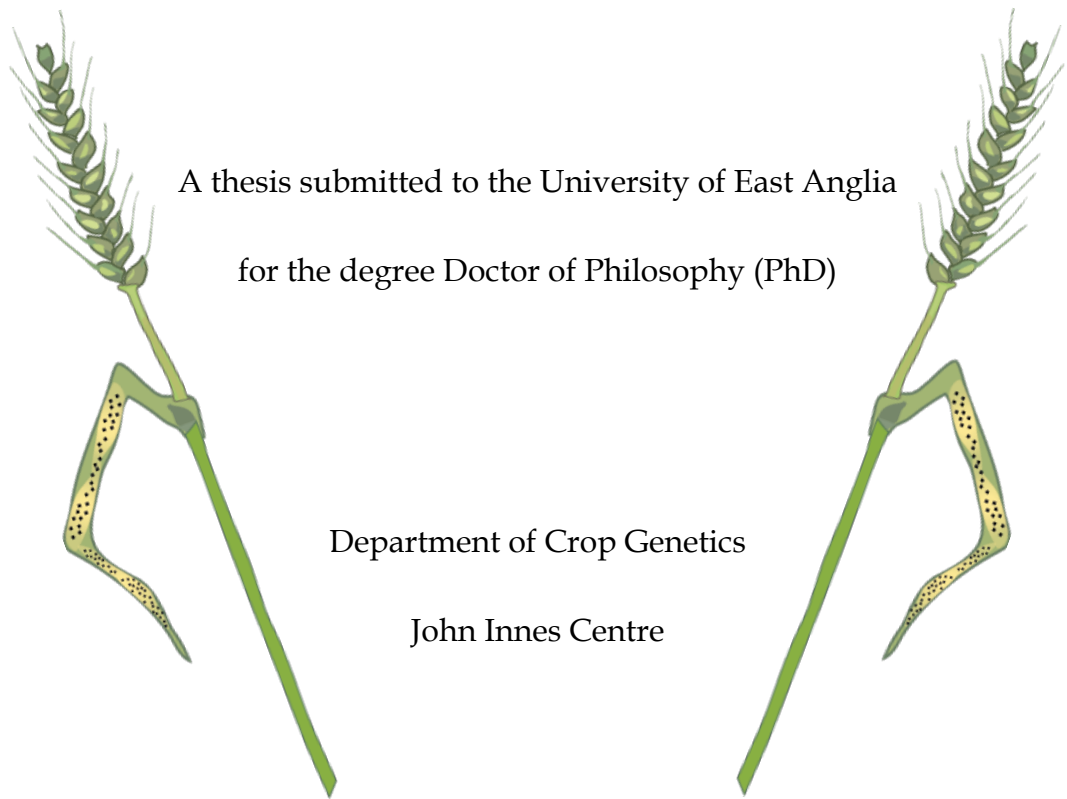


# EXPLORING THE GENETIC DIVERSITY IN WHEAT FOR RESISTANCE TO SEPTORIA TRITICI BLOTCH

Amber Noelle Hafeez



A thesis submitted to the University of East Anglia  
for the degree Doctor of Philosophy (PhD)

Department of Crop Genetics  
John Innes Centre

March 2022

© This copy of the thesis has been supplied on condition that anyone who consults it is understood to recognise that its copyright rests with the author and that use of any information derived therefrom must be in accordance with current UK Copyright Law. In addition, any quotation or extract must include full attribution.

'It is the nature of idea to be communicated: written, spoken, done. The idea is like grass.  
It craves light, likes crowds, thrives on crossbreeding, grows better for being stepped on.'

Ursula K. Le Guin, *The Dispossessed* (1974)

'I worked for chaff, and earning wheat  
Was haughty and betrayed.  
What right had fields to arbitrate  
In matters ratified?

I tasted wheat, - and hated chaff,  
And thanked the ample friend;  
Wisdom is more becoming viewed  
At distance than at hand.'

Emily Dickinson (1896)

# I. ABSTRACT

**S**eptoria tritici blotch (STB) is a foliar disease of wheat caused by the fungal pathogen *Zymoseptoria tritici* and is the third-most impactful wheat disease worldwide, due in part to the pathogen's widespread resistance to fungicides. It is therefore vital that more sources of host resistance are characterised and deployed.

Wild species contain multitudes of unexploited genetic variation, without the genetic bottlenecks and artificial selection pressures imposed upon crops. The D-genome progenitor of bread wheat, *Aegilops tauschii*, has shown near immunity to STB, yet this interaction is scarcely studied and little understood. Landraces are another valuable resource from which resistances that have been lost on the road to developing elite cultivars could be rediscovered. An example is the highly genetically and geographically diverse Watkins collection of pre-Green Revolution wheat landraces.

Association genetics was employed to investigate the genetic basis of resistance to *Z. tritici* in Watkins landraces by using whole-genome shotgun sequences for a set of 300 accessions. This led to the rediscovery of *Stb6* conferring resistance to the *Z. tritici* isolate IPO323. Subsequently, a candidate gene conferring resistance to IPO88004 and encoding a serine/threonine protein kinase was discovered on chromosome 6A, likely the previously-designated gene *Stb15*. The haplotype diversity of these genes in the panel was explored. A region on chromosome 4D associated with damage responses to IPO90012 was also investigated. Additionally, these methods were applied to an *Aegilops tauschii* diversity panel. Although the high prevalence of incompatible interactions limited the efficacy of this approach, several loci associated with necrosis responses were identified.

The identification of the third gene in the *Stb* canon, *Stb15*, provides valuable insights into the functional genetic architecture of *Z. tritici* resistance in wheat. Together, these results form a case study demonstrating both the power and limitations of association genetics for STB resistance gene discovery.

## **Access Condition and Agreement**

Each deposit in UEA Digital Repository is protected by copyright and other intellectual property rights, and duplication or sale of all or part of any of the Data Collections is not permitted, except that material may be duplicated by you for your research use or for educational purposes in electronic or print form. You must obtain permission from the copyright holder, usually the author, for any other use. Exceptions only apply where a deposit may be explicitly provided under a stated licence, such as a Creative Commons licence or Open Government licence.

Electronic or print copies may not be offered, whether for sale or otherwise to anyone, unless explicitly stated under a Creative Commons or Open Government license. Unauthorised reproduction, editing or reformatting for resale purposes is explicitly prohibited (except where approved by the copyright holder themselves) and UEA reserves the right to take immediate 'take down' action on behalf of the copyright and/or rights holder if this Access condition of the UEA Digital Repository is breached. Any material in this database has been supplied on the understanding that it is copyright material and that no quotation from the material may be published without proper acknowledgement.

## II. ACKNOWLEDGEMENTS

It feels as though I started this PhD a long time ago in a research institute far, far away...

I owe thanks to the many people who shared their time, expertise, and friendship with me over the course of this PhD. The main steps and people involved in the Watkins project are outlined in **Figure 1**. The project was managed by my supervisors Dr Brande Wulff and Prof James Brown, along with Dr Laetitia Chartrain; the four of us have had many productive brainstorming meetings over the last 4.5 years. Septoria experiments were conducted with assistance and training from Laetitia Chartrain and Rachel Burns. James Brown ensured that my manipulation and statistical analysis of the data were on track. Genotyping of the Watkins diversity panel was conducted by Dr Shifeng Cheng from material from Dr Simon Griffiths as part of the WatSeq collaboration between AGIS (Agricultural Genomics Institute Shenzhen) and JIC. Feng Cong and Xian Wenfei from Shifeng's team performed GWAS and subsequent peak-refining analyses. Dr Burkhard Steuernagel provided bioinformatics training and guidance for the haplotype analyses, and reassured me that I am capable of writing code. Dr Cyrille Saintenac provided material for the *Aegilops tauschii* project and I am grateful for his continued open collaboration. These experiments also owe thanks to Horticultural Services, especially Damian Alger who dealt with my CER-related neuroses with a smile and Lesley Phillips who always carefully looked after my plants.

I feel incredibly blessed to have been part of two wonderful research groups during my time at JIC. In the Wulff group, I made friends for life in my witches Dr Sreya Ghosh and Dr Clemence Marshal, who were generous in training me at the start of my PhD and who have supported me all the way through. I was also fortunate to be a student alongside Tom O'Hara, David Gilbert and Dr Ngoni Kangara, as well as our postdocs: Dr Burkhard Steuernagel, Dr Guotai Yu and Dr Sanu Arora. Finally, our work could not have been a success without the help of our RAs, Yajuan Yue and Macarana Forner. It is easy to work hard when you are surrounded by wonderful people, and the fact that many of us remain firm friends despite the scattering of our group several years ago speaks volumes. Brande has been an infinite source of both personal and professional support, wild science ideas and exasperating pranks over these past years, and I am incredibly grateful for his continued supervision all the way from KAUST.

The Brown and Nicholson lab tea break tradition kept me going through the long lockdown months. We persevered through wind and rain, shivering outside on benches spaced a safe distance apart, all in the name of hot drinks and conversation topics ranging from plant pathology to 'colanders for draining' to catching a bat with a pair of women's underwear. I have treasured being part of this tea-drinking elite and the endless supply of biscuits and cake has fuelled many pages of this thesis. I would like to thank the Brown group for their support and scientific input: Rachel Burns, Dr Elizabeth Orton, Dr Emily Beardon, Dr Cyrielle Ndouga and Oliver Powell. I am especially grateful to James Brown for his supervision and time spent immeasurably improving my understanding of both *Septoria* and statistics. Finally, my PhD would not have been possible without Laetitia, who always goes above and beyond as both a colleague and friend and who has taught me everything I know about working with *Septoria*. We have spent many days scoring side-by-side and going cross-eyed together.

I am so grateful to have experienced the patience, brilliance and dedication of all of the people listed above, who have made JIC feel like home as well as a workplace and who have helped me to become a scientist.

My final words of thanks go to my mother, Naomi Hafeez, for always encouraging me to work hard to make my own way in the world; my father, Dr Amer Hafeez, for pushing me towards science; and my grandparents, Margaret and Noel Dwyer, for never ceasing to believe in me.

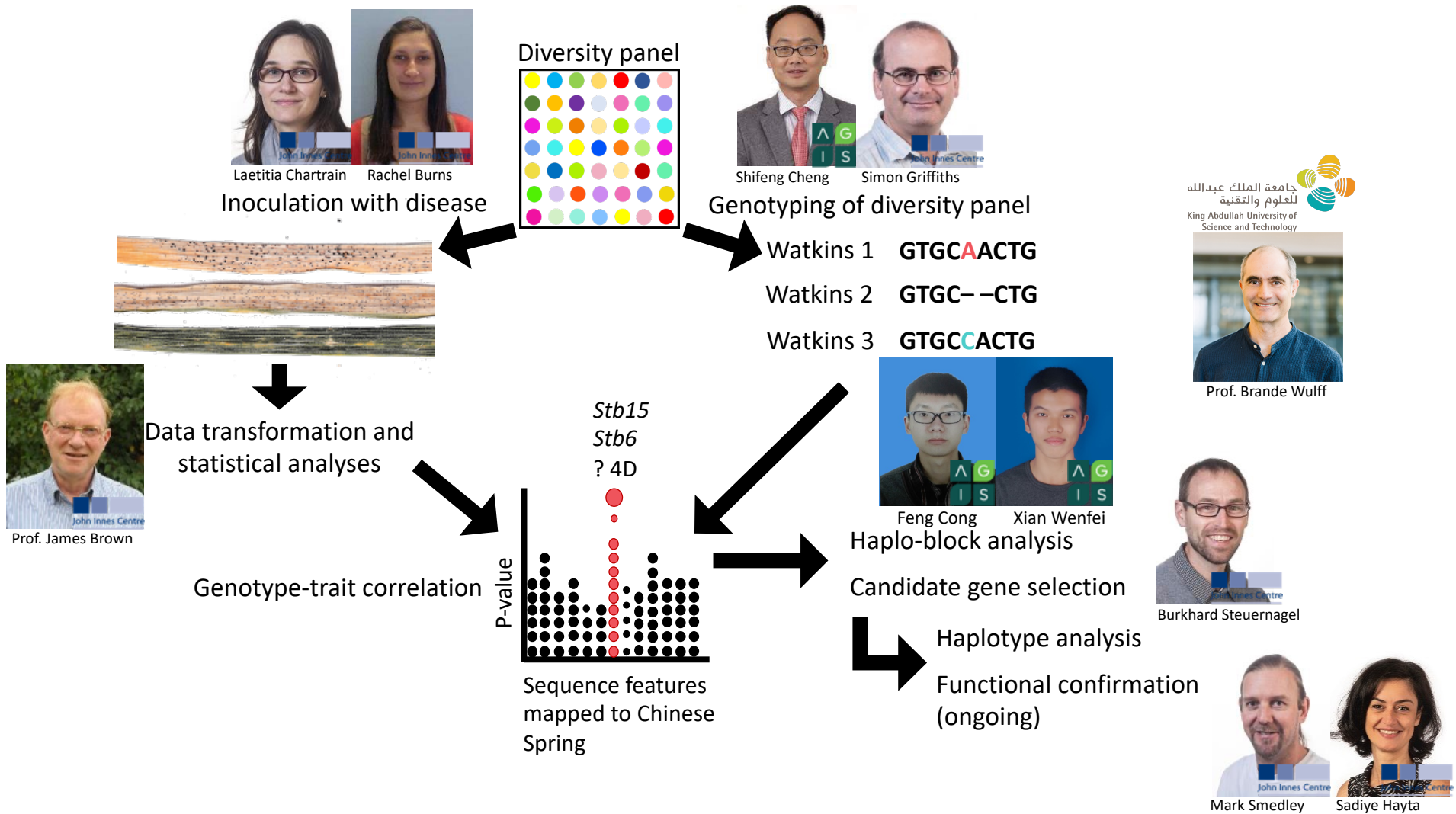


**Figure 1:** The main steps involved in my project on the Watkins landrace-Septoria interaction and the major collaborators involved along the way, without whom this project would not have been a success.

### III. ABBREVIATIONS

°C	degrees Celsius
[Chromosome]L	long arm of chromosome
[Chromosome]S	short arm of chromosome
%	percentage
\$	American Dollars
£	Great British Pounds
€	Euros
AUDPC	area under the disease progress curve
<i>Avr</i>	pathogen avirulence genes
bp	base pair
CER	controlled environment room
cm	centimetre
CRK	cysteine-rich receptor kinase
CS	Chinese Spring (wheat landrace)
DAMP	damage-associated molecular patterns
DMI	demethylation inhibitor
dpi	days post infection
DUF26	domain of unknown function 26
ETD	effector-triggered defence
ETI	effector-triggered immunity
EU	European Union
Gb	gigabase
GFF	general feature format
GFG	gene-for-gene
GTR-GAMMA	General Time Reversible model of nucleotide substitution under the Gamma model of rate heterogeneity
GUB-WAK	galacturonan-binding WAK domain
GWAS	genome-wide association study
h	hours
HR	hypersensitive response
HPC	high-performance computing
IGFG	inverse gene-for-gene
IP	invasion patterns
IPTR	IP-triggered receptor
JIC	John Innes Centre
k	thousand
kb	kilobases
L	litre
LD	linkage disequilibrium
LecRK	lectin receptor kinase
lgt	logit
m	metre
max.	maximum
Mb	megabases

ml	millilitre
mya	million of years ago
NIL	near-isogenic line
NLR	nucleotide-binding leucine-rich repeat receptor
OWWC	Open Wild Wheat Consortium
PAMP	pathogen-associated molecular pattern
PDA	potato dextrose agar
PPFD	photosynthetic photo flux density
PTI	PAMP-triggered immunity
QoI	quinone outside inhibitors
QTL	quantitative trait locus
R	disease resistance gene
RefSeq	reference sequence
RLK	receptor-like kinase
RLP	receptor-like protein
ROS	reactive oxygen species
S/TPK	serine/threonine protein kinase
SDHI	succinate dehydrogenase inhibitor
SHW	synthetic hexaploid wheat
SN	super necrosis
SNP	single nucleotide polymorphism
spp.	species
SRP	signal recognition particle
<i>Stb</i>	<i>R</i> gene for resistance to STB
STB	Septoria tritici blotch
TSV	tab-separated values format
TraesCS[5B][02] [G][236400]	RefSeq gene: <i>Triticum aestivum</i> Chinese Spring [chromosome] [annotation version][biotype][unique identifier]
UK	United Kingdom
VCF	Variant Call Format
WAK	wall-associated kinase
WGS	whole-genome shotgun
x	multiplication

# IV. TABLE OF CONTENTS

I. ABSTRACT .....	II
II. ACKNOWLEDGEMENTS .....	III
III. ABBREVIATIONS .....	VI
IV. TABLE OF CONTENTS .....	VIII
V. TABLE OF FIGURES .....	X
VI. TABLE OF TABLES.....	XV
VII. TABLE OF SUPPLEMENTARY TABLES.....	XVI
VIII. TABLE OF SUPPLEMENTARY SCRIPTS.....	XVII
<b>1. INTRODUCTION .....</b>	<b>1</b>
1.1. WHEAT: STAPLE CROP AND ACCOMMODATING HOST .....	1
1.2. IMPORTANCE AND LIFE CYCLE OF SEPTORIA TRITICI BLOTCH OF WHEAT .....	4
1.3. LOOKS LIKE WHEAT’S BACK ON THE MENU: EVOLUTION OF PATHOGENICITY .....	5
1.4. MANAGEMENT OF STB ON WHEAT .....	6
1.5. MODELS FOR PLANT IMMUNE RESPONSES .....	8
1.6. THE DEATH OF GRASS: GENETIC CONTROL OF DAMAGE RESPONSES.....	11
1.7. ALL THE SEPTORIA RESISTANCE IS A STAGE, AND ALL THE GENES AND QTLs MERELY PLAYERS.....	12
1.8. THE ROLE OF RLKs IN PLANT IMMUNE RESPONSES .....	14
1.9. QUANTITATIVE AND QUALITATIVE RESISTANCE.....	15
1.10. THE RISE AND FALL OF MAJOR GENE EMPIRES.....	18
1.11. ACHIEVING DURABLE FIELD RESISTANCE TO <i>Z. TRITICI</i> .....	19
1.12. EFFECTORS INVOLVED IN DEFENCE RESPONSES TO <i>Z. TRITICI</i> .....	21
1.13. COULD AN ATLAS UPHOLD <i>R</i> GENE DURABILITY AND STEWARDSHIP? .....	22
1.14. GENETIC DIVERSITY IN WHEAT’S BACK CATALOGUE .....	26
1.15. METHODS FOR THE RAPID CLONING OF RESISTANCE GENES .....	29
1.16. GENOME-WIDE ASSOCIATION STUDIES FOR CLONING RESISTANCE GENES .....	31
1.17. INTRODUCTION TO THE CURRENT STUDY .....	33
<b>2. EXPLORING THE INTERACTION BETWEEN <i>Z. TRITICI</i> AND <i>AEGILOPS TAUSCHII</i>.....</b>	<b>35</b>
2.1. INTRODUCTION .....	36
2.1.1. <i>Advantages of working with Ae. tauschii</i> .....	36
2.1.2. <i>Septoria resistance in the D-genome</i> .....	37
2.1.3. <i>Summary of chapter findings</i> .....	39
2.2. MATERIALS AND METHODS.....	40
2.2.1. <i>Plant and pathogen material</i> .....	40
2.2.2. <i>Experimental design for pathology assays</i> .....	45
2.2.3. <i>Standard infection protocol for pathology assays</i> .....	45
2.2.3. <i>Phenotype data collection</i> .....	48
2.2.4. <i>Statistical analysis</i> .....	48
2.2.5. <i>Association genetics</i> .....	49
2.3. RESULTS.....	50
2.4. DISCUSSION .....	60
<b>3. EXPLORING HOST-PATHOGEN INTERACTIONS BETWEEN WATKINS LANDRACES AND <i>Z. TRITICI</i> .....</b>	<b>65</b>
3.1. INTRODUCTION .....	66
3.1.1. <i>A landrace by any other name would prove as intractable</i> .....	66
3.1.2. <i>The collection of wheat landraces in the 20<sup>th</sup> century and unexpected theoretical journeys: there and back again</i> .....	68
3.1.3. <i>Studies of the Watkins collection and associated resources</i> .....	71
3.1.4. <i>Septoria isolates investigated in this chapter</i> .....	72
3.1.5. <i>Summary of chapter findings</i> .....	73
3.2. MATERIALS AND METHODS.....	74
3.2.2. <i>Plant and pathogen material</i> .....	75

3.3.	RESULTS.....	87
3.3.1.	<i>Responses of a reduced core set of Watkins landraces to eight Septoria isolates in detached leaf conditions.....</i>	87
3.3.2.	<i>Responses of the Watkins core 300 set to IPO323, IPO88004 and IPO90012.....</i>	97
3.3.3.	<i>The effect of inoculum dose on wheat responses to Z. tritici.....</i>	109
3.3.4.	<i>Identification of sources of broad-spectrum resistance within the Watkins collection for breeding.....</i>	115
3.4.	DISCUSSION.....	122
<b>4.</b>	<b>INTERROGATING THE GENETIC BASIS OF SEPTORIA RESISTANCE TO IPO323, IPO88004 AND IPO90012 IN THE WATKINS COLLECTION THROUGH ASSOCIATION GENETICS AND ANALYSIS OF WHOLE GENOME SHOTGUN SEQUENCES.....</b>	<b>127</b>
4.1.	INTRODUCTION.....	128
4.1.1.	<i>Solutions to the problem of STB.....</i>	128
4.1.2.	<i>Harnessing diversity for gene cloning.....</i>	128
4.1.3.	<i>Applications of cloned R genes.....</i>	129
4.1.4.	<i>Where did they come from, where did they go: the Stb genes of interest in this chapter.....</i>	130
4.1.5.	<i>Summary of chapter findings.....</i>	132
4.2.	MATERIALS AND METHODS.....	134
4.2.1.	<i>Association mapping.....</i>	134
4.2.2.	<i>Identification of candidate Stb genes.....</i>	134
4.2.3.	<i>Analysis of haplotypes of the identified candidate Septoria R genes.....</i>	134
4.2.4.	<i>Generation of a phylogenetic tree for Watkins core 300.....</i>	136
4.3.	RESULTS.....	137
4.3.1.	<i>Dissecting the response of Watkins landraces to IPO323 by GWAS.....</i>	137
4.3.2.	<i>Dissecting the response of Watkins landraces to IPO88004 by GWAS.....</i>	146
4.3.3.	<i>Dissecting the response of Watkins landraces to IPO90012 by GWAS.....</i>	158
4.4.	DISCUSSION.....	165
4.5.	CONCLUSION.....	167
<b>5.</b>	<b>GENERAL DISCUSSION.....</b>	<b>168</b>
<b>6.</b>	<b>REFERENCES.....</b>	<b>173</b>
<b>7.</b>	<b>APPENDIX.....</b>	<b>190</b>

# V. TABLE OF FIGURES

Figure 1: The main steps involved in my project on the Watkins landrace-Septoria interaction and the major collaborators involved along the way, without whom this project would not have been a success.....	v
Figure 2: The impact of wheat diseases on projected wheat yields. Figure reproduced from Hafeez et al. (2021).....	2
Figure 3: The number of designated major genes for resistance to diseases of wheat, arranged in order of their impact on wheat yields (top = most detrimental impact on wheat yields). Yield impact data from Savary et al. (2019). Gene designation data from supplementary table of Hafeez et al. (2021), based on the Komugi gene database ( <a href="https://shigen.nig.ac.jp/wheat/komugi/">https://shigen.nig.ac.jp/wheat/komugi/</a> ).....	3
Figure 4: Molecular interactions between hosts and pathogens or pests. Pathogens and pests secrete effectors upon colonisation of the host, either into the intracellular (i) or intercellular/apoplastic (ii) space (A). These bind host targets (iii) to manipulate the environment and aid in proliferation (B). In response, the host can detect the presence of effectors and initiate defence responses (C). This may be through direct binding of intracellular immune receptors (iv) and membrane-associated receptors for the recognition of apoplastic effectors (v) or indirect binding, <i>i.e.</i> the guard hypothesis (vi). Figure adapted from presentation slides shared by Brande Wulff, based on figures from Dodds and Rathjen (2010).....	10
Figure 5: The number of cloned major genes for resistance to diseases of wheat, arranged in order of their impact on wheat yields (top = most detrimental impact on wheat yields). Yield impact data from Savary et al. (2019). Gene designation data from supplementary table of Hafeez et al. (2021), based on the Komugi gene database ( <a href="https://shigen.nig.ac.jp/wheat/komugi/">https://shigen.nig.ac.jp/wheat/komugi/</a> ).....	13
Figure 6: The Cappuccino Model of plant disease resistance: there is an attractive froth layer comprising major <i>R</i> genes, which floats atop the caffeinated body of the drink that does the majority of the work in plant immune responses – the quantitative resistance genes (Brown, 2021).....	16
Figure 7: Sisyphus engaged in the seemingly ceaseless boom-and-bust cycle as it pertains to disease resistance genes. Research and breeding must identify and deploy new sources of resistance at great length and expense, which become widespread (the boom) only for the resistance to be quickly broken down by the pathogen due to deployment strategies that maximise pathogen evolutionary potential (the bust).....	18
Figure 8: Combining pathogen diversity data and <i>R</i> genes to build durable stacks and deploy them effectively. Pathogen populations in a region could be analysed for their effector complement and compatible <i>R</i> genes selected that recognise the most effectors (A). <i>R</i> genes can then be mobilised into wheat through crossing and marker-assisted selection (MAS) or by transformation (B). In the case of multi- <i>R</i> gene stacks, transformation as a cassette has the advantage that <i>R</i> genes would not become genetically separated. This would be beneficial for tracking stacks in breeding programmes. Cultivars containing these stacks can then be deployed in several ways: in a monoculture, as multilines (where plants differ only in the <i>R</i> gene stack they contain) or as multi- <i>R</i> gene stacks. The cultivars can then be rotated through years or growing seasons to continually change the <i>R</i> gene complement exposed to pathogen evolution (dynamic diversity; C). Figure reproduced from Hafeez et al. (2021).....	24
Figure 9: Atlas supporting wheat breeding. Wheat spike illustration adapted from Tobin Florio.....	25
Figure 10: Hybridisations, bottlenecks and inter-species crosses have influenced the genetic diversity of wheat during its speciation and domestication. 0.8 mya, <i>Triticum urartu</i> (AA) hybridised with a close relative of <i>Aegilops speltoides</i> (BB) to form allotetraploid emmer wheat, <i>Triticum turgidum</i> ssp. <i>dicoccoides</i> (AABB) (10.1). Hybridisation of tetraploid wheats and <i>Aegilops tauschii</i> resulted in the formation of hexaploid wheat 0.4 mya to 10,000 years ago (10.2). The thickness of coloured dot columns is proportionate to the	

geneflow from progenitor populations estimated by Zhou et al. (2020). Wheat breeding also introduced a genetic bottle neck (10.3). Over the past 100 years, the known native wheat *R* gene pool of 268 genes has been enriched with 198 exogenous *R* genes by inter-species crosses with the primary, secondary (e.g. *Ae. sharonensis*) and tertiary (e.g. *Thinopyrum elongatum*) gene pools (10.4). The secondary gene pool defined in this figure excludes *Ae. tauschii*. Figure reproduced from Hafeez et al. (2021).....27

Figure 11: The exponential growth in the number of cloned *R* genes from 1997 to 2021. Cloning method is coded by colour. The increase in the number of methods available for gene cloning, such as mutational genomics and association genetics, coincides with a rapid increase in the number of cloned genes. TACCA = targeted chromosome-based cloning via long-range assembly (Thind et al., 2017). The publishing of the wheat Chinese Spring reference genome (RefSeq v1.0) in 2017 is indicated. Figure based on Keller et al. (2018).30

Figure 12: A comparison of different methods for cloning *R* genes. Genetic structuring: mutational genomics and map-based cloning interrogate the narrow genetic base of just one to two accessions. On the other hand, the pangenome variation can be accessed through the use of a diversity collection for association genetics, without the need for lab-generated population structures. Genotyping: complexity-reduction strategies can be used, such as *R*-gene enrichment sequencing and chromosome flow sorting, whilst WGS sequencing is a more costly but potentially more informative and unbiased approach. Genotype-trait correlation: all three of these methods aim to discover a correlation between host genotypes and the trait of interest – ideally, leading to the identification of a candidate gene. This can be achieved by analysing mutations, mapping intervals or the significance of sequence features associated with the trait of interest (GWAS). Cloned gene(s): association mapping has the potential to identify multiple genes from one sequence-configured population, whilst mutational genomics and biparental mapping typically only allow the mapping of a single gene per population. Figure reproduced from Hafeez et al. (2021).....32

Figure 13: Comparison of spikes and chromosome numbers between wheat and *Ae. tauschii*. A genome = blue; B genome = red; D genome = green. ....36

Figure 14: Major genes and QTLs conferring resistance to *Z. tritici* that have been mapped to the D-genome chromosomes of wheat. Adapted and reproduced here with permission from Brown *et al.* (2015). ....38

Figure 15: Photos of some steps involved in seedling *Z. tritici* assays. Plants are sprayed on a turn table (A) and then placed inside propagators covered with black plastic bags for incubation (B). The second batch of seedlings can be seen at the one leaf stage in B and the 2-3 leaf stage, just prior to leaf cutting and inoculation, in C. Plants remain inside propagator bases after inoculation to enable watering from the bottom (C, right hand side). ....47

Figure 16: Phenotyping scale used for scoring seedling assays. Leaves are arranged according to their approximate pycnidia percentage cover, but necrosis was also scored. ....48

Figure 17: Leaf scan images of wheat and *Ae. tauschii* leaves inoculated with *Z. tritici* isolate IPO92006, 29 days post infection. Leaf images were selected to represent the major phenotypes observed: Taichung 29 (highly susceptible wheat control), BW\_21481 A (highly resistant); BW\_21481 B (wheat-like lesions bearing pycnidia); BW\_21200 (highly necrotic with scarce pycnidia); BW\_21133 (highly necrotic with a region densely populated with very small pycnidia); BW\_21092 (highly susceptible and densely populated with pycnidia) and BW\_21493 (presence of scarce pycnidia and melanised patches). BW\_21481 A and B are genetically identical replicates of the same accession....51

Figure 18: Estimated mean pycnidia and damage scores of wheat lines and 151 *Ae. tauschii* accessions inoculated with *Z. tritici* isolates cfz008 (left) and IPO323 (right). Wheat controls are labelled. There were no resistant controls for cfz008. For IPO323, Flame and Hereward were negative controls and Longbow and Riband were included as positive controls. Logit values of 2.5, 0, -2.5, -5 and -7.5 back-transform to 92%, 50%, 8%, 0.7% and 0.1%. ....55

Figure 19: Pycnidia and necrosis scores in response to IPO323 and cfz007 plotted against one another. ....55

Figure 20: Manhattan plot of IPO323 pycnidia phenotypes (calculated means from the last scoring day) associated with <i>k</i> -mers generated from <i>Ae. tauschii</i> whole-genome shotgun data. Reads were mapped to the <i>Ae. tauschii</i> reference genome AL8/78. Analysis and figure were generated by Kumar Gaurav. ....	56
Figure 21: Manhattan plot of cfz008 and IPO323 necrosis phenotypes (calculated means from the last scoring day) associated with <i>k</i> -mers generated from <i>Ae. tauschii</i> whole-genome shotgun data. Blue dots indicate an association with less necrosis (green leaf tissue); red dots signify an association with high necrosis. Larger dots indicate a greater number of associated <i>k</i> -mers. Major peaks are labelled for reference. Reads were mapped to assemblies of accessions with high necrosis, phased with the <i>Ae. tauschii</i> reference genome AL8/78. Analysis and figure were generated by Kumar Gaurav. ....	58
Figure 22: Manhattan plot of cfz008 and IPO323 necrosis phenotypes (calculated means from the last scoring day) associated with <i>k</i> -mers generated from <i>Ae. tauschii</i> whole-genome shotgun data and mapped to Chinese Spring RefSeq v1.0. Blue dots indicate an association with less necrosis (green leaf tissue); red dots signify an association with high necrosis. Larger dots indicate a greater number of associated <i>k</i> -mers. Major peaks are labelled for reference. Analysis and figure were generated by Kumar Gaurav. ....	59
Figure 23: Flow diagram giving an overview of the projects undertaken within this chapter. The main project is shaded in purple, whilst secondary projects are in blue. ....	74
Figure 24: Histograms of estimated means derived from the linear mixed model fitted to detached leaf response data of Watkins core 36 lines inoculated with eight <i>Z. tritici</i> isolates. ....	90
Figure 25: Relationship between pycnidia and damage estimated means derived from the linear mixed model fitted to detached leaf response data of Watkins core 36 lines inoculated with eight <i>Z. tritici</i> isolates. <i>R</i> gives the Pearson correlation score. Shaded area represents the 95% confidence interval. ....	91
Figure 26: Means of logit pAUDPC responses to single isolates plotted against the means of lines across all eight isolates. <i>R</i> gives the Pearson correlation score. Shaded area represents the 95% confidence interval. ....	93
Figure 27: Means of % maximum dAUDPC responses to single isolates plotted against the means of lines across all eight isolates. <i>R</i> gives the Pearson correlation score. Shaded area represents the 95% confidence interval. ....	94
Figure 28: A matrix of correlations between pycnidia (A) and damage (B) responses to <i>Z. tritici</i> isolates in the Watkins core 36 set and wheat controls in detached leaf conditions. Circle size and colour indicate the size of the coefficient of correlation (large positive or negative numbers have a larger circle size). Statistically significant Pearson's correlation scores are marked with an asterisk ( $p = 0.05$ ). ....	96
Figure 29: Leaf scan images of wheat and Watkins lines inoculated with <i>Zymoseptoria tritici</i> isolate IPO323 at 34 days post inoculation (seedlings around 7 weeks old). The key phenotypes observed were: full resistance, with leaves remaining green; clear susceptibility, with varying levels of fungal reproduction, and intermediate phenotypes, ranging from high necrosis with little/no spore production to mostly healthy leaves with single/few small lesions. ....	97
Figure 30: Histograms of lgt pAUDPC and % maximum dAUDPC of Watkins wheat landraces inoculated with <i>Z. tritici</i> isolates IPO323, IPO88004 and IPO90012. ....	101
Figure 31: Logit pAUDPC versus % maximum dAUDPC scores of Watkins wheat landraces inoculated with <i>Z. tritici</i> isolates IPO323, IPO88004 and IPO90012. Key wheat control lines are labelled. ....	101
Figure 32: Isolate logit pAUDPC and % maximum dAUDPC responses of Watkins landraces to IPO323, IPO88004 and IPO90012 plotted against one another. Key wheat lines are labelled. ....	103
Figure 33: Mean responses of Watkins and wheat lines to single isolates (IPO323, IPO88004 or IPO90012) plotted against the line mean across the other two isolates. Key wheat lines are labelled. ....	104
Figure 34: Mean logit pAUDPC scores of Watkins lines by ancestral group, against IPO323 (Netherlands), IPO88004 (Ethiopia) and IPO90012 (Mexico). Red numbers at the top of each graph indicate the number of lines in each category. ....	106

Figure 35: Box plots showing estimated logit AUDPC pycnidia and % maximum AUDPC damage scores of Watkins landrace and wheat cultivar lines with (1) and without (0) the presence of the super necrosis (SN) phenotype for each isolate. Numbers in red at the top of plot A show the sample size. ....	108
Figure 36: Logit AUDPC of pycnidia (A) and % maximum AUDPC damage (B) scores of a differential set of Watkins lines inoculated with IPO323 (purple) and IPO89011 (green) under four different inoculum doses (dose "3" = 10 <sup>3</sup> spores/ml <sup>-1</sup> , and so on).....	112
Figure 37: The mean % maximum pAUDPC (closed circles) and dAUDPC (open triangles) of 10 Watkins landraces and five wheat control lines tested under four different inoculum doses of IPO323 (red) and IPO89011 (blue). Dose "3" = 10 <sup>3</sup> spores/ml <sup>-1</sup> , and so on. Coloured dots are used to represent phenotypes observed previously for each isolate: green (resistant), pink (susceptible) or SN (yellow).....	114
Figure 38: Line means of damage (% max. dAUDPC) against pycnidia (logit pAUDPC) for Watkins landraces and wheat lines across six isolates (IPO87019, IPO89011, IPO90004, IPO94269, JIC040 and Cougar007). Lines included for their high resistance to IPO323, IPO90012 and IPO88004 are in teal; lines selected for general susceptibility are in pink; wheat controls are in black and the susceptible wheat line Longbow is highlighted in orange. Shaded area represents the 95% confidence interval. ....	120
Figure 39: Means of pycnidia (logit pAUDPC) for Watkins landraces and wheat lines in response to individual isolates plotted against the line means. Lines included for their high resistance to IPO323, IPO90012 and IPO88004 are in teal; lines selected for general susceptibility are in pink; wheat controls are in black and the susceptible wheat line Longbow is highlighted in orange. Shaded area represents the 95% confidence interval. ....	121
Figure 40: The pycnidia versus damage plot of IPO323 responses from Figure X. Lines are circled depending on responses falling into one of three categories: highly resistant, pycnidia cover increasing with damage or damage increasing independently of pycnidia.....	123
Figure 41: Flow chart of the steps taken to generate a SNP distance matrix based on regions extracted from the Watkins landrace WGS dataset. VCF = variant call format, TSV = tab-separated values format. ....	135
Figure 42: Manhattan plot showing associations between SNPs in the Watkins landrace collection and pycnidia, damage and super-necrosis responses to <i>Z. tritici</i> isolate IPO323. Figures produced by Feng Cong.....	138
Figure 43: Zoomed-in Manhattan plot of the 3A peak from the SNP-based GWAS with the IPO323 pycnidia phenotype from Shifeng <i>et al.</i> The LD heatmap is displayed below. Figure produced by Xian Wenfei. Blue square indicates the main area of the peak. Green square indicates that smaller haploblock within the blue square which is most highly associated with resistance. ....	140
Figure 44: Alignment of <i>Stb6</i> sequences in the sequenced wheat pangenome visualised in Geneious Prime. Yellow arrows = CDS, grey arrows = exons, red box = mRNA. ....	141
Figure 45: Heatmap displaying the distance between each pair of accessions in the Watkins collection, as well as some elite wheat lines. Pycnidia (pAUDPC) and damage (%max_dAUDPC) scores are plotted along the left-hand side. Accessions are grouped via a dendrogram. Haplotype groups are indicated with black outlines and labels. Groups 9 and 10 contained only one accession and are indicated with dashed lines.....	142
Figure 46: IGV visualisation of SNPs in the <i>Stb6</i> locus in the 13 lines which appeared to have the same <i>Stb6</i> haplotype as Chinese Spring but were susceptible to IPO323. Sites containing SNPs are indicated in the second panel. The third panel displays SNPs in the Watkins lines listed: grey bands indicate the same base as Chinese Spring, indigo bands indicate heterozygous SNPs, turquoise bands indicate homozygous SNPs and no/white bands indicate missing data. The bottom panel contains the GFF (general feature format) file, wherein thick bands represent exons and thinner bands represent introns. ....	143
Figure 47: Pycnidia (logit pAUDPC) scores plotted against damage (% max. dAUDPC) scores in response to IPO323, with colour coding to indicate haplotype clusters designated for <i>Stb6</i> . ....	144
Figure 48: Manhattan plots of logit pAUDPC (pycnidia) and % max. dAUDPC (damage) scores of Watkins lines inoculated with <i>Z. tritici</i> isolate IPO323 associated with genome-wide	

SNPs. 234 Watkins accessions carrying a functional version of <i>Stb6</i> were removed to leave a panel size of 66 accessions (plus three wheat cultivars).....	145
Figure 49: Manhattan plots showing association of SNPs mapped to Chinese Spring with logit pAUDPC, % maximum dAUDPC, SN (super necrosis) and SN with lines exhibiting high pycnidia values removed (clean SN only).....	147
Figure 50: Geneious screenshot showing an alignment of the TraesCS6A02G078700 gene in the wheat pangenome lines.....	150
Figure 51: SNP calls within the <i>Stb15</i> locus, visualised in IGV.....	151
Figure 52: Heatmap of distance in SNPs within the TraesCS6A02G078700 locus between Watkins accessions. Panel on left shows phenotype scores. Major haplotype groups are outlined in black and labelled with the names of key lines. ....	152
Figure 53: Pycnidia (logit pAUDPC) scores plotted against damage (% max. dAUDPC) scores in response to IPO88004, with colour coding to indicate haplotype clusters designated for <i>Stb15</i> . ....	155
Figure 54: Manhattan plot of Watkins SNPs associated with IPO88004 pycnidia data, with lines carrying the functional haplotype of <i>Stb15</i> candidate TraesCS6A02G078700 removed. .	157
Figure 55: Protein domains of the <i>Stb15</i> candidate TraesCS6A02G078700 predicted from the amino acid sequence in the Uniprot online database (uniprot.org). Length in pixels of each domain corresponds to the number of amino acids. SP = signal peptide, BT = bulb-type, S-Gly = S-locus glycoprotein, PAN = PAN/apple, TM = transmembrane. ....	158
Figure 56: Manhattan plot showing associations between SNPs in the Watkins landrace collection and pycnidia, damage and super-necrosis responses to <i>Z. tritici</i> isolate IPO90012. Figures produced by Feng Cong.....	160
Figure 57 (overleaf): Phylogenetic tree of the core 300 Watkins collection generated from Axiom breeder's array SNPs. Outer panels give additional information corresponding to each line. From the innermost panel: Ancestral group is indicated by colour (pink/green) and subgroups by colour intensity; STB response is indicated by lighter (more resistant) to darker (more susceptible) shades of orange (IPO323), purple (IPO88004) or blue (IPO90012); super necrosis presence (filled circle) or absence (blank) is indicated for each isolate; <i>Stb6</i> haplotype is colour-coded (Chinese Spring in pale blue); and, finally, <i>Stb15</i> haplotype is represented with functional <i>Stb15</i> alleles in black. For gene haplotypes, example wheat cultivars are given and labelled with R (resistant allele) or S (susceptible allele) where known. Yellow stars mark out clades which appear to contain highly Septoria-resistant lines. ....	162

## VI. TABLE OF TABLES

Table 1: <i>Aegilops tauschii</i> ssp. <i>strangulata</i> (Lineage 2) accessions included in the current study and their origins. Table adapted from Supplementary Table 2 of Arora et al. (2019). .....	40
Table 2: Wheat lines included in Septoria assays and reasons for their inclusion. Selections based on information from Arraiano & Brown (2006), Brown et al. (2015) and Chartrain et al. (2004). .....	44
Table 3: Isolates tested on the <i>Ae. tauschii</i> collection. For references re avirulences see Brown et al. (2015). Avirulence to <i>Stb16q</i> tested by Cyrille Saintenac (personal communication). .....	45
Table 4: ANOVA table for fixed effects of the linear mixed model fitted to logit pAUDPC values of <i>Ae. tauschii</i> accessions in response to IPO323 and cfz008. ....	53
Table 5: ANOVA table for fixed effects of the linear mixed model fitted to % maximum dAUDPC values of <i>Ae. tauschii</i> accessions in response to IPO323 and cfz008. ....	53
Table 6: Table of variance components for random effects of the linear mixed model fitted to logit pAUDPC and % maximum dAUDPC values of <i>Ae. tauschii</i> accessions in response to IPO323 and cfz008. ....	53
Table 7: Watkins landraces included in Septoria assays, their origin and core set designation. Ancestral groups are as described in Wingen et al. (2014). .....	75
Table 8: Wheat lines included in Septoria assays and reasons for their inclusion. The top section of the table includes wheat lines whose genomes have been sequenced. Selections based on information from Arraiano & Brown (2006), Brown et al. (2015) and Chartrain et al. (2004). .....	84
Table 9: Isolates tested on Watkins collection and sets of lines tested. S = seedling conditions, DL = detached leaf. For references re avirulence see Brown et al. (2015). Where the year of collection is not known, the paper wherein isolates are first described is given. ....	85
Table 10: ANOVA table of the linear mixed model on logit pAUDPC. ....	89
Table 11: ANOVA table of the mixed model on % maximum dAUDPC. ....	89
Table 12: Random effects of the linear mixed model fitted to logit pAUDPC and % maximum dAUDPC scores. ....	89
Table 13: ANOVA table of linear mixed model for logit pAUDPC scores from the Watkins 300 collection inoculated with IPO323, IPO88004 and IPO90012. Colons represent nested factors. ....	99
Table 14: ANOVA table of linear mixed model for % maximum dAUDPC scores from the Watkins 300 collection inoculated with IPO323, IPO88004 and IPO90012. Colons represent nested factors. ....	99
Table 15: Random effects of the linear mixed model fitted to logit pAUDPC and % maximum dAUDPC scores form the Watkins 300 collection inoculated with IPO323, IPO88004 and IPO90012. Colons represent nested factors. ....	99
Table 16: Summary of Watkins landrace ancestral groups (Wingen et al., 2014). ....	105
Table 17: Reasons for including lines in the “differential set” to test at different inoculum doses. ....	109
Table 18: ANOVA table of linear mixed model for logit pAUDPC scores from Watkins and wheat lines inoculated with IPO323 and IPO89011 at different inoculum doses ( $10^3$ , $10^4$ , $10^5$ or $10^6$ spores/ml). Colons represent nested factors. ....	111
Table 19: ANOVA table of linear mixed model for % maximum dAUDPC scores from Watkins and wheat lines inoculated with IPO323 and IPO89011 at different inoculum doses ( $10^3$ , $10^4$ , $10^5$ or $10^6$ spores/ml). Colons represent nested factors. ....	111
Table 20: Table of random effects from linear mixed models for logit pAUDPC and % maximum dAUDPC scores from Watkins and wheat lines inoculated with IPO323 and IPO89011 at different inoculum doses ( $10^3$ , $10^4$ , $10^5$ or $10^6$ spores/ml). ....	111
Table 21: Lines included in the test with scores for damage and pycnidia against IPO323, IPO90012 and IPO88004. Wheat cultivars and Chinese Spring (separated from Watkins landraces by a double line) were included as controls. Compatible interactions and lines included for their susceptibility are marked in pink. All other Watkins lines were included for their resistance to all three isolates. ....	116

Table 22: ANOVA table of linear mixed model for logit pAUDPC scores from Watkins and wheat lines. Colons represent nested factors.....	118
Table 23: ANOVA table of linear mixed model for % maximum dAUDPC scores from Watkins and wheat lines. Colons represent nested factors. ....	118
Table 24: Genes in the 6A peak and their function. Reasons for not selecting these genes as the <i>Stb15</i> candidate are given. ....	149
Table 25: Haplotypes identified by pheatmap $k=10$ and their SNP complement. Cells with the reference (Chinese Spring) genotype are in white. Cells with the ArinaLrFor genotype are in pink; other alternative alleles are in yellow cells.....	153
Table 26: Haplotypes identified by pheatmap $k=10$ and their SNP complement, manually curated to remove haplotypes of low confidence. Cells with the reference (Chinese Spring) genotype are in white. Cells with the ArinaLrFor genotype are in pink; other alternative alleles are in yellow cells. ....	154
Table 27: Haplotype groups in 800 Watkins lines and 250 additional wheat lines. 'Distance from' indicates the number of SNPs that are different in comparison to the named cultivar. .	156
Table 28: SNPs highly associated with super necrosis in response to IPO90012. Table provided by Shifeng Cheng and Feng Cong.....	161

## VII. TABLE OF SUPPLEMENTARY TABLES

Supplementary Table 1: Mean responses of <i>Ae. tauschii</i> and wheat accessions to <i>Z. tritici</i> isolates cfz008 and IPO323. Means are estimated from a linear mixed model fitted to both datasets (Chapter 2).....	190
Supplementary Table 2: Genes present in regions associated with necrosis response to <i>Z. tritici</i> isolate cfz008. Knetminer output for associated traits and functions of these genes is provided.....	194
Supplementary Table 3: Mean logit pAUDPC and % maximum dAUDPC values estimated from linear mixed models for the interactions between the Watkins core 300 and wheat controls and 7 <i>Z. tritici</i> isolates. ....	198
Supplementary Table 4: Mean logit pAUDPC and % maximum dAUDPC values estimated from linear mixed models for the interactions between the Watkins core 300 and wheat controls and <i>Z. tritici</i> isolates IPO323, IPO88004 and IPO90012. Super necrosis presence/absence is also given. ....	200
Supplementary Table 5: Haplotype groups assigned to each line in the Watkins core 300 based on SNPs within the <i>Stb6</i> and <i>Stb15</i> loci. ....	209

# VIII. TABLE OF SUPPLEMENTARY SCRIPTS

Supplementary Script 1: R code for transforming and fitting linear mixed models to STB phenotype data. Exported with <i>knitr</i> . .....	218
Supplementary Script 2: Python programme for generating SNP distance matrices from regions extracted from VCF files. ....	220
Supplementary Script 3: R code for generating heatmaps of haplotypes and defining clusters/haplotype groups. ....	226
Supplementary Script 4: Python script employed to convert from hapmap to fasta format, written with Oliver Powell. ....	227
Supplementary Script 5: Batch file used to run RaxML on the JIC high performance computing cluster, with arguments for tree generation specified. ....	228

# 1. INTRODUCTION

*Several figures and some of the writing in this chapter have been published previously in:*

Hafeez, A. N., Arora, S., Ghosh, S., Gilbert, D., Bowden, R. L., and Wulff, B. B. H. (2021). Creation and judicious application of a wheat resistance gene atlas. *Mol. Plant* **14**:1053–1070.

## 1.1. WHEAT: STAPLE CROP AND ACCOMMODATING HOST

**W**heat (*Triticum aestivum*) is the most widely grown crop in the world; 18% of the calories and 19% of the protein consumed by humankind are sourced from this staple food (FAOSTAT, 2017; <http://www.fao.org/faostat/en/#data/FBS>). Reductions in wheat yields can therefore have striking consequences. In 2010, poor wheat harvests led to increased bread prices in the Middle East and North Africa, which may have contributed to the fall of governments in these regions during the Arab Spring (Zurayk and Khalidi, 2011).

A major limitation to wheat production is diseases and pests, which reduce the world's harvest by an average of 21% compared to projected values each year (Savary et al., 2019; **Figure 2**). Over half of this loss is caused by the top four diseases (leaf rust, Fusarium head blight, Septoria tritici blotch and stripe rust). More than 90% of losses are accountable to the top 12 pathogens and pests. Sudden changes in pathogen populations or their spread in the environment can lead to epidemics and large-scale crop failure (Saari and Wilcoxson, 1974; Hovmøller et al., 2010; Islam et al., 2016). To minimise such risks, control methods have been employed, such as quarantine of material, pesticides, and breeding to combine desirable traits like grain yield with variation for enhanced disease resistance. An advantage of genetic disease resistance is that it reduces the optimal fungicide dose that is required to avoid epidemics (Te Beest et al., 2013) as well as the selection pressure on pathogens to evolve resistance to fungicides (Jørgensen et al., 2017). Chemical treatments can then be reduced along with their environmental and economic costs.

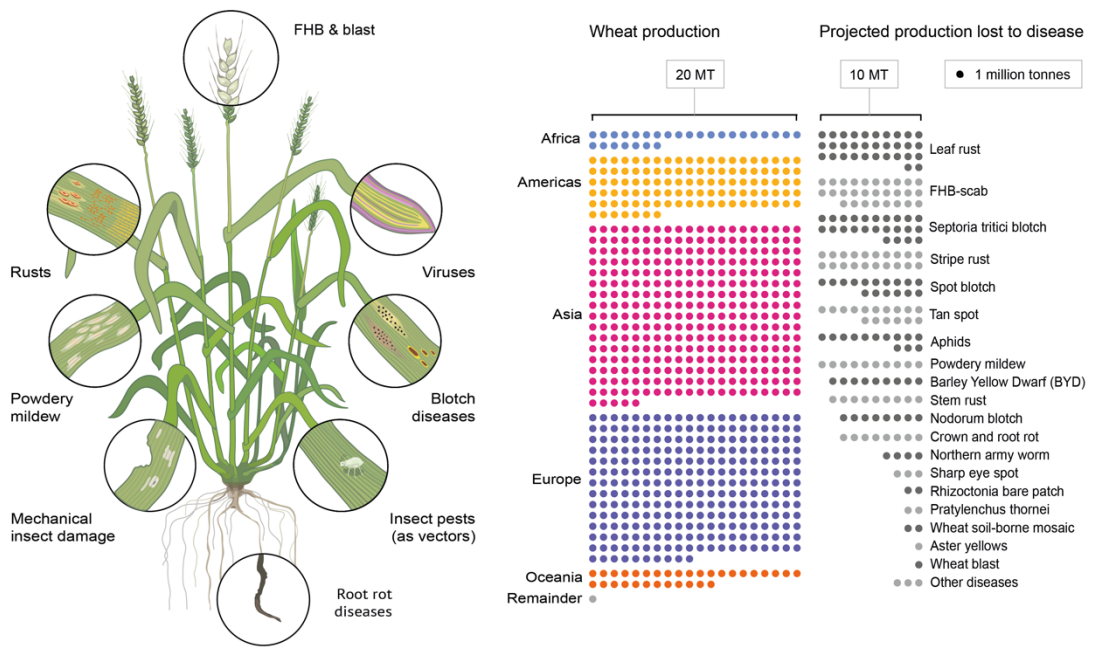


**Figure 2:** The impact of wheat diseases on projected wheat yields. Figure reproduced from Hafeez et al. (2021).

Much work across many pathosystems has led to the designation of 467 disease resistance genes in wheat, most of them for resistance to the wheat rust diseases and powdery mildew (**Figure 3**). There is a rift between the high importance of disease such as *Fusarium head blight* and *Septoria tritici blotch* in terms of yield impact and the comparatively small handful of genes that have been designated for resistance to these diseases. Bridging this gap would result in more resilient wheat crops, which would enhance food security for the oncoming challenges of climate change and population growth.

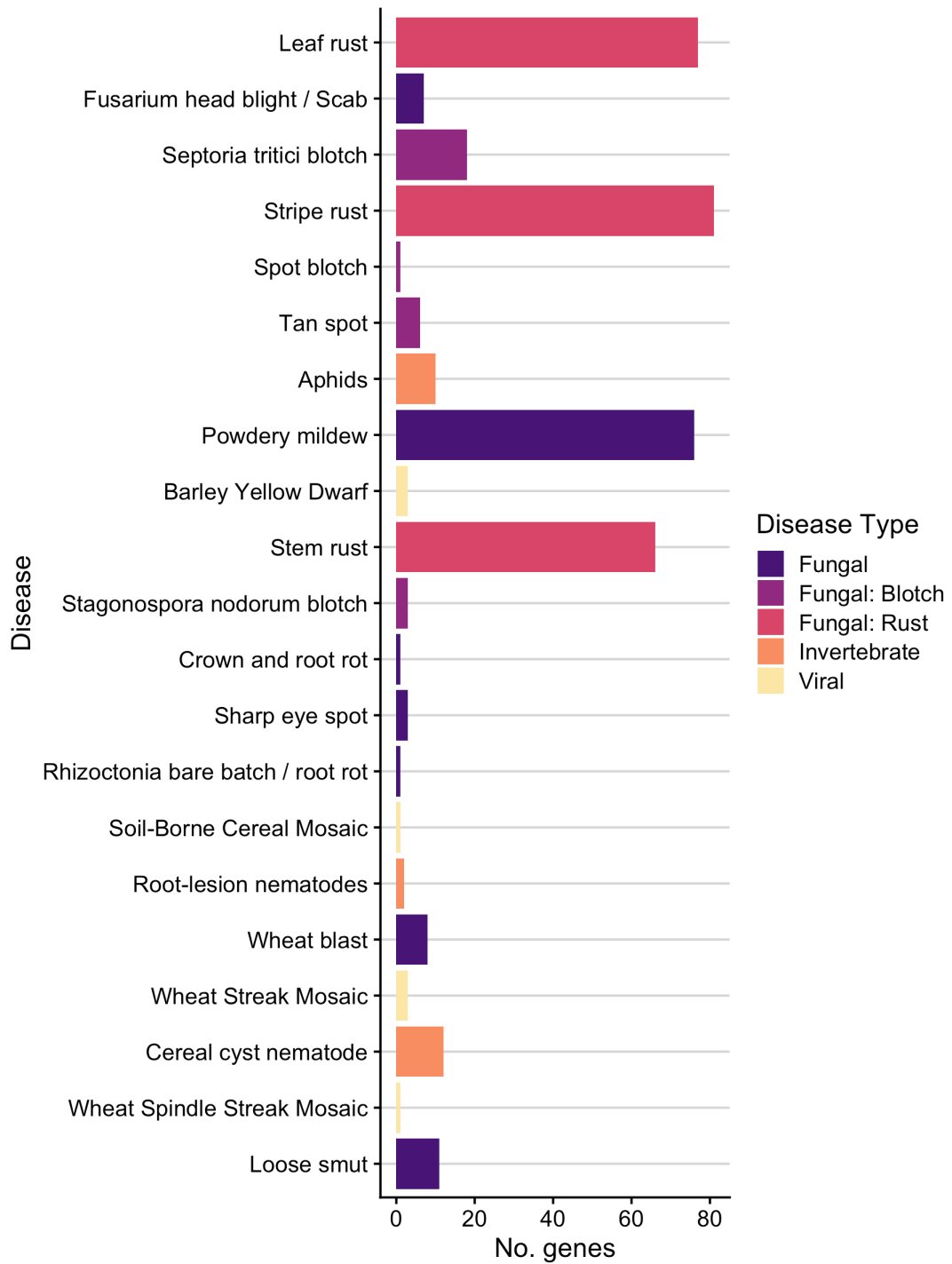


**Figure 3:** The number of designated major genes for resistance to diseases of wheat, arranged in order of their impact on wheat yields (top = most detrimental impact on wheat yields). Yield impact data from Savary et al. (2019). Gene designation data from supplementary table of Hafeez et al. (2021), based on the Komugi gene database (<https://shigen.nig.ac.jp/wheat/komugi/>).

## 1.2. IMPORTANCE AND LIFE CYCLE OF SEPTORIA TRITICI BLOTCH OF WHEAT

Throughout temperate climates worldwide, *Septoria tritici* blotch (STB) is a formidable foliar disease of wheat. In Europe, STB is the principle target of cereal fungicide, accounting for 70% of use at the cost of over \$400 million per year (O'Driscoll et al., 2014). STB is the second most important disease in the United States (costing around \$275 each year), and also afflicts Russia, Mexico and parts of South America. Serious losses due to STB were first reported in Italy in the 1890s (Cavara (1893), cited by Shipton et al. (1971)). By 1974, STB was claimed to be the most economically important leaf blotch disease in Asia and Africa following the introduction of high-yielding dwarf cultivars selected in the absence of the disease (Saari and Wilcoxson, 1974). STB still impacts Tunisia, Iran, Morocco and countries in East Africa (Ponomarenko et al., 2011). It is a disease of great social and economic importance threatening a staple crop for 35% of the world's population. The pursuit of new resistant wheat varieties can therefore only enhance food security.

STB is caused by the Dothideomycete fungus *Zymoseptoria tritici*. Infection occurs under conditions of prolonged, high relative humidity and temperatures above 7 °C (optimally around 20-25 °C), in the absence of desiccation (Eyal et al., 1997). Wind-dispersed, sexual ascospores form the primary inoculum and germinate within 12 hours in laboratory conditions. On the leaf surface, germinated spores overlook the thigmotrophic or chemotrophic signals utilised by other pathogens, instead growing randomly across the leaf surface until stomatal penetration is achieved after 24 hours, at a frequency of 25% (Kema et al., 1996a). This is followed by a latent period of asymptomatic growth where hyphae invade the surrounding apoplastic tissue, lasting between 8 and 14 days. *Z. tritici* does not deplete apoplastic nutrients during this phase (Keon et al., 2007). As there is also an absence of haustoria or other visible feeding structures, it is difficult to describe this phase as biotrophic, thus *Z. tritici* may be more accurately described as a latent necrotroph rather than a hemibiotroph (Sánchez-Vallet et al., 2015).

Once pre-pycnidia have formed, there is an abrupt switch to necrotrophy beginning in the sub-stomatal cavities (Shipton et al., 1971; Steinberg, 2015). Transcript analyses suggest that hypersensitive response-like activity (apoptosis) is elicited in host tissue at this stage through the release of pathogen toxin proteins (Keon et al., 2007). This results in the release of host nutrients and the rapid growth and proliferation of the pathogen. Symptoms begin as water-soaking and ultimately manifest as pycnidia, the asexual fruiting bodies, growing within necrotic lesions on the leaf surface.

Pycnidia spores may then spread by up to a meter through rain splash, allowing further cycles of colonisation within and between plants and consequently quick progress of the disease. When all host tissue is dead, the saprotrophic phase of growth commences, with the sexual fruiting bodies (pseudothecia) appearing 4-6 weeks after infection. It follows that ascospores are released or may overwinter to inoculate the same field in the succeeding growing season, hosted by wheat volunteers, weeds and, most significantly, crop debris (Suffert et al., 2011).

*Z. tritici* has a high evolutionary potential, exhibited by its adaptation of virulence to major and quantitative gene resistance in wheat cultivars. This is unsurprising when the pathogen's population biology is considered, elements of which are its large effective population size, high degree of gene flow and high levels of recombination observed in field populations worldwide (McDonald and Mundt, 2016).

### 1.3. LOOKS LIKE WHEAT'S BACK ON THE MENU: EVOLUTION OF PATHOGENICITY

'Disease is of no major concern to the host insofar as its ultimate survival is concerned. Both host and parasite had learned that the price of coexistence was less than the price of alternate superiority and inferiority. They had become, in a sense, the "odd couple" of the biological world.'

- R. R. Nelson (1978)

It is thought that *Z. tritici* diverged from *Septoria passerinii* around 68,500 years ago following specialisation of *S. passerinii* to a *Hordeum* host (Stukenbrock et al., 2007). *Z. tritici* then split from the wild population ~10,000 years ago (Stukenbrock et al., 2007), which is consistent with archaeological evidence demonstrating the domestication of its wheat host in the Fertile Crescent around the same time at the advent of modern agriculture (Salamini et al., 2002). Concurrent with this is phylogeographic localisation of the centre of origin for *Z. tritici* in the Middle East, with dispersal following the spread of wheat cultivation worldwide (Banke and McDonald, 2005). In this aspect, *Z. tritici* can be considered a domesticated disease.

Whilst the genetic diversity of wheat diminished in comparison to its progenitors under the constraints of agriculture, *Z. tritici* populations have expanded and accumulated greater genetic diversity than their wild relatives; this effect was apparent even when wild accessions were sampled from a broad geographic and host range (Stukenbrock et al., 2007). *Z. tritici* may be the sole recipient of this gene flow from wild populations – a possible mechanism for the gain of new virulence genes or pathogenicity factors. Gene flow between *Z. tritici* populations is such that they could in many cases be considered panmictic (Stukenbrock et al., 2007).

It seems clear that the development of great levels of gene flow and genetic diversity were key in the adaptation of *Z. tritici* to its wheat host. *Z. tritici* has high levels of genetic diversity which may be attributable in part to the legacy of serial introgressions of isolates from uncultivated grasses into the wheat-infecting population during domestication (Stukenbrock et al., 2007). *Z. tritici* has a large accessory genome of up to eight chromosomes; this may act as a cauldron for *de novo* gene evolution from non-coding DNA, and is enriched with pathogenesis-related genes (Badet et al., 2020). The high level of genetic redundancy in the *Z. tritici* genome allows for dispensability in the accessory genome, and functional redundancy in effectors could explain how *Z. tritici* populations are resilient to changes in host recognition (Badet et al., 2020). *Z. tritici* has also adapted a high rate of intron transposition, which may facilitate gene evolution (Torriani et al., 2011; Brunner et al., 2014). Highly plastic genomic regions containing high proportions of transposable elements may have developed to enhance the rapid evolution of virulence, resulting in highly polymorphic avirulence factors such as Avr3D1 (Meile et al., 2018b). An increase in specific transposable elements may have aided the pathogen in overcoming colonisation bottlenecks outside of its centre of origin as well as evolving fungicide resistance in North Africa (Oggenfuss et al., 2020).

#### 1.4. MANAGEMENT OF STB ON WHEAT

One of the most impactful consequences of its capacity for rapid adaptation is the resistance of *Z. tritici* to all unisite fungicides, primarily through modification or overexpression of their target sites (Omrane et al., 2017). Resistance to quinone outside inhibitors (Q<sub>o</sub>I) and azole fungicides was absent in 1992 isolates tested by Estep *et al.* (2015), but resistance to both fungicides appeared to be prevalent in the 2012 collection; the frequency of resistance alleles was highest at field sites with extensive fungicide use, highlighting the inefficacy of current management of this disease. Q<sub>o</sub>I resistance arose independently in several lineages through a single mutation to the mitochondrial

cytochrome b (cytb) protein. Multiple mutations to the nuclear *Cytochrome P450 Family 51 Subfamily A Member 1 (CYP51)* gene, conferring resistance to azole fungicides, are likely a consequence of diversifying selection and intragenic recombination among three phylogenetic clades of *Z. tritici* (Estep et al., 2015). DeMethylation Inhibitor (DMI) fungicide resistance is emerging in areas of intense wheat cultivation and isolates with reduced succinate dehydrogenase inhibitor (SDHI) sensitivity, as well as other resistances, have been reported at low frequencies since 2012 (FRAC, 2017; Rehfus et al., 2018). Perhaps most perturbing is that *Z. tritici* is capable of actively pumping out fungicides through overexpression of the *Major Facilitator Superfamily Transporter 1 (MFS1)* gene – a robust form of multidrug resistance that does not require adaptation to changes at individual active sites in the host (Omrane et al., 2017).

Even with an effective fungicide, a further challenge lies in the long latent period of *Z. tritici* after colonisation; fungicides are difficult to deploy effectively when the disease can only be detected after the destructive switch to necrotrophy. Coupled with restrictions in use due to the detrimental effects of many such chemicals on the environment, particularly within the EU (Hillocks, 2012), fungicides present an expensive and largely ineffective method for combating STB that may not be affordable for all afflicted countries. Resistance to the current chemistry is widespread, so new high-performance fungicides with multiple targets are needed for sustainable chemical control (Torriani et al., 2015). With 70% of wheat fungicides already targeted towards the management of *Z. tritici*, costing around €1 billion (Torriani et al., 2015), it is clear that new approaches are needed.

Genetic resistance in host plants is desirable as it can be effective at all developmental stages with little intervention from the farmer. The challenge lies in the identification of these genes and successful transfer into elite cultivars. Yet more imperative is the deployment of genetic resistance such that it is durable and broad-spectrum. Commercial cultivation of varieties with major-gene resistance can lead to rapid adaptation of the pathogen and breakdown of resistance in as little as five years, demonstrated by the case of the variety Gene, and this resistance can persist in the population even after use of the cultivar diminishes (Cowger et al., 2000). Releasing resistance genes as part of pyramids or stacks rather than singly reduces the likelihood that a pathogen will develop virulence. Even this method is unlikely to be effective if stacks consist of genes long exposed to agriculture; the development of resistance (*R*) gene stacks could be greatly facilitated by an increase in cloned resistance and avirulence genes as well as resistance from new and diverse germplasm.

## 1.5. MODELS FOR PLANT IMMUNE RESPONSES

‘The types of interaction between hosts and pathogens, particularly in relation to the durability of resistance, are so diverse that no single model can represent them.’

– Johnson (1984)

Reciprocal selection acts on hosts and parasites, resulting in the frequency of a gene in one species being dependent upon the fitness cost to the other species (Brown, 2015). More specifically, pathogens secrete molecules called effectors when they colonise a host (Figure 4). In turn, plant hosts have evolved resistance (*R*) genes, encoding immune receptors that recognise a subset of effectors encoded by avirulence genes (*Avrs*). This is known as the gene-for-gene (GFG) model (Flor, 1971). Defence responses are initiated when *Avr* molecules are detected by *R* proteins, which can limit pathogen proliferation in the host plant. Some interactions can better be described by the inverse GFG model, wherein pathogens evolve *Avrs* that bind host targets (Fenton et al., 2009). These host targets are known as effector-triggered susceptibility factors; an example is *Tsn1* which confers susceptibility in the presence of *ToxA* produced by necrotrophic pathogens such as *Parastagonospora nodorum* (Faris and Friesen, 2020).

*R* proteins can detect effectors through direct interaction (the “elicitor-receptor” model; Keen, 1990) or they can indirectly detect when effectors modify a host target (the “guard hypothesis”; Dangl and Jones, 2001). To prevent the pathogen from gaining an advantage upon effector binding, the host may also contain decoys that compete with operative targets and only exist to trigger host response upon interaction with corresponding *Avr* proteins (“decoy model”; van der Hoorn and Kamoun, 2008). Several models can be used to describe the course of these interactions.

In the zig-zag model of plant immunity (Jones and Dangl, 2006), microbial pathogens can be first recognised through pathogen-associated molecular patterns (PAMPs) by the host, resulting in PAMP-triggered immunity (PTI) or weak defence responses. PAMPs include conserved pathogen effectors as well as molecules essential to pathogen survival, such as chitin and flagellin. In response, pathogens can suppress PTI through secretion of effectors – molecules that interact directly or indirectly with the host to bring about disease. Many effectors are secreted by *Z. tritici* during the endophytic phase of growth within host leaf tissue; for example, *Z. tritici* upregulates the expression of *LysM* effectors that bind chitin to avoid detection by the plant (and therefore suppress PTI) during this phase (Marshall et al., 2011). Recognition of intracellular pathogen effectors by the plant

that would otherwise suppress defence responses during an incompatible interaction can lead to effector-triggered immunity (ETI), an accelerated PTI response that usually results in a hypersensitive cell death response (HR). These effectors are recognised by plant R proteins.

However, the zig-zag model falls short of encompassing the wide range of possible host immune responses and is most suited to describing interactions with intracellular, biotrophic pathogens. For example, responses to apoplastic pathogens do not usually result in HR; the necrotrophic growth phase of *Z. tritici* would likely be accelerated by this response (Stotz et al., 2014). Recognition of and response to apoplastic pathogens is more accurately described as effector-triggered defence (ETD); apoplastic pathogens are difficult to eradicate completely, thus *Z. tritici* can complete its life cycle through slow, symptomless growth even on a resistant host (Stotz et al., 2014). ETD in resistant hosts usually occurs at 10 dpi, when the pathogen would otherwise begin the switch from endophytic to necrotrophic growth. Perhaps to reduce the contribution of avirulent or fungicide-susceptible isolates to the gene pool, sexually-reproducing avirulent *Z. tritici* isolates switch to exclusive paternal parenthood which allows crosses between virulent and avirulent isolates to always result in virulent offspring (Kema et al., 2018).

Another nuance of these interactions is the distinction of seedling from adult plant resistance genes. Seedling resistance genes tend to be effective at all stages of development and confer major resistance, whilst adult plant resistance genes (APRs) typically manifest only in adult plants and have a quantitative effect (Ellis et al., 2014). Responses to the wheat rust diseases demonstrate the difference between these terms clearly, since seedling resistance results in HR while APRs lead to phenotypes such as 'slow rusting' which reduce the pathogen growth rate (Ellis et al., 2014). STB is also a disease of both the seedling and adult stages (Brown et al., 2015b).

French, Kim and Iyer-Pascuzzi (2016) propose an 'Invasion Model' to describe plant immunity as a surveillance system that is continually evolving mechanisms to detect pathogen infection. This model is more inclusive of responses to apoplastic and necrotrophic pathogens. Plants recognise invasion patterns (IP), including PAMPs, effectors and damage-associated molecular patterns (DAMPs). These IPs can then be recognised by IP-triggered receptors (IPTRs); in this way, PTI and ETI/ETD are assimilated into a continuum of immune responses. This model can also encompass quantitative disease resistance, which results in continuous distributions of resistance that do not fit neatly into other models (French et al., 2016). This may provide a more useful context for discussing the wheat-*Z. tritici* pathosystem.

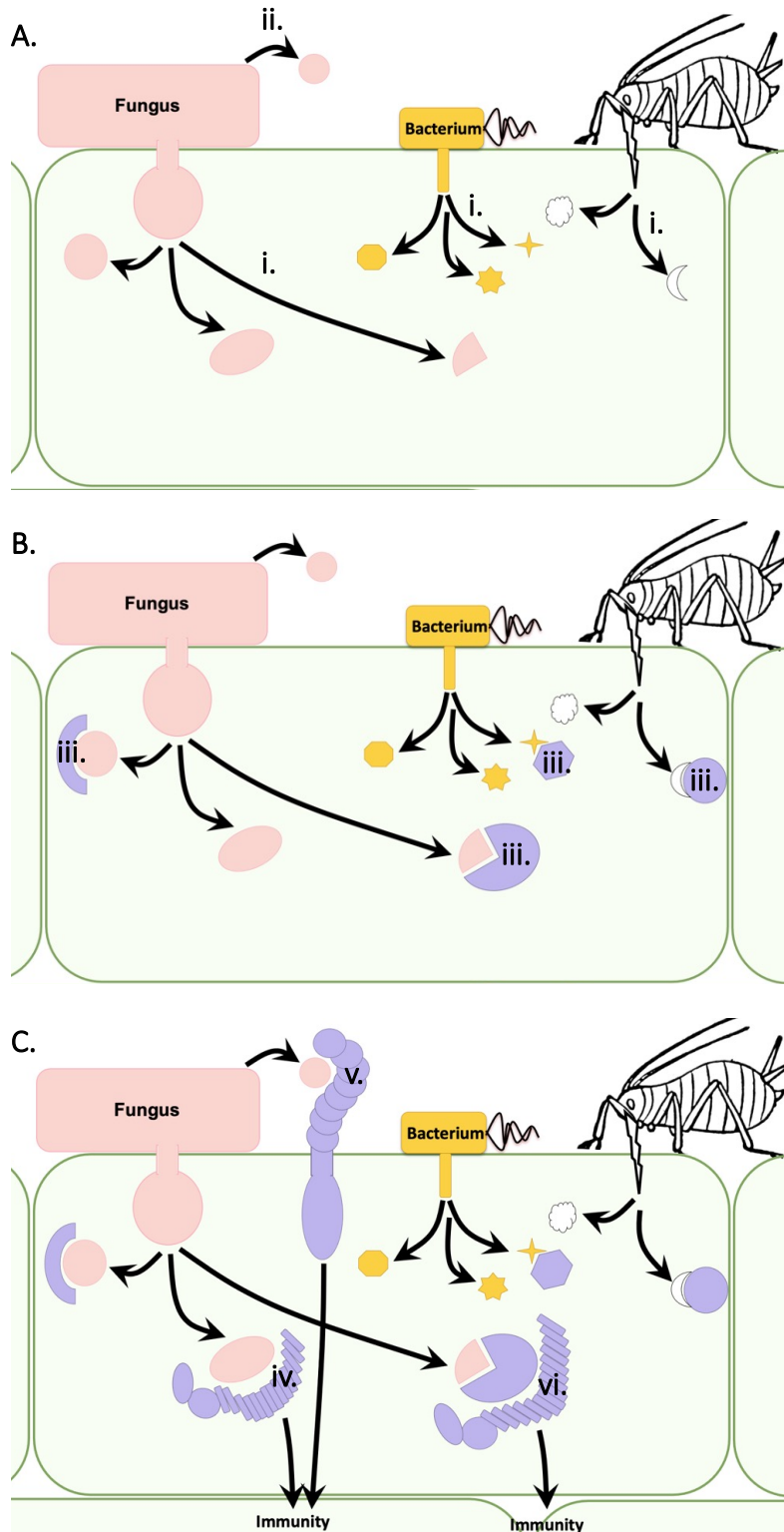


**Figure 4:** Molecular interactions between hosts and pathogens or pests. Pathogens and pests secrete effectors upon colonisation of the host, either into the intracellular (i) or intercellular/apoplastic (ii) space (A). These bind host targets (iii) to manipulate the environment and aid in proliferation (B). In response, the host can detect the presence of effectors and initiate defence responses (C). This may be through direct binding of intracellular immune receptors (iv) and membrane-associated receptors for the recognition of apoplastic effectors (v) or indirect binding, *i.e.* the guard hypothesis (vi). Figure adapted from presentation slides shared by Brande Wulff, based on figures from Dodds and Rathjen (2010).

## 1.6. THE DEATH OF GRASS: GENETIC CONTROL OF DAMAGE RESPONSES

There are still unanswered questions regarding the latent and necrotrophic phases of *Z. tritici*'s life cycle (Brennan et al., 2019), but the following model seems to explain the course of compatible interactions. The fungus does not appear to deplete host resources in during the latent phase (Keon et al., 2007); within 24 hours of spores making contact with the host plant, there is a rapid change in the transcriptional profile of *Z. tritici*, including upregulation of genes involved in metabolising the fungus' own lipids and fatty acids to support early colonisation (Rudd et al., 2015). However, there is evidence that *Z. tritici* may metabolise some nutrients in the apoplast during colonisation (Yang et al., 2013). Asymptomatic growth during the latent phase is achieved through the suppression of host defence responses at the transcription level (Yang et al., 2013). Once the fungus reaches a critical biomass and forms pre-pycnidia in the substomatal cavities, the switch to necrotrophy begins (Steinberg, 2015). In compatible interactions, it seems that the host detects *Z. tritici* effectors and triggers HR, a likely successful approach to defeating biotrophic pathogens which leads to the generation of reactive oxygen species (ROS) by the host (Brennan et al., 2019). Although *Z. tritici* is sensitive to ROS during the early stages of growth (Shetty et al., 2007), it has evolved to develop tolerance to the ROS during the necrotrophic phase through the production of several kinds of ROS-scavenging proteins (Yang et al., 2013). The breakdown of host cells due to HR, as well as limited cell wall degrading enzymes released by *Z. tritici* during the necrotrophic phase (Yang et al., 2013), serve to release nutrients into the apoplast that fuel the proliferation of the pathogen.

Kema *et al.* (1996b) suggested that both pycnidia and necrosis were capable of identifying a gene-for-gene interaction between resistance and virulence loci in *Z. tritici* and wheat, although they resulted in different clusters of cultivars and isolates suggesting that these two responses may be under different genetic control. Upon infection of *Z. tritici* isolates collected from durum wheat on bread wheat, Kema *et al.* (1996b) observed that small necrotic spots indicative of HR appeared. In the reverse situation, with bread wheat isolates inoculated onto durum wheat, large amounts of necrosis resulted along with little evidence of spore production. Histological studies showed that phenotypes with high necrosis and few pycnidia have low levels of colonisation, suggesting that this phenotype may imply avirulence (Kema et al., 1996b). The relationship between leaf necrosis and susceptibility is therefore not as straightforward as it may at first appear; the plant seems to be able to successfully restrict pathogen proliferation through HR in some cases. This could be because, as discussed above, *Z. tritici* is sensitive to ROS during the early stages of infection.

## 1.7. ALL THE SEPTORIA RESISTANCE IS A STAGE, AND ALL THE GENES AND QTLs MERELY PLAYERS

A great number of qualitative STB resistance genes have been mapped in wheat – 22 in all, distributed across 20 chromosomes. No *Stb* genes have yet been mapped to 5D. *Stb1* to *Stb18* as well as *StbWW* and *TmStb1* are described by Brown *et al.* (2015), whilst *Stb19* was mapped more recently (Yang *et al.*, 2018). In addition, 89 quantitative trait loci (QTLs) associated with resistance were mapped by 2015 (Brown *et al.*, 2015a). Many studies have been undertaken since, leading to the mapping of at least 31 additional QTLs for STB resistance (Kidane *et al.*, 2017; Vagndorf *et al.*, 2017; Yates *et al.*, 2019; Louriki *et al.*, 2021). Fine mapping of these genes as well as the identification of linked molecular markers is beneficial for advancing breeding programmes.

The realm of *Stb* gene cloning has recently begun to take off; it has been lagging behind gene cloning efforts in other wheat diseases (**Figure 5**). Brading *et al.* (2002) mapped a semi-dominant gene to the short arm of chromosome 3A conferring resistance to *Z. tritici* isolate IPO323 via a gene-for-gene relationship. Designated *Stb6*, it became the first *Stb* gene to be cloned and encodes a gene in the wall-associated receptor kinase (WAK) family, a subfamily within the receptor-like kinase (RLK) family in plants (Saintenac *et al.*, 2018). Susceptibility was found to be associated with non-synonymous mutations in the conserved region of the kinase domain and therefore may be induced by lack of kinase activity. *Stb6* is prevalent in wheat cultivars worldwide, which may have led to repeated selection by breeders despite the use of diverse germplasm (Brading *et al.*, 2002; Chartrain *et al.*, 2005c).

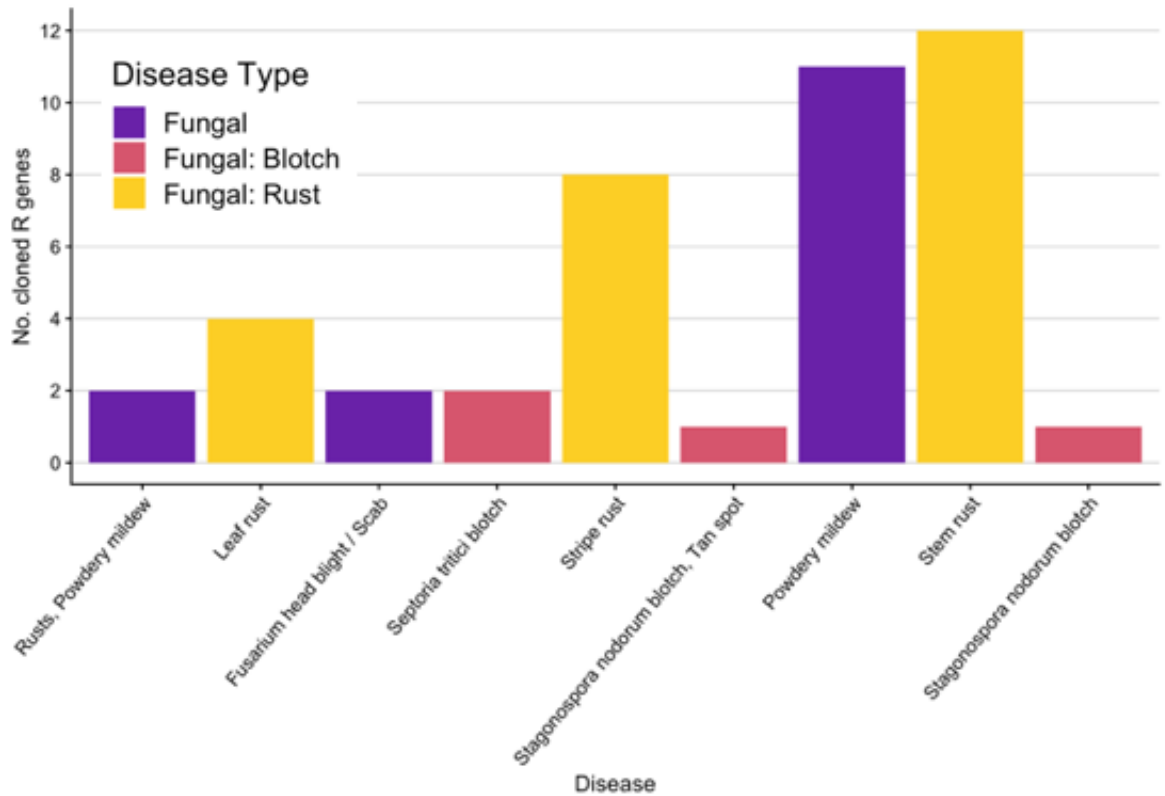


**Figure 5:** The number of cloned major genes for resistance to diseases of wheat, arranged in order of their impact on wheat yields (top = most detrimental impact on wheat yields). Yield impact data from Savary et al. (2019). Gene designation data from supplementary table of Hafeez et al. (2021), based on the Komugi gene database (<https://shigen.nig.ac.jp/wheat/komugi/>).

Mapped to chromosome 3D of the synthetic hexaploid wheat (SHW) line M3, *Stb16q* has demonstrated broad-spectrum resistance against a large number of *Z. tritici* isolates, as well as being expressed in both the adult and seedling stages (Ghaffary et al., 2012). The gene has recently been cloned by Saintenac et al. (2021), and found to encode a cysteine-rich receptor kinase (CRK).

Further cloned resistance genes will make valuable contributions to our understanding of how *Z. tritici* circumvents host resistance, as well as how this disease can be controlled.

## 1.8. THE ROLE OF RLKS IN PLANT IMMUNE RESPONSES

Although RLKs have ancient origins, the family expanded specifically in plants after their divergence from animals through tandem duplication and whole-genome duplication events (Shiu and Bleecker, 2003). These proteins consist of various subgroup-specific extracellular N-terminal domains, a transmembrane domain, and a kinase, typically a Serine/Threonine protein kinase (S/TPK) in plants, at the intracellular C-terminal end. Many of the extracellular domains of RLKs are mirrored by receptor-like proteins (RLPs), which often work together with RLKs during signalling (Jamieson et al.; Shiu and Bleecker, 2003). Three classes of RLKs that are involved in defence signalling in response to *Z. tritici* infection are described below.

### 1.1.1. Wall-associated kinases (WAKs)

WAKs contain a galacturonan-binding (GUB-WAK) domain. The *Arabidopsis thaliana* protein AtWAK1 recognises oligogalacturonides derived from cell wall pectins when they are broken down by pathogens and is involved in defence responses (Brutus et al., 2010). This is an example of race-non-specific resistance (the recognition of damage-associated molecular patterns). WAKs are also involved in several gene-for-gene interactions. One example is Stb6 and AvrStb6, described above. Rlm9 confers resistance to *Leptosphaeria maculans* strains expressing *AvrLm5-9* in oilseed rape; much like the Stb6-AvrStb6 interaction, the two proteins do not seem to interact directly (Larkan et al., 2020). The wheat WAK Snn1, on the other hand, does appear to interact directly with the SnTox1 effector secreted by *P. nodorum*, resulting in programmed cell death in the host and proliferation of the necrotroph (Liu et al., 2012; Shi et al., 2016). These three pathogens share similar lifestyles in that they primarily colonise the apoplast and have necrotrophic phases. However, in the case of Snn1, the WAK acts as a susceptibility factor that the pathogen uses to hijack host resistance pathways, whilst Stb6 and Rlm9 confer host resistance and may guard a host target. WAKs are reviewed in detail by Stephens et al. (2022).

### 1.1.2. Cysteine-rich receptor-like kinases (CRKs)

CRKs such as *Stb16q* have two extracellular domains of unknown function (DUF26) that contains conserved cysteine motifs (Vaattovaara et al., 2019). These proteins are involved in development and stress responses in rice and *Arabidopsis*, and have expanded in land

plants (Vaattovaara et al., 2019). DUF26 domains are structurally similar to fungal carbohydrate-binding lectins and may bind mannose; one of the DUF26 domains in *Stb16q* is similar to those in the GNK2 gene, which is known to bind mannose, lending more confidence to this theory (Saintenac et al., 2021).

### 1.1.3. Lectin receptor kinases (LecRKs)

Lectins are proteins that can selectively recognise and reversibly bind to glycans (Lannoo and Van Damme, 2014). LecRKs contain an N-terminal extracellular lectin domain. However, the nature of interactions between lectin domains in LecRKs and specific carbohydrates is not well understood (Lannoo and Van Damme, 2014). There are G-, C-, L- and LysM-type lectins; the latter domain type is commonly involved in interactions with fungi. LysM LecRKs recognise Glc-NAc moieties in fungal chitin as well as bacterial peptidoglycans, and are known to be involved in the initiation of defence responses (Buist et al., 2008). LysM effectors are produced by *Z. tritici* throughout the infection cycle to prevent the recognition of chitin (Yang et al., 2013).

From the few genes cloned so far, RLKs with carbohydrate recognition domains appear to be important for Septoria defence signalling. This could be indicative of the structure of other *Stb* genes. It will be exciting to further explore the diversity of Septoria resistance genes to better understand the mechanisms at work; if the guardee of *Stb6* could be identified, for example, this would be a huge step forward.

## 1.9. QUANTITATIVE AND QUALITATIVE RESISTANCE

The specific interactions between pathogen effectors and host receptors (resistance or *R* genes) during STB infection can be described as qualitative and GFG, as they are likely controlled by a single gene in both the host and the pathogen, as demonstrated for *Stb6* (Brading et al., 2002). It is also clear, however, that many QTLs contributing smaller but broad-spectrum quantitative effects are involved in resistance and may be more durable since they do not place strong selection pressures upon specific effectors in the pathogen (Brown et al., 2015b).

Major and quantitative genes affect host-pathogen interactions in different ways. Major genes reduce the initial amount of inoculum that can establish on the host, since, as described in the models above, this type of resistance operates quickly to prevent the

spread of pathogen infection (Van der Plank, 1963). Quantitative resistance can broadly be described as: ‘any resistance that is incomplete in an agricultural or horticultural situation’ (Cowger and Brown, 2019). It tends to be race non-specific and reduces the infection rate, for example by slowing lesion growth or spore production. Major gene resistance “helps to defeat itself”, since pathogens can often develop virulence quickly due to the strong selection pressure imposed (Van der Plank, 1963). Furthermore, the more popular a variety carrying a major-effect *R* gene is, the more virulent inoculum builds up during and between growing seasons and thus the more likely the gene is to be overcome. Typically, sources of major-gene resistance quickly dominate the pedigrees of popular varieties which aids in their breakdown (see Section 1.10). On top of this, the epistatic effect of major gene resistance reduces selection for quantitative resistance genes and results in them being eroded from the genepool (Van der Plank, 1963; Brown and Rant, 2013). The result is that major gene breakdown can lead to susceptibility greater than that of cultivars with no major *R* genes.

Despite the arguments above, research efforts focus primarily on major-effect resistance, which provides only short-term ‘froth’ on top of the more vital pool of quantitative resistance genes that are less easily overcome and provide more reliable outcomes for growers (Brown, 2021; **Figure 6**). Unfortunately, it is difficult to clone minor genes due to their small phenotypic effects; even major-gene cloning in Septoria is lagging behind other diseases of wheat (**Figure 5**), likely due to strong genotype-by-environment interactions that can confound mapping efforts.

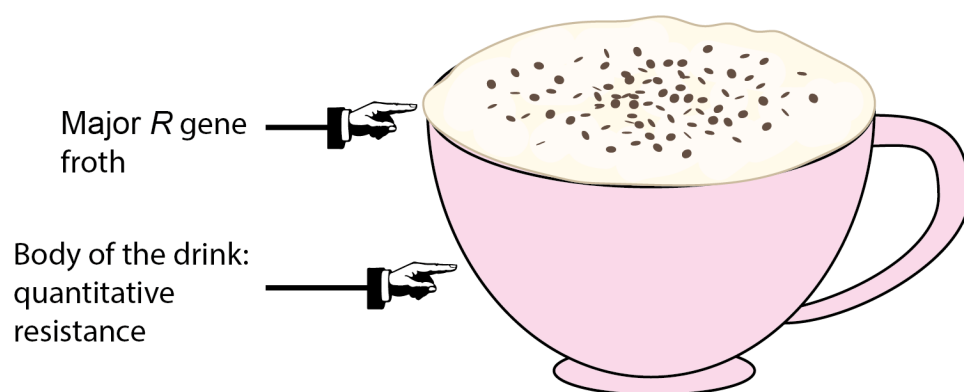


**Figure 6:** The Cappuccino Model of plant disease resistance: there is an attractive froth layer comprising major *R* genes, which floats atop the caffeinated body of the drink that does the majority of the work in plant immune responses – the quantitative resistance genes (Brown, 2021).

One problem is that major resistance genes can mask the effects of quantitative genes. This can lead to the Vertifolia effect, first observed in the potato late blight pathosystem, wherein quantitative resistance can be eroded due to reduced selection pressure caused by the presence of major *R* genes, pesticides or the absence of disease (Van der Plank, 1963; Brown and Rant, 2013). Major genes also provide yet another trait for breeders to keep track of during the complex process of selection. These issues could be overcome by truly treating major genes as the “froth” - by allowing conventional breeding to focus on agronomic traits of interest including quantitative disease resistance, followed by the engineering in of major genes in transgenic cassettes. This would allow the trend of incremental, yet highly impactful, increases in quantitative resistance breeding to continue unimpeded. The aim cannot be to remove the need for such practices, but perhaps to encourage growers to opt for wheat cultivars with extra “froth” rather than applying large quantities of fungicides, with strong background resistance firmly established as an insurance against extreme losses. Much like how a firm layer of froth in a cappuccino can prevent the body of the drink from spilling, the reduction in initial inoculum by major *R* genes can prolong the life and efficacy of both minor genes and fungicides. The best-case scenario would allow for synergy between these mechanisms of disease control.

## 1.10. THE RISE AND FALL OF MAJOR GENE EMPIRES

*Z. tritici* has been shown to adapt resistance to cultivars carrying major resistance genes very rapidly – an example of the boom-and-bust cycle of breeding for major resistance genes (**Figure 7**). This is illustrated by the following three cases.

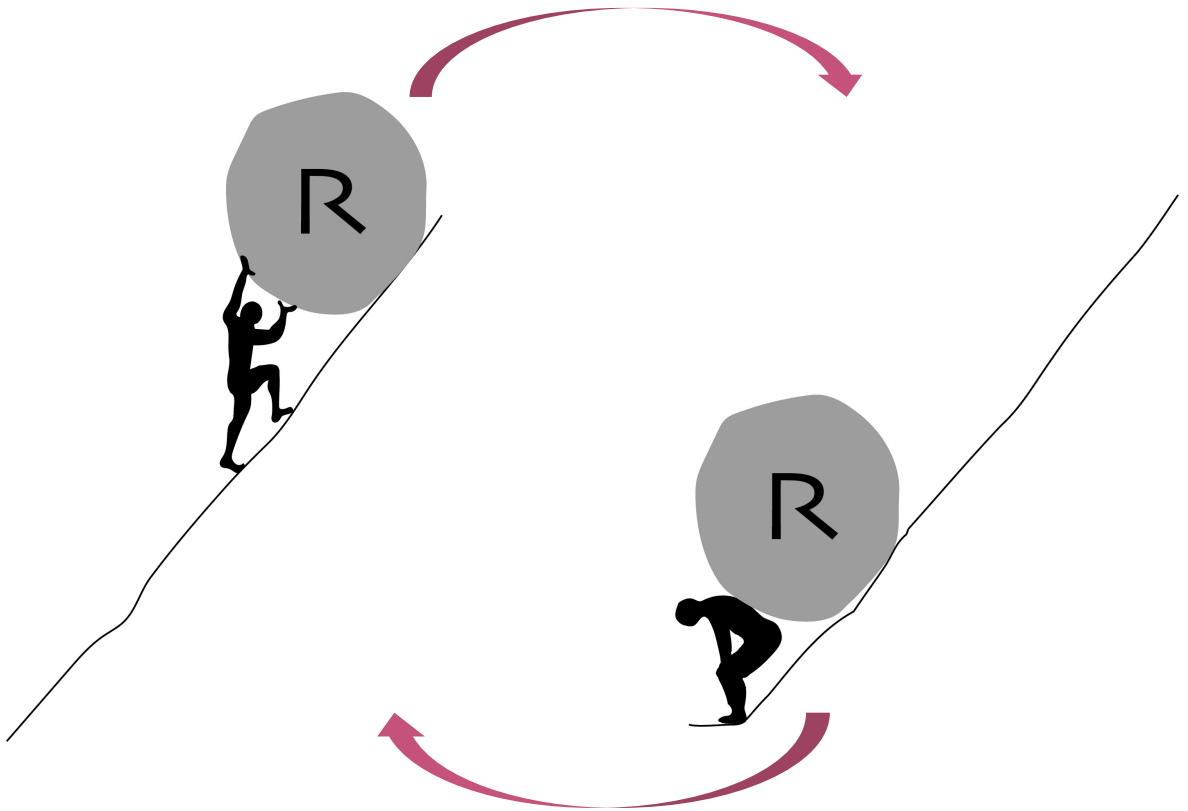


**Figure 7:** Sisyphus engaged in the seemingly ceaseless boom-and-bust cycle as it pertains to disease resistance genes. Research and breeding must identify and deploy new sources of resistance at great length and expense, which become widespread (the boom) only for the resistance to be quickly broken down by the pathogen due to deployment strategies that maximise pathogen evolutionary potential (the bust).

When the wheat cultivar Gene was commercially released in 1992, it had almost complete resistance to STB, likely due to the presence of the gene *Stb4* (Mundt et al., 1995; Cowger et al., 2000). A mere three years later, the resistance was being overcome by *Z. tritici* in Oregon, and virulence appeared to be fixed by 1997 despite a decline in cultivation of Gene (Cowger et al., 2000). This case was an early example of the ability of *Z. tritici* populations to overcome qualitative resistance rapidly.

*Stb16q* has been tested against a large number of *Z. tritici* isolates and shows strong resistance to all of them, as well as being expressed in both the adult and seedling stages (Ghaffary et al., 2012). The French cultivar Cellule was once of many to be subsequently

released carrying *Stb16q*, and became the third more frequently grown cultivar in France (Orellana-Torrejon et al., 2022). Unfortunately, STB symptoms on Cellule began to be observed in 2015 in France and in 2019 in Irish field populations (Kildea et al., 2020). This heralded the breakdown of *Stb16q* resistance and a reduction in the use of associated cultivars (Orellana-Torrejon et al., 2022) – the bust. Since it has emerged recently, it may not be too late to reduce *Stb16q* virulence in field populations of *Z. tritici* by restricting the deployment of cultivars carrying the gene to within mixtures; this could also help to evade the risk of superpathogen emergence (Orellana-Torrejon et al., 2022).

The UK wheat cultivar Cougar had notable STB resistance (rating of 7), leading to its addition to the UK recommended list in 2013. However, in 2015, moderate levels of disease were observed on this cultivar – the resistance source in Cougar and derived cultivars had been broken down (<https://ahdb.org.uk/news/septoria-tritici-disease-resistance-in-winter-wheat>). An AHDB investigation found that field isolates had broken down Cougar resistance exclusively. Subsequently, STB outbreaks in Ireland in 2020 were found to be associated with Cougar pedigree (Kildea et al., 2021). As the Cougar virulence continues to spread, further increasing durable resistance in current wheat varieties is a high priority.

### 1.11. ACHIEVING DURABLE FIELD RESISTANCE TO *Z. TRITICI*

Resistance can be defined as durable if it maintains its efficacy through prolonged and widespread use in an environment conducive to disease (Johnson, 1984). Qualitative resistance to *Z. tritici* is under risk of collapse through widespread use (see previous section). Given the huge quantities of time and resources required to develop resistant crop varieties, increasing durability is vital.

Agroecosystems have high host density and uniformity in plant architecture which form a dense canopy in which pathogens such as *Z. tritici* often thrive. Multiple *Z. tritici* genotypes can co-infect within single lesions; Linde, Zhan and McDonald (2002) found two to four *Z. tritici* genotypes of both mating types in four of five lesions analysed. The proximity of different genotypes, coupled with regular sexual reproduction, are a few factors enabling *Z. tritici* to evolve instantaneously through both horizontal and vertical gene transfer. Since even avirulent *Z. tritici* can complete their life cycle, populations can accumulate virulence sequentially rather than requiring simultaneous, independent

mutations. This drastically increases the probability of developing virulence to multi-*R*-gene-stacks (Mundt, 2018).

Closely-packed vegetation only compounds this issue, allowing rain splash to accelerate disease spread and permit panmixis. Cultivar mixtures have demonstrated benefits for yield stability and pathogen control (Gigot et al., 2013). Mixtures heterogeneous for plant height have shown a significant reduction in the area under the disease progress curve in comparison to pure stands; Vidal *et al.* (2017) suggested sensitivity of *Z. tritici* spread to canopy density and leaf wetness duration, both of which were lower in the stand heterogeneous for height. Gigot *et al.* (2013) found that a 1:3 susceptible:resistant wheat variety mixture resulted in reductions in disease impact of over 40% compared to the pure susceptible stand. The efficacy of resistant and susceptible cultivar mixtures could be explained by an increase in the frequency of avirulence alleles when sexual reproduction occurs between virulent and avirulent pathogen strains. This was observed in isolates under selection for fungicide and host gene resistance, due to exclusive paternal parenthood of avirulent strains (Kema et al., 2018). A shift in focus towards increasing the proportion of avirulence genes in the population, rather than outright elimination of the pathogen and creation of strong selection pressures, could yield more durable resistance. However, methods such as cultivar mixtures are not always appropriate for developed countries where large-scale agriculture requires monocultures.

Strong selection pressure from static, monoculture crop fields enhances the efficiency of directional selection to overcome host resistance. A dynamic diversity approach to disease management (McDonald, 2014) would involve strategic and frequent changes to the resistance repertoire present in the field at any one time, disrupting such selection in the pathogen (see Section 1.13).

Biological control could soon be a viable alternative to fungicide application, which is becoming ever less sustainable and effective. A study of bacteria isolated from Irish cereal fields found that the bacterium *Bacillus megaterium* has potential as a biological control for STB. The bacterium was able to retard *Septoria* growth by up to 80% in small-scale field trials on adult wheat plants over two growth seasons (Kildea et al., 2008). It would be relatively straightforward to apply mixtures of bacteria providing biological control to fields cycled according to dynamic diversity for durable protection.

## 1.12. EFFECTORS INVOLVED IN DEFENCE RESPONSES TO *Z. TRITICI*

*Z. tritici* effectors involved in a range of different interactions with wheat have been cloned and shed light on the complex ways in which these two organisms interact. Once both the *R* and *Avr* components of gene-for-gene interactions are cloned, it is possible to understand these interactions in much more detail, as demonstrated by some of the examples below.

A lysin domain effector, *Zt3LysM*, has been shown to bind chitin to suppress chitin-triggered immunity at the early stages of host colonisation (Marshall et al., 2011). The effector is upregulated during the asymptomatic stage of infection, and deletion mutants are unable to form lesions or pycnidia, likely due to the upregulation of host defence genes (Marshall et al., 2011).

*AvrStb6*, the pathogen effector corresponding to *Stb6*, has been cloned through a combined QTL-mapping and genome-wide association study (GWAS) approach and map-based cloning, respectively (Zhong et al., 2017; Kema et al., 2018). Yeast two-hybrid experiments did not show direct binding between *AvrStb6* and *Stb6*, which could mean that the assay attempted was not suitable as other factors are required for the interaction or possibly that *Stb6* encodes a guard for the target of *AvrStb6* (Saintenac et al., 2018). *AvrStb6* was present in all 142 *Z. tritici* accessions from three continents sampled by Brunner and McDonald (2018), with evidence of diversifying selection to escape host recognition. Clearly, *Stb6* and *AvrStb6* have long been coevolving, and further sets of host receptors and pathogen effectors, perhaps less widely adapted to by *Z. tritici*, must be cloned in order for this interaction to be fully understood as well as championed in the field.

The *Avr3D1* effector is specifically recognised by wheat hosts carrying the gene *Stb7* and is an example of a quantitative interaction wherein a defence response is elicited but the pathogen is still able to form lesions (Meile et al., 2018a). This demonstrates the fact that quantitative resistance genes can also have a gene-for-gene relationship with pathogen effectors.

*Z. tritici* also produces effectors to quell competition from other microorganisms and protect its niche. *Zt6*, a ribonuclease effector, has been demonstrated to be toxic to bacteria, yeasts and filamentous fungi, as well as causing a cell death response in wheat (Kettles et al., 2018).

### 1.13. COULD AN ATLAS UPHOLD *R* GENE DURABILITY AND STEWARDSHIP?

‘Go back young man and gather up your weary and defeated resistance genes of the past, take your currently successful genes, find some new ones if you can and build yourself a genetic pyramid.’

R. R. Nelson (1978)

Dynamic diversity could form part of a breeding and deployment strategy to maximise resistance durability (McDonald, 2014; **Figure 8**). With greater knowledge of the effector complement of pathogens, regional monitoring of pathogen populations could be used to track their effector complement and produce *R* gene combinations (stacks) that would provide durable resistance. This would prioritise *R* genes that are broad-spectrum. These genes could then be mobilised into wheat.

The process of combining resistance genes into an elite wheat background with minimal linkage disequilibrium (LD) can be time consuming – combining 12 genes for resistance to three diseases would require a minimum of 19 generations (Hafeez et al., 2021). This would take around four years if speed breeding were employed in a spring wheat background, and if the sources of resistance are hexaploid wheats. Combining *R* genes from wild species would take considerably longer. Another challenge is that the elite background will begin to lag in terms of yield within a few years, and the process of retaining many *R* genes that are genetically separated in new backgrounds would be difficult to manage. An alternative approach is to clone *R* genes and generate multi-*R*-gene stacks through DNA engineering and transformation. This approach has been demonstrated recently with a five-transgene stem rust *R*-gene stack which has been deployed in wheat and confers high levels of resistance in the field (Luo et al., 2021). It could one day be possible to produce such stacks for STB resistance if more *R* genes are cloned for resistance the disease. Resistance gene pyramids should, however, be treated as a ‘foam’ atop a strong ‘coffee’ base of minor genes, QTLs and adult plant resistance (APR) genes (see Section 1.9); for the cereal rusts, most published examples of durable pyramids indicate an association between durability and combining incompletely expressed APR with other genes (as reviewed by Mundt, 2018). This is even more important in stacks targeting *Z. tritici*, which frequently sexually reproduces (McDonald and Mundt, 2016). An advantage of stacking, especially through transgenic cassettes, is that it would not

disrupt the gradual process of breeding for increased background resistance to STB that has been successful over the decades (Brown, 2021).

Once genes are introduced into wheat cultivars, they can be deployed in monoculture, with a single *R* gene; as multilines, where plants are isogenic for different *R* genes; or as a monoculture of plants containing multi-*R* gene stacks. In the case of Septoria, a monoculture should best be treated as a last resort due to its capacity to evolve virulence rapidly. Rotating the *R* genes present within fields could help to slow this process, but the strategic rotation of multilines or multi-*R* gene stacks would be yet more effective (McDonald, 2014; Rimbaud et al., 2018). The method is effective because progress made by pathogens towards virulence within one season becomes a fitness disadvantage in the next when different host genotypes are introduced (Rimbaud et al., 2018). It is unlikely that gene or cultivar deployment could be coordinated across regions, leading to mosaics in the landscape. Mosaics can be effective in slowing the evolution of pathogen virulence (Djidjou-Demasse et al., 2017), but care must be taken not to allow the occurrence of green bridges between growing seasons – especially in the case of STB, which overwinters successfully on stubble and marginal hosts.

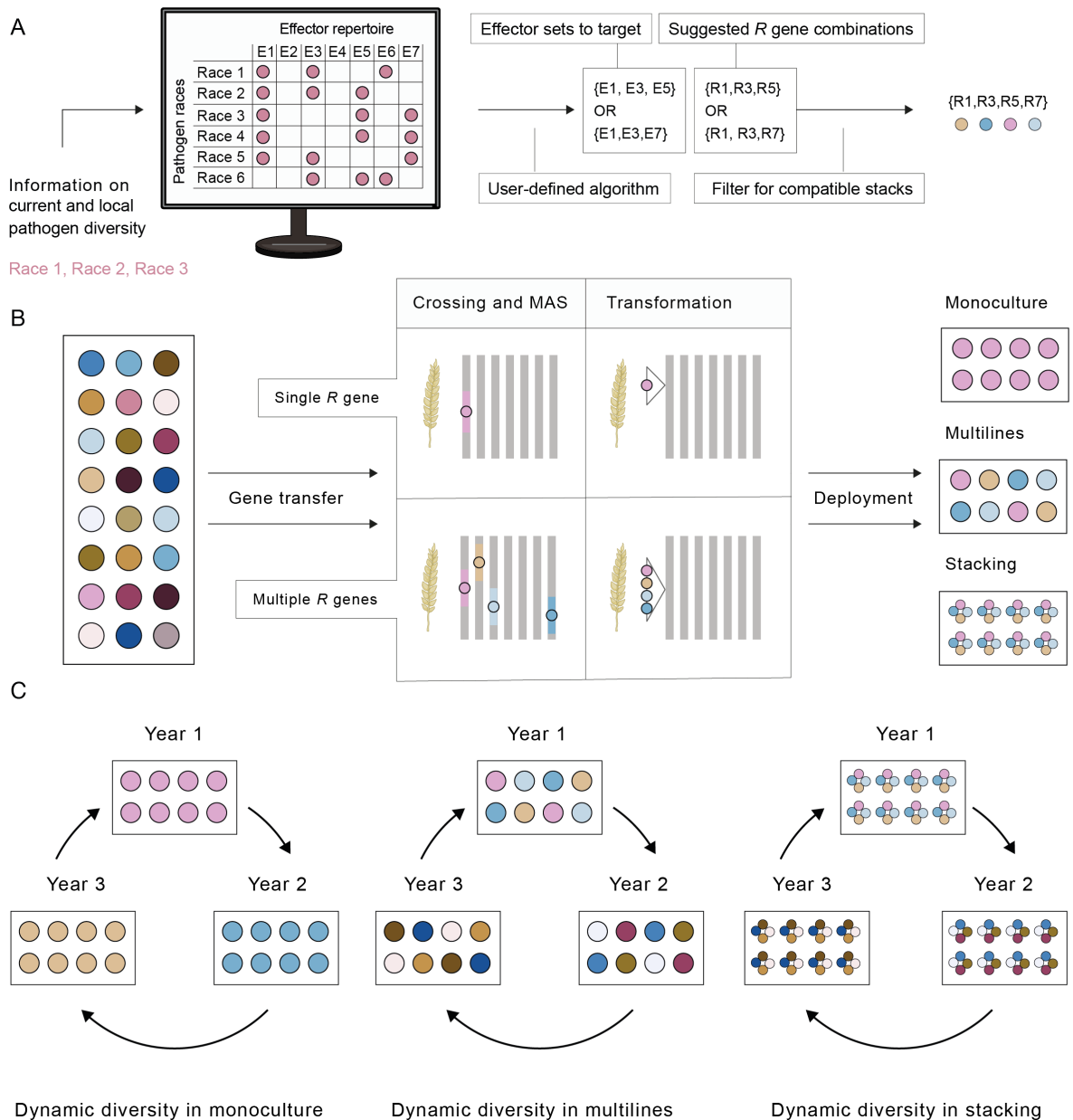


**Figure 8:** Combining pathogen diversity data and *R* genes to build durable stacks and deploy them effectively. Pathogen populations in a region could be analysed for their effector complement and compatible *R* genes selected that recognise the most effectors (**A**). *R* genes can then be mobilised into wheat through crossing and marker-assisted selection (MAS) or by transformation (**B**). In the case of multi-*R* gene stacks, transformation as a cassette has the advantage that *R* genes would not become genetically separated. This would be beneficial for tracking stacks in breeding programmes. Cultivars containing these stacks can then be deployed in several ways: in a monoculture, as multilines (where plants differ only in the *R* gene stack they contain) or as multi-*R* gene stacks. The cultivars can then be rotated through years or growing seasons to continually change the *R* gene complement exposed to pathogen evolution (dynamic diversity; **C**). Figure reproduced from Hafeez et al. (2021).



**Figure 9:** Atlas supporting wheat breeding. Wheat spike illustration adapted from Tobin Florio.

In summary, the ultimate breeder's tool could take the form of a 'wheat resistance gene atlas' – a matrix of pathogen *Avrs* and the *R* genes required to combat them (Hafeez et al., 2021). The pathotypes present in the environment could be evaluated each season, allowing breeders to choose varieties that provide the maximum protection whilst avoiding situations where lone effective *R* genes are left vulnerable to being overcome in the field (calculated by an algorithm). This responsiveness to new pathogen threats, combined with the development *R* gene stacks could allow durable, dynamic resistance to be achieved. If non-host resistance could also be incorporated, wheat may one day become a non-host for its major pathogens entirely.

The challenge for STB resistance is the lack of not only cloned but effective major effect or GFG resistance genes. One solution could be to study wild species and landraces for diverse sources of resistance that have not yet been exposed to modern field populations of *Z. tritici*. A key part of the strategy above is gene stewardship – the careful and responsible management of *R* genes to ensure that they remain effective during prolonged use (Hafeez et al., 2021). The first step in managing the distribution of *Stb* genes would be to clone them, create perfect markers and track their prevalence in global wheat germplasm. New sources of resistance will hopefully be cloned from wheat relatives and landraces, the release of which could be managed through patents or agreements with breeders. Perhaps if *Stb* genes are better managed and deployed such that virulent *Z. tritici* mutants are less likely to arise, they would last much longer than a scant few years.

#### 1.14. GENETIC DIVERSITY IN WHEAT'S BACK CATALOGUE

'In the great laboratory of Asia, Europe, and Africa, unguided barley breeding has been going on for thousands of years. Types without number have arisen over an enormous area. The better ones have survived. Many of the surviving types are old. Spikes from Egyptian ruins can often be matched with ones still growing in the basins along the Nile. The Egypt of the Pyramids, however, is probably recent in the history of barley. In the hinterlands of Asia there were probably barley fields when man was young. The progenies of these fields with all their surviving variations constitute the world's priceless reservoir of germplasm. It has waited through long centuries. Unfortunately, from the breeder's standpoint, it is now being imperilled. When new barleys replace those grown by the farmers of Ethiopia or Tibet, the world will have lost something irreplaceable.'

H. V. Harlan and M. L. Martini (1936)

The words above can easily be applied to the history of wheat breeding. The grass family, to which wheat belongs, is estimated to have originated around 77 million years ago (mya). The subfamily Pooideae, comprising oats, barley and wheat, diverged from rice (Eriocaulaceae) around 46 mya; from here, the Triticeae tribe, including barley and wheat, diverged from oats approximately 25 mya, with barley and wheat finally diverging around 13 mya (Gaut, 2002). Having arisen from ancient hybridisations between three diploid species, modern bread wheat (*Triticum aestivum*, AABBDD) has assimilated a vast amount of information across its 42 chromosomes (**Figure 10**). *Triticum urartu* (AA) hybridised with an unknown close relative of *Aegilops speltoides* (BB) to form tetraploid emmer wheat (*Triticum turgidum*) a few hundred thousand years ago in the Fertile Crescent (Marcussen et al., 2014; **Figure 10.1**). The cultivation of tetraploid wheats brought them into close contact with *Aegilops tauschii*, the D-genome donor of wheat and itself a product of hybrid speciation between the A and B genome donors ~5.5 mya (Marcussen et al., 2014; Singh et al., 2019). Rare hybridisation events between these species resulted in the formation of hexaploid wheat around 0.23-0.43 mya based upon genetic evidence, or possibly much later (around 10,000 years ago) according to fossil evidence (Marcussen et al., 2014; **Figure 10.2**).

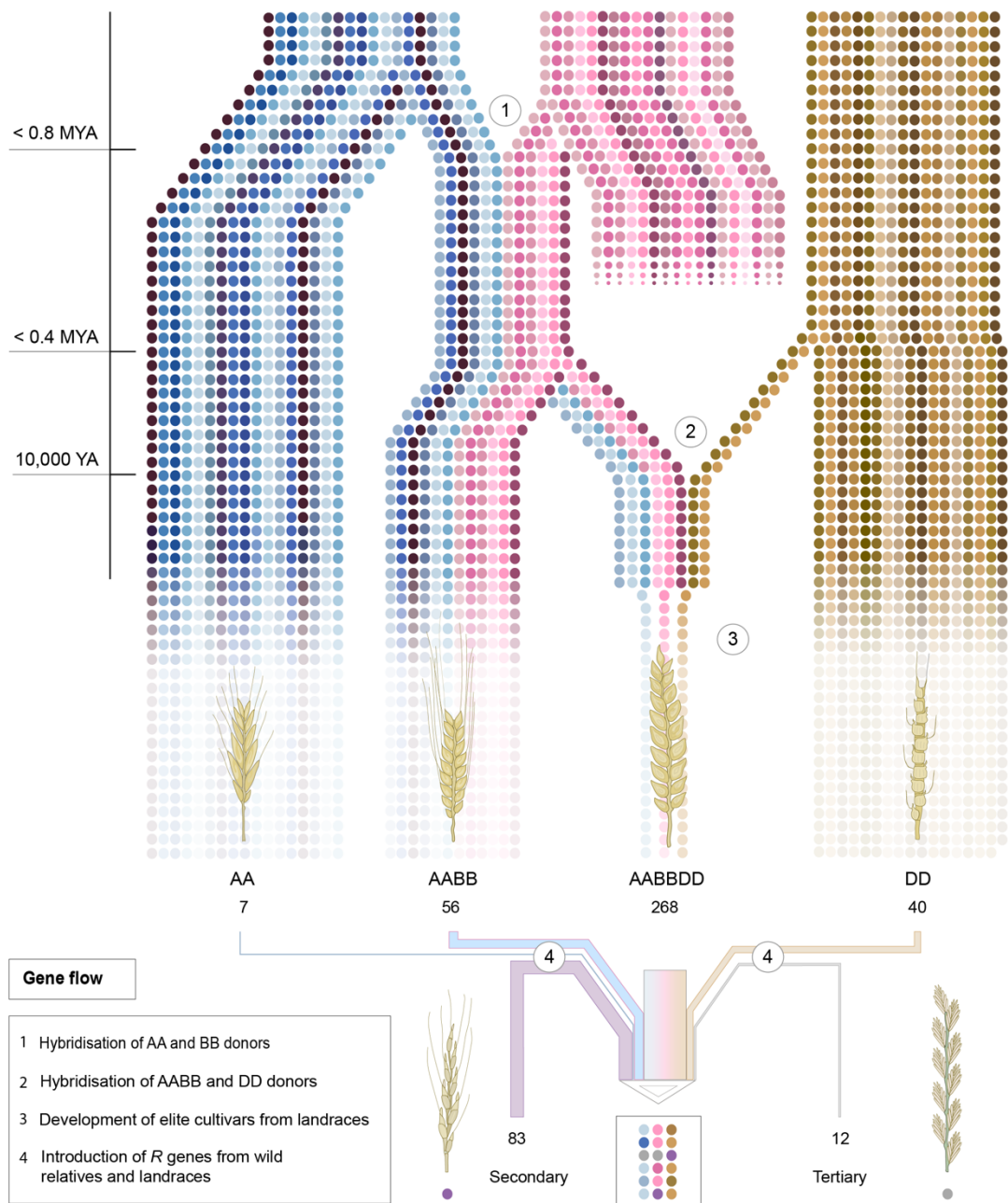


**Figure 10:** Hybridisations, bottlenecks and inter-species crosses have influenced the genetic diversity of wheat during its speciation and domestication. 0.8 mya, *Triticum urartu* (AA) hybridised with a close relative of *Aegilops speltoides* (BB) to form allotetraploid emmer wheat, *Triticum turgidum* ssp. *dicoccoides* (AABB) (10.1). Hybridisation of tetraploid wheats and *Aegilops tauschii* resulted in the formation of hexaploid wheat 0.4 mya to 10,000 years ago (10.2). The thickness of coloured dot columns is proportionate to the gene flow from progenitor populations estimated by Zhou et al. (2020). Wheat breeding also introduced a genetic bottle neck (10.3). Over the past 100 years, the known native wheat *R* gene pool of 268 genes has been enriched with 198 exogenous *R* genes by inter-species crosses with the primary, secondary (e.g. *Ae. sharonensis*) and tertiary (e.g. *Thinopyrum elongatum*) gene pools (10.4). The secondary gene pool defined in this figure excludes *Ae. tauschii*. Figure reproduced from Hafeez et al. (2021).

The two hybridisation events that formed hexaploid bread wheat introduced genetic bottlenecks since only a subset of the genetic diversity present in the wild populations became part of the tetraploid and hexaploid wheat gene pools. 57% of wild emmer

diversity was introgressed into bread wheat cultivars due to historic gene flow from multiple tetraploid taxa, but only 14% of the diversity in *Ae. tauschii* spp. *strangulata* was captured (Zhou et al., 2020). Researchers and breeders therefore continue to come back to progenitor species as well as landraces to recapture this genetic diversity for wheat improvement (**Figure 10.4**). Indeed, more than half of the *R* genes cloned in wheat have been contributed by species outside of bread and durum wheat (Hafeez et al., 2021).

Human selection has caused *Triticum* species, and indeed many cereal crops, to converge in their complement of domestication-related genes (Zhou et al., 2020). The rigours of human selection continued over the centuries and led to landraces (see Section 3.1) being developed into more modern, high-yielding cultivars – with some genetic diversity lost along the way (Wingen et al., 2014; Winfield et al., 2018; **Figure 10.3**). A key step in this process was the Green Revolution in the 1960s which involved the rapid development of wheat varieties that had beneficial traits, most importantly dwarf cultivars that did not lodge and which had increased yield, amenability to fertilisation and good resistance to wheat rust diseases (Borlaug, 1968). They were also developed to be successful in a broad range of environments, so that they could be deployed widely in the developing world. These cultivars were first grown in Mexico, followed by Asia and China, leading to a decline in the proportion of hungry people worldwide from 60% in 1960 to 17% in 2000 (Borlaug, 2007). CIMMYT continues to carry out this important work. To develop cultivars with broad-spectrum and durable resistance to diseases, amongst other key traits, CIMMYT heavily utilises the genetic diversity present in wild grasses and landraces of wheat (Singh et al., 2021; **Figure 10.4**).

The discovery that *Aegilops tauschii* (formerly *Triticum tauschii* or commonly goatgrass) was the D-genome progenitor of wheat in the 1940s led to a flurry of scientific interest in this genus and their genetic contributions to wheat polyploids (McFadden and Sears, 1947). This species is important with respect to several wheat diseases due to high rates of resistance, and STB is no exception. Having donated the D-genome chromosomes of wheat, this species, along with other wheat genome donors, may present sources of resistance that are more readily accessible for wheat breeding, with the added benefit of a smaller genome size compared to bread wheat. *Ae. tauschii* is discussed in detail in Section 0.

Wheat landraces are also a valuable resource for finding resistances that have been lost relatively recently on the road to developing elite cultivars, where the emphasis has been placed upon traits such as yield and short stature. This has been demonstrated by Kidane *et al.* (2017), who used a diversity panel of 293 Ethiopian durum wheat landraces and 25

durum wheat improved varieties, genotyped with >16,000 genome-wide polymorphic markers, to identify four putative novel STB resistance loci through a genome-wide association approach. Wheat landraces are discussed in detail in Section 3.1, particularly the Watkins collection of 826 pre-Green Revolution, tall wheat landraces collected from markets in 32 countries across Asia, Europe and Africa by A. E. Watkins in the 1930s.

Combined with high-quality reference genomes for wheat (International Wheat Genome Sequencing Consortium (IWGSC) et al., 2018; Walkowiak et al., 2020) and wild relatives such as *Ae. tauschii* (Luo et al., 2017), wild emmer (*Triticum turgidum* ssp. *dicoccoides*; Avni et al., 2017) and *Triticum urartu* (Ling et al., 2018), it is an exciting time to apply new approaches to cloning resistance genes in both old and new wheat, as well as its relatives.

### 1.15. METHODS FOR THE RAPID CLONING OF RESISTANCE GENES

There are numerous challenges involved in cloning *R* genes in wheat. Whilst studies on wild species may be hindered by poor agronomy (such as hard glumes that hinder seed harvesting and other unfavourable traits in *Ae. tauschii*, for example) cloning genes from bread wheat is made complex by its large genome size and difficulty of assembly, largely due to repetitive DNA as well as areas of suppressed recombination that hinder genetic mapping.

Complexity-reduction sequencing can ameliorate the problem by reducing sequencing costs as well as the difficulty of assembly and analysis of the data. Exome captures can reduce the amount of sequence dramatically by only including the gene portion of the genome, especially when a specific gene family is targeted, e.g. nucleotide-binding leucine-rich repeat receptors (NLRs) (Jupe et al., 2013; Steuernagel et al., 2016). The RLP and RLK gene families in plants are involved in extracellular recognition of pathogens; it is likely that many STB *R* genes encode RLKs, as is the case for *Stb6* and *Stb16q* (Saintenac et al., 2018; Saintenac et al., 2021). The implementation of RLK exome captures opens the door for cloning resistance genes involved in the extracellular recognition of a broad array of pathogens, from *Z. tritici* on wheat to phoma canker (*Leptosphaeria maculans*) on oilseed rape. An 'RLP/KSeq' pipeline for mapping RLPs and RLKs has been developed for *Solanum* species (Lin et al., 2020) and similar efforts have been ongoing in wheat (Saintenac et al. in Feechan et al., 2019). Increasing the number of cloned STB genes will inform strategies such as exome captures.

Another method for complexity reduction that does not require *a priori* knowledge of gene structure, and is therefore unbiased, is ‘MutChromSeq’ (Sánchez-Martín et al., 2016). In this method, mutant populations are generated, followed by chromosome flow sorting. The chromosome that the gene of interest has been mapped to can then be sequenced specifically – resulting in a 21-fold reduction in complexity of the hexaploid wheat genome, or a 7-fold reduction in diploids such as *Ae. tauschii*. By comparing loss-of-resistance mutants with the wildtype chromosome, causal resistance genes can be identified – although the large amount of data generated may be cumbersome to handle.

All of these methods have and will continue to increase the pace of resistance gene cloning (Figure 11).

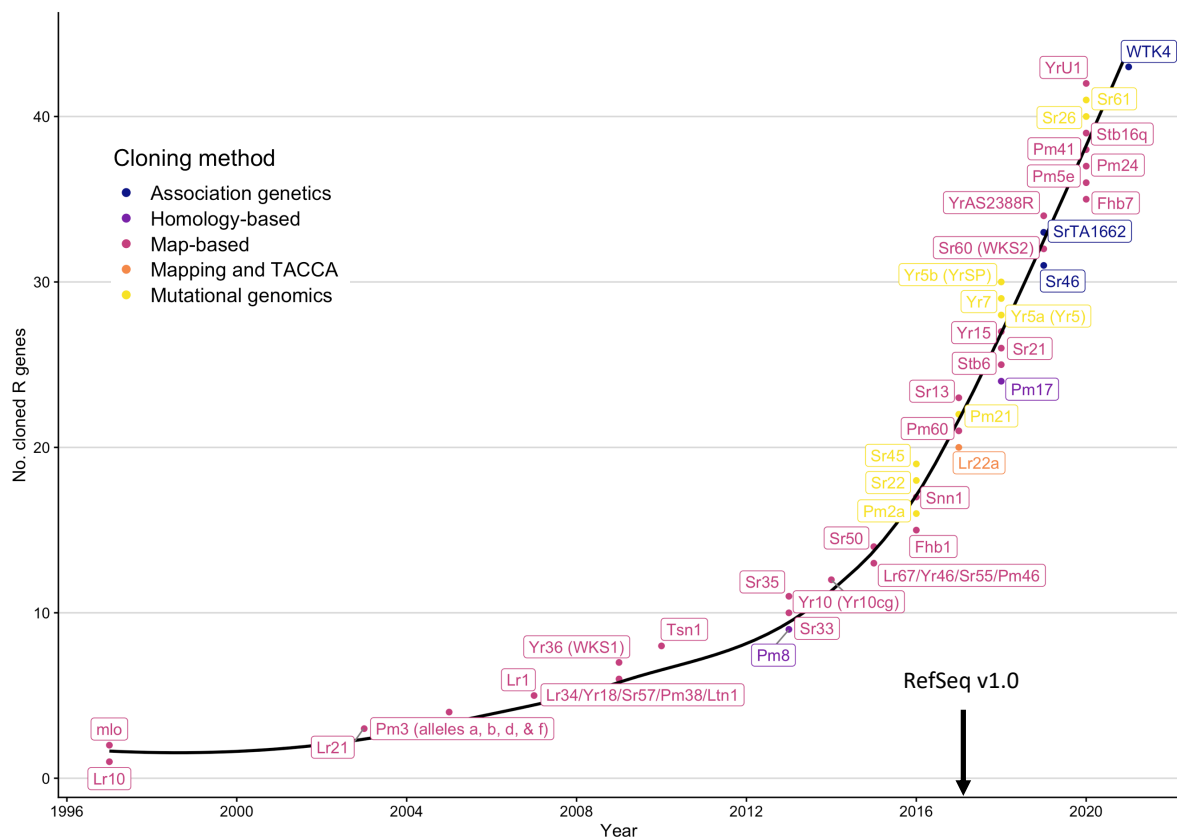


**Figure 11:** The exponential growth in the number of cloned *R* genes from 1997 to 2021. Cloning method is coded by colour. The increase in the number of methods available for gene cloning, such as mutational genomics and association genetics, coincides with a rapid increase in the number of cloned genes. TACCA = targeted chromosome-based cloning via long-range assembly (Thind et al., 2017). The publishing of the wheat Chinese Spring reference genome (RefSeq v1.0) in 2017 is indicated. Figure based on Keller et al. (2018).

## 1.16. GENOME-WIDE ASSOCIATION STUDIES FOR CLONING RESISTANCE GENES

The tedious business of generating loss-of-resistance mutant populations or biparental mapping populations remains a central component of many gene cloning efforts. This limits researchers to cloning one gene at a time, since each gene often requires its own lab-generated population structure (**Figure 12**). Mutational genomics is also challenging when working with diploids such as *Ae. tauschii*, as surplus mutations that deteriorate fitness can have a large effect due to the lack of genetic redundancy.

An alternative approach is to harness naturally-occurring population structures, by genotyping diversity panels: ‘collections of individual accessions representing the genetic and phenotypic diversity of a species’ (Hafeez et al., 2021). Although this requires a greater investment than genotyping a handful of mutants, the sequence-configured panel can be combined with multiple phenotype datasets to potentially clone many genes from a single population (**Figure 12**). For a truly unbiased approach, whole-genome shotgun (WGS) sequencing can be employed to access all of the genetic diversity in a panel. Commonly, sequence reads are aligned to a reference genome and the resulting SNP calls are used for GWAS. Another approach is to generate sub-sequences called  $k$ -mers from raw sequence reads to avoid mapping to a reference genome, which greatly simplifies the process of working with complex datasets and mitigates reference bias; the  $k$ -mers can then be employed for association genetics of traits of interest (Audano et al., 2018; Rahman et al., 2018; Arora et al., 2019; Voichek and Weigel, 2020; Gaurav et al., 2022). Methods for genotyping and utilising diversity panels are discussed in more detail in Hafeez et al. (2021).

Genetic association studies involve testing for correlations between disease responses and genetic variation to identify candidate genes or loci. Multiple phenotypes can be combined with whole-genome data time and time again to identify loci that can be used in breeding and gene cloning. The use of wild populations also presents the opportunity to understand genes and their evolution in a population-genetic context.

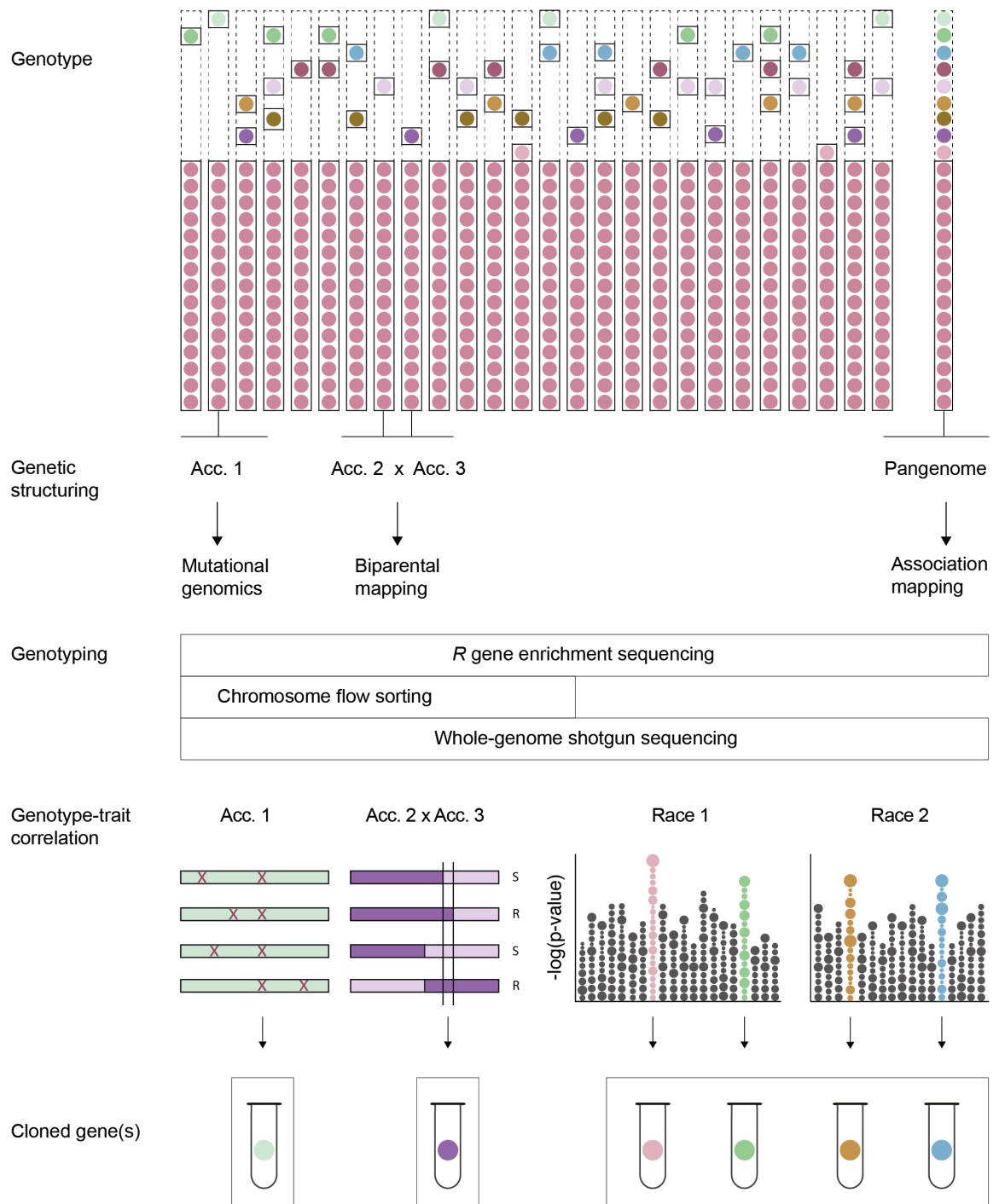


**Figure 12:** A comparison of different methods for cloning *R* genes. **Genetic structuring:** mutational genomics and map-based cloning interrogate the narrow genetic base of just one to two accessions. On the other hand, the pangenome variation can be accessed through the use of a diversity collection for association genetics, without the need for lab-generated population structures. **Genotyping:** complexity-reduction strategies can be used, such as *R*-gene enrichment sequencing and chromosome flow sorting, whilst WGS sequencing is a more costly but potentially more informative and unbiased approach. **Genotype-trait correlation:** all three of these methods aim to discover a correlation between host genotypes and the trait of interest – ideally, leading to the identification of a candidate gene. This can be achieved by analysing mutations, mapping intervals or the significance of sequence features associated with the trait of interest (GWAS). **Cloned gene(s):** association mapping has the potential to identify multiple genes from one sequence-configured population, whilst mutational genomics and biparental mapping typically only allow the mapping of a single gene per population. Figure reproduced from Hafeez et al. (2021).

## 1.17. INTRODUCTION TO THE CURRENT STUDY

There is much to discover about the structure and function of *Stb* genes, which confer resistance to the third-most-important disease of wheat worldwide, STB. The first step is to clone these genes in wheat and its relatives in order to investigate both known and novel sources of resistance. Well-curated and sequence-configured diversity panels of wheat relatives and landraces do not only provide inherent population structures amenable to genetic studies, but also allow us to gather additional information about the diversity of candidate genes. Studies employing association genetics are also efficient in that the same panel can be employed for multiple studies.

In this project, myself and my colleagues have explored STB resistance in two diversity panels. The first, *Aegilops tauschii*, is discussed in Chapter 2. The D-genome progenitor of wheat has contributed much to wheat breeding, including an STB resistance gene of recent importance, *Stb16q*. The diploid genome, high genetic diversity and apparent near-immunity to *Z. tritici* of *Ae. tauschii* makes it an attractive subject. We aimed to test the suitability of *Ae. tauschii* as a host for wheat-adapted *Z. tritici* isolates and hypothesised that *Stb* genes could be mapped in this system through association genetics. We also aimed to test the effect of the resistance gene *Stb16q* in the *Ae. tauschii* panel. These aims are addressed through the analysis of pycnidia and necrosis responses to two key isolates, IPO323 and cfz008.

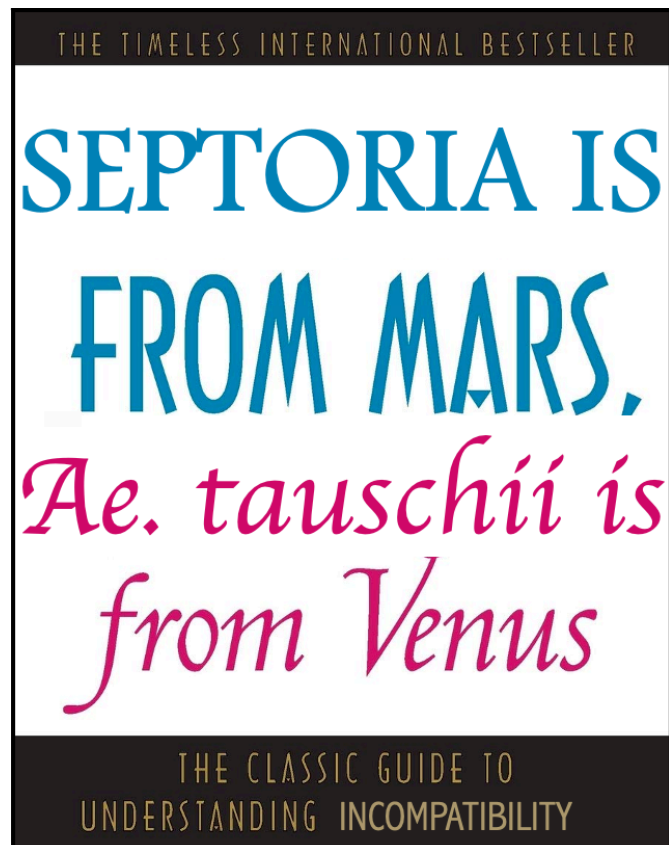
In Chapter 3, the second diversity panel we investigated is introduced: the Watkins collection of wheat landraces. This collection provides the opportunity to study interactions with STB in a well-adapted yet highly genetically diverse context. We tested the presence of genotype- and isolate-specific effects in responses of Watkins landraces to isolates of *Z. tritici* using linear mixed modelling, in both detached leaf and seedling conditions. Means were estimated from these models to reduce the impact of environmental experimental design factors on subsequent analyses. We hypothesised that certain phenotype distributions which appeared to be more binomial were likely to be more amenable to association mapping, and selected isolates eliciting such responses for testing on a larger subset of the Watkins diversity panel. We also hypothesised that damage phenotypes can be a useful measure of pathogen colonisation, whilst rapid-onset and widespread necrosis of leaf tissue may be associated with resistance or disease escape. These phenotypes and their relationship with pycnidia cover were investigated through inoculation of key lines with two isolates of *Z. tritici* and different inoculum doses. Finally, we predicted that there may be Watkins landraces that possess exceptional

broad-spectrum resistance. The most resistant lines were screened against a further set of six isolates, resulting in the identification of at least five lines with robust broad-spectrum resistance to *Z. tritici* that could be used in wheat pre-breeding.

In Chapter 4, association genetics is performed on 300 Watkins landraces with the aim of mapping loci linked with resistance to *Z. tritici* isolates. Phenotype data from IPO323 was employed to test the power of this method and data to detect the known Septoria resistance gene, *Stb6*. Following this proof-of-concept, analyses in Chapter 3 and the known presence of major genes conferring resistance to these isolates in wheat led us to predict that we would be able to map candidate genes for resistance to IPO88004 and IPO90012 via GWAS. This resulted in the successful mapping of an interval containing *Stb15*. Analyses of the region and haplotypes in the Watkins panel led to a candidate gene encoding a lectin receptor-like kinase (LecRK). Haplotypes were analysed for *Stb6* and the *Stb15* candidate gene, and we hypothesised that the removal of functional haplotypes of these genes from the GWAS would allow the detection of other resistance genes with smaller effects. This was not successful for IPO323 data, but the removal of the *Stb15* candidate did lead to a more defined and significant interval on chromosome 2B associated with resistance to IPO88004. We also hypothesised that there may be specific traits associated with the phenotype of early-onset and widespread necrosis (super necrosis) discussed in Chapter 3. Mapping this phenotype in IPO90012 led to the identification of a significant association on chromosome 4D.

The overall aim of this thesis is to evaluate the utility of diversity panels of wheat landraces and the diploid progenitor *Ae. tauschii* for mapping genes associated with responses to *Z. tritici*. I hope to increase our knowledge of the canon of *Stb* genes as well as identifying sources of resistance useful for wheat breeding.

2. EXPLORING THE INTERACTION BETWEEN  
*Z. TRITICI* AND *AEGILOPS TAUSCHII*



## 2.1. INTRODUCTION

### 2.1.1. Advantages of working with *Ae. tauschii*

There are many advantages to working with the D-genome progenitor of wheat, *Aegilops tauschii*. Firstly, it has a smaller (4.3 Gb) genome in comparison to the 16 Gb genome of wheat. *Ae. tauschii* is also a diploid, which makes its genetics simpler to understand and manipulate (**Figure 13**). Working in the D-genome alone can provide opportunities to study genes that may be masked by widespread genes on other subgenomes. An example for Septoria resistance is *Stb6*, which is in the A genome and widespread in bread wheat (Chartrain et al., 2005c); this gene may be masking a second source of resistance to the isolate IPO323 (Chartrain et al., 2005a).



**Figure 13:** Comparison of spikes and chromosome numbers between wheat and *Ae. tauschii*. A genome = blue; B genome = red; D genome = green.

One of the most favourable aspects of *Ae. tauschii* is the vast amount of resources available. Diversity from *Ae. tauschii* can be introduced into bread wheat through the generation of SHWs, formed by crossing *Ae. tauschii* with tetraploid wheats (McFadden and Sears, 1947). SHWs can harbour >80% more diversity in the D genome than elite wheats (Bhatta et al., 2018). The large number of SHWs already generated (Mujeeb-Kazi et al., 1996; Ogonnaya et al., 2013; Gaurav et al., 2022) can often mean that traits of interest from *Ae. tauschii* are already incorporated into SHWs. One of the two cloned *Stb* genes, *Stb16q*, was mapped to chromosome 3D of the SHW line M3, demonstrating the importance of Septoria resistance from *Ae. tauschii* (Ghaffary et al., 2012; Saintenac et al., 2021).

The genetic resources available for this species are now vast. A reference-quality genome assembly of accession AL8-78 has been generated (Luo et al., 2017) and whole-genome shotgun data (7.5 to 30x coverage) of 242 diverse *Ae. tauschii* accessions was generated by

the Open Wild Wheat Consortium (<http://www.openwildwheat.org/>; Gaurav et al., 2021b). This provides a huge and valuable resource for rapid gene cloning that can be used to accelerate wheat improvement.

### 2.1.2. Septoria resistance in the D-genome

A small amount of research has previously been published pertaining to the *Ae. tauschii*-*Z. tritici* interaction. Around 99% of the 127 *Ae. tauschii* accessions tested by Assefa and Fehrman (1998) were highly resistant to a mixed field culture of *Z. tritici* collected in Missouri; the majority were immune, with four accessions showing lesions and just one accession found to be susceptible. This is consistent with a study by McKendry and Henke (1994) that also found resistance and immunity in *Ae. tauschii* to be prevalent, especially south of the Caspian Sea in Iran and in eastern Afghanistan. A host of multiple-disease resistant *Ae. tauschii* lines have been observed from these regions, including to leaf rust, stem rust, powdery mildew and tan spot (Cox et al., 1992) as well as resistance to foliage-feeding aphids (Singh et al., 2018). More recently, Ajaz et al. (2021) found varying levels of resistance to *Z. tritici* amongst five *Ae. tauschii* accessions tested.

Three main lineages of *Ae. tauschii* have been identified: Lineage 1, comprised almost entirely of subspecies *tauschii*, is distributed in the eastern Caspian region, from Syria and Russia to Afghanistan, Pakistan and China; Lineage 2, composed mainly of ssp. *strangulata*, is distributed mostly westerly, in Iran, Azerbaijan and Georgia; Lineage 3 is restricted to present-day Georgia (Wang et al., 2013; Arora et al., 2017; Gaurav et al., 2022). The D-genome of modern bread wheat arose from *Ae. tauschii* accessions from both Lineage 1 and Lineage 3; such accessions are of particular interest for this reason, especially given high levels of multiple disease resistance (Cox et al., 1992) and *Z. tritici* resistance (McKendry and Henke, 1994) in Lineage 2 *Ae. tauschii* spp. *strangulata* accessions and superior dough quality (Delorean et al., 2021) and blast resistance (Arora et al., 2022) traits in Lineage 3.

There are several aspects of the *Aegilops tauschii* genome to which its valuable, multiple-disease resistance may be attributable. The reference-quality genome assembly of *Ae. tauschii* spp. *strangulata* accession AL8/78 revealed that the chromosomes of *Ae. tauschii* have been evolving an order of magnitude faster than other grasses (Luo et al., 2017). Large amounts of highly similar repeated sequences and dispersed duplicated genes (more than many other sequenced genomes) may cause frequent errors in recombination

that drive rapid genome evolution through gene duplications and structural chromosome changes (Luo et al., 2017). A fast pace of genome evolution is especially important in the context of maintaining resistance to dynamic pathogens such as *Z. tritici*.

Major genes for resistance to *Z. tritici* have already been mapped to the wheat D-genome chromosomes 1, 3, 6 and 7, with QTLs identified on all apart from chromosome 5D (Figure 14). *Stb16q* has been tested against a large number of *Z. tritici* isolates and shows strong resistance to all of them, as well as being expressed in both the adult and seedling stages (Ghaffary et al., 2012). This locus was discovered on chromosome 3D of the SHW line M3, and is therefore within the *Ae. tauschii* gene pool. Unfortunately, virulence to this gene has emerged in field populations in Ireland (Kildea et al., 2020) and France (Orellana-Torrejon et al., 2022). Investigating other sources of resistance to these virulent isolates is therefore of increasing priority.

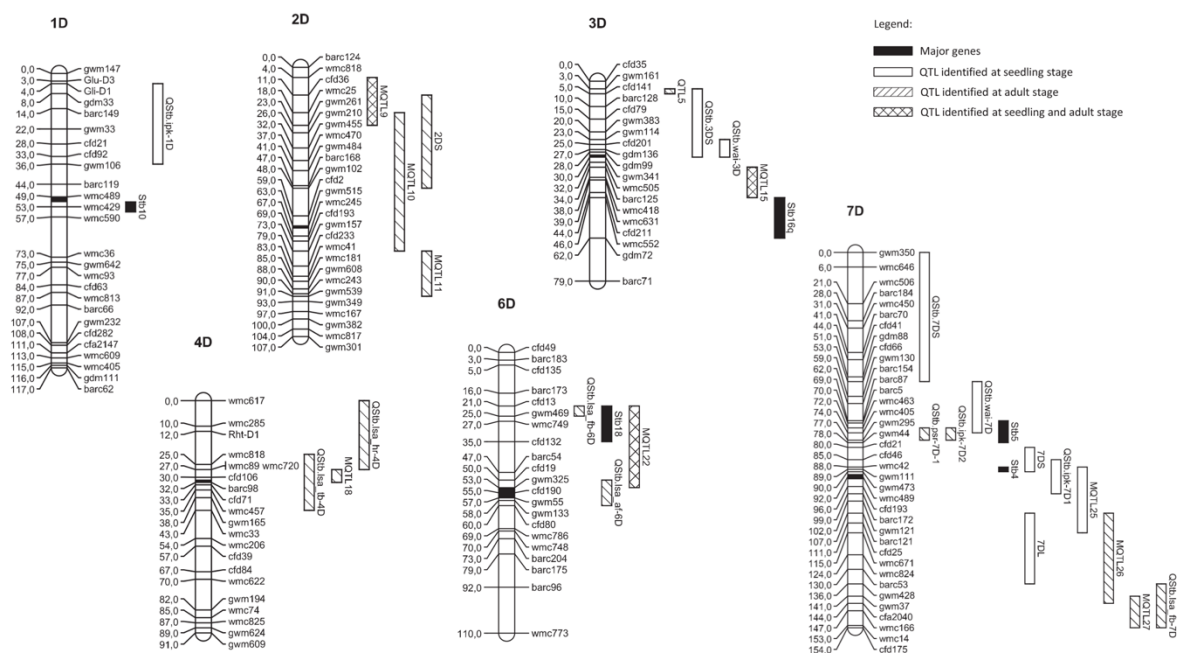


Figure 14: Major genes and QTLs conferring resistance to *Z. tritici* that have been mapped to the D-genome chromosomes of wheat. Adapted and reproduced here with permission from Brown et al. (2015).

With genetic diversity far exceeding that of its domesticated relative, there is every opportunity to unearth not just these sources of resistance in *Ae. tauschii*, but also resistances that were not incorporated or that have evolved in modern *Ae. tauschii* since the final polyploidisation of wheat. The significant challenge remaining is to find effective methods for dissecting the genetic basis of Septoria resistance in *Ae. tauschii*, starting with the pathology.

### 2.1.3. Summary of chapter findings

Responses of *Ae. tauschii* to wheat-adapted isolates of *Z. tritici* are suggestive of a marginal host relationship, similar to that observed in interactions with *Triticum monococcum* and *Brachypodium distachyon*. There were few compatible interactions between *Ae. tauschii* and the *Z. tritici* isolate IPO323, but a greater variety of responses was observed in response to cfz008 which is virulent to the *Ae. tauschii*-derived gene *Stb16q*. *k*-mer-based association mapping efforts using *Ae. tauschii* whole-genome shotgun data were not successful when pycnidia responses to either isolate were used. Necrosis responses, on the other hand, were associated with several loci, and the loci at 4DL and 6DS were associated with low levels of necrosis in response to both isolates. This could suggest that there are race-non-specific genes at these loci that confer a reduction in damage in *Ae. tauschii*. However, the strong effect of accession on necrosis data warrants further testing to determine whether these loci are associated with response to *Z. tritici*. There are also unanswered questions regarding the role of necrosis in Septoria interactions to consider.

## 2.2. MATERIALS AND METHODS

### 2.2.1. Plant and pathogen material

A panel of 151 non-redundant *Ae. tauschii* ssp. *strangulata* accessions (Lineage 2) was tested (Arora et al., 2019; Gaurav et al., 2022). These accessions originated from the region surrounding the Caspian Sea in the Middle East (**Table 1**).

**Table 1:** *Aegilops tauschii* ssp. *strangulata* (Lineage 2) accessions included in the current study and their origins. Table adapted from Supplementary Table 2 of Arora et al. (2019).

JIC GRU No.	Project Accession No.	Original Source	Country of Origin	State/Province/City
TOWWC002	BW_01001	NSGC	Iran	Mazandaran
TOWWC003	BW_01002	NSGC	Iran	Golestan
TOWWC004	BW_01003	NSGC	Iran	Golestan
TOWWC005	BW_01004	NSGC	Iran	Golestan
TOWWC006	BW_01005	NSGC	Iran	Mazandaran
TOWWC007	BW_01006	NSGC	Iran	Mazandaran
TOWWC008	BW_01007	ICARDA	Azerbaijan	Agsu
TOWWC009	BW_01008	ICARDA	Azerbaijan	Askeran
TOWWC010	BW_01009	ICARDA	Azerbaijan	Baku
TOWWC011	BW_01010	ICARDA	Azerbaijan	Aliabad
TOWWC012	BW_01011	ICARDA	Azerbaijan	Lankaran
TOWWC013	BW_01012	ICARDA	Azerbaijan	Shabran
TOWWC016	BW_01015	IPK	Azerbaijan	
TOWWC017	BW_01016	IPK	Azerbaijan	
TOWWC020	BW_01019	IPK	Azerbaijan	
TOWWC021	BW_01020	IPK	Azerbaijan	
TOWWC022	BW_01021	IPK	Azerbaijan	
TOWWC023	BW_01022	IPK	Azerbaijan	
TOWWC025	BW_01024	IPK	Turkmenistan	
TOWWC026	BW_01025	IPK	Armenia	
TOWWC027	BW_01026	IPK	Turkmenistan	
TOWWC028	BW_01027	IPK	Armenia	
TOWWC031	BW_01030	Vavilov Institute	Russia	North Caucasian
TOWWC032	BW_01031	KSU	Uzbekistan	
TOWWC033	BW_01032	KSU	Turkey	Shemsdin
TOWWC034	BW_01033	KSU	Turkey	Shemsdin
TOWWC040	BW_01039	KSU	Azerbaijan	
TOWWC042	BW_01041	KSU	Azerbaijan	Shaki
TOWWC043	BW_01042	KSU	Azerbaijan	Ismaili
TOWWC044	BW_01043	KSU	Azerbaijan	Fizuli
TOWWC045	BW_01044	KSU	Azerbaijan	Zangilan

TOWWC046	BW_01045	KSU	Azerbaijan	Basut-Chay State Reserve
TOWWC047	BW_01046	KSU	Armenia	
TOWWC048	BW_01047	KSU	Armenia	
TOWWC049	BW_01048	KSU	Armenia	
TOWWC050	BW_01049	KSU	Uzbekistan	Zangiota
TOWWC051	BW_01050	KSU	Syrian Arab Republic	Ras al-Ayn
TOWWC056	BW_01055	KSU		
TOWWC057	BW_01056	KSU	Georgia	Kumisi
TOWWC058	BW_01057	KSU	Georgia	Kumisi
TOWWC059	BW_01058	KSU	Georgia	Signhnaghi
TOWWC060	BW_01059	KSU	Georgia	Signhnaghi
TOWWC061	BW_01060	KSU	Azerbaijan	Shirvan
TOWWC063	BW_01062	KSU	Azerbaijan	Shirvan
TOWWC064	BW_01063	KSU	Azerbaijan	Saatly
TOWWC066	BW_01065	KSU	Azerbaijan	Shamakhi
TOWWC067	BW_01066	KSU	Azerbaijan	Shamakhi
TOWWC069	BW_01068	KSU	Azerbaijan	Agsu
TOWWC070	BW_01069	KSU	Azerbaijan	Agsu
TOWWC071	BW_01070	KSU	Azerbaijan	Agsu
TOWWC072	BW_01071	KSU	Azerbaijan	
TOWWC073	BW_01072	KSU	Azerbaijan	
TOWWC074	BW_01073	KSU	Azerbaijan	
TOWWC075	BW_01074	KSU	Azerbaijan	
TOWWC077	BW_01076	KSU	Azerbaijan	
TOWWC078	BW_01077	KSU	Azerbaijan	
TOWWC079	BW_01078	KSU	Azerbaijan	
TOWWC080	BW_01079	KSU	Iran	
TOWWC082	BW_01081	KSU	Turkey	Hakkari
TOWWC083	BW_01082	KSU	Turkey	Hakkari
TOWWC084	BW_01083	KSU	Iran	Mazandaran
TOWWC085	BW_01084	KSU	Iran	Mazandaran
TOWWC086	BW_01085	KSU		
TOWWC087	BW_01086	KSU	Iran	Amol
TOWWC088	BW_01087	KSU	Former USSR	
TOWWC089	BW_01088	KSU	Russian Federation	
TOWWC090	BW_01089	KSU	Turkmenistan	Balkan
TOWWC092	BW_01091	KSU	Azerbaijan	Shabran
TOWWC095	BW_01094	KSU	Iran	Mazandaran
TOWWC096	BW_01095	KSU	Iran	Golestan
TOWWC097	BW_01096	KSU	Iran	Hamadan
TOWWC098	BW_01097	KSU	Iran	Aliabad
TOWWC099	BW_01098	KSU	Iran	Mazandaran
TOWWC100	BW_01099	KSU	Iran	Guilan
TOWWC101	BW_01100	KSU	Iran	Golestan
TOWWC103	BW_01102	KSU	Azerbaijan	Goychay

TOWWC104	BW_01103	KSU	Azerbaijan	
TOWWC105	BW_01104	KSU	Azerbaijan	Sabirabad
TOWWC106	BW_01105	KSU	Azerbaijan	
TOWWC107	BW_01106	KSU	Azerbaijan	
TOWWC108	BW_01107	KSU	Azerbaijan	Masalli
TOWWC109	BW_01108	KSU	Azerbaijan	Shamakhi
TOWWC110	BW_01109	KSU	Azerbaijan	Shamakhi
TOWWC112	BW_01111	KSU	Azerbaijan	Shamakhi
TOWWC113	BW_01112	KSU	Azerbaijan	Shamakhi
TOWWC114	BW_01113	KSU	Azerbaijan	Kutkashen
TOWWC115	BW_01114	KSU	Azerbaijan	Yardymli
TOWWC116	BW_01115	KSU	Turkmenistan	
TOWWC117	BW_01116	KSU	Azerbaijan	
TOWWC118	BW_01117	KSU	Azerbaijan	
TOWWC119	BW_01118	KSU	Azerbaijan	Shamakhi
TOWWC120	BW_01119	KSU	Azerbaijan	Agsu
TOWWC121	BW_01120	KSU	Azerbaijan	Shaki
TOWWC122	BW_01121	KSU	Azerbaijan	Kutkashen
TOWWC123	BW_01122	KSU	Azerbaijan	Davachi
TOWWC124	BW_01123	KSU	Azerbaijan	Ezmarail
TOWWC125	BW_01124	KSU	Azerbaijan	Shamakhi
TOWWC126	BW_01125	KSU		
TOWWC127	BW_01126	KSU		
TOWWC129	BW_01128	KSU		
TOWWC130	BW_01129	KSU		
TOWWC131	BW_01130	KSU	Iran	Gilan
TOWWC133	BW_01132	KSU	Iran	Guilan
TOWWC134	BW_01133	KSU	Iran	Markazi
TOWWC135	BW_01134	KSU	Russian Federation	Dagestan
TOWWC136	BW_01135	KSU	Iran	Alborz
TOWWC137	BW_01136	KSU	Iran	Tehran
TOWWC138	BW_01137	KSU	Iran	Mazandaran
TOWWC139	BW_01138	KSU	Iran	Mazandaran
TOWWC140	BW_01139	KSU	Iran	Alborz
TOWWC141	BW_01140	KSU	Iran	Mazandaran
TOWWC142	BW_01141	KSU	Iran	Mazandaran
TOWWC143	BW_01142	KSU	Iran	Gorgan
TOWWC144	BW_01143	KSU	Iran	Aliabad-e Katul
TOWWC145	BW_01144	KSU	Iran	Aliabad-e Katul
TOWWC147	BW_01146	KSU	Iran	Golestan
TOWWC148	BW_01147	KSU	Iran	Golestan
TOWWC149	BW_01148	KSU	Iran	Golestan
TOWWC152	BW_01151	KSU	Iran	Mazandaran
TOWWC153	BW_01152	KSU	Iran	Mazandaran
TOWWC154	BW_01153	KSU	Iran	Mazandaran
TOWWC155	BW_01154	KSU	Iran	Mazandaran

TOWWC156	BW_01155	KSU	Iran	Mazandaran
TOWWC157	BW_01156	KSU	Iran	Mazandaran
TOWWC159	BW_01158	KSU	Iran	Mazandaran
TOWWC160	BW_01159	KSU	Iran	Mazandaran
TOWWC162	BW_01161	KSU	Iran	Guilan
TOWWC163	BW_01162	KSU	Iran	Guilan
TOWWC164	BW_01163	KSU	Iran	Guilan
TOWWC165	BW_01164	KSU	Iran	Gilan
TOWWC166	BW_01165	KSU	Iran	Gilan
TOWWC167	BW_01166	KSU	Iran	Gilan
TOWWC168	BW_01167	KSU	Iran	Ardabil
TOWWC169	BW_01168	KSU	Iran	
TOWWC171	BW_01170	KSU	Iran	East Azerbaijan
TOWWC172	BW_01171	KSU	Iran	Mazandaran
TOWWC173	BW_01172	KSU	Iran	Mazandaran
TOWWC176	BW_01175	KSU	Iran	Mazandaran
TOWWC177	BW_01176	KSU	Iran	Mazandaran
TOWWC178	BW_01177	KSU	Iran	Mazandaran
TOWWC179	BW_01178	KSU	Iran	Mazandaran
TOWWC180	BW_01179	KSU	Azerbaijan	Shamakhi
TOWWC182	BW_01181	KSU	Azerbaijan	Shamakhi
TOWWC183	BW_01182	KSU	Azerbaijan	
TOWWC185	BW_01184	KSU	Armenia	Yerevan
TOWWC186	BW_01185	KSU	Georgia	Tbilisi
TOWWC187	BW_01186	KSU	Georgia	Gori
TOWWC190	BW_01189	CSIRO	Iran	Gorgan
TOWWC191	BW_01190	CSIRO	Iran	
TOWWC193	BW_01192	UC Davis	Armenia	
TOWWC194	BW_01193	UC Davis	Iran	Mazandaran

Various wheat control lines were included in all assays, with lines selected based on known response to *Septoria* (relevant isolates listed) or due to strategic importance (**Table 2**).

**Table 2:** Wheat lines included in *Septoria* assays and reasons for their inclusion. Selections based on information from Arraiano & Brown (2006), Brown et al. (2015) and Chartrain et al. (2004).

\*Seed provided by Cyrille Saintenac, INRA, France.

Line	Reason for inclusion
Bastard II	Resistant to IPO92006
Tadina*	Contains the D-genome gene <i>Stb4</i>
CS (Chinese Spring) Synthetique/Synthetic 6x*	Contains the D-genome gene <i>Stb5</i>
Taichung 29	Highly susceptible control
Riband	Susceptible to IPO323 and IPO92006
Hereward	Resistant to IPO323, contains <i>Stb6</i>
Cellule	Widely resistant, resistant to IPO92006
CS <i>Stb16q</i> *	Near-isogenic line of Chinese Spring with <i>Stb16q</i>
CS <i>stb16q</i> *	Near-isogenic line of Chinese Spring without <i>Stb16q</i>
Flame	Resistant to IPO323, contains <i>Stb6</i>
KK	Susceptible to IPO94269, resistant to IPO323
Longbow	Widely susceptible control

IPO323 was tested as it is the reference isolate of *Z. tritici* and elicits consistent phenotypes in wheat. The isolates cfz006, cfz008 and cfz013 were isolated by INRA BIOGER and the Kema lab at Wageningen University & Research (WUR) from *Z. tritici* field populations in France growing on the cultivar Cellule. These isolates were known to be virulent on *Stb16q* and included in order to test for resistance in the *Ae. tauschii* panel that is not masked by *Stb16q*.

**Table 3:** Isolates tested on the *Ae. tauschii* collection. For references re avirulences see Brown *et al.* (2015). Avirulence to *Stb16q* tested by Cyrille Saintenac (personal communication).

Isolate	Year Isolated	Origin	Known avirulence to <i>R</i> genes
IPO323	1981	The Netherlands	<i>Stb5, Stb6, Stb18, Stb16q.</i>
Cfz006	2016	Northern France	Virulent on <i>Stb16q.</i>
Cfz008	2016	Northern France	Virulent on <i>Stb16q.</i>
Cfz013	2016	Paris, France	Virulent on <i>Stb16q.</i>

### 2.2.2. Experimental design for pathology assays

An alpha lattice design was used as the experiment consisted of incomplete blocks (40-well seedling trays). This allowed the effects of tray and position in the CER (controlled environment room) to be estimated through subsequent statistical analyses. The design was generated using the ALPHA setting of the Gendex programme from Design Computing (<http://designcomputing.net/gendex/>). This programme is based on the design principles set out in Patterson and Williams (1976).

### 2.2.3. Standard infection protocol for pathology assays

The following methods are based on those described by Arraiano *et al.* (2001a), which in turn closely followed the methods set out by Kema *et al.* (Kema *et al.*, 1996b).

Multiple seeds of the lines tested were pre-germinated in petri dishes on filter paper (Whatman 90 mm, Whatman International Ltd, Hadstone, UK) and 4 ml of 0.2 ppm gibberellic acid added. Petri dishes were placed in the dark at room temperature for 48

hours, then moved to the lab bench in daylight for a further 24 hours. Germinated seeds were then planted in John Innes peat-based F2 compost in 40-well trays. Trays were placed in a Conviron controlled environment cabinet with a 16-hour photoperiod: day temperature 18°C, night temperature 12°C. When the second leaf was fully expanded, usually at around 14 days after germination, inoculum was prepared.

Sporulating cultures of *M. graminicola* were grown on potato dextrose agar (PDA) plates for five to seven days under near ultra-violet light (Snijders Micro Clima-Series™ Economic Lux Chamber, Snijders Labs, Tilburg, The Netherlands) for 16 h per day at 18°C. Cultures were then flooded with 3 ml of sterile distilled water and scraped to release conidia. The concentration of conidial suspension was then adjusted to the desired inoculum concentration; this was typically 10<sup>6</sup> spores ml<sup>-1</sup>. This was adjusted down from 10<sup>7</sup> spores/ml based on the findings of Fones et al. (2015). Conidial concentration was assessed through the use of a Fuchs-Rosenthal counting chamber (Hawksley, Lancing, UK) using the equation: (average spore number) x 16 x 5000. For the experiment testing the effect of inoculum dose, serial dilutions were employed to achieve concentrations of 10<sup>6</sup>, 10<sup>5</sup>, 10<sup>4</sup> and 10<sup>3</sup> spores mL<sup>-1</sup>. Two drops of polyoxyethylene-sorbitan monolaurate (Tween-20; Sigma-Aldrich Chemie GmbH, Germany) were added per 50 ml of spore suspension.

Excess leaves were cut away so that only the primary seedling leaf remained. Seedlings were then evenly sprayed with spore suspension (20 ml per tray), assisted by the use of a turn table (home-made at the JIC), using a Clarke Wiz Mini Air Compressor spray gun kit (Clarke Tools, Dunstable, England).

#### 2.2.3.1. Seedling assays

Assays on *Ae. tauschii* were performed in a walk-in cabinet with conditions: 16 hour photoperiod, 20°C day and 16°C night temperature, humidity of 70%, and photosynthetic photon flux density (PPFD) of 334 microEinstein/m<sup>2</sup> at plant height. Trays were placed on matting atop metal racks which allowed drainage of excess water. Two metal racks were used, each surrounded by a plastic tent to maintain high humidity around the plants. After inoculation, plants were placed in propagators, two trays per propagator, which were closed and covered with a black plastic bag for dark incubation. Black bags were removed after 48 hours and propagator lids were kept over trays until seven days after inoculation to increase humidity and therefore the success of infection by *Z. tritici*. New

leaf growth was cut back 2 times per week (every two to three days) to keep the inoculated leaf healthy and facilitate scoring. These steps are pictured in **Figure 15**.



**Figure 15:** Photos of some steps involved in seedling *Z. tritici* assays. Plants are sprayed on a turn table (A) and then placed inside propagators covered with black plastic bags for incubation (B). The second batch of seedlings can be seen at the one leaf stage in B and the 2-3 leaf stage, just prior to leaf cutting and inoculation, in C. Plants remain inside propagator bases after inoculation to enable watering from the bottom (C, right hand side).

#### 2.2.3.2. Detached leaf assays

Detached leaf assays were carried out as described by Arraiano et al. (2001a). Inoculated leaves were left to dry for 30 min before ~3.5 cm sections were cut from the middle of the primary leaves.

50 mL of water agar (10 g L<sup>-1</sup>) containing 100 mg L<sup>-1</sup> benzimidazole (Sigma), used to delay senescence and reduce contamination, was dispensed into non-sterile clear polystyrene boxes (8x12x2 cm). Rectangular sections (3x9 cm) were cut from the centre of the agar. Seedling leaf sections were laid, adaxial side upwards, across the gap so that the cut ends rested on the agar. The presence of a gap underneath the leaves aided in preventing water soaking and contamination by other microorganisms. Up to ten leaf sections were fitted into each box before strips of agar were laid over the edges of the leaf sections. This served to hold the leaf sections in place and reduce their exposure, thereby delaying senescence. The boxes were closed and covered with a black plastic bag for dark incubation in the same cabinet used previously for growth on PDA plates. Black bags were removed after 48 hours.

### 2.2.3. Phenotype data collection

The percentage of leaf area covered by pycnidia and necrosis (**Figure 16**) was scored three to five times at intervals of two to five days over a period of 10 to 32 days post inoculation, depending on disease progress.

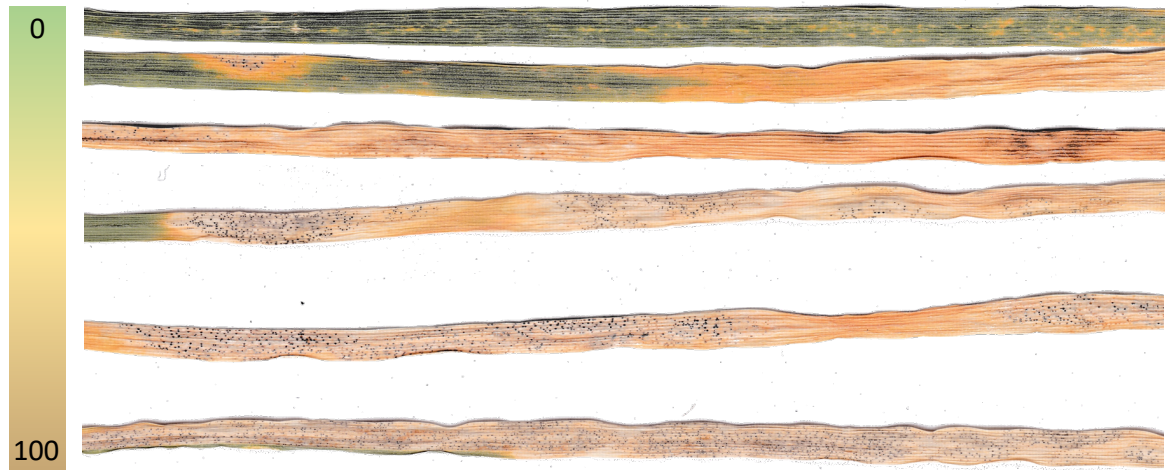


**Figure 16:** Phenotyping scale used for scoring seedling assays. Leaves are arranged according to their approximate pycnidia percentage cover, but necrosis was also scored.

For detached leaf assays, phenotyping was carried out using a dissecting WILD M3Z microscope at 20x magnification. For seedling assays, phenotyping was carried out by eye.

### 2.2.4. Statistical analysis

The area under the disease progress curve (AUDPC) was calculated for each dataset by calculating the sums of the below equation for each consecutive pair of scoring days:

$$\text{Difference between scoring days} * (\text{score from day 1} + \text{score from day 2})/2$$

This gives the area of the trapezium formed between each pair of scoring days on a graph of disease severity over time.

Since the scores had a bounded outcome (from 0 to 100), they were transformed to logits to normalise the data distribution for statistical analysis, where score = the AUDPC of pycnidia or damage). A standard logit transformation would designate the maximum and

minimum score values, 0 and the max AUDPC, as undesignated transformed values. To prevent this, the empirical logit transformation was used wherein a small number was added to each score and to the maximum score used in the transformation (Collett, 2003; McGrann et al., 2014). The number used was the lowest possible non-zero score:  $a$ , calculated as the difference between the first two scoring days multiplied by 0.5, divided by 4. The transformation was thus as follows:

Equation 1 
$$\mathbf{Logit\ } x = \mathbf{log\ } \frac{x+a}{(100+a) - x}$$

The data was then analysed for the effects of blocking and other factors using linear mixed modelling, to account for both random and fixed effects, via the package *lsmmeans* in R. If only fixed effects were involved, the native R analysis of variance (*avov*) function was used. For *Ae. tauschii* assays, the models included the blocking factors: Tent (two plastic humidifying tents described above), Tray (p40 seedling trays) and Block (10-plant quarter sections of each seedling tray).

Nested deviance tests were conducted to determine the most concise models that explained as much of the variation in phenotype as possible. Plots of residuals were then examined to determine model fit. Models were fitted to the % of the maximum possible AUDPC if the residual plots from logit AUDPC models were not adequate; this was often the case with damage data, which was often more normally distributed in its raw form than pycnidia data. The estimated mean pycnidia and damage scores for each genotype were obtained through the R *emmeans* package.

An example script for performing the analyses above is provided in **Supplementary Script 1**.

#### 2.2.5. Association genetics

GWAS was performed by Kumar Gaurav using a pre-publication version of the Open Wild Wheat Consortium (OWWC) *Ae. tauschii* whole-genome shotgun  $k$ -mer GWAS pipeline (Gaurav et al., 2022).

### 2.3. RESULTS

Three isolates from Cyrille Saintenac were tested on wheat controls and *Ae. tauschii* accessions: cfz006, cfz008 and cfz013. Cfz006 and cfz013 were avirulent on the Chinese Spring near-isogenic lines (NILs) for *Stb16q*, likely due to the presence of *Stb6*. Cfz008 was equally and significantly virulent on both NILs as well as Tadinia, so was selected for screening on the panel of 151 *Ae. tauschii* accessions as there appeared to be little avirulence to this isolate in the D genome of wheat (data not shown). Cfz008 was, however, avirulent to CS Synthetique, so is likely avirulent to *Stb5*. The reference isolate IPO323 was also screened, due to its reliable proliferation in artificial conditions and avirulence to *Stb16q*.

A range of phenotypes were observed in response to *Z. tritici* isolates (**Figure 17**), described below to give an idea of the responses in *Ae. tauschii* that were difficult to measure. The susceptible wheat cultivar Taichung 29 was included for comparison. It is clear from these images that pycnidia forming on *Ae. tauschii* were smaller than those on wheat. Often, completely necrotic leaves with a sparse covering of pycnidia were observed (as in BW\_21200). Dense pycnidia coverage was sometimes observed, either as smaller patches (BW\_21133) or, rarely, covering large areas of the leaf (BW\_21092). Both phenotypes were very difficult to observe when scoring seedling experiments by eye due to the small size of the pycnidia – it is likely that many leaves were underscored. Far more rarely, lesions bearing pycnidia, similar to those observed in wheat, were observed. This was often associated with whitening of the infected tissue, thought to be due to excessive mycelial growth. Susceptible phenotypes were also often inconsistent – BW\_21481 B was the exception amongst three other replicates of BW\_21481 which appeared extremely green and resistant as in the image for BW\_21481 A. Finally, a common response was the “black spots” observed on necrotic leaves, sometimes alongside pycnidia (BW\_21493).

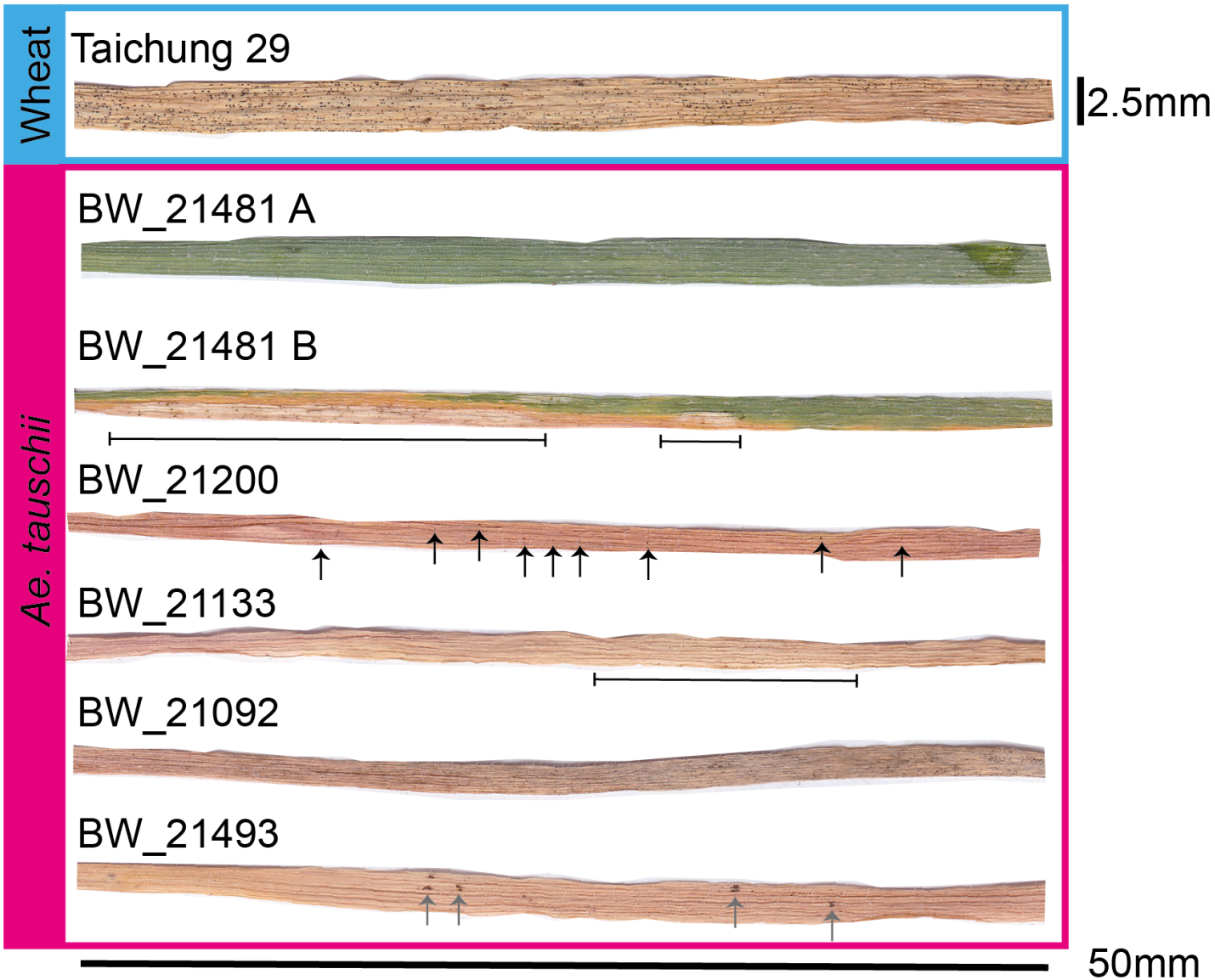


**Figure 17:** Leaf scan images of wheat and *Ae. tauschii* leaves inoculated with *Z. tritici* isolate IPO92006, 29 days post infection. Leaf images were selected to represent the major phenotypes observed: **Taichung 29** (highly susceptible wheat control), **BW\_21481 A** (highly resistant); **BW\_21481 B** (wheat-like lesions bearing pycnidia); **BW\_21200** (highly necrotic with scarce pycnidia); **BW\_21133** (highly necrotic with a region densely populated with very small pycnidia); **BW\_21092** (highly susceptible and densely populated with pycnidia) and **BW\_21493** (presence of scarce pycnidia and melanised patches). BW\_21481 A and B are genetically identical replicates of the same accession.

The linear mixed model used for analysis of both pycnidia and necrosis data consisted of Isolate, Accession, the Isolate-by-Tent interaction and Isolate-by-Accession interaction as fixed effects (**Table 4**; **Table 5**). The Isolate-by-Tent-by-Tray and Isolate-by-Tent-by-Tray-by-Block interactions were fitted as random effects (**Table 6**). There was a significant effect of isolate on pycnidia and necrosis responses as well as the isolate-by-accession interaction (although this was a smaller effect). This suggests that responses to *Ae. tauschii* were isolate-specific. There was also an effect of accession genotype on Septoria response. Damage appeared to be more affected by host genotype than by isolate. It is important to note that the isolate effect also encompasses an experiment effect – as the isolates were screened at different times. Means between tents only significantly differed for necrosis data; this phenotype may be more sensitive to environmental variation. Line means in response to both isolates are provided in **Supplementary Table 1**.

The Isolate-by-Tent-by-Tray and Isolate-by-Tent-by-Tray-by-Block effects only accounted for 8.6 and 2.2% of the variance for damage, and 6.0 and 6.3% of the variance for pycnidia, respectively. 89% of the residual variance for damage and 87% for pycnidia was unexplained and likely due to variation in responses of individual replicate leaves.

**Table 4:** ANOVA table for fixed effects of the linear mixed model fitted to logit pAUDPC values of *Ae. tauschii* accessions in response to IPO323 and cfz008.

Term	Mean Square	Numerator DF	Denominator DF	F value	Pr(>F)
Isolate	43.60	1	33	18.57	<0.001
Accession	11.63	162	1111	4.95	<0.0001
Isolate:Tent	6.22	2	33	2.65	0.09
Isolate:Accession	4.12	152	1110	1.75	<0.0001

**Table 5:** ANOVA table for fixed effects of the linear mixed model fitted to % maximum dAUDPC values of *Ae. tauschii* accessions in response to IPO323 and cfz008.

Term	Mean Square	Numerator DF	Denominator DF	F value	Pr(>F)
Isolate	2848.10	1	34	4.17	0.05
Accession	4460.2	162	1126	6.52	<0.0001
Isolate:Tent	3854.7	2	34	5.64	0.008
Isolate:Accession	1119.1	152	1125	1.63	<0.0001

**Table 6:** Table of variance components for random effects of the linear mixed model fitted to logit pAUDPC and % maximum dAUDPC values of *Ae. tauschii* accessions in response to IPO323 and cfz008.

Term	Logit pAUDPC		% max. dAUDPC	
	Variance	Std. Dev	Variance	Std. Dev
Isolate:Tent:Tray	0.16	0.40	66.22	8.14
Isolate:Tent:Tray:Block	0.17	0.41	16.99	4.12
Residual	2.35	1.53	683.65	26.15

There was little virulence to *Ae. tauschii* accessions in terms of pycnidia production compared to responses seen in susceptible wheat controls, which were all above the regression line in response to cfz008 (**Figure 18**). This was particularly true for IPO323, in response to which significant pycnidia cover was extremely rare although there was much variation in necrosis cover. As expected, the virulence of cfz008 on *Stb16q* resulted in increased disease cover in the panel, but there were still many accessions presenting very good resistance to this isolate.

Although the linear mixed model suggested that there was a significant difference between the means of necrosis values between isolates (**Table 5**), the responses were very strongly correlated (**Figure 19**). This confirms that accession is the most important factor when it comes to necrosis. Conversely, pycnidia responses were weakly correlated.

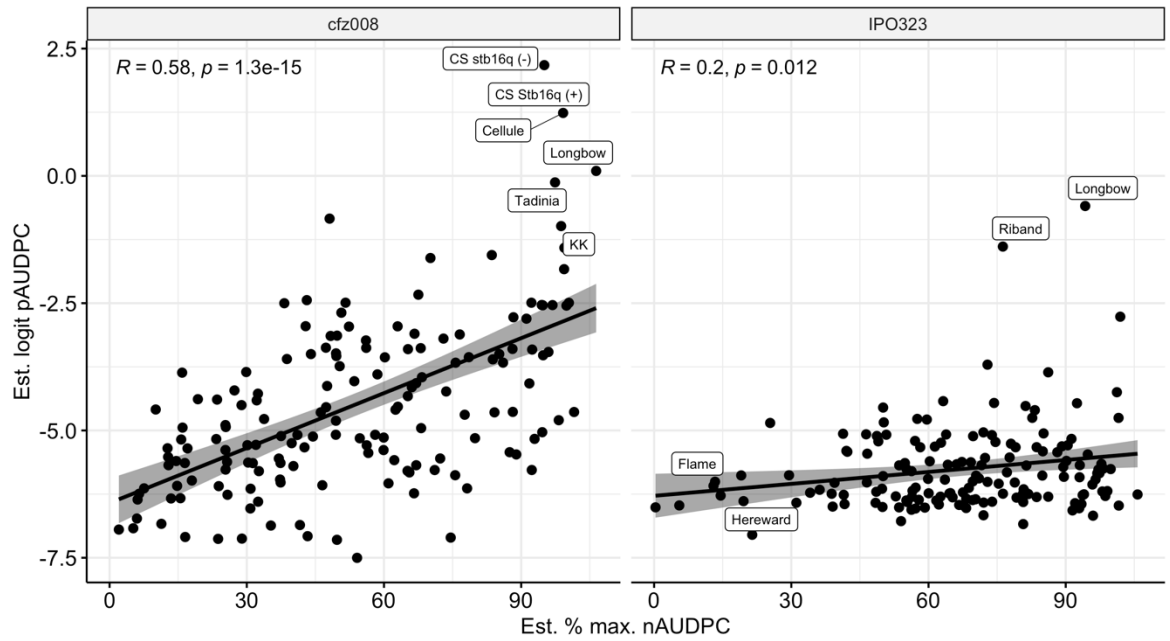


**Figure 18:** Estimated mean pycnidia and damage scores of wheat lines and 151 *Ae. tauschii* accessions inoculated with *Z. tritici* isolates cfz008 (left) and IPO323 (right). Wheat controls are labelled. There were no resistant controls for cfz008. For IPO323, Flame and Hereward were negative controls and Longbow and Riband were included as positive controls. Logit values of 2.5, 0, -2.5, -5 and -7.5 back-transform to 92%, 50%, 8%, 0.7% and 0.1%.

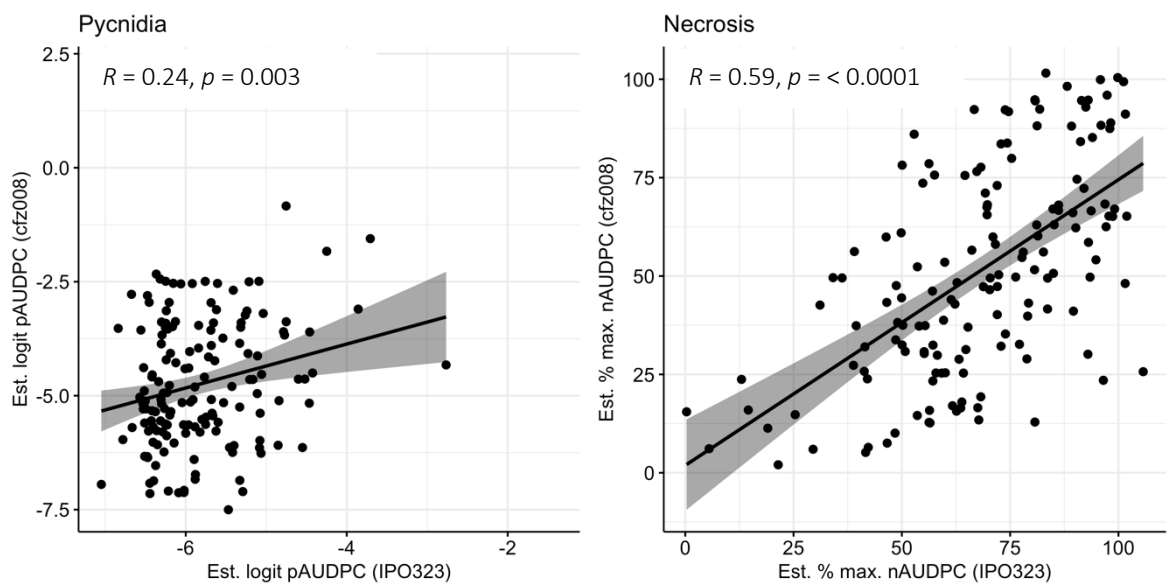


**Figure 19:** Pycnidia and necrosis scores in response to IPO323 and cfz007 plotted against one another.

These *Septoria* phenotypes (both pycnidia and damage for both isolates) were then combined with whole-genome shotgun sequences of the *Ae. tauschii* in a *k*-mer-based GWAS. Unfortunately, no clear association was found between pycnidia phenotypes and *k*-mers generated from *Ae. tauschii* whole-genome shotgun data (example plot for IPO323 pycnidia data is displayed in **Figure 20**). There are many cases where *k*-mers form horizontal lines across the plot, likely arising from a lack of phenotypic diversity across the panel leading to resistance being confounded with large differences in genotype. These analyses were performed on calculated line means from the last scoring day; it is possible that more refined results could be garnered from rerunning the analysis with the more thoughtfully manipulated datasets described above, but the likelihood seems low given the below plot.

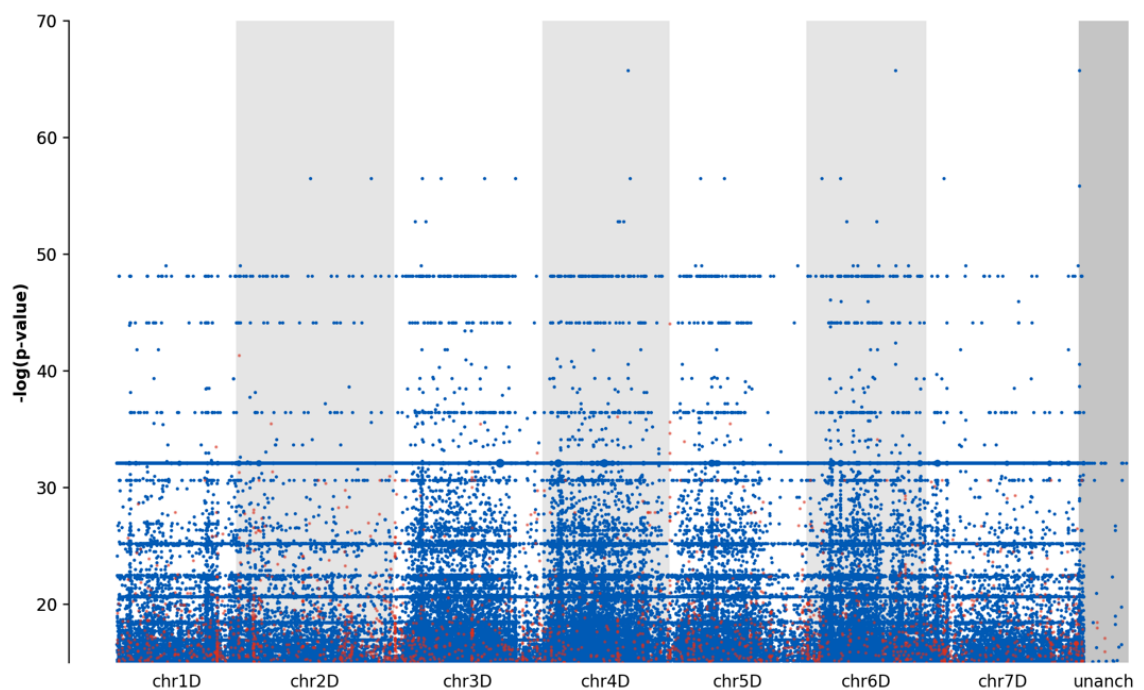


**Figure 20:** Manhattan plot of IPO323 pycnidia phenotypes (calculated means from the last scoring day) associated with *k*-mers generated from *Ae. tauschii* whole-genome shotgun data. Reads were mapped to the *Ae. tauschii* reference genome AL8/78. Analysis and figure were generated by Kumar Gaurav.

As observed above, there was more diversity in necrosis responses of *Ae. tauschii* when infected by *Z. tritici*. When the GWAS was carried out on this data, several loci were found to be associated with necrosis, all located towards the telomeres (**Figure 2121**). Blue 1-4 were associated with lower necrosis in response to cfz008 and were located on 2DS, 3DS, 4DL and 6DS. Interestingly, both Blue 3 and Blue 4 were also associated with lower necrosis in response to IPO323, although there was more noise in this plot. This suggests that these loci are isolate-non-specific. Two major loci (Red 1 and Red 2) were associated with high necrosis, located on 3DL and 5DL. There were also red *k*-mers at the same locus as Blue 4 (6DS). This could mean that there are two alleles at this locus, associated with high or low necrosis.

The experiment with necrosis data was repeated with reads mapped to Chinese Spring RefSeq v1.0. Most of the peaks observed when the data was mapped to *Ae. tauschii* were also present in Chinese Spring (**Figure 22**). The exception was Blue 4, which did not seem to be present at all in the Chinese Spring plots. Many of the peaks (Red 1, Blue 3 and Red 2) appeared less discreet when mapped to Chinese Spring. Red *k*-mers associated with high necrosis were present in the Blue 1 and 3 loci (associated with low necrosis when mapped to *Ae. tauschii*), suggesting that Chinese Spring carries a susceptible/high necrosis allele at these loci. The genes present within Chinese Spring peaks are listed in **Supplementary Table 1**.

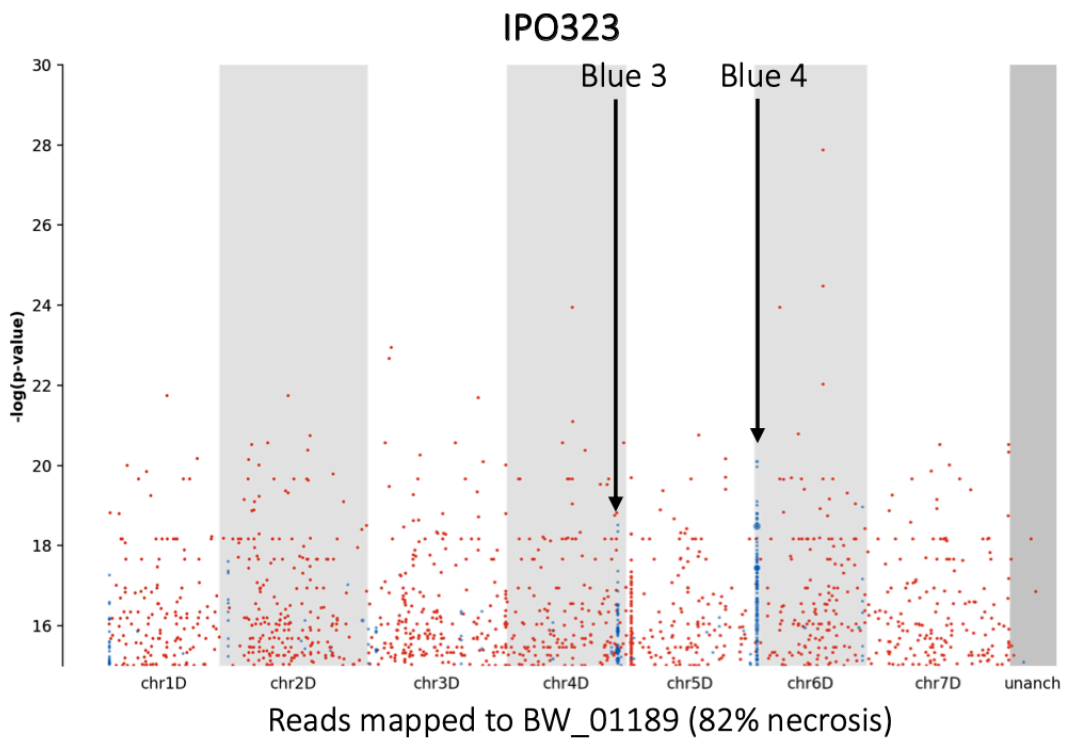
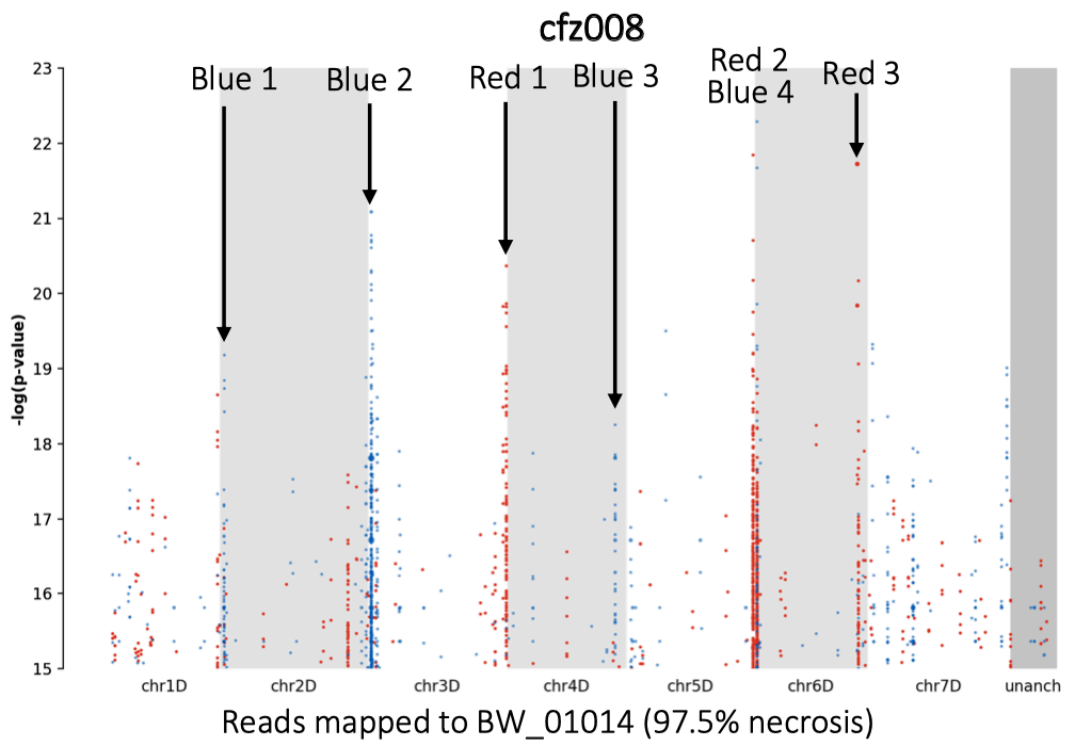


**Figure 21:** Manhattan plot of cfz008 and IPO323 necrosis phenotypes (calculated means from the last scoring day) associated with *k*-mers generated from *Ae. tauschii* whole-genome shotgun data. Blue dots indicate an association with less necrosis (green leaf tissue); red dots signify an association with high necrosis. Larger dots indicate a greater number of associated *k*-mers. Major peaks are labelled for reference. Reads were mapped to assemblies of accessions with high necrosis, phased with the *Ae. tauschii* reference genome AL8/78. Analysis and figure were generated by Kumar Gaurav.

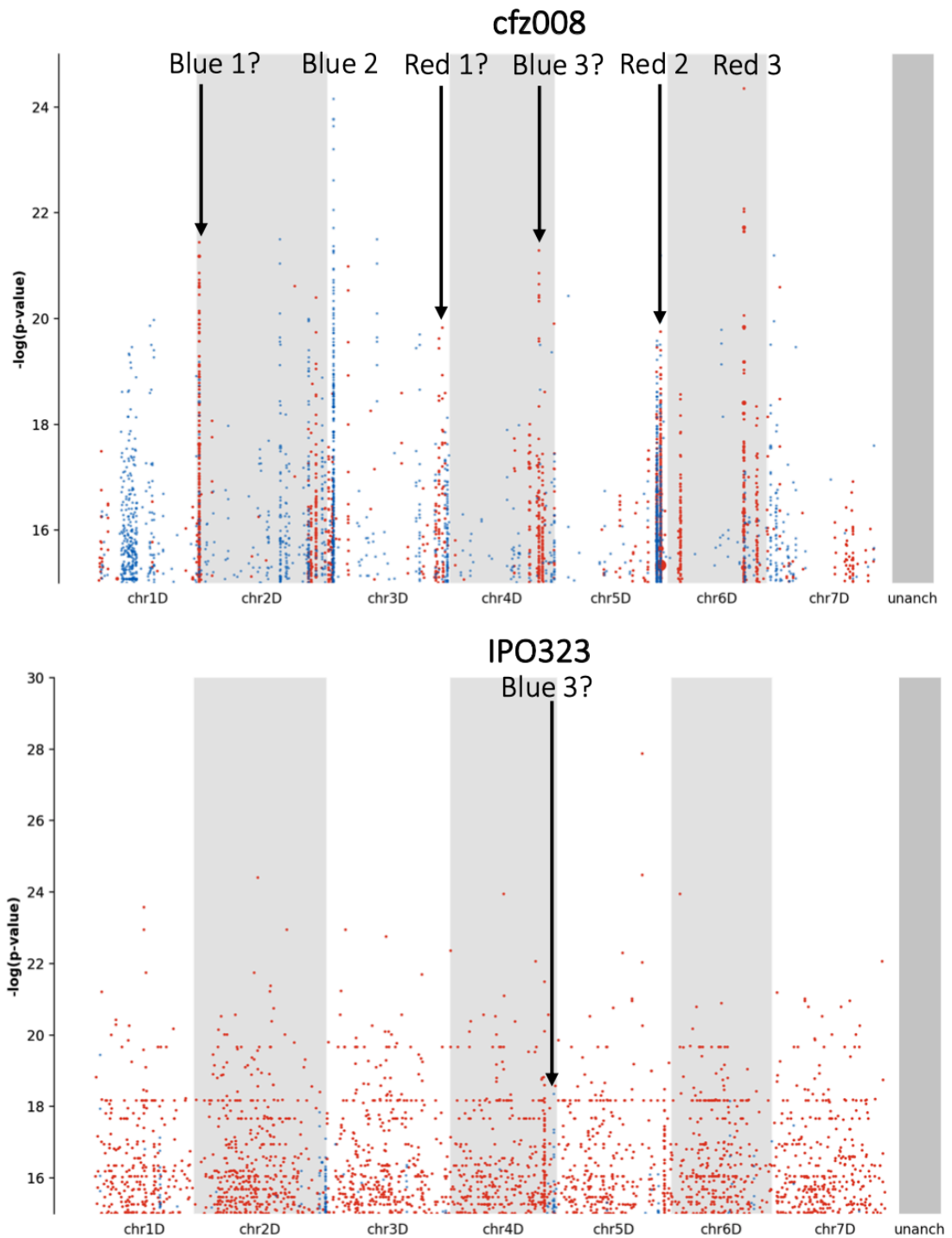


**Figure 22:** Manhattan plot of cfz008 and IPO323 necrosis phenotypes (calculated means from the last scoring day) associated with *k*-mers generated from *Ae. tauschii* whole-genome shotgun data and mapped to Chinese Spring RefSeq v1.0. Blue dots indicate an association with less necrosis (green leaf tissue); red dots signify an association with high necrosis. Larger dots indicate a greater number of associated *k*-mers. Major peaks are labelled for reference. Analysis and figure were generated by Kumar Gaurav.

## 2.4. DISCUSSION

There were very few *Ae tauschii* accessions that were susceptible to IPO323 based on pycnidia data compared to responses of Watkins lines (**Figure 31**). *Stb16q* appears to be quite important for Septoria resistance in this species, as virulence of cfz008 to this gene resulted in more diverse phenotypes during infection; however, even screening with an *Stb16q*-virulent isolate was not sufficient to obtain diverse enough phenotypes for GWAS. The phenotypes observed are not easily compared with wheat, due to the sparse and small nature of the pycnidia – even leaves with high pycnidia scores would have a much lower spore load compared to susceptible wheat leaves. Furthermore, the frequently observed phenotype (in response to IPO323 in particular) where many leaves had high necrosis values was much more frequent in *Ae. tauschii* than in wheat landraces (**Figure 31**). These differences could mean that *Ae. tauschii* has more minor genes that reduce pathogen reproduction, or that *Z. tritici* growth is different in a non-wheat background (or both).

In *Ae. tauschii*, 87 and 89% of the residual variance in pycnidia and necrosis, respectively, was unexplained and likely due to variation in responses of individual replicate leaves. This suggests that it is difficult to control for variation in the *Z. tritici*-*Ae.tauschii* interaction, and it may be fruitful to repeat experiments. However, the experiment was large enough to be able to detect significant variation between accessions and isolate-by-accession interactions, so the most likely limiting factor is the lack of susceptible lines in terms of pycnidia response. Residual variance in interactions with Watkins landraces was comparatively low (**Table 15**), demonstrating the more consistent and predictable pycnidia phenotypes that can be observed when *Z. tritici* is inoculated on more compatible hexaploid wheats. This would also be due to the fact that a higher proportion of total variance was explained by the fixed effect of variation between accessions, due to there being more susceptible lines in the assays of Watkins landraces. Overall, it appears that there is little susceptibility to STB in *Ae. tauschii* in terms of lesions bearing pycnidia.

Although the necrosis phenotype appeared to be quite strong, with many clear resistant and susceptible accessions as well as many intermediate responses, it is not entirely clear whether high necrosis is caused by the pathogen making a switch to necrotrophy, or by *Ae. tauschii*'s own defence responses. This is made more complex by the presence of wholly necrotic leaves with very little pycnidia, or with small patches of pycnidia that often only appeared on the leaf tip – especially when the leaf tip had fallen into the wet matting beneath the seedling trays. Therefore, it is difficult to interpret the loci associated

with necrosis responses. Some loci appeared to be associated with less necrosis in *Ae. tauschii* and high necrosis in Chinese Spring, suggesting allelic rather than presence-absence variation between the two phenotypes. The Blue 3 peak was not detected when reads were mapped to Chinese Spring; if a candidate gene can be identified in this region, its presence in other wheat lines could be tested. It may be that the locus is specific to *Ae. tauschii*. Within all of the peaks mapped to Chinese Spring, Knetminer identified genes that were associated with disease resistance (**Supplementary Table 2**). However, it is difficult to predict what genes involved in necrosis response to *Z. tritici* may be like, as none have yet been cloned. Furthermore, necrosis responses appeared to differ more between accessions than between isolates, so it would be beneficial to perform a mock inoculation to control for accession-specific necrosis responses (a similar method was used by Ajaz et al. (2021)). This would ensure that any candidate regions investigated are specifically associated with responses to isolates of *Z. tritici*.

Kema *et al.* (1996b) suggested that pycnidia and necrosis were separately capable of identifying gene-for-gene interactions between resistance and virulence loci in *Z. tritici* and wheat, although they resulted in different clusters of cultivars and isolates suggesting that these two responses may be under different genetic control. Upon infection of *Z. tritici* isolates collected from durum wheat on bread wheat, Kema *et al.* (1996b) observed that small necrotic spots indicative of a hypersensitive response appeared. In the reverse situation, with bread wheat isolates on durum wheat, large amounts of necrosis resulted along with little evidence of spore production. The response of *Ae. tauschii* seems to be very much comparable to the latter interaction. Histological studies showed that phenotypes with high necrosis and few pycnidia have low levels of colonisation, suggesting that, although necrosis is brought about by the pathogen, it may imply avirulence (Kema *et al.*, 1996b). Microscopy or chitin binding assays could be used to investigate the extent of pathogen colonisation in necrotic leaves, to examine the relationship between necrosis and colonisation in *Ae. tauschii*.

The failure of the pathogen to produce pycnidia in some interactions could be due to the relative lack of coevolution of *Z. tritici* isolates collected from bread wheat with *Ae. tauschii*. This seems to be especially true in the case of IPO323; as mentioned above, virulence of cfz008 to *Stb16q* seems to allow the pathogen to overcome some incompatibility barriers. More isolates could be tested to evaluate how line-specific the high necrosis phenotype is, as well as the extent of pycnidia production that is possible on *Ae. tauschii*. Screening more isolates and comparing to cfz008 responses could also add to our knowledge of the importance of *Stb16q*. It is possible that the recent gain of virulence

to *Stb16q* in *Septoria* populations is akin to a host jump – this gene seems to have provided *Ae. tauschii* with adequate protection against a huge range of *Z. tritici* isolates, perhaps for thousands of years, but was defeated relatively quickly when deployed in wheat fields. The *Stb16q*-virulent isolate cfz008 that developed on Cellule was then able to cause susceptibility in *Ae. tauschii*. *Stb16q* can therefore be seen as a cautionary tale in the utilisation of wheat genetic resources for *Septoria* resistance.

Seifbarghi *et al.* (2009) found that *Septoria* spp. isolated from *Ae. tauschii* were so specialised that they did not infect any other hosts, including other *Aegilops* species, and *Z. tritici* isolates from wheat were unable to infect *Ae. tauschii* even though these bread-wheat adapted strains did infect *Triticum dicoccum*, *T. durum* and *T. compactum*. This suggests that *Ae. tauschii* may have some singular characteristics that enable only specifically-adapted *Septoria* species to achieve consistent or widespread virulence. Seifbarghi *et al.* (2009) also reported that symptoms in *Ae. tauschii* took longer to appear than wheat-adapted *Z. tritici* on wheat (2 months compared to 15 days); that lesions were more necrotic than grey or brown, as seen in wheat; that pycnidia were sparse, small and often solitary; and, finally, that disease severity was greater in older leaves. These observations largely align with those described in this chapter, suggesting that small, sparse pycnidia on a backdrop of extensive necrosis is the most likely ‘susceptible’ phenotype in *Ae. tauschii* when infected with wheat-pathogenic isolates. Very similar non-host or marginal host responses were observed in the interaction between *Brachypodium distachyon* and *Z. tritici* (O’Driscoll *et al.*, 2015).

In the interaction between *Z. tritici* and *Triticum monococcum*, some pycnidia-like phenotypes were observed that were in fact incompatible interactions leading to the formation of immature pycnidia (Jing *et al.*, 2008). They also observed blackened stomata, likely caused by melanisation of the fungus in the substomatal cavity. Many of the pycnidia scores gathered in this chapter likely represent these phenotypes rather than properly developed pycnidia. In particular, blackened patches observed in accessions such as BW\_21493 (**Figure 17**) more clearly appear to be melanised stomata rather than fruiting bodies. This would need to be confirmed through more detailed phenotyping under a microscope; however, to screen the panel of 151 accessions this way would require more sources of variance to be introduced, such as other scorers or multiple batches. It could be interesting to investigate whether there are particular genes for marginal host resistance to *Septoria* that have been conserved across grasses like *Ae. tauschii*, *T. monococcum* and *B. distachyon*, and whether there could be applications for these in wheat breeding. Although some of these phenotypes are associated with necrosis,

they also greatly reduce the amount of spore production by, for example, arresting fungal development in the substomatal cavity, which could have a positive impact at the field and landscape scale. This comes with the caveat that it is difficult to introgress traits from wild species into crops, especially if they are polygenic.

One explanation for the sparse pycnidia development on *Ae. tauschii* could be that the stomatal penetration efficiency of *Z. tritici* on this species is low. When individuals from multiple lesions coalesce, *Z. tritici* seems to be more efficient at filling sub-stomatal cavities with pycnidia, resulting in a higher density of these structures (Fones et al., 2015). It has been demonstrated that the stomatal density of the adaxial leaf surface can impact resistance of *Gentiana triflora* to the related pathogen *Septoria gentianae* (Tateda et al., 2019). The stomata of *Ae. tauschii* and *B. distachyon* are distinctly smaller than those of wheat (Toda et al., 2021), which could possibly have an effect on *Z. tritici* penetration. Assays of stomatal penetration efficiency as in the study by Fones et al. (2015) could be carried out to allow more precise observation of lesion formation in *Ae. tauschii* and answer this question.

Ajaz et al. (2021) found evidence of both broad-spectrum and isolate-specific interactions between *Ae. tauschii* and *Z. tritici*, and some interactions appeared to consistently result in susceptibility. Therefore, it seems there is scope to improve the consistency and diversity of responses in this system with different isolates, conditions or host genotypes. The challenge may lie in finding a panel large and responsive enough to facilitate *R* gene cloning via association genetics. It would be interesting to discover whether the most susceptible line in the Ajaz et al. (2021) study carried *Stb16q*, and therefore whether its absence could explain much of the susceptibility to *Z. tritici* that was observed.

STB could be allowed to develop for 2 months or longer, as was done for the *Ae. tauschii*-adapted *Septoria* isolate tested by Seifbarghi et al. The cabinets employed in this thesis were not at the correct containment level for such experiments due to the risk of sexual reproduction. It is possible that *Septoria* development on *Ae. tauschii* is accelerated during the production of pseudothecia later in the infection. It could also be fruitful to test more isolates that are adapted to *Ae. tauschii*. Isolates from the Middle East where *Ae. tauschii* is most common, and where wheat and *Z. tritici* have been coevolving for the longest, may infect *Ae. tauschii* between growing seasons, for example. Another way to gain clearer phenotypes in this interaction could be to use pathogen culture filtrates or to extract apoplastic fluid from susceptible wheat lines infected with *Z. tritici* and infiltrate the fluid into *Ae. tauschii* leaves. This should result in easily reproducible and scorable phenotypes

as it removes the barrier of host colonisation, which may be even more of an obstacle when wheat-adapted isolates are inoculated onto *Ae. tauschii*. Such methods are often successful in the *Parastagonospora nodorum*-wheat and *Cladosporium fulvum*-tomato pathosystems, even more so if effectors can be purified and infiltrated (Liu et al., 2012; De Wit, 2016). In order to investigate non-host resistance genes in *Ae. tauschii*, susceptible accessions could be crossed over several generations to gain extremely susceptible variants. These lines could then be crossed to accessions that are immune to STB in order to map and clone non-host resistance genes. This approach has been employed to investigate non-host resistance genes for wheat leaf rust in barley (Wang et al., 2019).

As discussed above, there are several avenues through which the interaction between *Ae. tauschii* and *Z. tritici* could be better understood and applied to wheat breeding. However, since the interaction is not straightforward to dissect, conducting STB research on SHWs to access D genome diversity may be more practical. When working with wild grasses there are obstacles such as poor growth habit and the encasement of seed in thick glumes which hinder germplasm multiplication and approaches like biparental mapping. If association genetics could effectively be employed for Septoria resistance in *Ae. tauschii*, some of these hurdles could be overcome; but it seems to be the case that the disadvantages outweigh the advantages for this system. Since the key goal of this work was to identify candidate genes for STB resistance via GWAS, it seemed most prudent to change focus to a more well-adapted panel of hexaploid wheat landraces, the Watkins collection. This work is described in the following two chapters.

### 3. EXPLORING HOST-PATHOGEN INTERACTIONS BETWEEN WATKINS LANDRACES AND *Z. TRITICI*

‘Such balanced populations - variable, in equilibrium with both environment and pathogens, and genetically dynamic - are our heritage from past generations of cultivators. They are the result of millennia of natural and artificial selections and are the basic resources upon which future plant breeding must depend.’

J. R. Harlan (1975)

### 3.1. INTRODUCTION

#### 3.1.1. A landrace by any other name would prove as intractable

**L**andraces are likely to contain untapped diversity for many traits, including disease resistance. According to Villa et al. (2005), crop landraces can be defined as:

‘a dynamic population(s) of a cultivated plant that has historical origin, distinct identity and lacks formal crop improvement, as well as often being genetically diverse, locally adapted and associated with traditional farming systems.’

The duration of use for individual landraces can be measured in decades to centuries; a minimum age of ‘one farmer generation’ has been proposed (Villa et al., 2005). This highlights the intimate connection of landraces to people and place. Generations of farmer seed selection and saving in a specific location led to local adaptation and the development of recognisable characteristics within landraces, whilst seed exchange networks enabled the introduction of new local or exotic germplasm, maintaining genetic diversity (Villa et al., 2005). The boundary between wild relatives, landraces and cultivars is not always clear; landraces can range from naturally-selected ecotypes that have not been fully domesticated to cultivars that have been grown without high selection pressure for specific traits and uniformity, thus backpedalling to landrace status (Villa et al., 2005). In cereals, novel uses or the presence of unusual traits, such as horny wheat or six-row barley, may be enough to define a landrace, since formal crop improvement has acted to eradicate such features (Villa et al., 2005).

It is often assumed that modern cultivars are less well-adapted to suboptimal or low input environments than landraces (for example, such an outcome is described as ‘inevitable’ by Villa et al. (2005)). Voss-Fels et al. (2019) demonstrated that breeding has increased cultivar performance in both high and low input environments over the last fifty years; breeding in a high-input environment therefore does not seem to make cultivars less viable when inputs are reduced, so the above assumption may be incorrect (although this study did not look at landraces, but older cultivars). A feature of landraces is that they are often incredibly locally-adapted; therefore, their advantages can be more obvious when they are grown in the relatively narrow ranges of conditions in which they can excel. Although cultivars are also more well-adapted to certain regions, many breeding

programmes involve trialling cultivars across many regions of a country or even continent (e.g. CIMMYT), resulting in cultivars that are more generally successful rather than ones that exploit resources better at a smaller scale.

In arid to Mediterranean conditions tested in Israel, landraces of bread and durum wheat were little impacted by aridity but were still outperformed in terms of yield and other traits by modern cultivars; the best-performing landrace had 80.4% of the yield of modern cultivars (Frankin et al., 2021). Much of the yield disparity was likely due to lodging, so the introduction of reduced height genes to these landraces could perhaps close the yield gap in arid environments. Again, however, this did not survey the strengths of locally adapted landraces (those used in the above study were exotic). Mexican wheat landraces were found to have a better capacity for extracting water from the deepest part of the soil and establishing early groundcover, amongst other traits, that gave them an advantage over Mexican cultivars under drought stress conditions (Reynolds et al., 2007). Likewise, landraces from Iran, Turkey and Afghanistan outcompeted similarly-adapted cultivars in two of four sites tested, despite high disease pressure (Morgounov et al., 2021). Again, lodging was an issue for some landraces. These studies demonstrate how specific adaptations in landraces could be promising breeding targets for improving cultivars.

Another factor is yield stability – the inherently diverse population structure of landraces may result in ‘built-in’ insurance of yields in the face of adverse conditions (Villa et al., 2005). For example, landraces of crops such as rice, pearl millet and sorghum are often favoured for yield stability, and farmer surveys in the Iberian Peninsula have shown that landraces are preferred due to their enhanced disease resilience, local adaptation and cultural importance such as cooking characteristics and tradition (Calvet-Mir et al., 2011; Ficiyan et al., 2018). Furthermore, regions that cultivate landraces also typically have high overall agrobiodiversity due to small-scale farming, which may enhance the resilience of the whole region against crop failure (Ficiyan et al., 2018). This may result in better yields over time compared to modern cultivars, but trials may not test landraces as they were originally developed (as diverse collections of recognisably similar germplasm) but rather as single accessions planted in monoculture. The process of reducing the diversity of landraces to single accessions for the purpose of curating diversity panels must result in the loss of diversity; furthermore, it confounds some of the key characteristics of landraces – that they are dynamic and diverse. The full benefits of traditional landrace-based agricultural systems in marginal or highly specialised environments are therefore very difficult to test and compare to modern cultivars. It seems clear that the true nature of landraces is something so ephemeral and intimately

connected to cultural practices and place that it cannot be easily captured or replicated. The most representative way to evaluate the strengths of landraces in agriculture may be to evaluate *in situ* those currently still being maintained within more traditional farming systems, for example in parts of Tajikistan where landraces are favoured for their adaptation to high altitude and suitability for home breadmaking (Husenov et al., 2021).

It seems important to keep in mind the cultural and historical significance of landraces. Their traditional names and specific end-uses, for example, may be lost once they are reduced to a numerical identifier within a diversity collection. More concerningly, the priority placed upon some elements within the definition of landraces may be given more weight than others, which could influence the landrace material and associated cultural heritage that is ultimately conserved. In the UK, the most important traits were defined as heterogeneity (by collection curators) or uniqueness of traits (by plant breeders) (Villa et al., 2005).

Although modern cultivars have many benefits, such as performing exceptionally in high-input and broad-ranging environments, landraces can still compete in terms of specialist traits and even yield. Therefore, there are still benefits that can be garnered from looking back at the landraces which gave rise to modern wheat.

### 3.1.2. The collection of wheat landraces in the 20<sup>th</sup> century and unexpected theoretical journeys: there and back again

By the end of the 20<sup>th</sup> century, 75% of the crop genetic diversity was lost worldwide and over 90% of crop varieties had disappeared from agricultural systems (FAO, 1998; <http://www.fao.org/3/y5609e/y5609e02.htm>). The rollout of modern, high-yielding cultivars likely contributed to this, particularly during the Green Revolution, and, as the importance of landrace diversity and its decline began to be recognised, collectors began attempting to preserve this germplasm in earnest (Harlan, 1975):

‘We could afford to squander our genetic resources because we never had much of our own, and we could always send collectors to such places as Turkey, Afghanistan, Ethiopia, India, Southeast Asia, China, Mexico, Colombia, and Peru and assemble all the diversity we could use.’

The work of N. I. Vavilov in preserving and understanding crop diversity in the early 20<sup>th</sup> century was landmark. The Russian collection of plant genetic resources, established in 1894, is one of the oldest in the world, and was later named the Vavilov Institute of Plant Genetic Resources (VIR); the collection grew from 301 accessions in 1901 to 325,000 in 2015 (Dzyubenko, 2018). Vavilov dedicated the first part of his career to collecting and investigating genetic resources for staple crops and their wild relatives, which led to the identification of new species of wheat (Vavilov, 1931) and informed the development of later theories. Before Vavilov's work, species were considered the basic units of diversity; through his differential method of taxonomy, the diversity below the species level (infraspecific diversity) was recognised and species were divided into subspecies, varieties and forms as we understand them today (Hawkes, 1999). Their relation to geography was also better understood. Vavilov (1922) stated that: 'the more we study our plants and animals, the more variable they are, the more varieties we find among Linnean species'. He separated wheat into eight Linnean species, with bread wheat divided into around 60 classes based on: beardedness, ear colour, ear smoothness/hairiness (awns), seed colour, and habit (winter/spring). Vavilov observed 'parallelism' of these varietal groups repeated in all wheat species, illustrating the 'law of homologous series' in which varieties in one crop species are likely to be present in another related species – an example of convergent evolution (Vavilov, 1922). These ideas were put forward in the hope that they could be used to define more systematic classification systems for crops. He also noted the determination of up to 220 racial differences within single varieties of wheat. This is perhaps illustrative of the diversity still present within cultivars at that time, which was beginning to be broken down into more uniform groups.

Vavilov also developed the theory that there were centres of diversity for crop species, generated through a combination of geographical and human diversity that allowed the interactions between tribes employing ancient agricultural techniques to generate diverse crops (Vavilov, 1926, cited by Harlan, 1975). He wanted to discover the 'bricks and mortar' from which modern cultivars were derived, for the benefit of the Soviet Union and 'socialistic agriculture' (Vavilov, 1931):

'We study the construction of primitive agricultural implements in order to get indications for the construction of modern machinery'

The centre of species formation of wheat was designated as South-Western Asia, which is consistent with modern analyses which point to the Fertile Crescent (Pont et al., 2019). The greatest diversity of bread wheat was found in eastern Afghanistan, so this was

determined as the precise centre of origin (Watkins, 1933). The varying microclimates of mountainous and tropical regions were recognised as cauldrons for generating inter- and intra-species diversity of crops. Vavilov's career is an example of how the study of diversity in itself can provide fundamental insights, as well as providing more tangible outcomes by generating genetic resources for breeding.

The belief in the value of the germplasm collection at VIR was so strong amongst scientists at the time that many died in their attempts to protect it during the siege of Leningrad by the Axis powers during World War 2, from 1941 to 1944 (Loskutov, 1999). Vavilov himself had already been arrested by this time for his outspoken and 'anti-Soviet' defence of genetics. Research and maintenance of the collections continued throughout this period, despite the constant threats of bombing and starvation. Strict control measures were in place 24 hours a day to protect the collections from theft by the starving population of Leningrad. Many researchers at the institute starved to death whilst steadfastly protecting collections of wheat, rice, peas and corn (Loskutov, 1999). Because of these unfathomable efforts, a vast and unique source of crop diversity has been preserved until the present day.

Contemporaries of Vavilov also collected wheat around this time. For example, John Percival, the first Professor of Agricultural Botany at the University of Reading in 1909, collected 2,500 wheat accessions as well as publishing a monograph of wheat (Bunting, 2001). A. E. Watkins from the School of Agriculture at Cambridge was inspired by Vavilov's work (Wingen et al., 2014) and exchanged material with him and John Percival amongst others working in wheat (Miller et al. 2001). The lines of thinking below (Watkins, 1933) foreshadow the gathering of a landrace collection that would later be used to contribute valuable insights into the genetic groups present in wheat and their geographic origins:

'The cultivators may have attained only a low level of culture, and thousands of years may have elapsed before they produced a civilization of which the marks have endured. But to know where the different species of cultivated plants originated must help to trace the origins and diffusion of civilizations.'

Watkins gathered bread and durum wheat landraces from local farmers and markets in the 1920s and 1930s, mostly in Asia and Europe (Wingen et al., 2014). He also used his connections with the London Board of Trade to gather landraces from further regions, in Africa and Australia – in total, landraces were gathered from 34 countries. The collection

was at one time comprised of over 7,000 diploid, tetraploid and hexaploid accessions, but many were lost in storage to grain moth during the Second World War. Today, 826 viable bread wheat landraces remain, which along with additional diploid and tetraploid lines comprise the modern collection of 1,300 accessions in total, housed at the John Innes Centre in Norwich, UK (Miller et al., 2001).

As discussed above, this collection can at best provide a snapshot of the wheats that were being grown during the collection period, and cannot represent the true variety within landraces at that time. Watkins' key interest was in the genetics of ear characteristics which he used to classify the accessions, such as awning and the colouration of grains and glumes (Miller et al., 2001). This led to publications elucidating the genetic control of awning as well as the inheritance of glume shape. As such, there may be a bias in the collection, since Watkins selected plants which exhibited phenotypes that he was interested in (Miller et al., 2001). But, ultimately, this has little bearing on the utility of the collection. Within a diversity collection as large as the Watkins, it is amazing to consider the centuries of history, people and practices that led to the development of each accession, and how these histories have manifested in swathes of genetic diversity that can be explored and used to bolster our modern cultivars.

The specific interest of this thesis, the investigation of diverse germplasm for *Septoria tritici* blotch resistance, can be framed within the visions of scientists like Watkins and Vavilov: what can the diversity of a trait like *Septoria* resistance tell us about the history of wheat in the world, and how can we use this information to prepare for the future?

### 3.1.3. Studies of the Watkins collection and associated resources

The Watkins collection has been genotyped with 41 microsatellite markers, used to demonstrate a level of genetic diversity above that of a modern collection of European winter bread wheat from 1945-2000 – although the European collection was much narrower in geographic scope (Wingen et al., 2014). In 2018, 804 Watkins accessions were genotyped to a higher density (35k Wheat Breeders' Array – 32,443 polymorphic markers) (Winfield et al., 2018). Accessions were assigned to three clusters: Asia & Middle East, Western Europe & North Africa and Eastern Europe & Asia. The collection was also compared with 1003 modern, elite hexaploid bread wheat accessions from across Africa, Australia, the Americas, the Middle East and Europe. This was a more appropriate comparison than the 2014 study. 32.2% of markers from the 820 k Axiom Array were

unique to 120 core accessions from the Watkins collection, whilst 21.5% were unique to 145 core accessions from the elite collection, demonstrating the genetic diversity waiting to be unlocked within the Watkins collection.

As well as revealing the ancestry of modern wheat, the Watkins collection has been used to identify novel resistance loci for eyespot (Burt et al., 2014) and rust (Bansal et al., 2011; Toor et al., 2013; Bansal et al., 2013; Randhawa et al., 2015). A study by Doohan et al. (2021) identified Watkins lines with very good resistance to up to five isolates of *Z. tritici*, highlighting the potential utility of the panel for breeding in this key trait. Genomic selection for leaf, yellow and stem rust resistance has also been demonstrated in a subset of Watkins lines (Daetwyler et al., 2014).

These landraces have large tetraploid or hexaploid genomes, but research is facilitated by the growing genetic and genomic tools that have been developed, such as a nested association mapping panel (Wingen et al., 2017), RenSeq data and, most astoundingly for a collection of over 800 wheats, whole-genome shotgun data (the WatSeq collaboration between JIC and AGIS). Combined with high-quality reference genomes for wheat (International Wheat Genome Sequencing Consortium (IWGSC) et al., 2018; Walkowiak et al., 2020) and wild relatives such as *Ae. tauschii* (Luo et al., 2017; Zhou et al., 2021), wild emmer (*Triticum turgidum* ssp. *dicoccoides*; Avni et al., 2017) and *Triticum urartu* (Ling et al., 2018), it is an exciting time to apply new approaches to cloning resistance genes in both old and new wheat, as well as their relatives.

#### 3.1.4. Septoria isolates investigated in this chapter

In this chapter, a range of Septoria isolates were screened against subsets of the Watkins collection. Three Dutch isolates have been included: IPO323, IPO89011 and IPO94269. IPO323 was used to map and subsequently clone the resistance gene *Stb6* in cultivars Flame and Hereward, and Chinese Spring, respectively (Brading et al., 2002; Saintenac et al., 2018). There is also evidence of a second unidentified gene for resistance to IPO323 in the cultivar KK (Chartrain et al., 2005a). IPO89011 was used to map the *Stb9* resistance gene to 2BL in cultivars Courtot and Tonic (Chartrain et al., 2009). Finally, two sources of resistance to IPO94269 have been identified – *Stb5* and *Stb10* (Arraiano et al., 2001b; Chartrain et al., 2005a).

Ethiopian isolate IPO88004 is avirulent to *Stb15* and was used to designate and map this gene to the short arm of chromosome 6A in the wheat cultivar Arina (Arraiano et al., 2007). The Mexican isolate IPO90012 was used to map the *Stb11* gene to the short arm of chromosome 1B in the line TE9111 (Chartrain et al., 2005b). Also isolated from Mexico, IPO90004 is a widely virulent isolate with uncharacterised resistance present in the cultivar Olaf (Kema et al., 1996b). Two other widely-virulent isolates were included – IPO92006 and JIC040. Resistance to the Portuguese isolate IPO92006 has been identified in the wheat line Bastard II (Arraiano and Brown, 2006) and Cellule (data in this chapter). Cellule is known to carry the gene *Stb16q*, which suggests that this may be the source of resistance in both cultivars. JIC040 was isolated in Norfolk around 2010 and was also found to be avirulent to Cellule (data in this chapter) – so *Stb16q* may provide resistance to both of these isolates that may have a functional avirulence gene recognised by *Stb16q*.

*Z. tritici* resistance in the UK wheat cultivar Cougar was specifically broken down in 2015 (<https://ahdb.org.uk/news/septoria-tritici-disease-resistance-in-winter-wheat>), and there have since been Cougar-associated STB outbreaks in Ireland (Kildea et al., 2021). As the Cougar virulence continues to spread, further increasing durable resistance in current wheat varieties is a high priority. To this end, a Cougar Collection of *Z. tritici* was isolated by Sarah Holdgate (NIAB) in 2015 and 2016 including the Cougar007 isolate used in the present study.

### 3.1.5. Summary of chapter findings

A key finding of this chapter is that there is a huge amount of diversity in the responses of the Watkins collection to the *Z. tritici* isolates tested – from near immunity to up to eight isolates to extreme susceptibility far beyond the responses seen in the wheat positive controls, and the full range of phenotypes in between.

There is evidence of isolate-specific effects in the strong genotype-by-isolate interactions which resulted from statistical analysis of all assays in this chapter. This is also demonstrated by the divergence of responses from line means for particular isolates. Furthermore, some of the isolates tested elicit very similar responses from the Watkins lines tested, whilst others seem to employ a different line of attack.

The relationship between pycnidia and damage responses was examined: damage may be a useful indicator of pathogen colonisation when pycnidia cover is low or null, and there

are Watkins lines which have consistently low damage scores. Further investigation could show that such lines permit less pathogen colonisation than others. Additionally, a new trait was observed, deemed “super necrosis”. The consistent manifestation of this trait is measurable, is isolate and genotype specific, and seems to be associated with resistance in the epidemiological sense that it prevents spore formation.

The above observations can be used to determine the most suitable isolate and germplasm combinations for genetic studies (**Chapter 5**). Furthermore, the broad-spectrum resistance observed in some Watkins landraces could be introduced into breeding programs.

### 3.2. MATERIALS AND METHODS

An overview of the experiments discussed in this chapter is provided below (**Figure 23**).

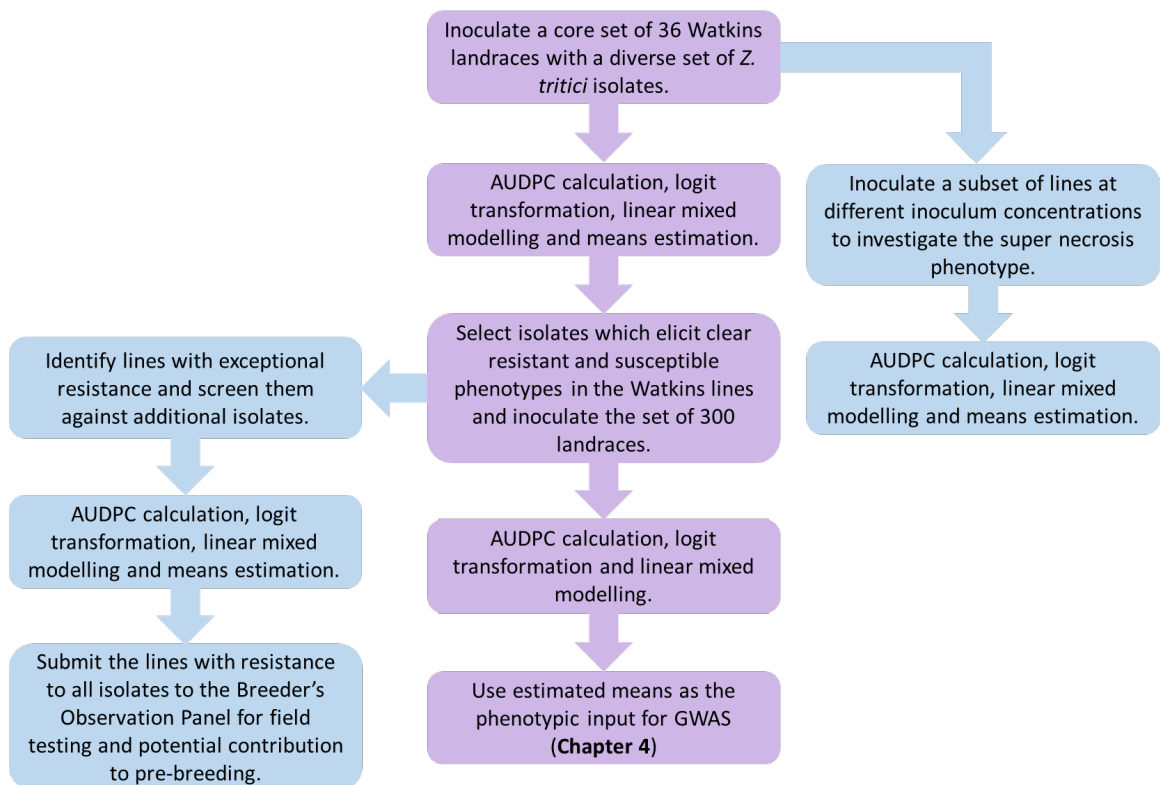


**Figure 23:** Flow diagram giving an overview of the projects undertaken within this chapter. The main project is shaded in purple, whilst secondary projects are in blue.

### 3.2.2. Plant and pathogen material

Of the total 826 lines in the Watkins collection, core sets representing the majority of genetic variation present in spring growth types have been determined (Luzie Wingen, JIC). In this chapter, the core 300 and core 36 diversity sets have been employed. These vary greatly in both their geographic and genetic diversity (**Table 7**). Wheat varieties were also included due to prior knowledge of their responses to *Z. tritici* isolates or because of their associated genetic resources (**Table 8**).

**Table 7:** Watkins landraces included in Septoria assays, their origin and core set designation.

Ancestral groups are as described in Wingen *et al.* (2014).

ID	Core 36	Country of Origin	Ancestral Group	Group Code
W004		Iraq	1.3.C-E-Asia	1.3
W007		Australia	2.4.S-Med-Afr	2.4
W008		Portugal	2.4.S-Med-Afr	2.4
W012		India	2.3.E-Eur	2.3
W015		Yugoslavia	2.3.E-Eur	2.3
W023		Australia	2.5.N-Med	2.5
W024		Australia	2.2.N-Eur-Asia	2.2
W030		Australia	Mix 1.2:4	1.2
W032		India	1.4.Eur-Asia	1.4
W034		India	1.4.Eur-Asia	1.4
W042		France	2.2.N-Eur-Asia	2.2
W044		Morocco	2.4.S-Med-Afr	2.4
W045		Syria	2.4.S-Med-Afr	2.4
W046		Crete	Mix 2.2:3	2.2
W053		Spain	2.4.S-Med-Afr	2.4
W063		Spain	2.3.E-Eur	2.3
W066		Spain	2.4.S-Med-Afr	2.4
W067		Spain	2.3.E-Eur	2.3
W079		India	2.4.S-Med-Afr	2.4
W081		India	2.3.E-Eur	2.3
W082		India	2.2.N-Eur-Asia	2.2
W083		Spain	2.4.S-Med-Afr	2.4
W088		Poland	1.3.C-E-Asia	1.3
W094		India	2.5.N-Med	2.5

W103		Italy	2.5.N-Med	2.5
W104		Italy	2.1.S-Eur-Asia	2.1
W106		France	2.5.N-Med	2.5
W114		Yugoslavia	1.1.USSR	1.1
W115		Yugoslavia	2.4.S-Med-Afr	2.4
W117		Spain	2.5.N-Med	2.5
W124		India	1.4.Eur-Asia	1.4
W125		India	Mix 2.1:3	2.3
W126		India	1.4.Eur-Asia	1.4
W127		India	1.1.USSR	1.1
W129		India	2.3.E-Eur	2.3
W130		Spain	2.5.N-Med	2.5
W136		Australia	2.4.S-Med-Afr	2.4
W138		Australia	2.2.N-Eur-Asia	2.2
W139		France	2.5.N-Med	2.5
W141		China	2.4.S-Med-Afr	2.4
W145		Spain	2.4.S-Med-Afr	2.4
W149		United Kingdom	2.2.N-Eur-Asia	2.2
W151		Portugal	2.5.N-Med	2.5
W153		Portugal	1.3.C-E-Asia	1.3
W155		Portugal	1.1.USSR	1.1
W160		Spain	Mix 2.1:5	2.1
W164		India	2.1.S-Eur-Asia	2.1
W166		India	1.4.Eur-Asia	1.4
W167		India	2.4.S-Med-Afr	2.4
W181		Poland	2.2.N-Eur-Asia	2.2
W186		Italy	2.3.E-Eur	2.3
W187		Italy	2.5.N-Med	2.5
W189		France	2.2.N-Eur-Asia	2.2
W199		India	Mix 1.3:4	1.4
W206		India	Mix 2.1:2:3	2.3
W209	Yes	Egypt	1.3.C-E-Asia	1.3
W213		Morocco	2.3.E-Eur	2.3
W216		Morocco	2.4.S-Med-Afr	2.4
W218		Tunisia	2.4.S-Med-Afr	2.4
W219	Yes	Spain	2.4.S-Med-Afr	2.4

W222		Crete	2.4.S-Med-Afr	2.4
W223		Burma	2.4.S-Med-Afr	2.4
W224		China	2.4.S-Med-Afr	2.4
W228		Spain	2.4.S-Med-Afr	2.4
W229		Portugal	2.5.N-Med	2.5
W231		Hungary	2.2.N-Eur-Asia	2.2
W232	Yes	India	2.5.N-Med	2.5
W233		India	2.3.E-Eur	2.3
W237		Iran	1.4.Eur-Asia	1.4
W238		Iran	1.4.Eur-Asia	1.4
W239		Spain	Mix 2.4:5	2.5
W240	Yes	Iran	2.5.N-Med	2.5
W241		India	1.1.USSR	1.1
W242	Yes	India	1.4.Eur-Asia	1.4
W246		India	1.3.C-E-Asia	1.3
W248		India	2.5.N-Med	2.5
W254		Morocco	2.5.N-Med	2.5
W260		Canary Islands	2.4.S-Med-Afr	2.4
W262		Canary Islands	2.4.S-Med-Afr	2.4
W264		Canary Islands	Mix 2.4:5	2.4
W268	Yes	Spain	2.5.N-Med	2.5
W271	Yes	Spain	1.3.C-E-Asia	1.3
W273	Yes	Spain	1.3.C-E-Asia	1.3
W277	Yes	Spain	2.1.S-Eur-Asia	2.1
W286		Greece	2.4.S-Med-Afr	2.4
W290		Crete	1.3.C-E-Asia	1.3
W291		Cyprus	Mix 2.3:4	2.4
W292	Yes	Cyprus	2.3.E-Eur	2.3
W293		Turkey	2.4.S-Med-Afr	2.4
W297	Yes	Turkey	1.1.USSR	1.1
W298		Turkey	1.4.Eur-Asia	1.4
W299		Turkey	1.3.C-E-Asia	1.3
W300		Turkey	1.3.C-E-Asia	1.3
W301	Yes	Turkey	2.5.N-Med	2.5
W302		Syria	1.1.USSR	1.1
W304		Syria	2.4.S-Med-Afr	2.4

W305		Egypt	2.4.S-Med-Afr	2.4
W308		Iran	1.4.Eur-Asia	1.4
W315		China	2.1.S-Eur-Asia	2.1
W316		China	1.2.Chi-Ind	1.2
W317	Yes	China	Mix 1.1:3	1.1
W321		China	1.2.Chi-Ind	1.2
W339		Portugal	2.5.N-Med	2.5
W346		Bulgaria	2.3.E-Eur	2.3
W347		Bulgaria	2.3.E-Eur	2.3
W349		Bulgaria	2.5.N-Med	2.5
W351		Yugoslavia	2.3.E-Eur	2.3
W352		Yugoslavia	1.4.Eur-Asia	1.4
W355		Yugoslavia	2.2.N-Eur-Asia	2.2
W356		Yugoslavia	2.2.N-Eur-Asia	2.2
W360		Yugoslavia	1.1.USSR	1.1
W361		Yugoslavia	2.3.E-Eur	2.3
W363		Yugoslavia	Mix 1.3:4	1.4
W370		Yugoslavia	2.5.N-Med	2.5
W376		Iran	1.1.USSR	1.1
W379		Iran	1.3.C-E-Asia	1.3
W381	Yes	India	1.3.C-E-Asia	1.3
W382		India	1.1.USSR	1.1
W387		Spain	2.4.S-Med-Afr	2.4
W394		Portugal	Mix 1.3:4	1.4
W396		Portugal	2.5.N-Med	2.5
W397		Portugal	2.5.N-Med	2.5
W398		Palestine	2.4.S-Med-Afr	2.4
W399	Yes	China	1.2.Chi-Ind	1.2
W400		China	1.2.Chi-Ind	1.2
W401		Portugal	2.4.S-Med-Afr	2.4
W403		Spain	1.1.USSR	1.1
W404	Yes	Iran	1.1.USSR	1.1
W405		Iran	1.4.Eur-Asia	1.4
W406		India	1.3.C-E-Asia	1.3
W407	Yes	India	1.3.C-E-Asia	1.3
W409		India	1.4.Eur-Asia	1.4

W412		India	2.5.N-Med	2.5
W413		India	1.3.C-E-Asia	1.3
W414		India	2.3.E-Eur	2.3
W419		India	1.3.C-E-Asia	1.3
W420		India	1.3.C-E-Asia	1.3
W423	Yes	India	1.3.C-E-Asia	1.3
W424		India	1.4.Eur-Asia	1.4
W426	Yes	India	1.4.Eur-Asia	1.4
W428		India	1.3.C-E-Asia	1.3
W429		India	1.4.Eur-Asia	1.4
W430		India	1.3.C-E-Asia	1.3
W433		India	1.4.Eur-Asia	1.4
W435		China	1.3.C-E-Asia	1.3
W440		China	1.2.Chi-Ind	1.2
W444		China	2.4.S-Med-Afr	2.4
W446		China	1.2.Chi-Ind	1.2
W448		Romania	1.2.Chi-Ind	1.2
W449	Yes	Romania	1.2.Chi-Ind	1.2
W453		Afghanistan	2.4.S-Med-Afr	2.4
W456		Afghanistan	1.4.Eur-Asia	1.4
W458		Afghanistan	2.4.S-Med-Afr	2.4
W460		Afghanistan	2.2.N-Eur-Asia	2.2
W463		Afghanistan	2.5.N-Med	2.5
W465		Afghanistan	1.4.Eur-Asia	1.4
W468		Afghanistan	2.2.N-Eur-Asia	2.2
W470		Afghanistan	2.3.E-Eur	2.3
W471		Afghanistan	2.1.S-Eur-Asia	2.1
W473		Afghanistan	1.1.USSR	1.1
W474		Afghanistan	1.3.C-E-Asia	1.3
W475		Afghanistan	1.4.Eur-Asia	1.4
W478		Afghanistan	1.4.Eur-Asia	1.4
W483		Poland	2.5.N-Med	2.5
W484		Italy	2.3.E-Eur	2.3
W485		Algeria	1.4.Eur-Asia	1.4
W486		USSR	1.1.USSR	1.1
W487		USSR	1.4.Eur-Asia	1.4

W492	Spain	Mix 2.2:5	2.2
W493	Tunisia	1.1.USSR	1.1
W496	Morocco	2.4.S-Med-Afr	2.4
W505	Iran	1.3.C-E-Asia	1.3
W507	Australia	2.1.S-Eur-Asia	2.1
W509	Portugal	1.3.C-E-Asia	1.3
W512	India	1.4.Eur-Asia	1.4
W513	Iran	1.4.Eur-Asia	1.4
W515	Iran	2.5.N-Med	2.5
W517	India		
W520	India	2.1.S-Eur-Asia	2.1
W522	India	1.1.USSR	1.1
W528	China	1.4.Eur-Asia	1.4
W530	Afghanistan	2.1.S-Eur-Asia	2.1
W534	Morocco	2.3.E-Eur	2.3
W538	Tunisia	Mix 2.4:5	2.4
W541	Spain	2.5.N-Med	2.5
W543	Spain	2.5.N-Med	2.5
W546	Spain	2.4.S-Med-Afr	2.4
W547	Spain	1.3.C-E-Asia	1.3
W549	Spain	2.5.N-Med	2.5
W551	Spain	2.5.N-Med	2.5
W552	Canary Islands	2.4.S-Med-Afr	2.4
W557	Canary Islands	1.4.Eur-Asia	1.4
W560	Greece	2.4.S-Med-Afr	2.4
W561	Crete	1.3.C-E-Asia	1.3
W562	Greece	2.3.E-Eur	2.3
W563	Crete	2.4.S-Med-Afr	2.4
W565	Greece	1.3.C-E-Asia	1.3
W566	Greece	1.3.C-E-Asia	1.3
W568	China	1.3.C-E-Asia	1.3
W571	Turkey	2.5.N-Med	2.5
W572	Syria	1.4.Eur-Asia	1.4
W573	Turkey	1.4.Eur-Asia	1.4
W574	Turkey	1.3.C-E-Asia	1.3
W576	Iran	1.4.Eur-Asia	1.4

W578		Iran	2.4.S-Med-Afr	2.4
W579		Iran	1.4.Eur-Asia	1.4
W580	Yes	Iran	1.4.Eur-Asia	1.4
W583		China	1.2.Chi-Ind	1.2
W587		China	1.3.C-E-Asia	1.3
W590		Portugal	2.1.S-Eur-Asia	2.1
W591		Portugal	1.3.C-E-Asia	1.3
W594		Portugal	1.3.C-E-Asia	1.3
W596		Portugal	1.3.C-E-Asia	1.3
W598	Yes	Portugal	2.5.N-Med	2.5
W604		Spain	1.4.Eur-Asia	1.4
W605		Greece	1.1.USSR	1.1
W607		Yugoslavia	2.5.N-Med	2.5
W611		Yugoslavia	1.1.USSR	1.1
W614		Yugoslavia	2.1.S-Eur-Asia	2.1
W619		Yugoslavia	2.1.S-Eur-Asia	2.1
W622		Bulgaria	2.3.E-Eur	2.3
W623		Bulgaria	2.3.E-Eur	2.3
W625		Iran	1.3.C-E-Asia	1.3
W627		Iran	1.2.Chi-Ind	1.2
W629		Iran	1.2.Chi-Ind	1.2
W633		India	1.1.USSR	1.1
W637		Turkey	2.3.E-Eur	2.3
W639		Crete	2.5.N-Med	2.5
W644		India	1.3.C-E-Asia	1.3
W646		India	1.2.Chi-Ind	1.2
W648		China	1.3.C-E-Asia	1.3
W649		China	1.2.Chi-Ind	1.2
W650	Yes	China	1.1.USSR	1.1
W653		China	1.2.Chi-Ind	1.2
W655		China	1.2.Chi-Ind	1.2
W657		China	1.2.Chi-Ind	1.2
W662		Romania	2.3.E-Eur	2.3
W667		Afghanistan	2.4.S-Med-Afr	2.4
W668		Yugoslavia	1.4.Eur-Asia	1.4
W670		Poland	Mix 2.3:5	2.3

W671	Yes	USSR	1.4.Eur-Asia	1.4
W673		USSR	1.3.C-E-Asia	1.3
W676		Tunisia	2.3.E-Eur	2.3
W678		Iran	1.4.Eur-Asia	1.4
W680	Yes	Italy	1.4.Eur-Asia	1.4
W681	Yes	Iran	2.4.S-Med-Afr	2.4
W683		Spain	2.5.N-Med	2.5
W685		Spain	Mix 2.4:5	2.5
W690		Greece	2.5.N-Med	2.5
W694		India	1.2.Chi-Ind	1.2
W695		China	1.4.Eur-Asia	1.4
W697		India	1.1.USSR	1.1
W698		China		
W700		China	1.1.USSR	1.1
W704		Iran	1.3.C-E-Asia	1.3
W705		Iran		
W707		India	1.2.Chi-Ind	1.2
W711		India	1.3.C-E-Asia	1.3
W719		China	1.3.C-E-Asia	1.3
W721		China	1.3.C-E-Asia	1.3
W722		China	2.2.N-Eur-Asia	2.2
W724		India	2.2.N-Eur-Asia	2.2
W726		China	1.2.Chi-Ind	1.2
W727		China		
W728		Iraq	1.2.Chi-Ind	1.2
W729	Yes	Iran		
W731	Yes	India	1.4.Eur-Asia	1.4
W732		India	1.4.Eur-Asia	1.4
W737		Italy	2.3.E-Eur	2.3
W742		Algeria	2.4.S-Med-Afr	2.4
W743		USSR		
W746		USSR	1.1.USSR	1.1
W747	Yes	Ethiopia	1.1.USSR	1.1
W749		USSR	1.1.USSR	1.1
W750		USSR		
W752		USSR		

W759		USSR	Mix 2.1:5	2.5
W760	Yes	USSR	Mix 1.1:4	1.1
W769	Yes	Algeria	1.1.USSR	1.1
W770		USSR	Mix 2.4:5	2.5
W771	Yes	USSR	1.2.Chi-Ind	1.2
W773	Yes	USSR	1.3.C-E-Asia	1.3
W774		Ethiopia	1.3.C-E-Asia	1.3
W775		USSR	1.1.USSR	1.1
W777		Finland	1.2.Chi-Ind	1.2
W784		Italy	1.2.Chi-Ind	1.2
W788	Yes	USSR	1.1.USSR	1.1
W789		USSR	1.1.USSR	1.1
W794		USSR	1.4.Eur-Asia	1.4
W802		USSR	1.1.USSR	1.1
W803		India	1.2.Chi-Ind	1.2
W804		USSR	2.2.N-Eur-Asia	2.2
W806	Yes	Italy	1.4.Eur-Asia	1.4
W811		Tunisia	1.2.Chi-Ind	1.2
W814		Tunisia	1.3.C-E-Asia	1.3
W816		Italy	Mix 1.2:4	1.4
W823		China	1.2.Chi-Ind	1.2
W824		China	1.2.Chi-Ind	1.2
W827	Yes	China	1.2.Chi-Ind	1.2
W903		India	1.1.USSR	1.1

**Table 8:** Wheat lines included in Septoria assays and reasons for their inclusion. The top section of the table includes wheat lines whose genomes have been sequenced. Selections based on information from Arraiano & Brown (2006), Brown et al. (2015) and Chartrain et al. (2004).

Line	Reason for inclusion
Chinese Spring	Wheat reference genome (International Wheat Genome Sequencing Consortium (IWGSC) et al., 2018)
ArinaLrFor	Wheat pangenome (Walkowiak et al., 2020)
Baj	Wheat pangenome (Walkowiak et al., 2020)
Cadenza	Wheat pangenome (Walkowiak et al., 2020) TILLING population
CDC Landmark	Wheat pangenome (Walkowiak et al., 2020)
Lancer	Wheat pangenome (Walkowiak et al., 2020)
Paragon	Wheat pangenome (Walkowiak et al., 2020) Paragon x Watkins RIL populations
Robigus	Wheat pangenome (Walkowiak et al., 2020)
Baldus	Susceptible to IPO323, resistant to IPO89011
Bastard II	Resistant to IPO92006
Cellule	Widely resistant, resistant to IPO92006
Chaucer	Susceptible to IPO323
Courtout	Susceptible to IPO89011, resistant to IPO90012
Flame	Resistant to IPO323
Gene	Susceptible to CA30, resistant to IPO94269
KK	Susceptible to IPO94269, resistant to IPO323
Longbow	Widely susceptible
Olaf	Resistant to IPO90012

A range of *Z. tritici* isolates have been tested on the Watkins core collections (**Table 9**). These isolates were selected because of known avirulences to *Stb* genes of interest, or because resistance to these isolates is rare and finding new sources of resistance to them would be useful.

**Table 9:** Isolates tested on Watkins collection and sets of lines tested. S = seedling conditions, DL = detached leaf. For references re avirulence see Brown *et al.* (2015). Where the year of collection is not known, the paper wherein isolates are first described is given.

\* Based on experiments undertaken during my PhD.

\*\* Kema et al. (Kema et al., 1996b)

Isolate	Origin	Year collected	Known avirulence to <i>R</i> genes or cultivars	Watkins lines tested
IPO323	The Netherlands	1981	<i>Stb5, Stb6, Stb18</i>	Core 300 (S) Core 36 (DL) Dose effect set (S)
IPO88004	Ethiopia	1988	<i>Stb15</i>	Core 300 (S) Resistant lines (S)
IPO90012	Mexico	Kema et al. (1996b)	<i>Stb11</i>	Core 300 (S) Core 36 (DL)
IPO87019	Uruguay	Kema et al. (1996b)	<i>Stb7</i>	Resistant lines (S)
IPO89011	The Netherlands	1989	<i>Stb5, Stb9, Stb18</i>	Core 36 (DL) Dose effect set (S) Resistant lines (S)
IPO90004	Mexico	Kema et al. (1996b)	Widely virulent. Avirulent on Olaf**.	Resistant lines (S)
IPO92006	Portugal	Kema et al. (1996b)	Widely virulent. Avirulent on Cellule*.	Core 36 (DL)
IPO94269	The Netherlands	Kema et al. (1996b)	<i>Stb5, Stb10</i>	Core 36 (DL) Resistant lines (S)
CA30	California	(Somasco et al., 1996)	<i>Stb4</i>	Core 36 (DL)
Cougar007	UK	2015/2016	Widely virulent. Isolated from susceptible Cougar plants.	Resistant lines (S)
JIC040	Norfolk, UK	2012/2013	Widely virulent. Avirulent on Cellule*.	Core 36 (DL)

Methods for seedling pathology assays were broadly as described in section **2.2.** (distinctions described below).

### 3.2.3. Cabinet conditions for pathology assays

Trays were placed in a Conviron controlled environment cabinet with the following conditions: temperature of 18°C day/12°C night, humidity of 85%, 16-h photoperiod and a (PPFD) of 350 microEinstein/m<sup>2</sup> at plant height.

### 3.2.4. Phenotype data collection

Necrosis and chlorosis were recorded together as the 'damaged' leaf area.

Super necrosis (SN) was scored for large seedling assays of the core 300 Watkins collection. This was recorded as a qualitative trait (SN/non-SN; 1/0) when leaves became almost completely necrotic after the first or second scoring day. These scores were then manually checked to determine the most representative scoring day for SN response in each test. Line SN was determined by selecting lines for which more than half of replicates were scored as SN and the remaining replicates were highly damaged; this was to account for genotype-by-environment interactions which may have resulted in slower necrosis response in some replicates.

### 3.3. RESULTS

“I ought to propitiate you, for, to tell the truth, I am bound to bore you with figures. Statistics are rarely attractive to a listening audience; but they are necessary evils, and those of this evening are unusually doleful. Nevertheless, when we have proceeded a little way on our journey I hope you will see that the river of figures is not hopelessly dreary.”

The Wheat Problem – Sir W. Crookes (1917)

#### 3.3.1. Responses of a reduced core set of Watkins landraces to eight *Septoria* isolates in detached leaf conditions

The core set of 36 landrace lines was screened with eight *Z. tritici* isolates across three experiments/batches: CA30, IPO323, IPO88004, IPO89011, IPO90012, IPO92006, IPO94269 and JIC040. This was conducted in detached leaf conditions within agar boxes.

A linear mixed model was fitted to the transformed data. Some detached leaf boxes were mistakenly made up with half the concentration of agar typically used for *Septoria* assays (5 g/L<sup>-1</sup> rather than 10 g/L<sup>-1</sup>), so an Agar effect with two levels (full or half) was added to the model. Experiment describes the effect of the three batches in which isolates were inoculated onto plants. The JIC040 inoculation was replicated in two of these batches. Replicate describes the five biological replicates of each accession-isolate combination. Agar was fitted as a fixed effect, along with Experiment and the interaction between Lines and Isolates. Box (the agar box, nested within Isolate and Replicate) and the Line by Experiment effect were fitted as random effects. This model resulted in a good model fit for the both the damage and pycnidia datasets; for damage, % max. dAUDPC resulted in the best fit, with residuals roughly normally distributed, and the best fit for pycnidia was achieved with the logit pAUDPC dataset.

For both traits, there was a significant effect of isolate as well as an isolate-by-line interaction (**Table 10, Table 11**). This suggests that responses of the lines included were isolate-specific. Of the random effects that were fitted to pycnidia (logit pAUDPC) and damage (% max. dAUDPC) data, lines within experiments explained 12.5% and 5.8% of variance, whilst box explained 4.9% and 34% of variance, respectively. The Experiment:Line effect for pycnidia was also small compared to its standard error, suggesting that the relative susceptibility of lines is fairly consistent across experiments.

These values were relatively small in comparison to the larger residual terms which accounted for 82.6% and 60.2% of variance for pycnidia and damage datasets, respectively. This demonstrates a large effect of individual leaves or replicates within the experiment compared to other experimental design factors.

The flatter distributions of wheat response data to IPO323, IPO89011, IPO90012 and IPO88004 can be explained by more extreme phenotypes and fewer intermediate phenotypes in comparison to the other isolates tested (**Figure 24**). This could mean that a significant proportion of varieties in the panel have very strong resistance, possibly controlled by major genes. These isolates were then selected as those of the greatest interest for testing on a larger set of Watkins lines as they were deemed most likely to allow the identification of candidate resistance genes in subsequent analyses.

IPO92006 and JIC040 were the most aggressive isolates tested – there was little resistance in the core set to these isolates. Conversely, a greater range of resistant phenotypes were observed in response to IPO90012 and IPO94269. There was a strong correlation between damage and pycnidia for almost all isolates (**Figure 25**), although the responses were only weakly correlated for IPO323. Gene was included as a resistant control for CA30 based on previous work (Chartrain et al., 2004), but in this experiment the line had a high pycnidia score and was as susceptible as the positive control Baldus. A study of 12 *Z. tritici* isolates previously showed no evidence of isolate-specific interactions of wheat lines with CA30 (Chartrain et al., 2004), so the lack of resistance response in Gene is not necessarily representative of CA30-specific resistance in the panel (e.g. deriving from *Stb4*).

**Table 10:** ANOVA table of the linear mixed model on logit pAUDPC.

Term	Mean Square	Numerator DF	Denominator DF	F value	Pr(>F)
Agar	69.08	1	116.82	20.42	<0.0001
Experiment	601.07	1	35.46	177.68	<0.0001
Line	14.23	46	14.09	4.21	<0.0001
Isolate	188.35	7	96.05	55.68	<0.0001
Line:Isolate	9.67	258	119.14	2.86	<0.0001

**Table 11:** ANOVA table of the mixed model on % maximum dAUDPC.

Term	Mean Square	Numerator DF	Denominator DF	F value	Pr(>F)
Agar	342.60	1	123.44	1.48	0.23
Experiment	766.64	1	37.11	3.32	0.08
Line	1068.10	46	11.64	4.62	<0.01
Isolate	2254.75	7	131.26	9.76	<0.0001
Line:Isolate	488.37	258	112.97	2.11	<0.0001

**Table 12:** Random effects of the linear mixed model fitted to logit pAUDPC and % maximum dAUDPC scores.

Term	Logit pAUDPC		% max. dAUDPC	
	Variance	Std. Dev	Variance	Std. Dev
Isolate:Rep:Box	0.20	0.45	130.63	11.43
Experiment:Line	0.51	0.71	22.33	4.73
Residual	3.38	1.84	231.13	15.20

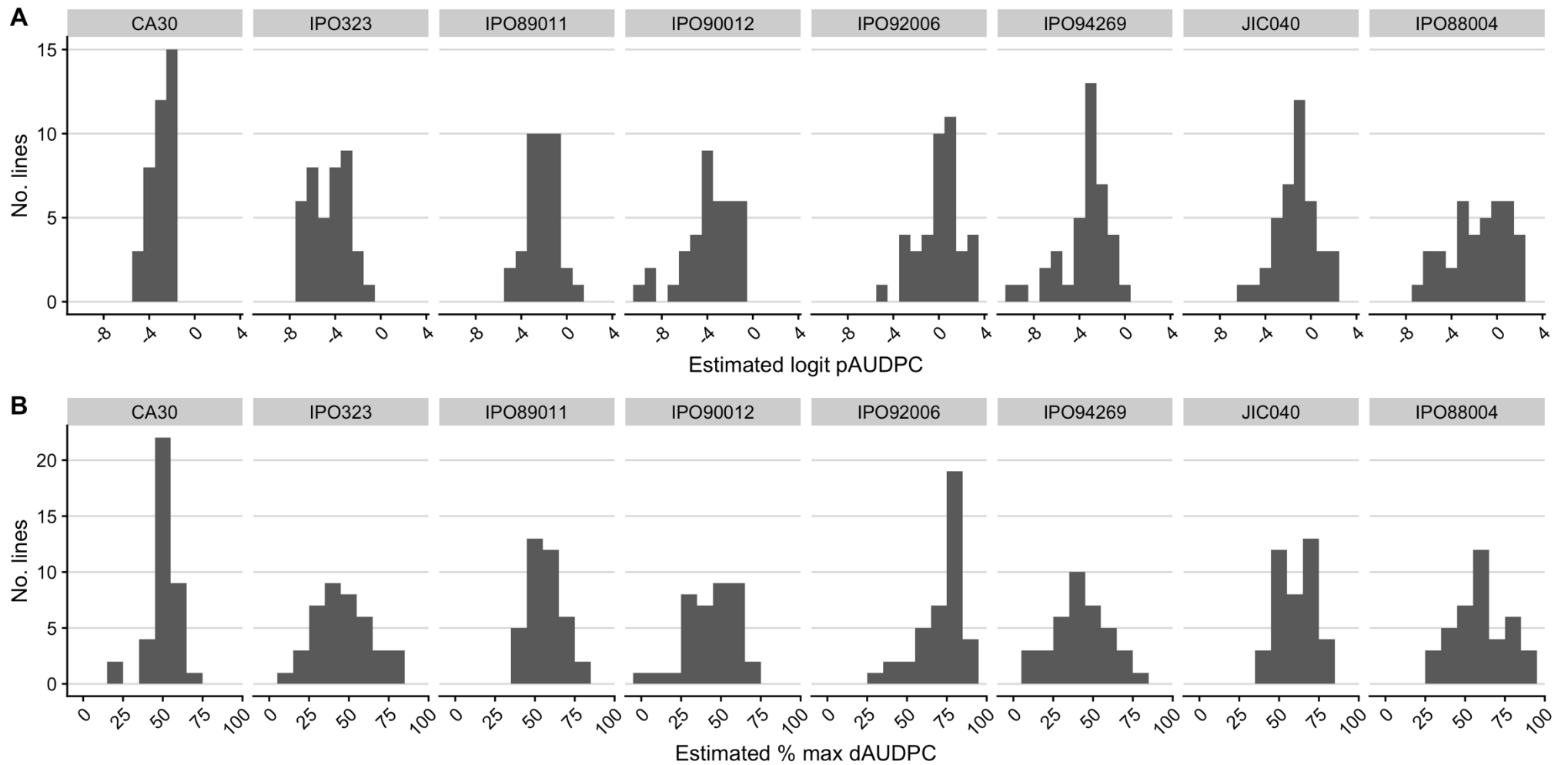


**Figure 24:** Histograms of estimated means derived from the linear mixed model fitted to detached leaf response data of Watkins core 36 lines inoculated with eight *Z. tritici* isolates.

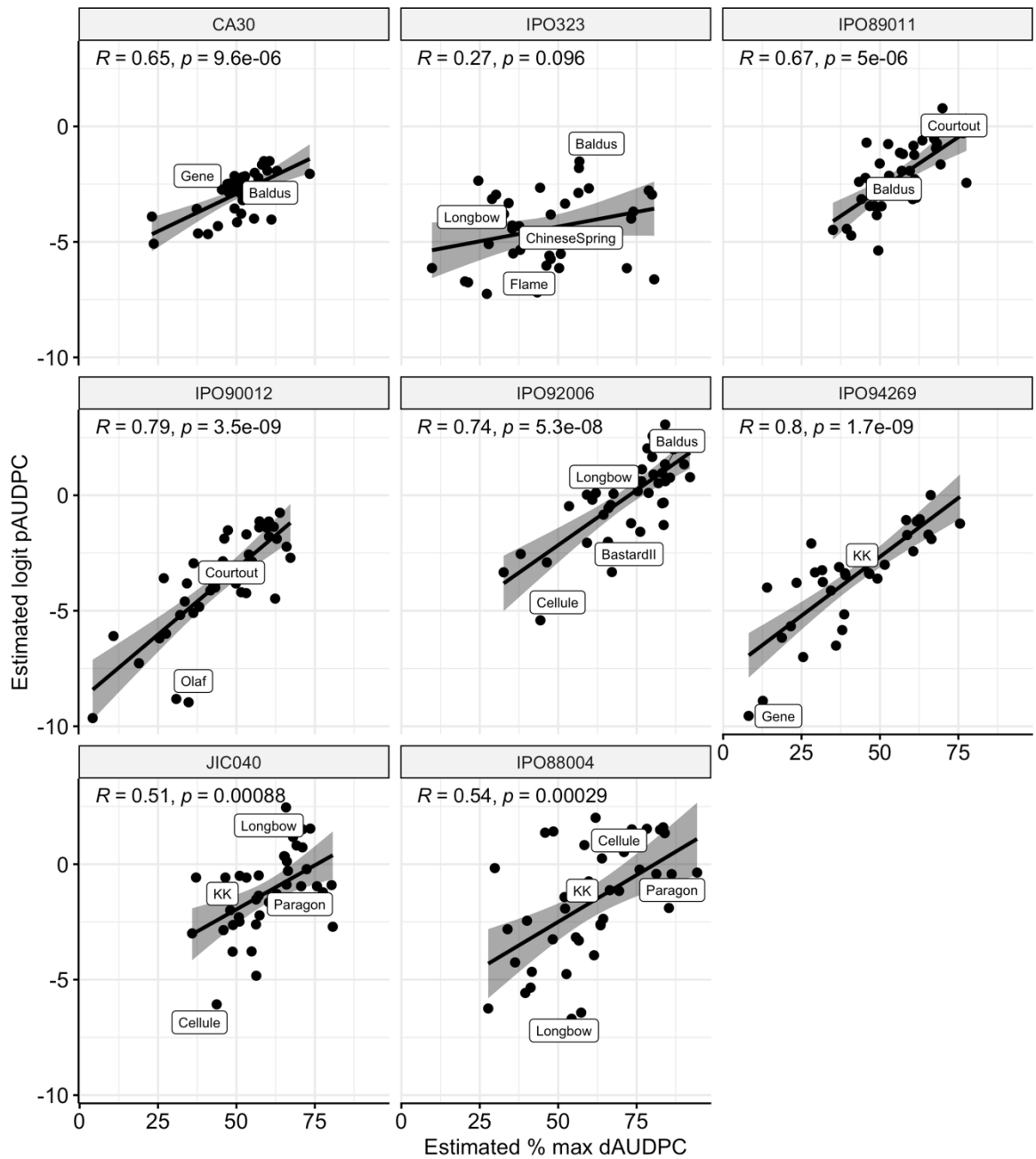


**Figure 25:** Relationship between pycnidia and damage estimated means derived from the linear mixed model fitted to detached leaf response data of Watkins core 36 lines inoculated with eight *Z. tritici* isolates. *R* gives the Pearson correlation score. Shaded area represents the 95% confidence interval.

To examine isolate-specificity further, the estimated means for the responses of lines to a particular isolate were plotted against the means of lines in response to all isolates (**Figure 26** and **Figure 27**). Responses to CA30 and IPO89011 did not correlate significantly with the line mean for pAUDPC. This suggests that responses are more isolate-specific – the genes controlling resistance to these two isolates may be independent of those for resistance to the other six. Responses to IPO323, IPO88004, IPO90012, IPO92006, IPO94269 and JIC040 were well-correlated with the mean line pAUDPC, which suggests that many lines responded similarly to all of the isolates tested.

From the below figures, it is clear that there were some isolate-specific interactions, particularly with IPO89011 and CA30 for which responses did not correlate with the mean response across isolates. However, isolate-specificity tended to differ between the pycnidia and damage datasets. W449 was more resistant than average to CA30 in terms of both pycnidia and damage, with a number of other lines resistant for pycnidia only (W769, W671, W407, W426, W242 and W827). W806 was more resistant to IPO323 than expected based on both pycnidia and damage scores, whilst W424 and W650 appeared to be outliers for pycnidia scores alone. Damage scores for IPO88004 were close to the line means, but W771, W423 and W240 appeared to show specific resistance to the isolate in terms of pycnidia response. For IPO89011, W273 showed a specific resistance response in terms of both damage and pycnidia, whilst W773 was highly resistant in the pycnidia dataset only. W268 was more resistant than average to IPO94269 (pycnidia and damage) and IPO92006 (damage only). The damage response of W277 also appeared to be specific to IPO92006. Finally, W760 was specifically resistant to IPO90012 in terms of both damage and pycnidia, whilst W271 was notably resistant in terms of pycnidia response alone. The overall picture is that both damage and pycnidia responses can be isolate-specific, but not necessarily under the same genetic control as there are differences depending on host genotype or isolate.

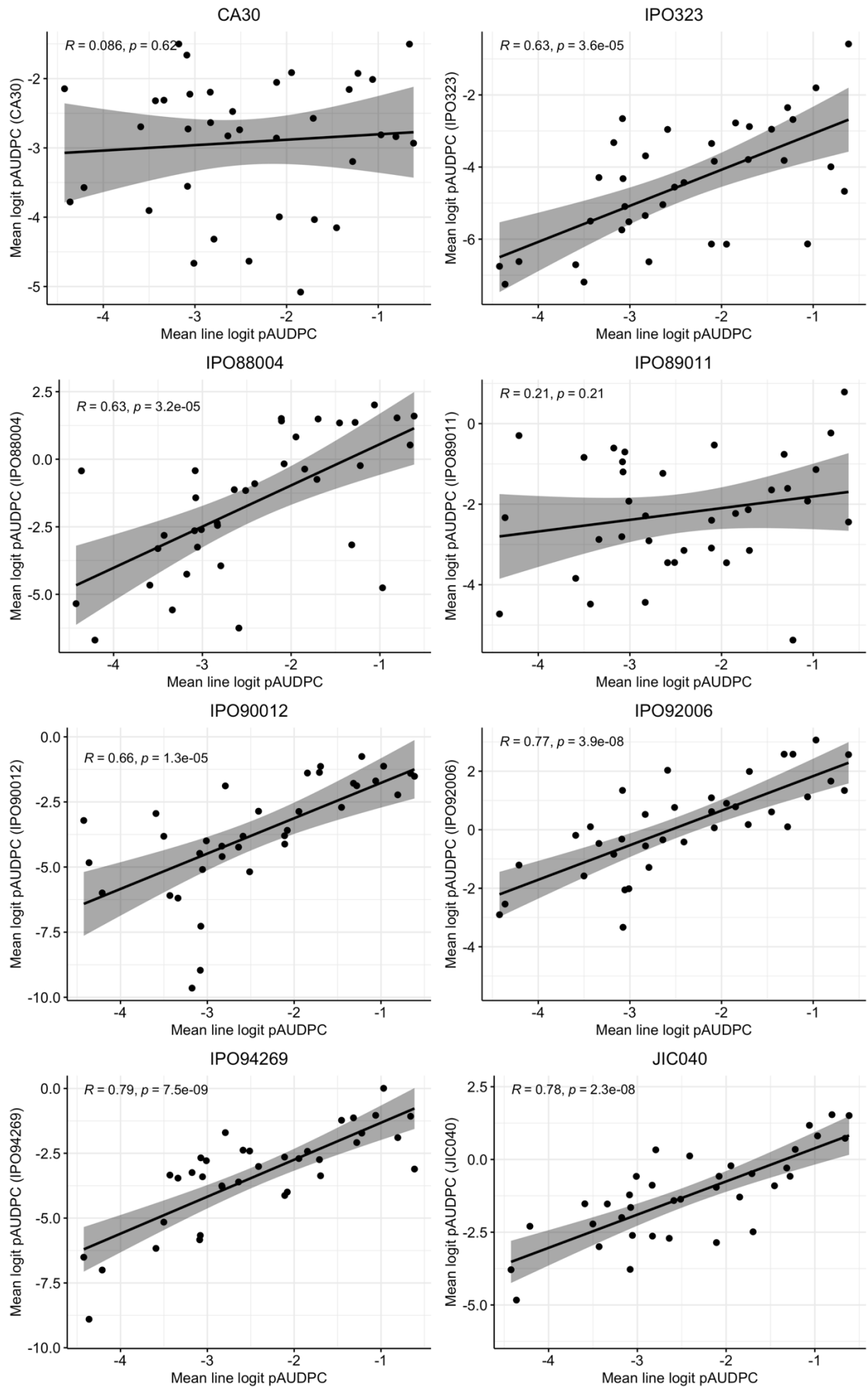


**Figure 26:** Means of logit pAUDPC responses to single isolates plotted against the means of lines across all eight isolates.  $R$  gives the Pearson correlation score. Shaded area represents the 95% confidence interval.

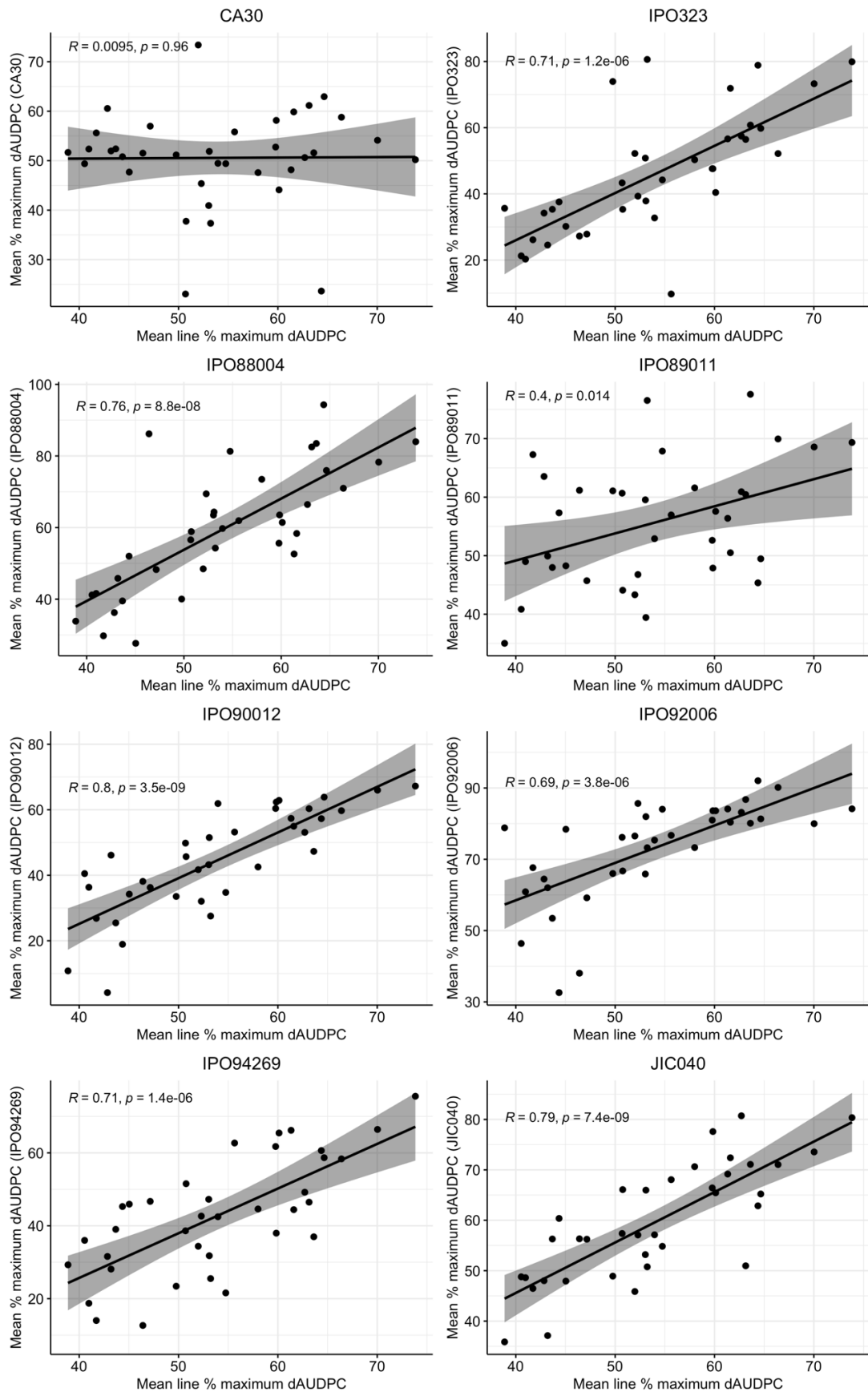


**Figure 27:** Means of % maximum dAUDPC responses to single isolates plotted against the means of lines across all eight isolates. *R* gives the Pearson correlation score. Shaded area represents the 95% confidence interval.

Of the isolates tested, responses to CA30 were the most divergent as they did not correlate significantly with pycnidia or damage responses to any other isolates (**Figure 28**).

Pycnidia responses to IPO89011 were also distinct from other isolates, although damage responses correlated with IPO323 and IPO88004. JIC040, IPO90012, IPO94269 and IPO92006 responses clustered together in terms of both pycnidia and damage scores, with responses to all of these isolates significantly positively correlated with one another.

IPO88004 pycnidia responses were only significantly positively correlated with IPO90012, whilst IPO323 correlated significantly with IPO94269, JIC040 and IPO92006. The damage responses to both IPO88004 and IPO323 were significantly positively correlated with damage responses to all isolates apart from CA30. Overall, there were more similarities between isolates when looking at damage data, with the exception of CA30 which did not have a significant relationship with any other isolates (also demonstrated by the plot of CA30 responses against line means, **Figure 26** and **Figure 27**). This demonstrates that damage responses can be isolate-specific, but are perhaps less so than pycnidia responses.

CA30 was quite aggressive compared to some other isolates tested (**Figure 24**), so it is possible that the Watkins landraces tested have not adapted much resistance to the perhaps distinct virulence mechanisms of isolate CA30. IPO323, IPO94269 and IPO89011 all originate from The Netherlands and share avirulence on *Stb5* (Arraiano et al., 2001b), but responses to IPO89011 were very distinctive. Possibly, *Stb5* is not prevalent in the Watkins lines tested as it typically has a strong effect (Arraiano et al., 2001b).

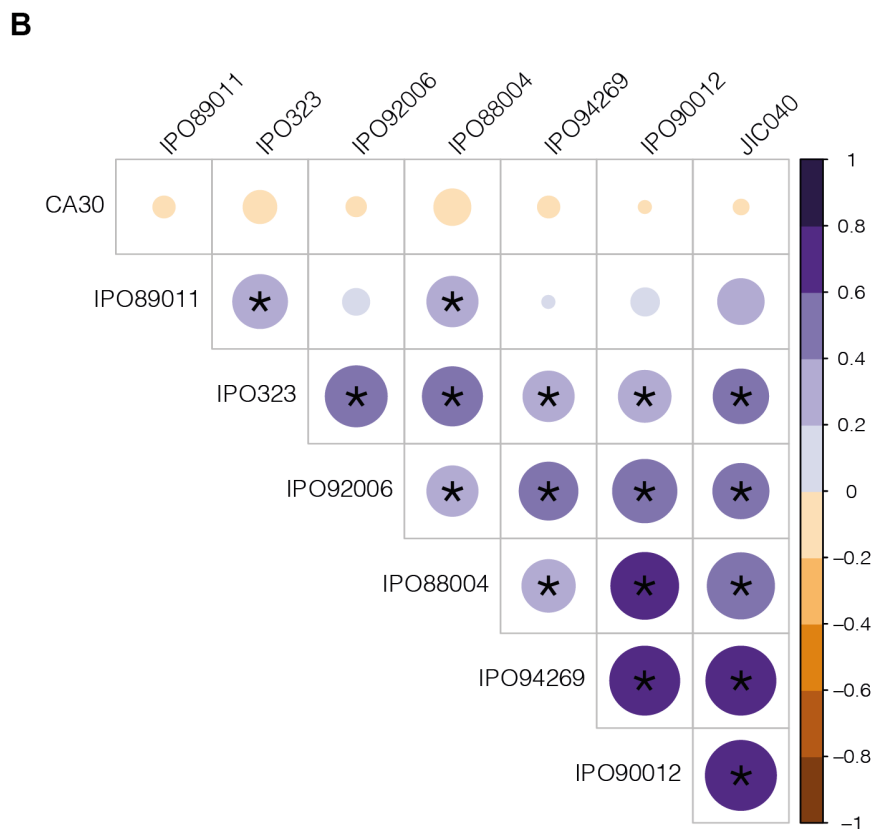
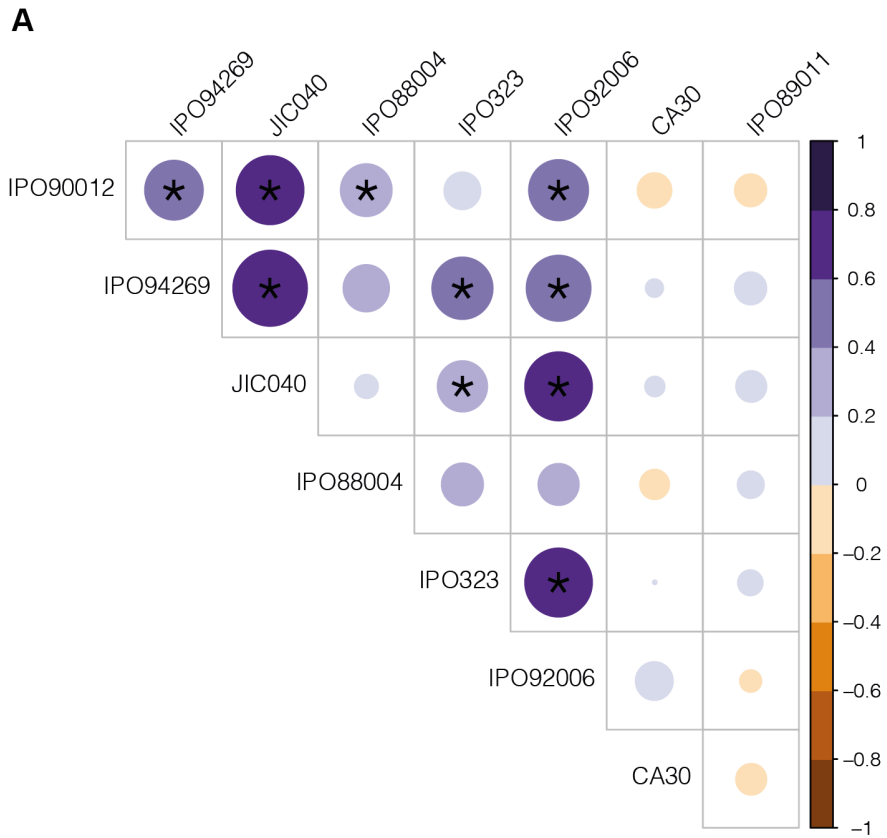


**Figure 28:** A matrix of correlations between pycnidia (A) and damage (B) responses to *Z. tritici* isolates in the Watkins core 36 set and wheat controls in detached leaf conditions. Circle size and colour indicate the size of the coefficient of correlation (large positive or negative numbers have a larger circle size). Statistically significant Pearson's correlation scores are marked with an asterisk ( $p = 0.05$ ).

### 3.3.2. Responses of the Watkins core 300 set to IPO323, IPO88004 and IPO90012

A range of phenotypes were observed in response to the three isolates tested on the Watkins core 300 set, and, although the data is quantitative in nature, phenotypes can be separated into several categories (**Figure 29**).



**Figure 29:** Leaf scan images of wheat and Watkins lines inoculated with *Zymoseptoria tritici* isolate IPO323 at 34 days post inoculation (seedlings around 7 weeks old). The key phenotypes observed were: full resistance, with leaves remaining green; clear susceptibility, with varying levels of fungal reproduction, and intermediate phenotypes, ranging from high necrosis with little/no spore production to mostly healthy leaves with single/few small lesions.

The main effect of Isolate on pycnidia scores was not significant, with a  $p$ -value just above 0.05, but there was a significant effect of the Isolate-by-Line interaction on both pycnidia and damage scores (**Table 13**). This suggests that pycnidia levels were similar between isolates, and differences between isolates resulted in large part from their interaction with different host genotypes. The main effect of Isolate appeared to have more impact on damage scores, for which the effect was significant (**Table 14**). The main effect of Line on pycnidia scores was also significant, which emphasises the importance of genotype in these interactions. The effect sizes of Line, Isolate and the Line by Isolate interaction were of similar magnitudes, so it seems that all three of these effects are important in determining disease response. Different scorers did not appear to significantly impact either pycnidia or damage scores; scorers were from the same lab, which may have facilitated consistent scoring.

In both the pycnidia and damage models, Batch explained the greatest amount of variance of the random effects, comprising 12.3% and 31.4%, respectively (**Table 15**). Batch captures the effects of the two separate sowing, inoculation and scoring events, so it is unsurprising that there was some variance. However, for the pycnidia dataset, the variance component for Batch was small compared to its standard deviation. The most important source of variation in both datasets arose from individual replicate plants across all levels (the residual variance), but even this was small. A greater number of replicate plants would therefore provide a more accurate measure of *Septoria* response – although the present experimental design was still effective enough to lead to the identification of significant Line and Line-by-Isolate effects.

**Table 13:** ANOVA table of linear mixed model for logit pAUDPC scores from the Watkins 300 collection inoculated with IPO323, IPO88004 and IPO90012. Colons represent nested factors.

Term	Mean Square	Numerator DF	Denominator DF	F value	Pr(>F)
Isolate	21.45	2.00	3.10	8.53	0.05
Line	28.49	322.00	3539.20	11.34	<0.0001
Scorer	5.89	2.00	46.80	2.34	0.11
Isolate:Line	14.40	624.00	3535.20	5.73	<0.0001

**Table 14:** ANOVA table of linear mixed model for % maximum dAUDPC scores from the Watkins 300 collection inoculated with IPO323, IPO88004 and IPO90012. Colons represent nested factors.

Term	Mean Square	Numerator DF	Denominator DF	F value	Pr(>F)
Isolate	607.48	2.00	3.00	12.46	0.03
Line	427.76	322.00	3523.50	8.77	<0.0001
Scorer	3.78	2.00	60.10	0.08	0.93
Isolate:Line	219.63	624.00	3502.20	4.51	<0.0001

**Table 15:** Random effects of the linear mixed model fitted to logit pAUDPC and % maximum dAUDPC scores from the Watkins 300 collection inoculated with IPO323, IPO88004 and IPO90012. Colons represent nested factors.

Term	Logit pAUDPC		% max. dAUDPC	
	Variance	Std. Dev	Variance	Std. Dev
Isolate:Batch:Rep:Box:Tray			0.54	0.74
Isolate:Batch:Rep:Box	0.11	0.33	2.19	1.48
Isolate:Batch:Rep	0.01	0.12	0.00	0.00
Isolate:Batch	0.37	0.61	23.56	4.85
Residual	2.51	1.59	48.75	6.98

There was more resistance to IPO323 in the panel compared to IPO88004 and IPO90012, which were progressively more virulent (**Figure 30**). Whilst IPO323 and IPO88004 had large left-hand tails for pycnidia scores (due to a high level of resistance in the panel), the distribution of scores in response to IPO90012 was relatively flat. Damage scores appeared to be able to explain some of the variation in pycnidia for all three isolates, given significant positive Pearson correlation scores (IPO323:  $R = 0.29$ ,  $p = 1.4 \times 10^{-7}$ ; IPO88004:  $R = 0.57$ ,  $p = 2.2 \times 10^{-16}$ ; IPO90012:  $R = 0.37$ ,  $p = 4.4 \times 10^{-12}$ ; **Figure 31**). In the case of IPO323, the data appeared to bifurcate into two distinct groups: a group where pycnidia cover seemed to increase with damage, and another where pycnidia cover remained relatively low whilst damage increased. Many lines from the latter group were designated as “super necrotic”, since they were observed to rapidly accumulate high damage whilst maintaining very low pycnidia scores. Many lines had very low scores for both pycnidia and damage cover in response to IPO323. A triangular distribution is seen in **Figure 31** for both IPO88004 and IPO90012 as pycnidia scores cannot be present without damage, but there was much variation in the amount of pycnidia that were produced given the amount of damage.

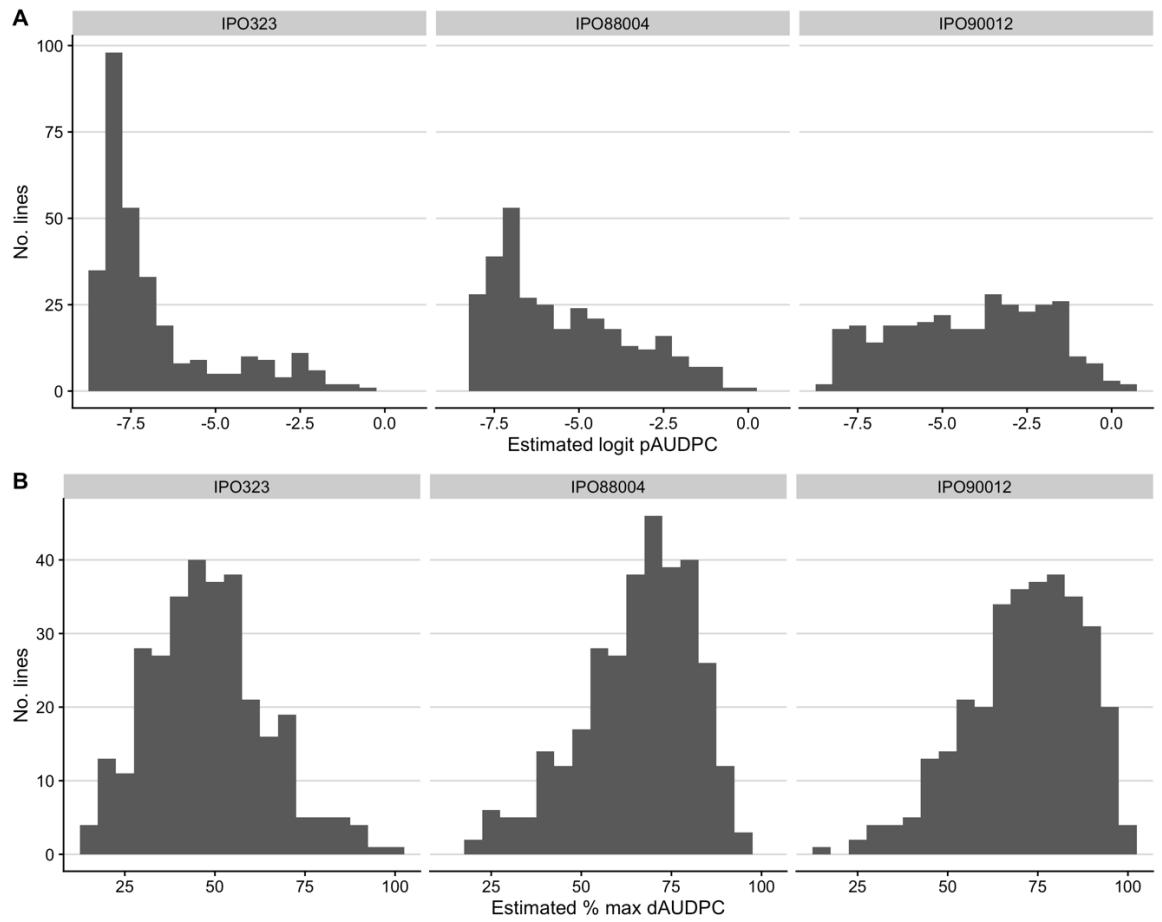


**Figure 30:** Histograms of logit pAUDPC and % maximum dAUDPC of Watkins wheat landraces inoculated with *Z. tritici* isolates IPO323, IPO88004 and IPO90012.

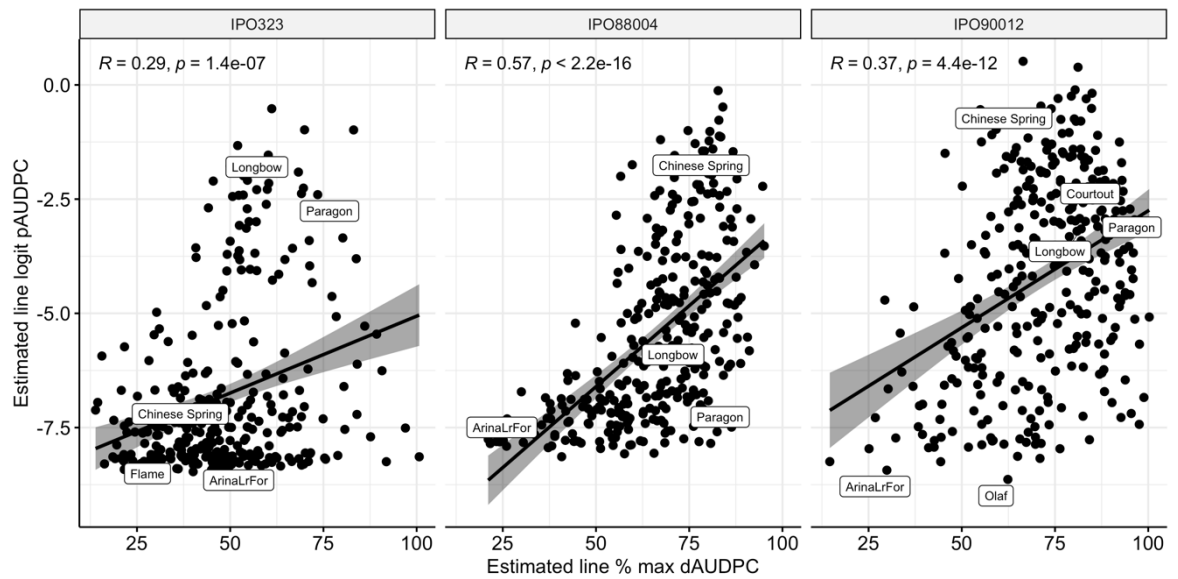


**Figure 31:** Logit pAUDPC versus % maximum dAUDPC scores of Watkins wheat landraces inoculated with *Z. tritici* isolates IPO323, IPO88004 and IPO90012. Key wheat control lines are labelled.

There appeared to be some correlation between responses to IPO323 and IPO90012, as well as between IPO90012 and IPO88004 (**Figure 31**). Interestingly, the correlation between IPO323 and IPO90012 was stronger in the damage than the pycnidia response; this could be due to relatively low pycnidia production in the IPO323 assay overall. The opposite was true for the correlation between IPO90012 and IPO88004. Responses to IPO323 and IPO88004 did not appear to be correlated.

When means against single isolates were plotted against means across the other two isolates (**Figure 32**), there was a clear clustering of lines to the bottom of the IPO323 pycnidia plot, as there was less disease than was exhibited in response to the other two isolates. There were also many lines that are more susceptible than would be predicted by the regression line; Baj in particular appears to show specific susceptibility to IPO323. There was a stronger correlation of responses to IPO88004 and IPO90012 with responses across all isolates, and the damage response of IPO323 was more in line with that of other isolates. This may indicate that there is a large degree of non-race-specific *Septoria* responses in the Watkins collection. It could also indicate that the genetic basis of resistance to these isolates, in particular IPO88004 and IPO90012, is similar. Due to the similarity of responses to these two isolates, a better picture of isolate specificity to IPO323 could be gained by performing this analysis with a larger number of genetically diverse isolates. However, it appears that IPO88004 and IPO323 induce more isolate-specific responses than IPO90012 in the lines tested.

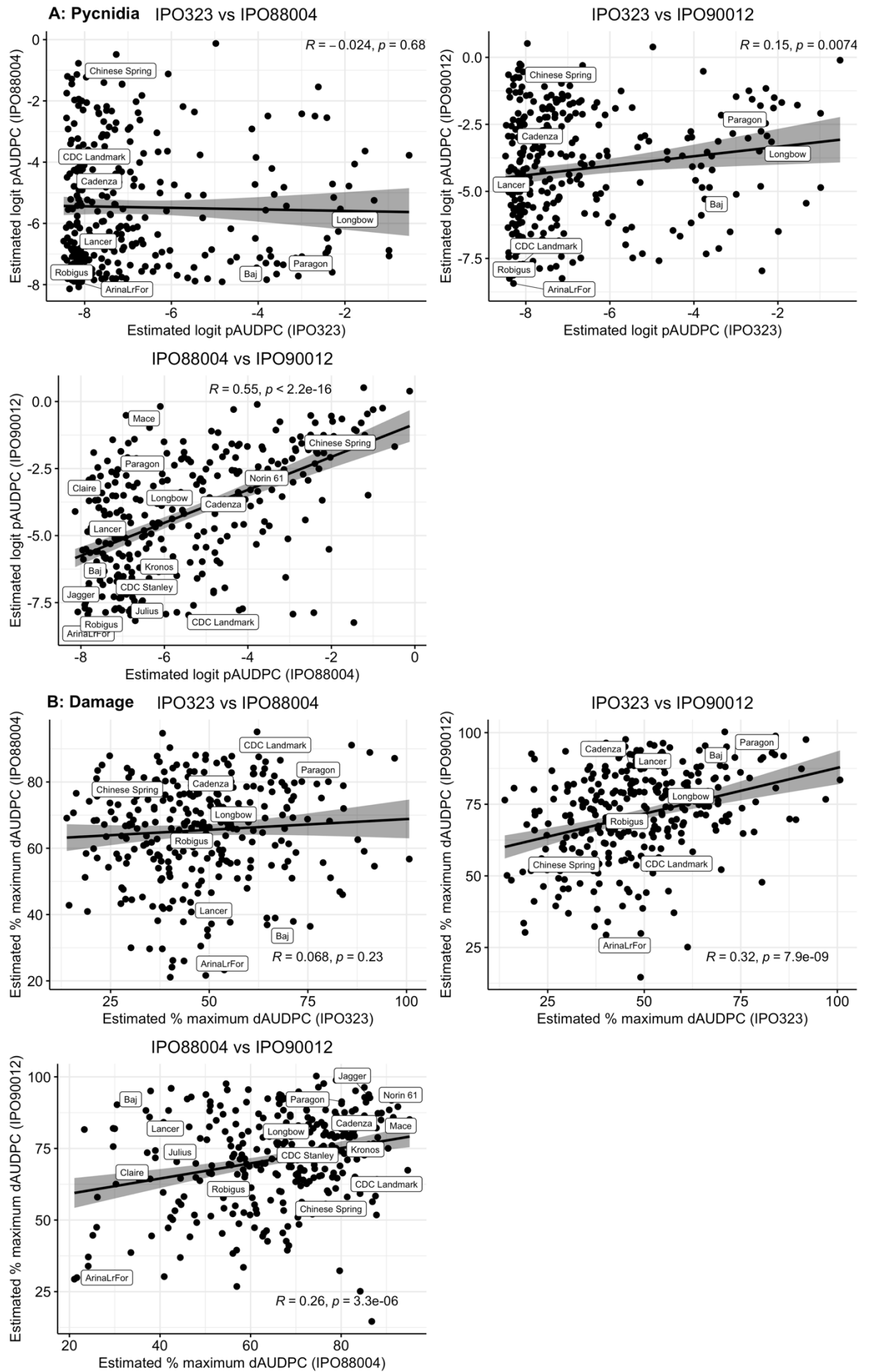
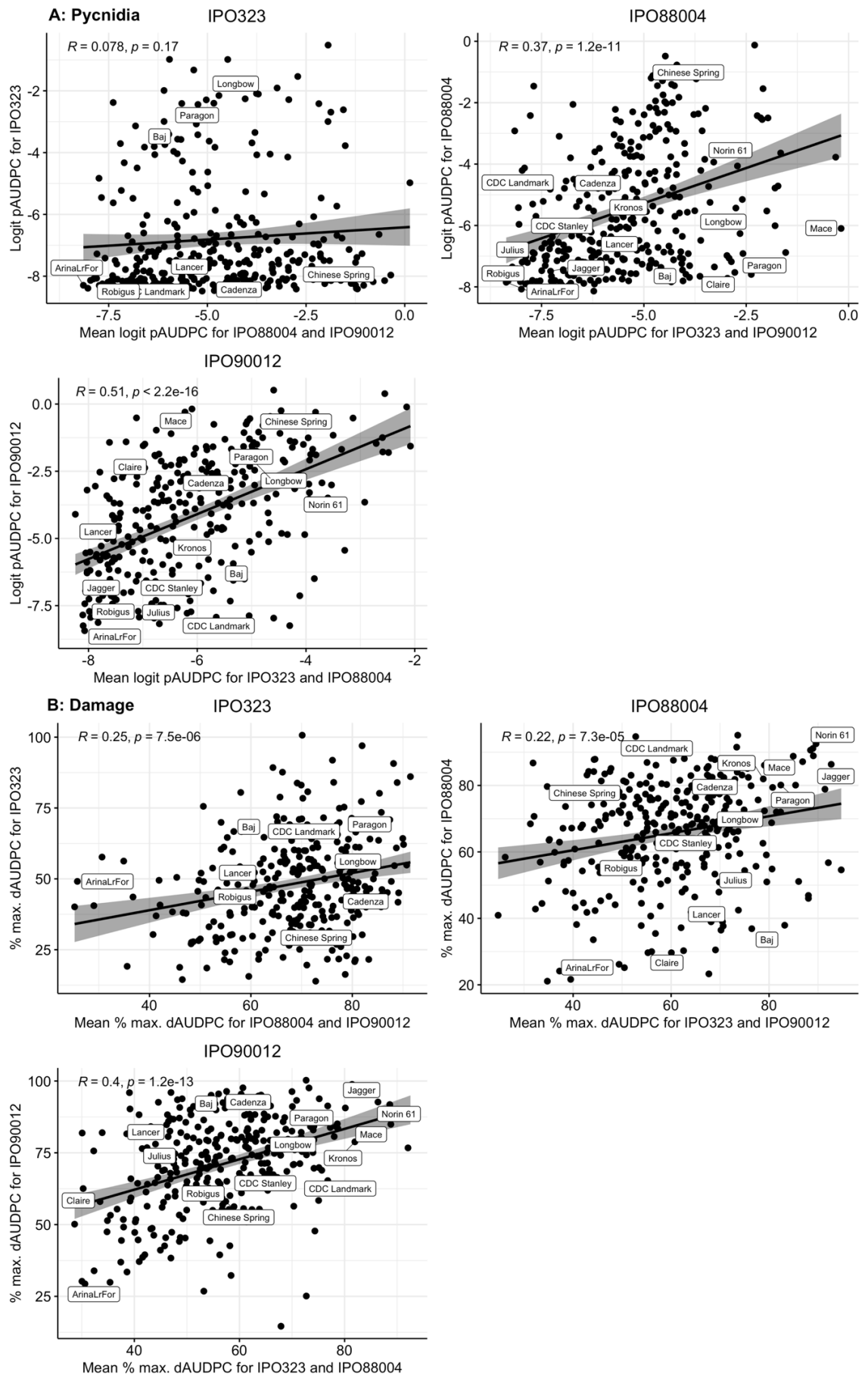


Figure 32: Isolate logit pAUDPC and % maximum dAUDPC responses of Watkins landraces to IPO323, IPO88004 and IPO90012 plotted against one another. Key wheat lines are labelled.



**Figure 33:** Mean responses of Watkins and wheat lines to single isolates (IPO323, IPO88004 or IPO90012) plotted against the line mean across the other two isolates. Key wheat lines are labelled.

### 3.3.2.1. *Septoria* response by ancestral group

Watkins landraces fall into two key ancestral groups, which are further divided into 9 subgroups (Wingen et al., 2014; **Table 16**). Generally, a broad range of pycnidia scores was observed within each ancestral group (**Figure 34**). Groups 1.2 (China/India) and 2.3 (East Europe) had particularly low scores in response to IPO323, within a narrow range. This appears to be IPO323-specific resistance since the groups also contained lines susceptible to IPO88004 and IPO90012. Group 2.1 (South Europe/Asia) appeared to be the most resistant to IPO88004 and IPO90012, suggesting there may be a gene or genes for resistance to these isolates within this group. Although most groups show a range of responses, it may be useful to use ancestral groups as a guide for expanding the panel from the larger collection of over 800 landraces when it is suspected that there may be rare alleles of interest present. Group 2.1, for example, consists of only 12 lines, which may reduce the power of GWAS to identify a region controlling resistance.

**Table 16:** Summary of Watkins landrace ancestral groups (Wingen et al., 2014).

Group Code	Geographic regions
1.1	Russia
1.2	China/India
1.3	Central/East Asia
1.4	Europe/Asia
2.1	South Europe/Asia
2.2	North-west Europe
2.3	East Europe
2.4	South Mediterranean/Africa
2.5	North Mediterranean

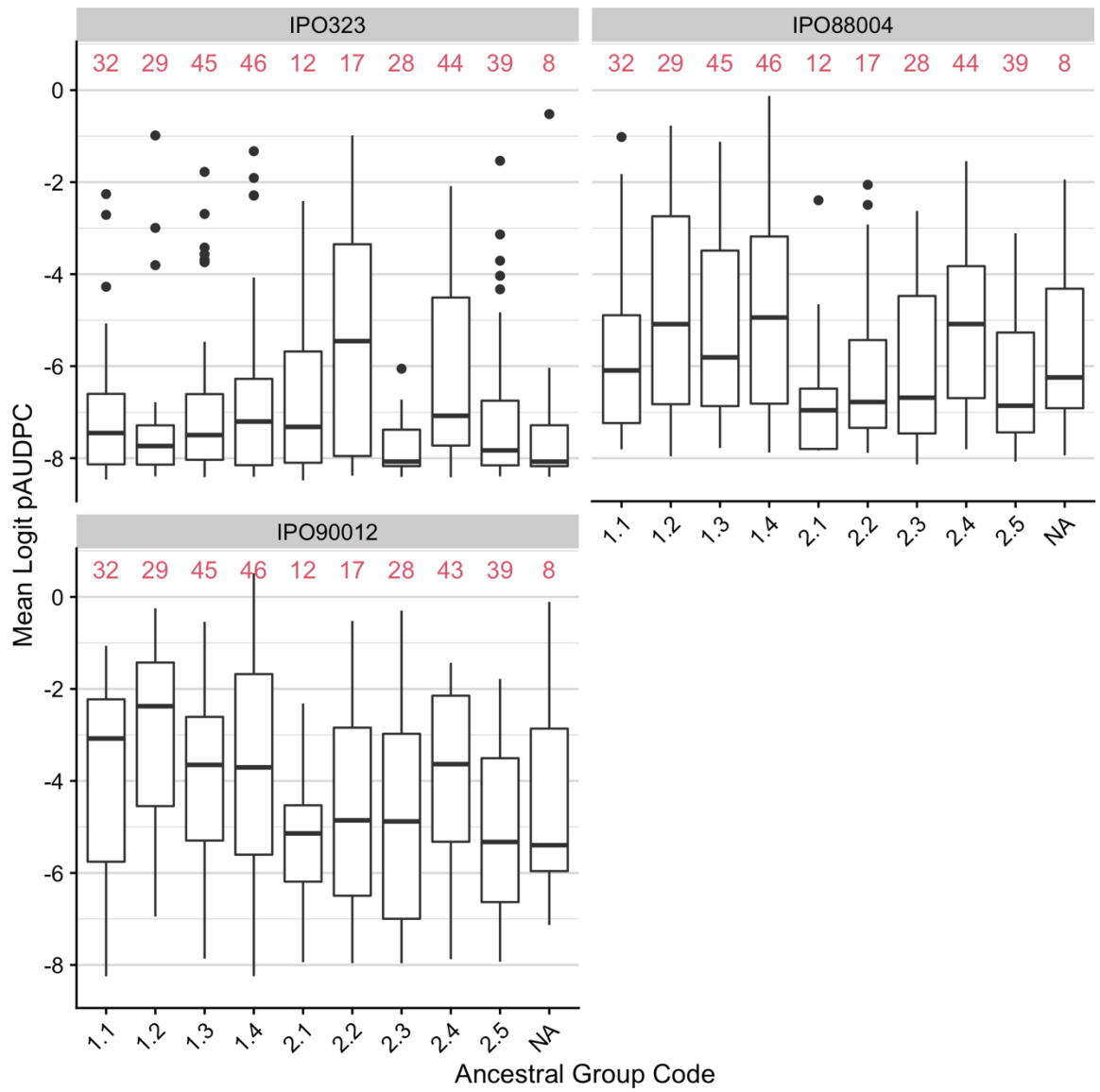


**Figure 34:** Mean logit pAUDPC scores of Watkins lines by ancestral group, against IPO323 (Netherlands), IPO88004 (Ethiopia) and IPO90012 (Mexico). Red numbers at the top of each graph indicate the number of lines in each category.

### 3.3.2.2. *Dissecting the damage response and 'super necrosis'*

During the course of the above assays, we observed a phenotype where some leaves would develop necrosis rapidly across the whole leaf within the first few days of scoring, which was often not associated with lesions or pycnidia. We called this phenotype 'super necrosis' or SN. As expected, lines scored positive for SN have higher damage scores than other lines. SN lines only appeared to be associated with increased pycnidia in response to IPO88004; they had the same or less pycnidia cover in response to IPO323 and IPO90012 (**Figure 35**). With IPO323 and IPO90012, the susceptibility and SN responses were more distinct. No line was scored for SN with more than one isolate, suggesting the response is highly specific to certain line and isolate combinations. The relationship between damage and super necrosis responses is therefore not clear - lines exhibiting super necrosis are not more or less likely to have high levels of pycnidia (typical susceptibility) in general, although the relationship may be more tightly correlated in response to some isolates.

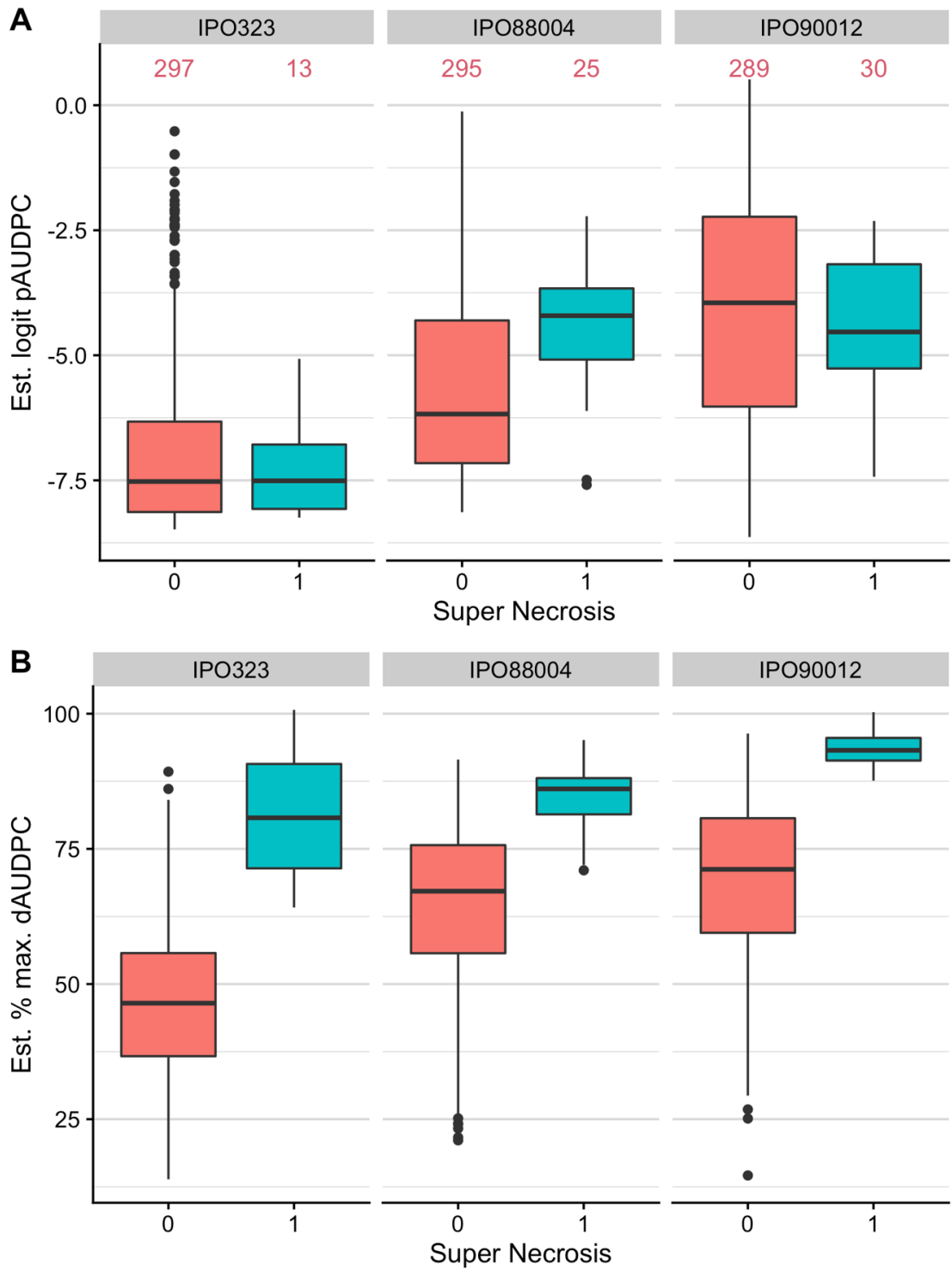


**Figure 35:** Box plots showing estimated logit AUDPC pycnidia and % maximum AUDPC damage scores of Watkins landrace and wheat cultivar lines with (1) and without (0) the presence of the super necrosis (SN) phenotype for each isolate. Numbers in red at the top of plot A show the sample size.

### 3.3.3. The effect of inoculum dose on wheat responses to *Z. tritici*

It has previously been demonstrated that the inoculum doses often used in Septoria pathogenicity assays may be excessively high and overwhelm plant defence responses, causing some variation in virulence to be masked (Fones et al., 2015). We hypothesised that the SN phenotype, where leaves exhibit high levels of rapid-onset necrosis but little or no pycnidia, could be a result of symptom saturation, which would be confirmed if pycnidia are produced when these lines are inoculated at lower inoculum doses. Four inoculum doses of two *Z. tritici* isolates, IPO323 and IPO89011, were screened on a differential set of 10 Watkins lines to investigate this.

Lines were selected based on their response to IPO323 and other isolates in previous assays (**Table 17**). Specifically, they were selected from the assay testing the core 300 lines in the Watkins panel with IPO323 and the detached leaf assay of IPO89011 and other isolates.

**Table 17:** Reasons for including lines in the “differential set” to test at different inoculum doses.

Line	Origin	Reason for inclusion
W268	Spain	Very resistant to IPO323. Susceptible to IPO89011.
W273	Spain	SN response with no pycnidia in response to IPO323. Highly resistant to IPO89011.
W277	Spain	Highly resistant to IPO323. Susceptible to IPO89011.
W317	China	Highly resistant to IPO323. Susceptible to IPO89011 but resistant to other isolates tested in the detached leaf assays – IPO89011-specific susceptibility.
W407	India	SN response to IPO323. Susceptible to IPO89011.
W423	India	Highly resistant to IPO323. Intermediate resistance to IPO89011.
W731	India	Highly resistant to IPO323. Intermediate resistance to IPO89011.
W747	Ethiopia	SN response to IPO323. Susceptible to IPO88004.
W771	USSR	Very susceptible line. High damage and pycnidia scores in response to IPO323. Susceptible or intermediate response to other isolates.
W773	USSR	Very susceptible to IPO323 and IPO89011.

The logit and % max. AUDPC values were calculated as previously described. A linear mixed model was fitted to the data with the main and interacting effects of Line, Isolate and Dose as fixed effects and the Tray as a random effect (**Table 18, Table 19, Table 20**). The estimated marginal means were obtained using this model, although the model assumptions were violated somewhat by the heavy-tailed distributions of the data. This could be because the lines included were selected based on their more extreme phenotypes relative to the rest of the core set, so there were fewer intermediate phenotypes observed. This was especially evident at high doses and particularly in IPO323 where responses formed binomial distributions (**Figure 36**). It also suggests that differences in phenotype (e.g. resistant vs susceptible) may become more evident at higher doses, particularly for damage responses.

**Table 18:** ANOVA table of linear mixed model for logit pAUDPC scores from Watkins and wheat lines inoculated with IPO323 and IPO89011 at different inoculum doses ( $10^3$ ,  $10^4$ ,  $10^5$  or  $10^6$  spores/ml). Colons represent nested factors.

Term	Mean Square	Numerator DF	Denominator DF	F value	Pr(>F)
Isolate	127.32	1	5.24	65.53	<0.001
Dose	183.19	3	5.22	94.29	<0.0001
Line	151.41	14	430.66	77.93	<0.0001
Isolate:Dose	7.68	3	5.22	3.95	0.083
Isolate:Line	108.93	14	430.66	56.07	<0.0001
Dose:Line	7.41	42	428.06	3.82	<0.0001
Isolate:Dose:Line	8.44	42	428.06	4.34	<0.0001

**Table 19:** ANOVA table of linear mixed model for % maximum dAUDPC scores from Watkins and wheat lines inoculated with IPO323 and IPO89011 at different inoculum doses ( $10^3$ ,  $10^4$ ,  $10^5$  or  $10^6$  spores/ml). Colons represent nested factors.

Term	Mean Square	Numerator DF	Denominator DF	F value	Pr(>F)
Isolate	29439.00	1	5.31	260.99	<0.0001
Dose	33406.00	3	5.27	296.17	<0.0001
Line	5378.00	14	425.33	47.68	<0.0001
Isolate:Dose	1617.00	3	5.27	14.34	0.006
Isolate:Line	2459.00	14	425.33	21.80	<0.0001
Dose:Line	763.00	42	417.45	6.76	<0.0001
Isolate:Dose:Line	480.00	42	417.45	4.26	<0.0001

**Table 20:** Table of random effects from linear mixed models for logit pAUDPC and % maximum dAUDPC scores from Watkins and wheat lines inoculated with IPO323 and IPO89011 at different inoculum doses ( $10^3$ ,  $10^4$ ,  $10^5$  or  $10^6$  spores/ml).

Term	Logit pAUDPC		% max. dAUDPC	
	Variance	Std. Dev	Variance	Std. Dev
Line	0.04	0.21	0.70	0.84
Residual	1.94	1.39	112.80	10.62

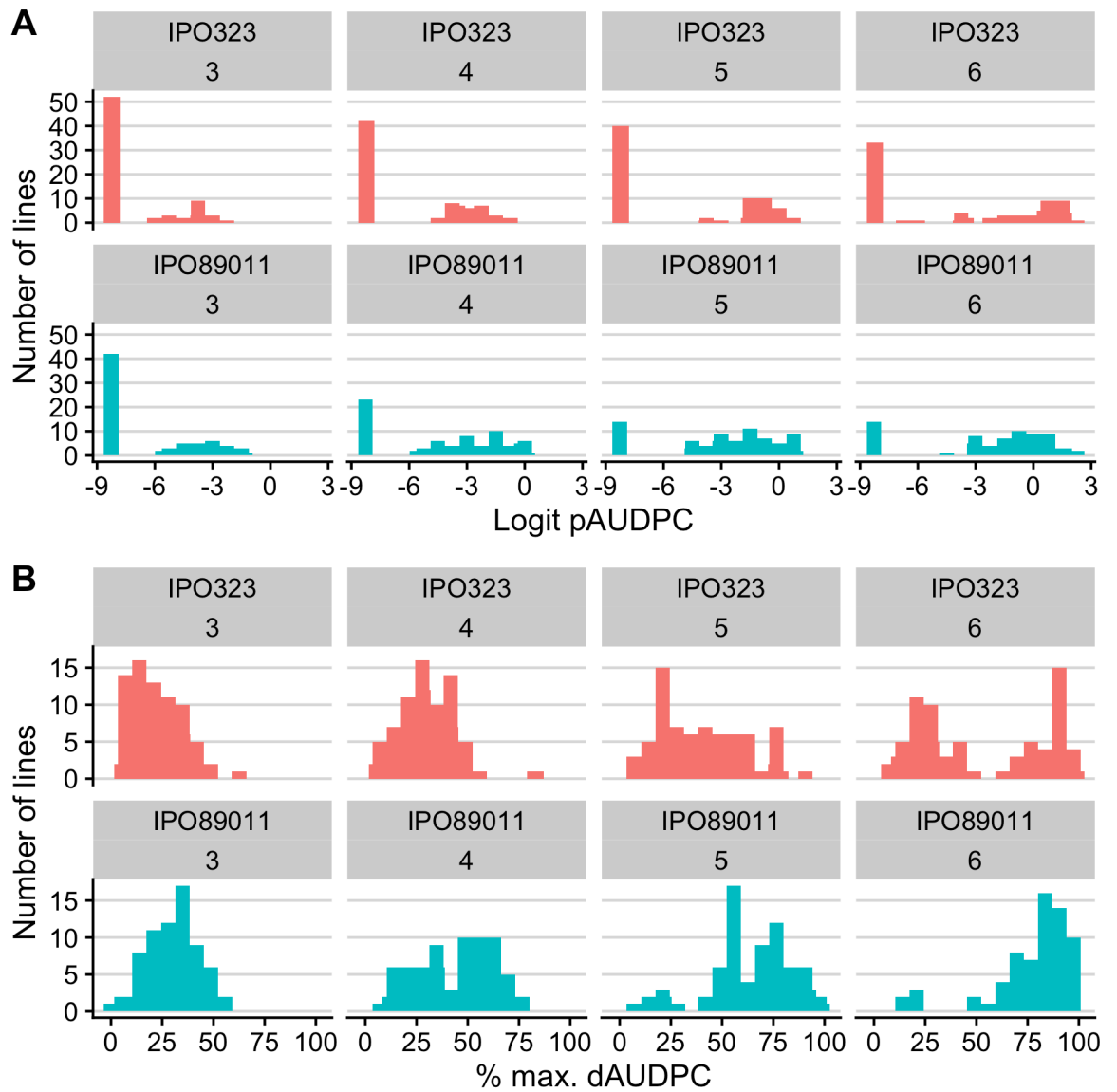


**Figure 36:** Logit AUDPC of pycnidia (A) and % maximum AUDPC damage (B) scores of a differential set of Watkins lines inoculated with IPO323 (purple) and IPO89011 (green) under four different inoculum doses (dose “3” =  $10^3$  spores/ml<sup>-1</sup>, and so on).

All fixed terms appeared to have a significant effect on both pycnidia and damage scores, with the exception of the Isolate-by-Dose interaction which did not significantly impact pycnidia scores. An interaction between isolate and dose was not expected, but the result was likely impacted by the fact that many lines had little or no pycnidia cover across all doses (**Figure 37**), thus making it appear that responses to isolates were often consistent across doses. On the other hand, damage often increased with dose and this occurred more frequently in response to IPO89011 in the lines tested, which may account for the Isolate by Dose interaction (although the F statistic was low in comparison to the main effects). The largest effects were from the main effects of Isolate, Dose and Line; these were of a similar magnitude for pycnidia data but for damage the main effect of Line was five to six times smaller than the other main effects. This could be due to the tighter relationship of damage with dose and isolate as described above. The interaction effects of Line by Dose and Line by Dose by Isolate were small compared to the main effects of Line, Isolate and Dose. The significant Isolate by Line effect demonstrates that the phenotypes observed were often isolate-specific, as expected due to the lines that were chosen for the experiment; this was especially true for pycnidia data where the F statistic was more than twice as large as that for damage. This lends some confidence to the results, as well as the fact that most lines had similar responses to these isolates as observed in previous assays (summarised with dot annotations in **Figure 37**). However, the Isolate by Line effect was smaller for damage (~10x smaller than the main effects of Isolate and Dose), which is consistent with above observations that damage is less isolate-specific than pycnidia cover.

In general, damage cover increased with inoculum dose, even when pycnidia cover remained low (**Figure 37**). This suggests that damage is indicative of increased pathogen colonisation at higher inoculum doses and is not just a random effect resulting only from ageing leaves or the surfactant, for example. There were cases where damage increased with dose while pycnidia scores remained low at all doses. Baldus and Watkins lines W317 and W747, for example, were previously found to be susceptible to IPO89011 and accumulated high damage but very few or no pycnidia at high doses in the present assay; Courtot exhibited a similar phenotype despite having previously been scored as resistant to IPO89011. Therefore, although damage can clearly provide information about pathogen colonisation due to its relationship with dose, its relationship to pycnidia development is not always consistent. Lines which have previously been scored as either susceptible or resistant both exhibited high necrosis phenotypes.

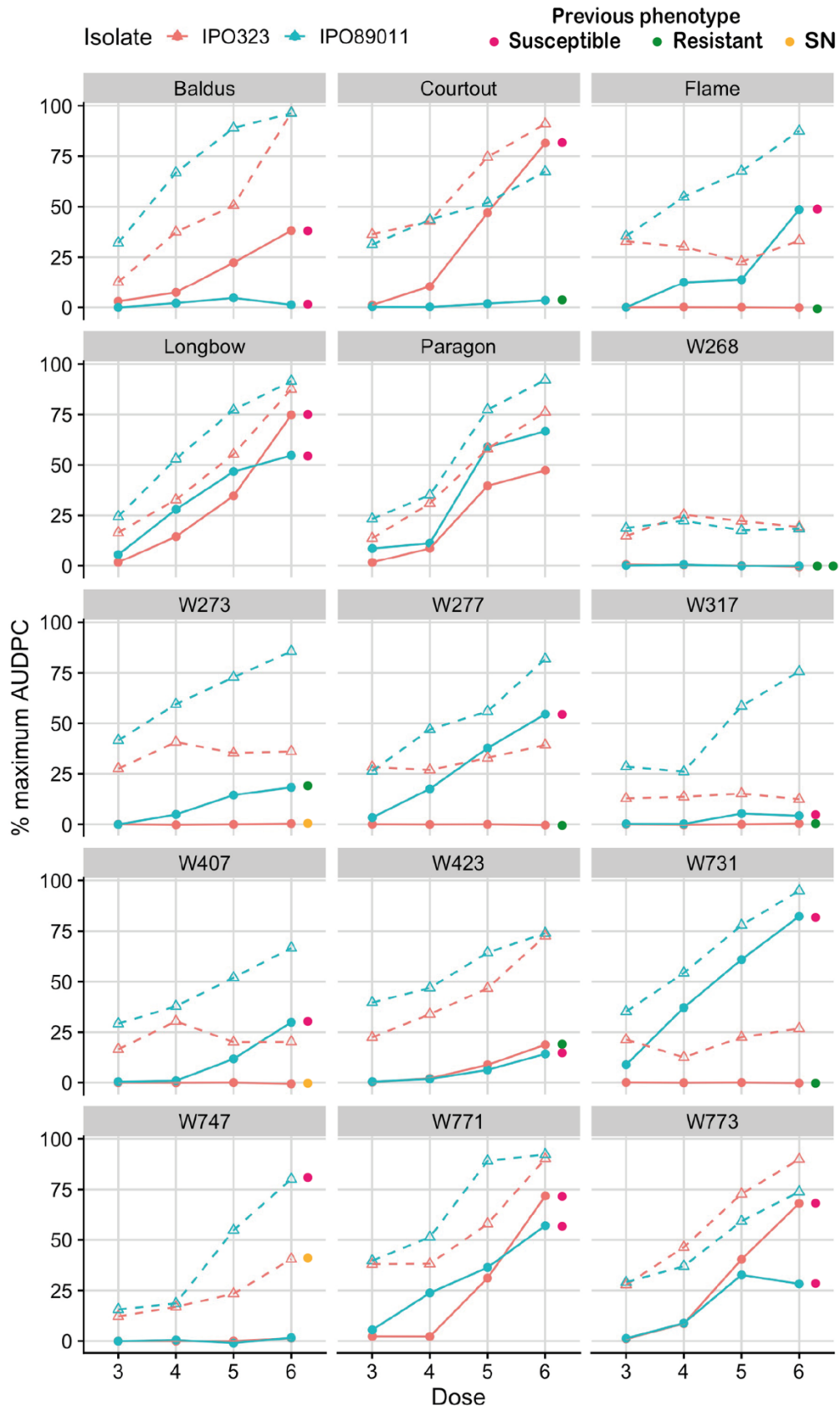


**Figure 37:** The mean % maximum pAUDPC (closed circles) and dAUDPC (open triangles) of 10 Watkins landraces and five wheat control lines tested under four different inoculum doses of IPO323 (red) and IPO89011 (blue). Dose “3” =  $10^3$  spores/ml<sup>-1</sup>, and so on. Coloured dots are used to represent phenotypes observed previously for each isolate: green (resistant), pink (susceptible) or SN (yellow).

On the other hand, low damage scores were often scored across all inoculum doses of a particular isolate. This phenotype was observed in response to both IPO323 and IPO89011 in W268, and in W273, W277, W317, W407 and W731 in response to IPO323. This phenotype of damage stability over increasing inoculum dose could be a useful measure of resistance. There may be biological differences between responses to *Z. tritici* in lines which experience increasing damage vs lines with stable damage levels – it may separate lines which allow extensive pathogen colonisation from those that do not, when identical null pycnidia scores may indicate that similar interactions are occurring.

W273, W407 and W747 were previously scored as SN in response to IPO323, and in the present assay exhibited no pycnidia production across all doses in response to IPO323 coupled with low to intermediate levels of damage (20 to 40% of the maximum AUDPC). This suggests that the SN phenotype previously observed may correspond to a resistance response, as lower doses of inoculum simply reduced the total amount of damage observed but did not result in an increase in pycnidia production. It also appears that the SN response is difficult to replicate, and may sometimes manifest as a more standard resistance response (resulting in low levels of damage and pycnidia cover) when assays are repeated.

#### 3.3.4. Identification of sources of broad-spectrum resistance within the Watkins collection for breeding

Based on the seedling assays of the Watkins core 300 (4.3.2), lines were selected which were resistant to all three isolates tested – IPO323, IPO90012 and IPO88004 (**Table 21**). Tests against six further isolates (IPO87019, IPO89011, IPO90004, IPO94269, JIC040, Cougar007) were conducted to assess the breadth of resistance exhibited by these lines. Some lines exhibiting general susceptibility were also included.

**Table 21:** Lines included in the test with scores for damage and pycnidia against IPO323, IPO90012 and IPO88004. Wheat cultivars and Chinese Spring (separated from Watkins landraces by a double line) were included as controls. Compatible interactions and lines included for their susceptibility are marked in pink. All other Watkins lines were included for their resistance to all three isolates.

Line	IPO323		IPO88004		IPO90012	
	logit pAUDPC	% max dAUDPC	logit pAUDPC	% max dAUDPC	logit pAUDPC	% max dAUDPC
ArinalrFor	-8.29	49.11	-7.85	21.64	-8.43	29.90
Chinese Spring	-7.56	33.44	-1.40	81.34	-1.09	58.06
Courtot	-	-	-	-	-2.74	87.62
Longbow	-2.15	60.34	-6.26	73.83	-3.15	82.02
Olaf	-	-	-	-	-8.63	62.35
Paragon	-2.40	73.46	-6.91	80.12	-2.76	91.33
Robigus	-8.30	41.34	-7.35	58.70	-8.13	64.96
W083	-7.98	48.48	-7.02	67.88	-7.78	42.63
W114	-8.18	19.14	-7.01	40.93	-6.65	30.26
W187	-8.07	36.95	-7.90	38.14	-7.71	44.46
W199	-4.98	30.27	-0.13	82.75	0.39	81.17
W209	-8.14	43.44	-7.31	37.82	-6.67	64.37
W223	-2.61	59.67	-1.54	71.08	-1.57	61.94
W248	-8.32	30.36	-5.22	44.48	-6.60	36.92
W268	-8.23	29.35	-6.98	57.42	-6.52	48.73
W315	-8.09	21.47	-7.83	68.45	-7.94	41.09
W356	-3.78	40.84	-2.49	71.56	-0.52	73.99
W361	-8.41	49.49	-7.21	56.96	-7.28	26.82
W397	-8.24	40.55	-7.81	24.14	-6.28	33.91
W401	-2.42	52.28	-2.55	76.25	-1.80	82.87
W414	-7.15	40.12	-7.76	21.09	-4.71	29.36
W572	-7.49	49.60	-7.65	33.57	-7.02	38.64
W579	-8.32	29.80	-6.60	67.31	-6.20	53.33
W607	-7.85	27.08	-6.59	56.92	-6.99	39.50
W611	-8.39	46.09	-7.81	62.67	-8.25	44.35
W619	-7.28	33.08	-7.80	45.29	-7.79	58.19
W639	-8.15	28.79	-7.79	44.65	-6.19	55.39
W662	-8.15	37.12	-7.17	54.00	-7.72	57.78
W724	-7.10	45.62	-6.78	53.73	-6.57	45.33
W743	-8.28	27.61	-6.88	43.29	-7.13	53.25

Prior to statistical testing, pycnidia data was logit transformed to normalise the data, as the distribution was heavily skewed to the left. Damage data was taken as the percentage of the maximum AUDPC, as this provided the best model fit in later tests.

Separate models were fitted to the pycnidia and damage data. The model fit for pycnidia was singular when any combination of Scorer (fixed) and Tray and Box (random) was included, likely because these factors are confounding. After performing nested deviance checks, a fully fixed model was fitted with Scorer and Isolate by Line interaction as effects, using the `aov()` function in R. For damage, there was a significant effect of including Box as a random effect along with the fixed effect of Scorer, so the final model included Scorer and Isolate by Line interaction as fixed effects and Box as a random effect.

The analysis indicated that the effects of Line and the Line-by-Isolate interaction had a significant effect on both pycnidia and damage phenotypes (**Table 22**, **Table 23**). There was also a significant main effect of Isolate on pycnidia scores but not damage, suggesting that particular isolates were more likely to generate characteristic levels of pycnidia than damage across the lines tested. There was also a significant effect of Scorer on the pycnidia scores, although this term also largely encompasses the random effect of Box since each box was scored by one scorer. For damage, the effect of Scorer was not significant but the random effect of Box explained 7.5% of the total residual variance (193.26).

**Table 22:** ANOVA table of linear mixed model for logit pAUDPC scores from Watkins and wheat lines. Colons represent nested factors.

Term	Mean Square	DF	F value	Pr(>F)
Isolate	3169.3	5	17.15	<0.0001
Line	7830.6	32	42.37	<0.0001
Scorer	1420.4	1	7.69	<0.01
Line:Isolate	850.2	154	4.55	<0.0001
Residuals	184.8	715		

**Table 23:** ANOVA table of linear mixed model for % maximum dAUDPC scores from Watkins and wheat lines. Colons represent nested factors.

Term	Mean Square	Numerator DF	Denominator DF	F value	Pr(>F)
Isolate	623.0	5	4.68	3.49	0.1057
Line	7752.5	32	711.42	43.38	<0.0001
Scorer	235.4	1	5.00	1.32	0.3030
Line:Isolate	850.4	154	710.42	4.76	<0.0001

Line means across all isolates tested were estimated based on the above models. Most lines tested were much less susceptible than Longbow, the general susceptible control, on average (**Figure 38**). The lines included for their general susceptibility were all more susceptible than the wheat controls included – perhaps due to a lack of background resistance to Septoria.

All responses to particular isolates were strongly correlated with line means (**Figure 39**); this result was likely biased due to the fact that lines were selected for broad-spectrum resistance and susceptibility. However, although W209 was selected for its resistance to IPO323, IPO88004 and IPO90012, it was more susceptible than Longbow to JIC040 and Cougar007 and scored similarly to Longbow in response to the other isolates tested. This demonstrates the importance of testing against a large panel of isolates to identify broad-spectrum resistance.

Lines such as W114, W662 and W743 had less consistent responses, scoring above or below the expected values in response to different isolates. Such lines are less favourable candidates for studying durable broad-spectrum resistance. W361, W572 and W611 were selected as the best candidates due to reliable high levels of resistance and have been included in the UK Breeders' Observation Panel for testing in field conditions (ongoing).

Many lines exhibiting good resistance to the currently very problematic Cougar race were identified. Cellule was highly resistant to Cougar007 (-7.7 logit pAUDPC), suggesting that the key Septoria resistance in Cellule (*Stb16q*) is different to that of Cougar. Cellule, W083, W114, W187, W268, W572, W611 and W639 appear to all be excellent sources of resistance to Cougar007 and could be good targets for including in European pre-breeding programmes to enhance the resistance of Cougar-derived wheat lineages. Depending on local *Z. tritici* populations and the prevalence of *Stb7* in breeding lines, W114 and W639 may be less desirable due to their susceptibility to IPO87019 (both) and IPO90004 (W639).

W248 was selected for inclusion based on its exceptional green leaf area in comparison to other resistant lines. It continued to hold up in this regard with damage levels well below that of Longbow in response to all six isolates tested, demonstrated by its position to the far left in Figure 38. However, this line exhibited similar areas of pycnidia to Longbow in response to Cougar007 (**Figure 39**), which may make it less desirable for breeding given the current *Z. tritici* field population.

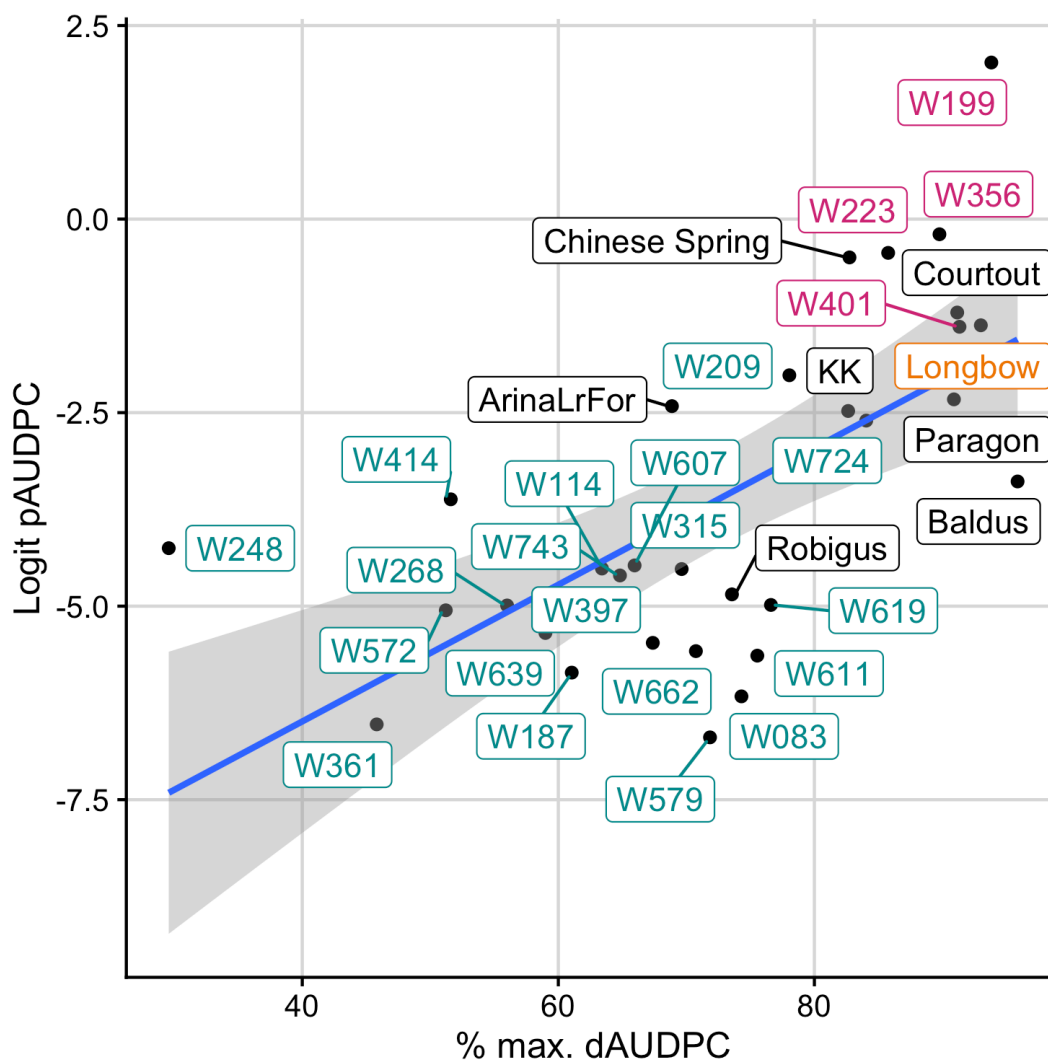


**Figure 38:** Line means of damage (% max. dAUDPC) against pycnidia (logit pAUDPC) for Watkins landraces and wheat lines across six isolates (IPO87019, IPO89011, IPO90004, IPO94269, JIC040 and Cougar007). Lines included for their high resistance to IPO323, IPO90012 and IPO88004 are in teal; lines selected for general susceptibility are in pink; wheat controls are in black and the susceptible wheat line Longbow is highlighted in orange. Shaded area represents the 95% confidence interval.



### 3.4. DISCUSSION

There was a huge amount of diversity in the responses of the Watkins collection to the *Z. tritici* isolates tested, and evidence of strong genotype-by-isolate interactions. Some Watkins lines, such as those described in section 3.3.4, exhibited levels of broad-spectrum resistance above that observed in the wheat lines tested, including those with good broad-spectrum resistance like ArinaLrFor. The Septoria isolates tested were isolated from the field within the last 30 years, so are much more modern than the Watkins landraces (~1930s). The enhanced resistance could therefore be due to the presence of *R* genes to which more recent *Z. tritici* populations have lost virulence, or have never been exposed. Five Watkins lines with exceptional broad-spectrum resistance to many or all (three lines) of the isolates tested in this chapter were submitted for potential use as pre-breeding material. In a limited number of cases, ancestral group appeared to explain resistance response: groups 1.2 (China/India) and 2.3 (East Europe) w.r.t. IPO323 and group 2.1 (South Europe/Asia) w.r.t. IPO90012 and IPO88004. There may have been more selection for STB resistance within these groups, as well as geographical variation.

Some lines also had extremely susceptible phenotypes. This could be explained by a lack of background resistance in comparison to even the more susceptible wheat lines. This highlights the success of modern breeding in enhancing background resistance (Brown, 2021), which can be the difference between a susceptible cultivar with a few lesions and one completely covered in large, spore-rich pycnidia which would greatly exacerbate epidemics. An example can be provided by comparing the two susceptible lines in Figure 29, Watkins landrace W729 and wheat variety Paragon. The extreme susceptibility of some of the landraces tested would make them ideal candidates for crossing to wheat lines with partial resistance to attempt to map such genes.

IPO92006 and JIC040 were the most broadly virulent isolates tested – there was little resistance in the core set to these isolates and responses to them were strongly correlated in the core 36 set of lines. Cellule is known to have the broad-spectrum Septoria resistance gene *Stb16q* in the absence of *Stb6*. This line exhibited good performance against both aggressive isolates, so it is possible that *Stb16q* recognises effectors produced by both isolates. Isolate-specific interactions could be further investigated through methods such as median tetrad analysis to identify specific susceptibility or resistance responses of wheat lines to *Z. tritici* isolates (Brown et al., 2001).

There appeared to be three types of response to IPO323: resistant lines with very little pycnidia and damage cover, lines where pycnidia cover increases with damage and lines where damage increases independently of pycnidia cover (**Figure 40**). This resulted in few lines having responses that fell close to the regression line. It could be that these three groups represent distinct responses to *Z. tritici*. Coupled with the weak correlation observed between pycnidia and damage scores for IPO90012, these results support observations made by Kema *et al.* (1996b) that necrosis and pycnidia scores may be under different genetic control. Furthermore, upon infection of *Z. tritici* isolates collected from bread wheat on durum wheat, Kema *et al.* (1996b) observed large amounts of necrosis along with little evidence of spore production. It is possible that the group of Watkins lines that had high damage but low pycnidia scores were exhibiting an incompatible response like that observed between bread-wheat-adapted *Septoria* isolates and durum wheat. The IPO323 dataset in particular could be used to identify the genetic basis of this phenotype through association genetics by mapping to the sequenced wheat line CDC Landmark, which also exhibited a high damage/low pycnidia phenotype. Damage and pycnidia responses to IPO88004 were better correlated; perhaps this isolate is better adapted to infection of Watkins landraces, or there is more overlap between the genes controlling damage and pycnidia in response to this isolate.

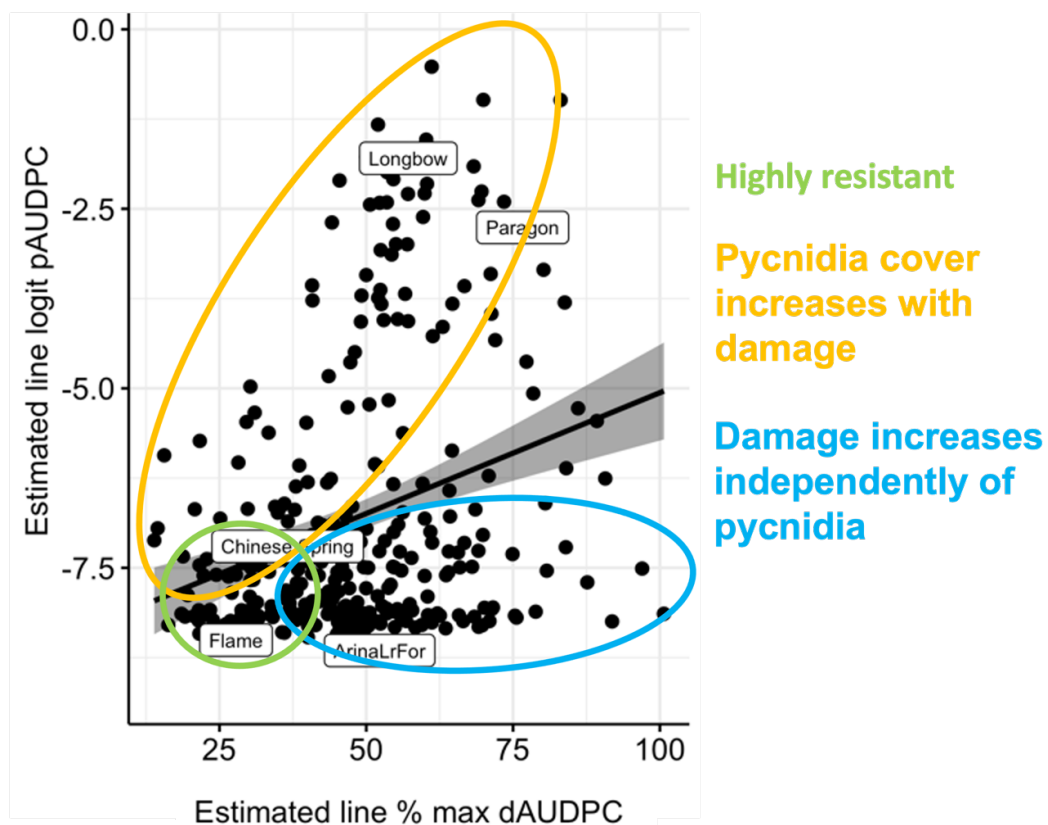


**Figure 40:** The pycnidia versus damage plot of IPO323 responses from Figure X. Lines are circled depending on responses falling into one of three categories: highly resistant, pycnidia cover increasing with damage or damage increasing independently of pycnidia.

An assay investigating the phenotypic effect of different inoculum doses was carried out to test whether lines exhibiting the SN phenotype were experiencing symptom saturation because of the high inoculum dose typically used in our lab ( $10^6$  spores/ml), as suggested by Fones et al. (2015). The experiments indicated that the SN phenotype previously observed may correspond to a resistance response, as lower doses of inoculum simply reduced the total amount of damage observed but did not result in an increase in pycnidia production. It also appears that the SN response is difficult to replicate and may sometimes manifest as a green resistance response when assays are repeated. Although assays were prepared using the same methods and took place in the same growth chamber, it could be that there were additional unaccounted for variables that resulted in a resistant green rather than an SN response. Therefore, it could be that lines dismissed as susceptible in some assays due to unusually high levels of necrosis may in fact be found to be resistant if assays are repeated. It would be interesting to pinpoint the genetic differences between resistant lines which remain reliably green and those that do not. In conclusion, we rejected the hypothesis that SN responses were caused by leaves becoming overwhelmed by the pathogen. SN appears to be isolate and genotype specific and associated with resistance.

The experiments testing different inoculum doses showed that damage generally increases with inoculum dose, sometimes accompanied by little or no pycnidia production. Damage may therefore be a useful measure of pathogen colonisation alongside pycnidia scores. Damage also sometimes does not increase across doses, which may indicate more stable resistance; this 'damage stability' phenotype could potentially be used as a measure of resistance. There may be biological differences between responses to *Z. tritici* in lines which experience increasing damage versus lines with stable damage levels - it may separate lines which allow extensive pathogen colonisation from those that do not, when identical null pycnidia scores in these lines may indicate that similar interactions are occurring. Further investigation of this phenotype either through microscopy or chitin binding assays could reveal whether 'damage stability' is indeed caused by a lack of pathogen colonisation. Similarly, it would be interesting to confirm colonisation levels within leaves that have a SN phenotype. Damage manifestation during colonisation by *Z. tritici* is likely a complex trait and reducing it to composite parts, such as SN and damage stability, for example, may aid in mapping the genetic components that control it.

The amount of initial inoculum ( $x_0$ ) was adjusted in the dose effect experiment – this could be considered a form of ‘sanitation’. If a simplified model of disease progress holds true, this should reduce the proportion of disease observed ( $x$ ) (Van der Plank, 1963):

Equation 2 
$$x = x_0 e^{rt}$$

However, this did not always hold true in the experiment described in this chapter. It could be because of the role of major-effect *R* genes in reducing  $x_0$ , therefore confounding the effect of inoculum dose. The lack of increase in  $x$  at higher doses could also be explained by a reduction in  $r$ , the apparent infection rate, in some lines. Reductions in  $r$  could have been caused by the presence of quantitative resistance genes that slowed disease progress or spore development. The time during which infection had occurred ( $t$ ) was constant due to the design of the experiment, so the task remains to somehow distinguish whether  $r$  or  $x_0$  was responsible for the lack of increased disease sometimes observed at higher inoculum doses. It is also possible that a combination of factors is at play – that some sources of partial resistance in the lines tested were most effective at reducing the infection rate when  $x_0$  was low, resulting in damage instability at high doses, whilst this was not an issue in lines exhibiting damage stability. As postulated above, this damage stability phenotype may be under different genetic control compared to phenotypes where damage increases with inoculum dose. The contrast between the different responses observed in these experiments show that the efficacy of partial resistance can be affected by  $x_0$  – but not always. No matter the genotype, the total diseased area was always lowest at the lowest inoculum concentration, so  $x_0$  was the greatest factor determining phenotype and even highly susceptible varieties are difficult to distinguish from resistant ones at inoculum concentrations of  $10^3$  spores/ml when working with AUDPC phenotypes.

Higher doses ( $10^6$  spores/ml) resulted in more clearly delineated phenotypes over a broader range when compared to responses at a lower dose ( $10^3$  spores/ml). The highly susceptible phenotypes observed at high doses in the present experiment may be an example of virulence deficiencies being masked in those lines that exhibited highly susceptible phenotypes, as suggested by Fones et al. On the other hand, our results may be in contrast to the suggestion that symptom saturation at high doses reduces the ability to observe differences in virulence – in this experiment, whether due to saturation or not, high doses enabled better differentiation of resistant and susceptible phenotypes. Furthermore, as discussed above, higher spore densities may reveal differences in pathogen colonisation that are not apparent at lower densities. This may of course be due

to our conditions being suboptimal, which would increase the coalescence threshold compared to Fones et al. The method of spray inoculation would introduce more variation in the spore concentration reaching each leaf than the more precise method of pipetting used by Fones et al.

#### 3.4.1. Conclusion

These results demonstrate the utility of preliminary pathology tests on relatively small sets of lines for evaluating the presence of isolate-specific or quantitative interactions for evaluation in further (*e.g.* larger scale) studies. By screening a large diversity collection against multiple isolates, it was possible to identify lines with broad-spectrum resistance and further test these with additional isolates. This led to the identification of sources of broad-spectrum resistance to up to eight isolates, including a currently problematic Cougar race of *Z. tritici*, which can be mobilised in wheat pre-breeding. Furthermore, relationships between pycnidia and necrosis were examined, resulting in inferences about the super necrosis and damage stability phenotypes which are associated with resistance.

4. INTERROGATING THE GENETIC BASIS OF  
SEPTORIA RESISTANCE TO IPO323,  
IPO88004 AND IPO90012 IN THE  
WATKINS COLLECTION THROUGH  
ASSOCIATION GENETICS AND ANALYSIS OF  
WHOLE GENOME SHOTGUN SEQUENCES

'Science is magic that *works*.'

Kurt Vonnegut, *Cat's Cradle* (1963)

## 4.1. INTRODUCTION

### 4.1.1. Solutions to the problem of STB

The majority of cereal fungicide applications in Europe are targeted towards control of STB (O'Driscoll et al., 2014). At the same time, the high priority assigned to genetic resistance to STB in breeding programmes has led to substantial increases in background resistance over the last few decades (Brown, 2021). This should provide good control of the disease, especially since these two methods of control are synergistic; genetic resistance can reduce the selection pressure on pathogens to evolve resistance to fungicides and vice versa (Jørgensen et al., 2017). However, historically *Z. tritici* has evolved resistance to fungicides and virulence to resistant cultivars rapidly and, despite gains in genetic resistance and frequent fungicide applications, such situations can still arise. A recent example is the evolution of isolates virulent on the UK cultivar Cougar which has an unmapped source of resistance, threatening yields of this cultivar as well as its descendants. Therefore, it is important to not only identify more sources of resistance to STB but also to understand how these genes may function and how this information can be harnessed to further understand and enhance resistance to the disease in wheat. This could lead to the development of new weapons in our arsenal to fight STB.

### 4.1.2. Harnessing diversity for gene cloning

The population structuring of diversity panels through naturally-occurring recombination events over many generations makes them ideal for genetic mapping. The use of such populations can be more efficient than mutational genomics or biparental mapping, for example, as a single population can be curated and genotyped for use in mapping many traits. GWAS of whole-genome sequenced diversity panels combined with informative phenotype datasets can be powerful enough to map down to a small LD block or even a single gene (Gaurav et al., 2022). A common approach is to align sequence reads to a reference genome and use the resulting SNPs in the population for GWAS. Further detail on GWAS for gene cloning can be found in **Section 1.16** and Hafeez et al. (2021).

#### 4.1.3. Applications of cloned *R* genes

Once *R* genes are cloned, new possibilities for enhancing host resistance open up. *R* genes can be combined into transgenic cassettes which can be introduced at a single locus (Wulff and Moscou, 2014). This has the benefit of behaving like a resistance injection into host plants, providing disease resistance whilst maintaining background genetics. It also ensures that *R* genes do not become genetically separated, thus making them easier to track in breeding programmes. The presence of several resistance genes together reduces the selection pressure on the pathogen to overcome any single gene, which should increase the effective life of all genes in the stack (Wulff and Moscou, 2014; Hafeez et al., 2021). A five-transgene cassette conferring stem rust resistance has successfully been implemented in wheat (Luo et al., 2021). A greater number of cloned genes for STB resistance could enable such stacks to be employed in the future.

Understanding the structure and function of *R* genes can also provide new opportunities. *R* gene specificity can be manipulated and expanded through single amino acid changes. This was demonstrated by Segretin et al. (2014) in the case of *R2a*, which was engineered to enable recognition of both variants of the *Avr3a* effector of *Phytophthora infestans*, the oomycete that causes potato blight. De la Concepcion et al. (2019) were also successful in engineering the rice gene *PikP* to recognise multiple variants of the *Magnaporthe oryzae* (rice blast) effector *AvrPik*. Natural allele diversity has also been harnessed to identify targets for gene editing, such as a single amino acid variant in the wheat *Pm2* gene that was identified in an *Ae. tauschii* diversity panel which induces a variant-specific hypersensitive response (Manser et al., 2021).

With a greater arsenal of cloned *R* genes for resistance to STB, combined with detailed studies of their structure and function, stacks of natural and synthetic *R* genes could be deployed in wheat to enhance resistance and increase yields. GWAS of the Watkins collection using diverse isolates of *Z. tritici* could be an efficient method for increasing the currently small pool of two cloned *Stb* genes (*Stb6* and *Stb16q*: Saintenac et al., 2018; Saintenac et al., 2021) that scientists have to work with.

#### 4.1.4. Where did they come from, where did they go: the *Stb* genes of interest in this chapter

Phenotyping a diversity panel is no small task, and as such the isolates used must be considered carefully to make the best use of available resources. The reference isolate of *Z. tritici*, IPO323, was included for two main reasons. Firstly, the isolate produces reliable results on wheat cultivars, making it an ideal candidate for use in a large experiment which is difficult to repeat. When tested on wheat landraces, the isolate elicited consistent resistant and susceptible responses (**Chapter 3**). Secondly, and most importantly, this isolate was used to map and clone the resistance gene *Stb6* (Brading et al., 2002; Saintenac et al., 2018). This provided an opportunity to attempt to re-clone *Stb6* to prove that the methods employed in this study are robust and powerful enough to clone an STB resistance gene. The success of this experiment would indicate whether further tests with different isolates were worthwhile with respect to achieving the aims of this project, *i.e.*, if they would lead to the positive result of strong genetic associations and candidate *R* genes.

Subsequently, two additional isolates were selected to be screened on the 300-line Watkins diversity set based on results from screens on the 36-line core set, selected to be representative of the genetic and geographic diversity present in the wider collection. Isolates were chosen that elicited a broad range of responses in the host plants, ranging from highly resistant or immune to highly susceptible with almost the whole of the leaf covered in pycnidia. Additionally, isolates with known avirulences conferred by major genes in wheat were favoured. The final selection of isolates was IPO88004 and IPO90012.

##### 4.1.4.1. *Stb6*

*Stb6* has been mapped and cloned to the distal end of chromosome 3A (Brading et al., 2002; Saintenac et al., 2018). It was first identified in the UK cultivars Flame and Hereward and confers resistance to the Dutch *Z. tritici* isolate IPO323. This gene is widely present, having been identified in 18% of 238 European wheat cultivars tested by Arraiano and Brown (2006) as well as being present in the reference landrace Chinese Spring. *Stb6* is prevalent in wheat cultivars worldwide due to repeated selection by breeders despite the use of diverse germplasm, resulting in it having been introduced into wheat breeding programmes on six separate occasions (Brading et al., 2002; Chartrain et al., 2005c).

Resequencing of *Stb6* exons in 98 wheat lines as well as some progenitor species led to the identification of 17 haplotypes, eight of which were present in bread wheat (Saintenac et al., 2018). A single SNP present in the kinase domain of *Stb6* in the wheat cultivar Courtout is sufficient to induce susceptibility, whilst other susceptible cultivars such as Longbow, Kronos and Riband contain eight SNPs, mostly in the kinase domain. The cultivars Balance, Skyfall and Veranopolis appear to have a functional version of *Stb6* despite one to two SNPs shortly downstream of the galacturonan-binding domain. *Triticum dicoccum* also had a resistant haplotype, suggesting that *Stb6* has been conserved since the early days of wheat domestication (Saintenac et al., 2018). The function of the majority of the haplotypes identified in this study is not known.

Although *AvrStb6* is widespread (Brunner and McDonald, 2018), virulence to *Stb6* is common, almost reaching fixation in the European population of *Z. tritici*. Notwithstanding, the presence of markers associated with *Stb6* still appears to be associated with resistance to *Z. tritici* (Brown et al., 2015b). Increased understanding of the allelic diversity of *Stb6* could therefore be of interest to breeders, as matching these alleles to phenotypes could help in predicting *Stb6* function in the field. Such studies may even uncover targets for gene editing; this has been demonstrated in *Ae. tauschii*, where a single-amino acid variant was discovered and introduced into the wheat *Pm2* gene to induce a variant-specific hypersensitive response (Manser et al., 2021).

#### 4.1.4.2. *Stb15*

*Stb15* was previously mapped to the short arm of chromosome 6A in the resistant Swiss cultivar Arina where it provides resistance to the Ethiopian *Z. tritici* isolate IPO88004 (Arraiano et al., 2007). This gene is widely found in European winter wheat – 60% of cultivars tested carry the gene, although it is not associated with resistance in field conditions (Arraiano and Brown, 2006; Arraiano et al., 2007). The mapping interval for *Stb15* is very large – one and a half chromosome arms between the markers *gwm459* (6A:680,551,3) and *gwm334* (6A:924,927,5). Efforts to reduce this interval and produce perfect markers would aid in monitoring the distribution of this gene in wheat fields.

ArinaLrFor, sequenced as part of the wheat pangenome (Walkowiak et al., 2020), is likely to carry the functional version of *Stb15*. This line is a cross between Forno, known to be susceptible to IPO88004, and Arina, and is highly resistant to IPO88004 (Arraiano et al., 2007b; **Figure 31**). The chromosome-level assemblies available for this line are therefore an asset to the mapping of *Stb15*. Another advantage is the strong gene-for-gene effect observed in interactions involving *Stb15*, which is relatively rare in Septoria-wheat interactions and increases the probability of being able to associate this potentially strong phenotype with sequence features via GWAS. As only two major genes have been cloned for resistance to STB, there is much left to discover about the function and diversity of these immune receptors. *Stb15* is therefore an ideal next target for *Stb* cloning studies.

#### 4.1.4.3. *Stb11*

*Stb11* has been mapped to the short arm of chromosome 1B in the line TE9111 and confers resistance to the Mexican isolate IPO90012 (Chartrain et al., 2005b). It is located close to the mapped locations of *Stb2* and *StbWW* – it is unclear whether or not these are the same genes, spread in global wheat breeding through CIMMYT breeding lines (Brown et al., 2015a). If this gene were cloned, perfect markers could be designed that would aid in the tracking of *Stb11* in breeding programmes; this would be a step towards separating the effects of *Stb11* from other genes and assessing its impact on disease resistance in the field.

#### 4.1.5. Summary of chapter findings

The aim of this chapter was to test the efficacy of whole-genome shotgun GWAS in wheat for cloning *Stb* genes, and to identify novel loci associated with resistance.

The phenotyping and GWAS methods described in Chapters 3 and 4 proved sufficient to re-clone the resistance gene *Stb6*; this proof-of-concept provided us with the confidence needed to pursue the mapping of other *Stb* genes in the same way. This led to the identification of a high-confidence candidate for the previously-mapped gene *Stb15* on 6AS, using the isolate IPO88004. The candidate gene encodes a G-type lectin RLK, following the pattern of other cloned *Stb* genes. An additional source of resistance to IPO88004 was mapped to chromosome 2B. We then attempted to use responses to the isolate IPO90012 to map a

candidate for *Stb11*. No significant associations were detected when employing pycnidia data, but an interval on 4D was associated with damage and super (rapid-onset) necrosis responses.

Haplotypes of *Stb6* and the *Stb15* candidate were explored in the Watkins collection. There appeared to be ten groups for *Stb6* and four key groups for *Stb15*. When haplotypes associated with resistance to IPO323 were removed from the analysis, the dataset appeared to be insufficient to map any additional intervals. However, the same analysis for IPO88004/*Stb15* resulted in the peak associated with resistance on 2B to become more refined and significant, facilitating future cloning efforts at this locus. Similarly, when the GWAS analyses on the IPO90012 damage and super necrosis datasets are compared, the interval associated with these traits was clearer when mapping with super necrosis data. These experiments demonstrate the utility of multiple, refined phenotype datasets for running different permutations of GWAS analyses.

## 4.2. MATERIALS AND METHODS

### 4.2.1. Association mapping

GWAS was performed by collaborators at the Agricultural Genomics Institute at Shenzhen, China (AGIS), led by Shifeng Chen, as part of a collaboration with JIC headed by Simon Griffiths ('WatSeq'). Watkins and wheat accessions were mapped to the reference genome of Chinese Spring and SNPs were called. The resulting genome-wide VCF files were combined with Septoria phenotype data (**Chapter 3**) for association genetics using a method based on the genome-wide efficient mixed-model association method (GEMMA; Zhou and Stephens, 2012). Manhattan plots were generated and shared with my team, as well as raw output files for some (but not all) of the analyses on Septoria phenotypes.

AGIS scientists (Feng Kong and Wen Fei) also analysed the LD block containing the SNPs most tightly correlated with Septoria response traits and shared their interpretations.

### 4.2.2. Identification of candidate *Stb* genes

Candidate Septoria resistance genes were identified by selecting the most likely candidate from the genes in the LD block most highly associated with Septoria response. A number of factors were considered, such as: the SNP *p*-value (for association with Septoria response), gene class, the presence of differential SNPs between susceptible and resistant wheat varieties, and the strength of correlation of predicted resistant haplotypes with the phenotypes (as presence-absence variation was typically not observed).

### 4.2.3. Analysis of haplotypes of the identified candidate Septoria *R* genes

#### 4.2.3.1. *Haplotypes in the wheat pangenome*

BLAST searches of candidate genes were performed against the wheat pangenome using an online Galaxy server (<https://galaxy-web.ipk-gatersleben.de/>; Altschul et al., 1997; Camacho et al., 2009; Cock et al., 2015) hosting BLAST databases generated from pseudomolecule and scaffold-level assemblies produced by Walkowiak et al. (2020).

Complete sequences of the top hits were then extracted from the assembled genomes using the *samtools getfasta* commandline function. These were then loaded in Geneious Prime 2020.2.5 and alignments were generated, allowing for manual evaluation of the haplotypes or alleles present. IGV (interactive genomics viewer; Robinson et al., 2011) was also used for data visualisation.

#### 4.2.3.2. VCF parsing to generate a distance matrix

A python script was written to identify the haplotypes of the candidate *Stb* genes identified (Figure 41; Supplementary Script 2). The script parsed variant call format files (VCFs) generated from the alignment of Watkins and wheat lines to Chinese Spring by AGIS. This produced a matrix of distances between all accessions which could be used to determine haplotype groups.

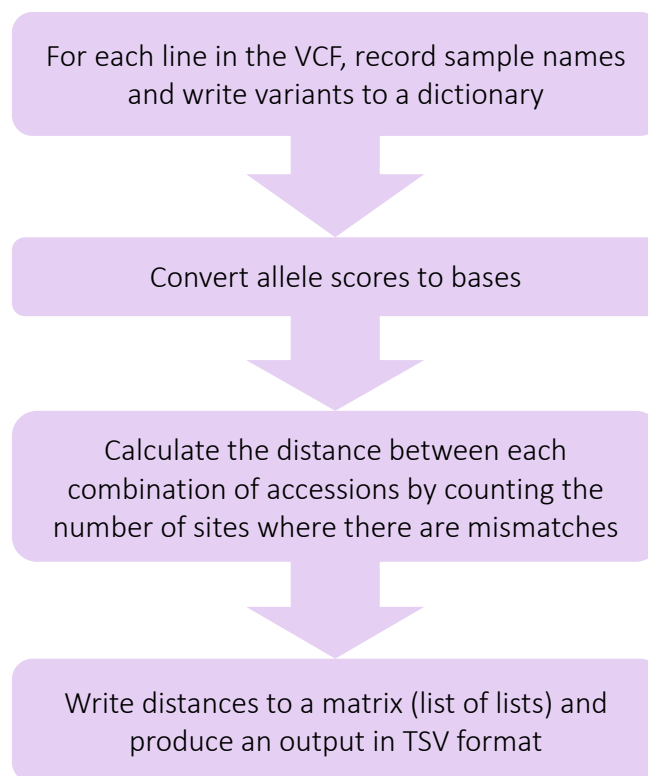


**Figure 41:** Flow chart of the steps taken to generate a SNP distance matrix based on regions extracted from the Watkins landrace WGS dataset. VCF = variant call format, TSV = tab-separated values format.

#### 4.2.3.3. Generation of heatmaps for haplotype identification

The R package *pheatmap* was used to generate heatmaps arranged in dendrograms from distance matrices, including associated phenotype data (**Supplementary Script 3**). Various iterations of the VCF parsing script described above were run and plotted in order to identify the most useful variation for haplotype calling. Ultimately, the whole gene sequence was analysed (rather than, for example, exons alone).

The dendrogram produced was manually analysed to estimate the number of haplotype groups present. Clusters were then estimated using the *cutree* function in *pheatmap* and examined; several iterations were performed to determine the most informative number of clusters/haplotypes.

#### 4.2.4. Generation of a phylogenetic tree for Watkins core 300

Axiom Breeder's array data for the Watkins core 300 collection was provided in hapmap format by Luzie Wingen. This data is also available at [wisplandrangepillar.jic.ac.uk](http://wisplandrangepillar.jic.ac.uk). For subsequent analysis, the data was converted from hapmap to fasta format using a short python script (**Supplementary Script 4**). As the markers were co-dominant and heterozygosity was common, the fasta sequence consisted of two sites per SNP – one for each homologue. This approach was chosen as admixture is typically common in landrace populations, so it seemed appropriate to treat each homologue as a separate allele.

The file was then opened in MEGA and exported as a PHYLIP file with non-variable sites removed. This reduced the total number of sites from 28,918 (from 14,459 codominant SNPs) to 23,021 variable sites. The tree-calculating software RaxML was used; **Supplementary Script 5** was employed to run the analysis on the JIC high performance computing (HPC) cluster. The number of bootstrap replicates was set to autoMRE to allow RaxML to execute the optimal number of bootstrap searches (up to a maximum of 1000). The GTR-GAMMA substitution model was used: the General Time Reversible model of nucleotide substitution under the Gamma model of rate heterogeneity. An ascertainment bias correction was added to this model, which corrects for the bias introduced by the exclusion of SNPs with extreme

allele frequencies (in contrast to analysing whole-genome data). The standard Paul Lewis correction was employed (Lewis, 2001).

The web-based visualisation tool iTOL (<https://itol.embl.de>; Letunic and Bork, 2021) was then used to circularise the tree and to annotate various datasets around it. The tree was rooted at the midpoint since the outgroups for this dataset were not known/consciously employed (Kinene et al., 2016).

## 4.3. RESULTS

### 4.3.1. Dissecting the response of Watkins landraces to IPO323 by GWAS

#### 4.3.1.1. *Results of GWAS on IPO323 data*

GWAS was performed using IPO323 pycnidia and damage phenotypes combined with SNP data from the Watkins collection, mapped to Chinese Spring. There was a peak on chromosome 3A that was associated with both damage and pycnidia responses, but the association for super necrosis was very noisy with no clear candidate regions (**Figure 42**; work by Feng Cong). SNPs in the 3A peak were very highly associated with pycnidia, with a  $-\log_{10} p$ -value of almost 30.

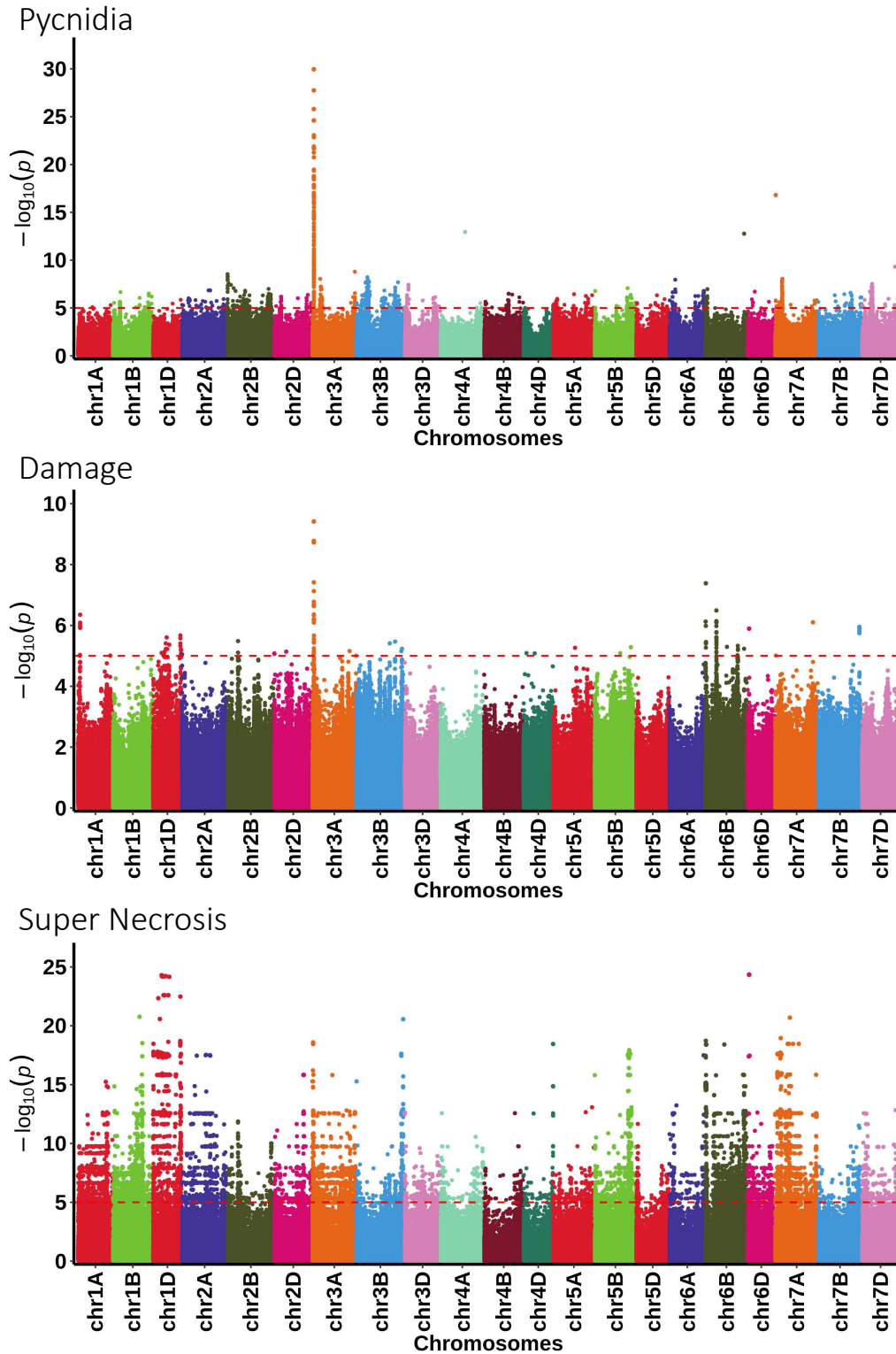


**Figure 42:** Manhattan plot showing associations between SNPs in the Watkins landrace collection and pycnidia, damage and super-necrosis responses to *Z. tritici* isolate IPO323. Figures produced by Feng Cong.

At the 3A locus, an LD block extending from around 26.10 to 27.50 Mb was identified (**Figure 43**, blue box; work and figure by Xian Wenfei). Within this larger block, a smaller haploblock was identified which was most highly associated with resistance, from around 26,035,170 to 26,238,727 bp (**Figure 43**, green box). This region was 204 kb and contained 6 genes; one of these was *Stb6*.

A search of this region in Knetminer (<https://knetminer.com/>; Hassani-Pak et al., 2021) indicated that there are five other annotated genes in the 'green box' region. In addition to *Stb6*, three of these genes encoded plasma membrane-localised proteins with kinase domains: TraesCS3A02G049375 (at 26,140,557), TraesCS3A02G049600 (at 26,229,850) and TraesCS3A02G049400 (at 26,194,495). These could be paralogues. There were two other annotated genes: TRAESCS3A02G049300 and a plant signal recognition particle (SRP) RNA, ENSRNA050023766.

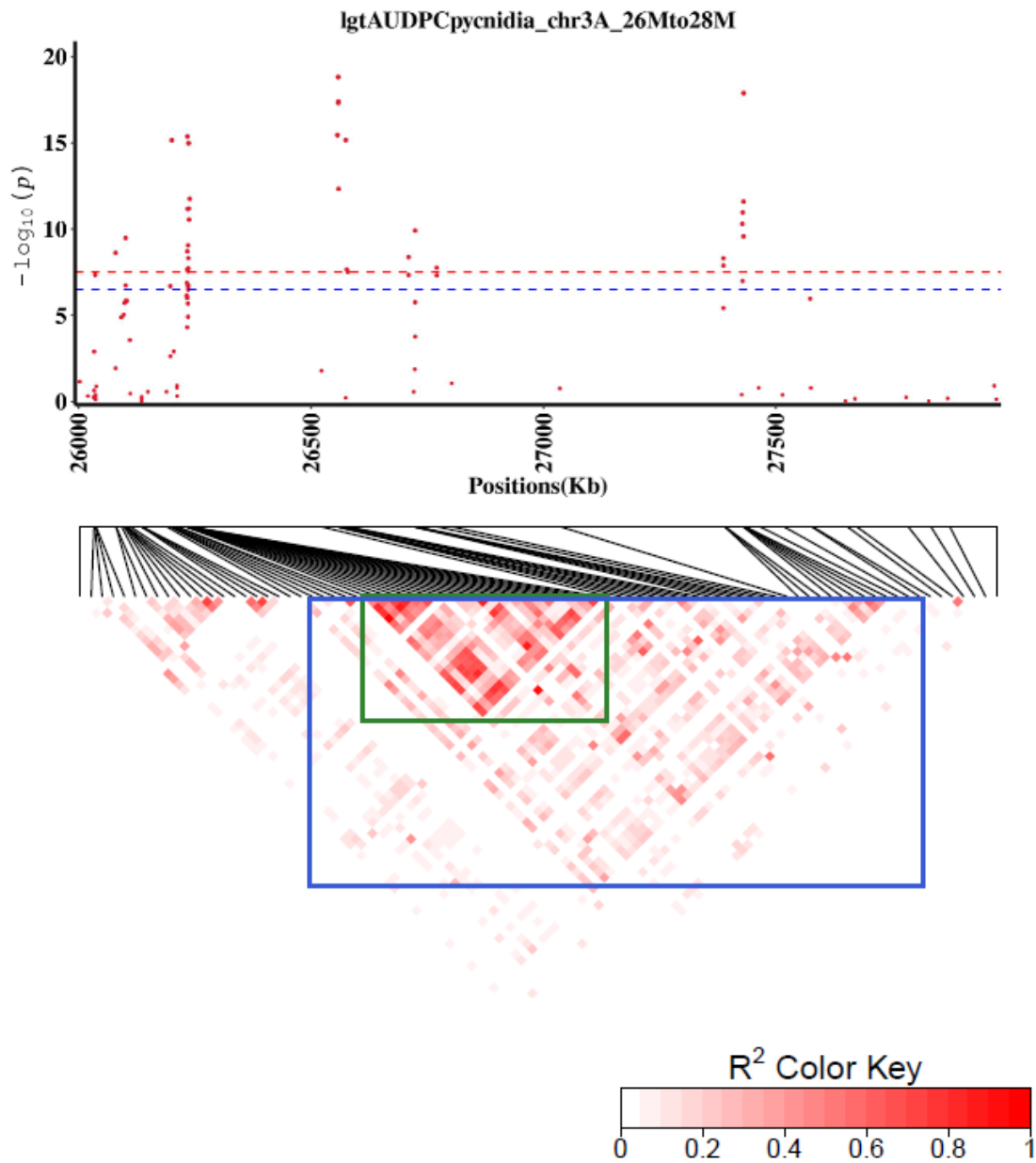


**Figure 43:** Zoomed-in Manhattan plot of the 3A peak from the SNP-based GWAS with the IPO323 pycnidia phenotype from Shifeng *et al.* The LD heatmap is displayed below. Figure produced by Xian Wenfei. Blue square indicates the main area of the peak. Green square indicates that smaller haplotype block within the blue square which is most highly associated with resistance.

#### 4.3.1.2. *Stb6* in the wheat pangenome

There appeared to be five haplotypes in the wheat pangenome. *Triticum spelta* has a SNP at position 2,790 relative to the reference genome, Chinese Spring (**Figure 44**). Robigus and Jagger have a SNP in the first exon of the gene, whilst Cadenza, Julius, Landmark, Claire and Mace have a SNP nine bp after the end of the third exon. Weebill and Lancer had a 219 bp insertion in an intron as well as a SNP in the fourth exon.

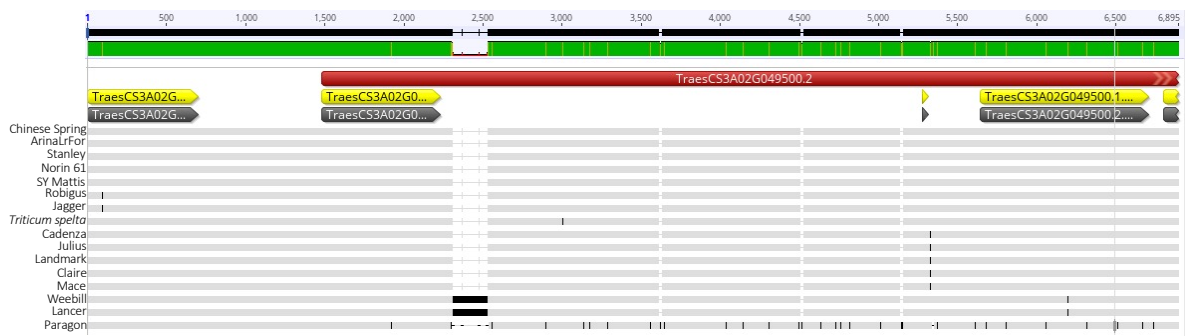


**Figure 44:** Alignment of *Stb6* sequences in the sequenced wheat pangenome visualised in Geneious Prime. Yellow arrows = CDS, grey arrows = exons, red box = mRNA.

#### 4.3.1.3. *Analysis of Stb6 haplotypes present in the Watkins collection and their correlation with phenotypes*

When distance in SNPs was plotted in a heatmap, it became clear that there were several distinct haplotype groups which corresponded to the phenotypes observed in seedling trials (**Figure 45**). By visual inspection of the dendrogram, there appeared to be around 11 major groups. When  $k=11$  was used, however three groups contained only one accession; WATDE0021 only differed from group 6 accessions in heterozygosity at a single site, so  $k=10$  was used to combine these two groups.

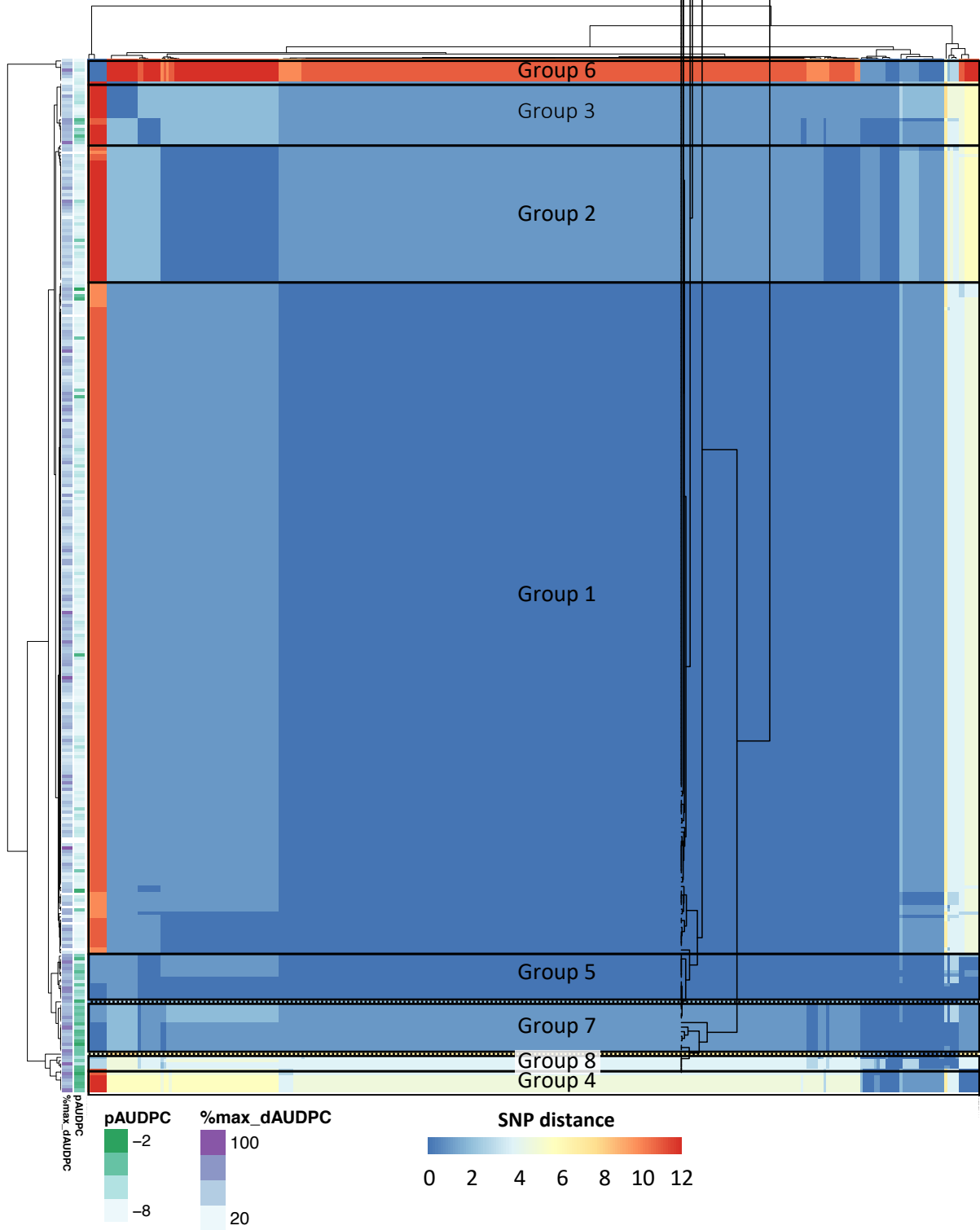


**Figure 45:** Heatmap displaying the distance between each pair of accessions in the Waktins collection, as well as some elite wheat lines. Pycnidia (pAUDPC) and damage (%max\_dAUDPC) scores are plotted along the left-hand side. Accessions are grouped via a dendrogram. Haplotype groups are indicated with black outlines and labels. Groups 9 and 10 contained only one accession and are indicated with dashed lines.

There were 13 lines which appeared to have the Chinese Spring haplotype of *Stb6* but were susceptible to IPO323 (Figure 46). Where SNPs in the panel relative to Chinese Spring had been designated, no homozygous SNPs were called within exons in these lines. There were, however, some sites at which there was missing data. This could be due to poor mapping/alignment to Chinese Spring, either due to limited data quality/coverage or because the sequence had so diverged from Chinese Spring that it was not possible to map it correctly with the approach used.

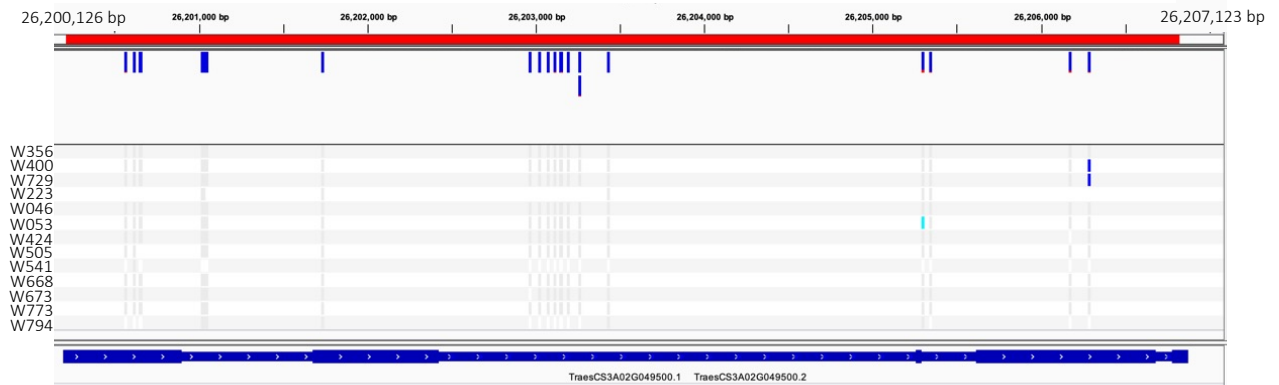


**Figure 46:** IGV visualisation of SNPs in the *Stb6* locus in the 13 lines which appeared to have the same *Stb6* haplotype as Chinese Spring but were susceptible to IPO323. Sites containing SNPs are indicated in the second panel. The third panel displays SNPs in the Watkins lines listed: grey bands indicate the same base as Chinese Spring, indigo bands indicate heterozygous SNPs, turquoise bands indicate homozygous SNPs and no/white bands indicate missing data. The bottom panel contains the GFF (general feature format) file, wherein thick bands represent exons and thinner bands represent introns.

Haplotypes were calculated based on the whole gene sequence. The SNP after the third exon, present in wheat lines such as Cadenza, Julius, Landmark, Claire and Mace, did not appear to have an effect on phenotype since the phenotype distribution was very similar to that of the Chinese Spring haplotype group (**Figure 47**). Group 4, containing Longbow and Paragon, was clearly associated with susceptibility; this was also true of groups 5, 7 and 8. Group 6 appeared to be resistant.

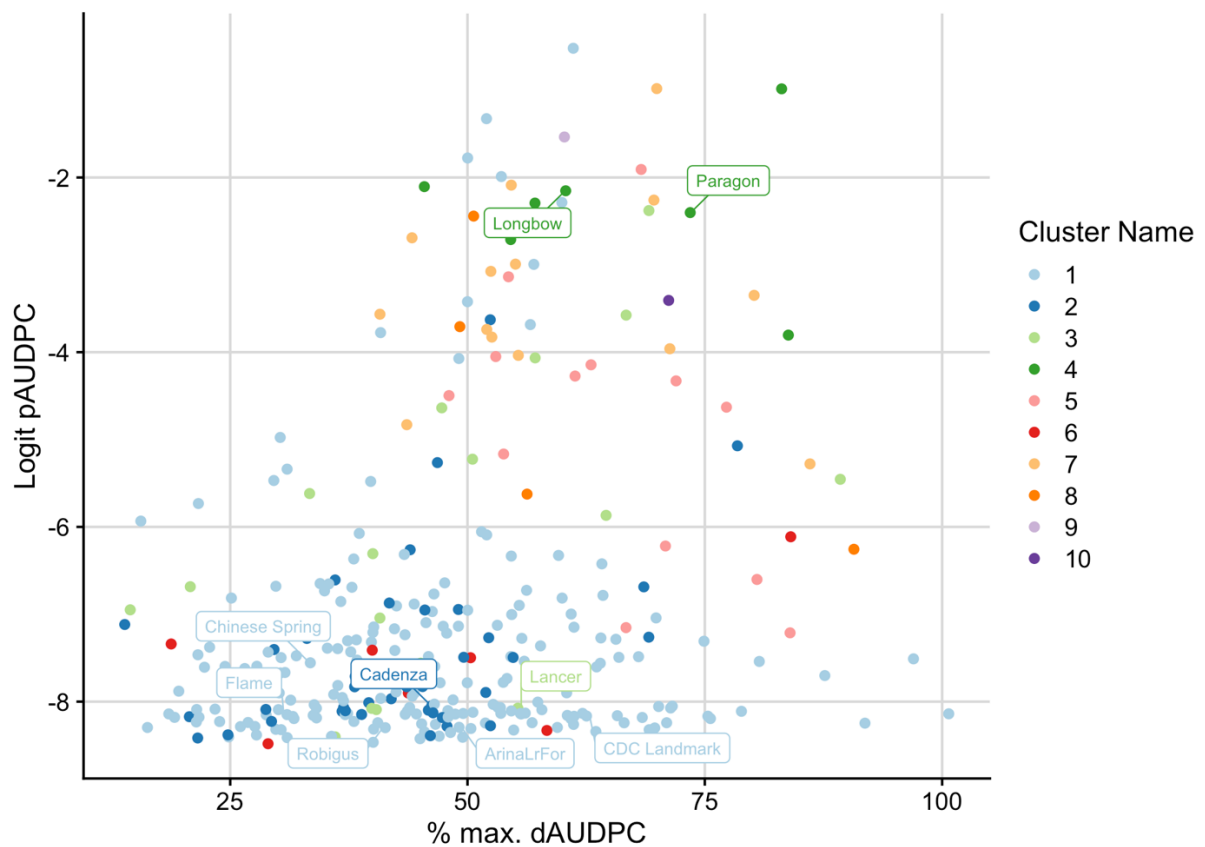


**Figure 47:** Pycnidia (logit pAUDPC) scores plotted against damage (% max. dAUDPC) scores in response to IPO323, with colour coding to indicate haplotype clusters designated for *Stb6*.

#### 4.3.1.4. Rerunning the GWAS in the absence of functional *Stb6* haplotypes

The GWAS was rerun with accessions carrying functional haplotypes of *Stb6* removed (*i.e.* groups 1, 2 and 6), to investigate whether functional copies of *Stb6* could be masking the effects of other *R* genes. Unfortunately, there seemed to be too few accessions in the panel that were resistant to IPO323 in the absence of *Stb6* to be able to identify any other regions associated with resistance to IPO323 (**Figure 48**).

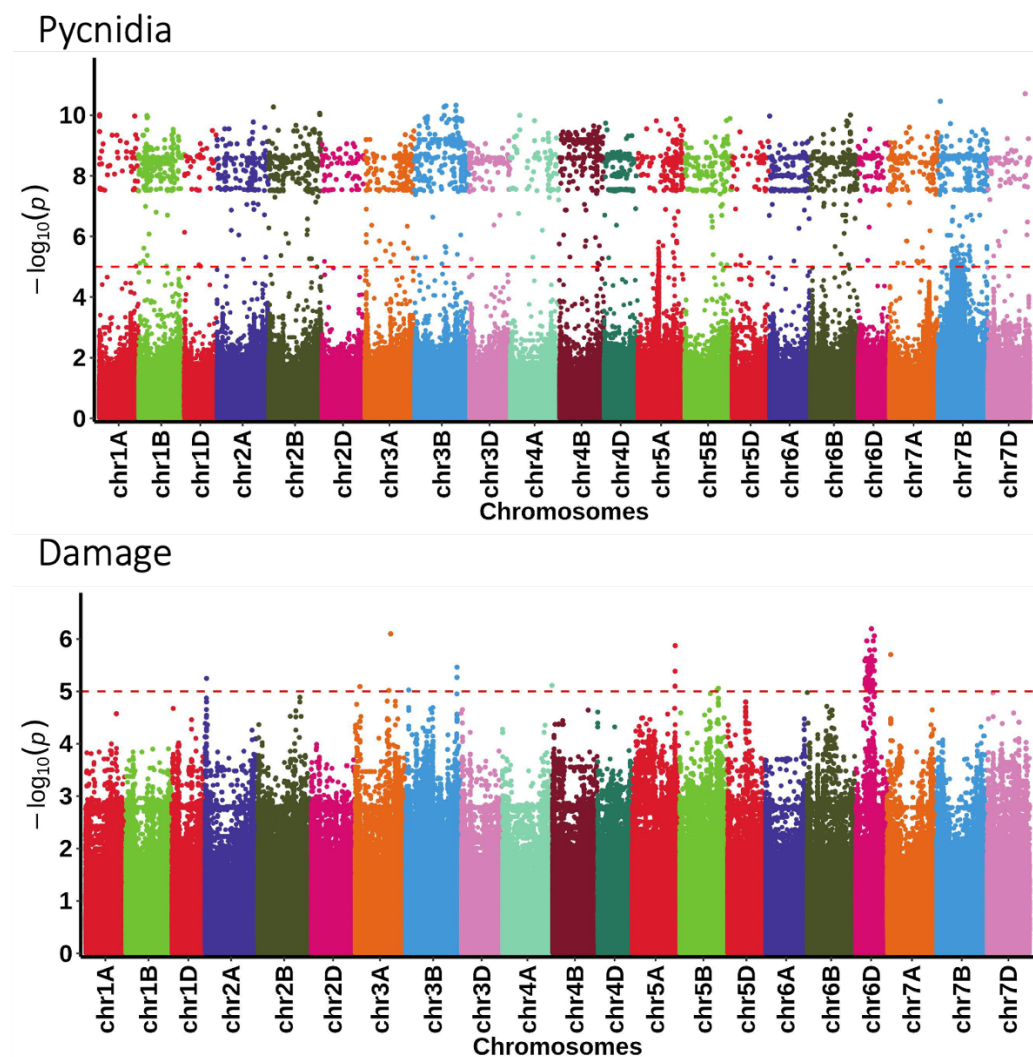


**Figure 48:** Manhattan plots of logit pAUDPC (pycnidia) and % max. dAUDPC (damage) scores of Watkins lines inoculated with *Z. tritici* isolate IPO323 associated with genome-wide SNPs. 234 Watkins accessions carrying a functional version of *Stb6* were removed to leave a panel size of 66 accessions (plus three wheat cultivars).

### 4.3.2. Dissecting the response of Watkins landraces to IPO88004 by GWAS

#### 4.3.2.1. *Results of GWAS on IPO88004 data*

Several regions were associated with IPO88004 phenotypes. The clearest association was on chromosome 6AS, as this locus had the highest p-value for both the pycnidia and damage traits (**Figure 49**). There was also a significant peak associated with pycnidia cover on chromosome 2BL; the locus did not appear to explain much variation in damage. The picture for super necrosis data was more difficult to interpret: many loci across the genome contained highly associated SNPs, with p-values highest in the peak on 5AL. The GWAS was run a second time for super necrosis data, with lines that had enough pycnidia to be considered susceptible removed. This test was performed to see whether more standard susceptible phenotypes, with high pycnidia as well as necrosis, were under different genetic control to the super necrosis phenotypes seen in response to IPO323, which typically consisted of high necrosis with little to no pycnidia cover. The peak at 5AL once again dominated in this second dataset, but chromosome 2AL and very large areas of chromosome 2B, amongst others, were also very highly associated with the trait. This was likely due to population structure effects since the test was run on relatively few lines (17 in total; **Supplementary Table 4**).

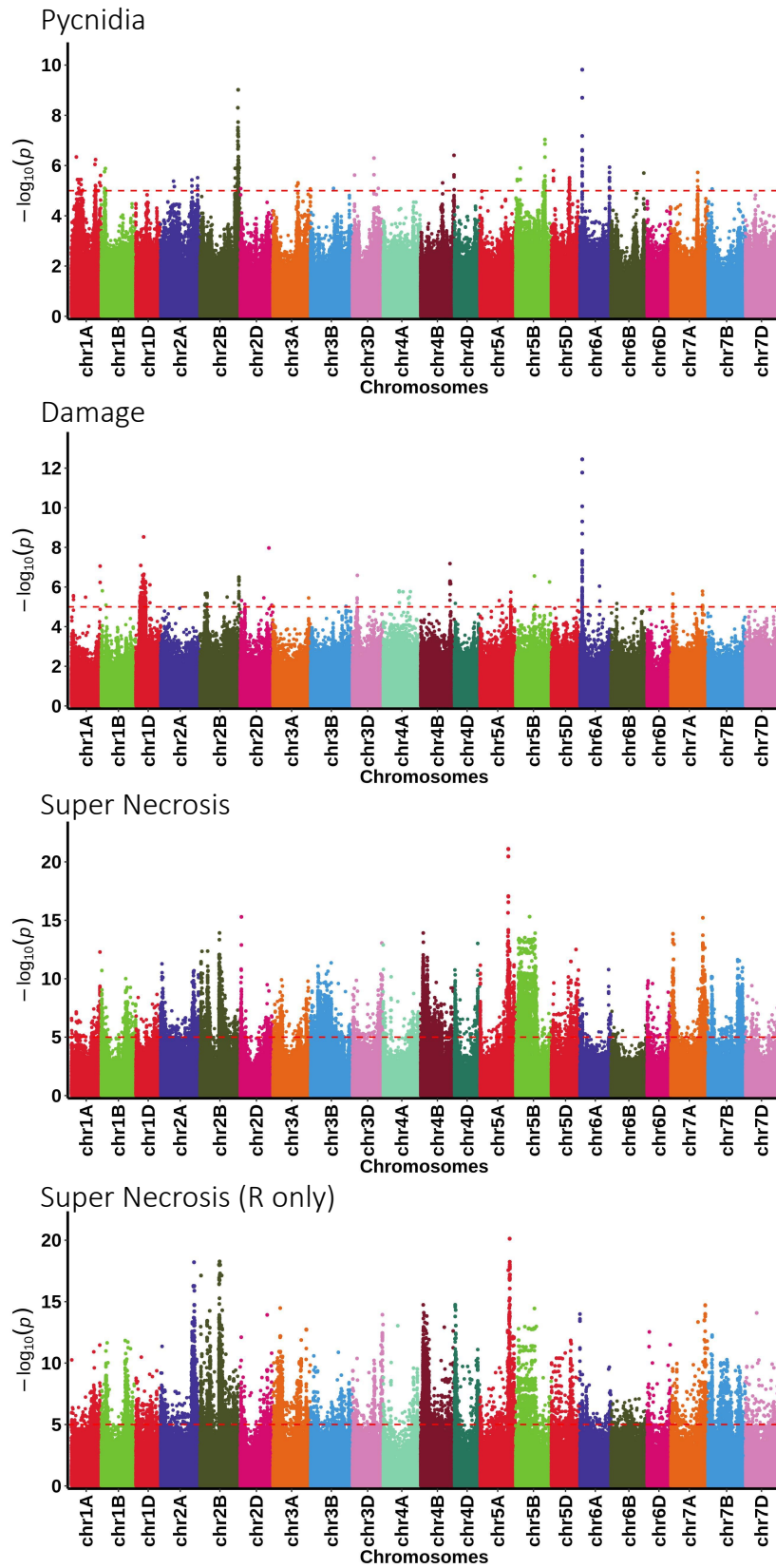


**Figure 49:** Manhattan plots showing association of SNPs mapped to Chinese Spring with logit pAUDPC, % maximum dAUDPC, SN (super necrosis) and SN with lines exhibiting high pycnidia values removed (clean SN only).

The most significant peak associated with pycnidia was on chromosome 6A between 485,003,26 and 485,994,21, with a length of 99.1 kb. This region contained six genes (**Table 24**). One of these genes, TraesCS6A02G078700, was predicted to encode a serine/threonine receptor kinase. Since the previously cloned *Stb6* and *Stb16q* genes also contain this domain, it was selected as the most likely candidate. Evidence was also gathered to evaluate whether the other genes in the region could be excluded as candidates. By looking at the VCFs called against Chinese Spring, the SNP variation in these genes could be compared between Arina (known to carry a functional copy of *Stb15*) and Chinese Spring (known to be susceptible to IPO88004). No SNPs were called in Arina against Chinese Spring within the sequences for TraesCS6A02G078600 and TraesCS6A02G078500, which excluded these two genes as candidates. When a haplotype analysis was performed on the remaining three genes, Arina copies of the genes did not correlate as well with responses to IPO88004. This analysis is described in **section 4.3.2.2** for TraesCS6A02G078700.

**Table 24:** Genes in the 6A peak and their function. Reasons for not selecting these genes as the *Stb15* candidate are given.

Annotation	Gene Name	Start	Length	Protein	Reason for exclusion
TRAESCS6A02G078600	APUM23	48516680	5780	Pumilio homolog 23	Arina has the same genotype as Chinese Spring.
TRAESCS6A02G079000	S6PDH	48563464	3903	Aldo_ket_red domain-containing protein	Lots of SNPs in Arina. Looking at the haplotype heatmap, the association with resistance phenotype is not as strong as for TraesCS6A02G078700.
TRAESCS6A02G078800	PEX16	48552372	4331	Peroxisomal membrane protein PEX16	No SNPs in exons detected.
TRAESCS6A02G078900	SRK6	48556992	4149	Uncharacterised protein	4 SNPs in Arina. Looking at the haplotype heatmap, the association with resistance phenotype is not as strong as for TraesCS6A02G078700.
TRAESCS6A02G078700		48525265	3354	Receptor-like serine/threonine-protein kinase	-
TRAESCS6A02G078500		48509308	1890	Uncharacterised, LRR superfamily related domain	Arina has the same genotype as Chinese Spring.

#### 4.3.2.2. Haplotypes of *Stb15* and their function in the Watkins collection

There appeared to be three main groups of haplotypes in the wheat pangenome lines (**Figure 50**). There was a group of lines with the ArinaLrFor phenotype, including Julius, Claire, Robigus and the *Triticum spelta* accession. The presence of the gene in *Triticum spelta* suggests that it is highly conserved. The rest of the lines had the Chinese Spring genotype, but in some genotypes (Chinese Spring, Cadenza, Norin 61, Paragon and Landmark) a large insertion of up to 1,314 bp was present in an intron.

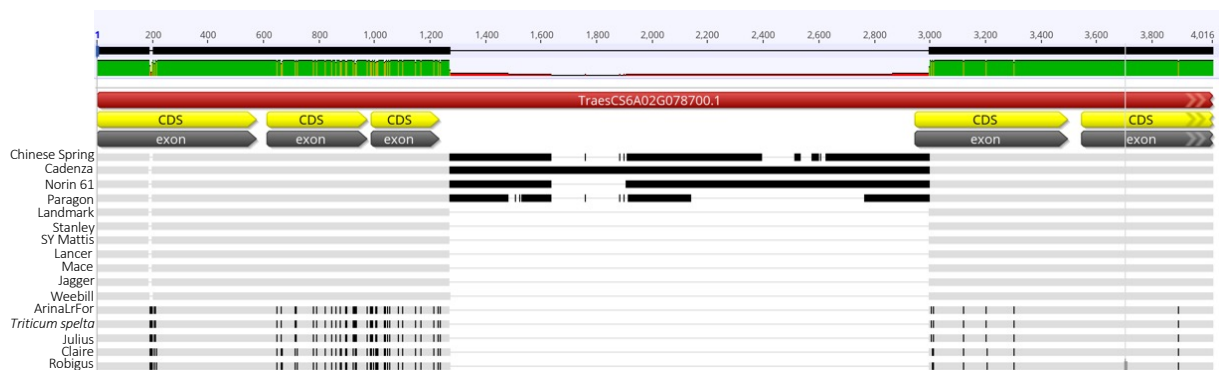


**Figure 50:** Geneious screenshot showing an alignment of the TraesCS6A02G078700 gene in the wheat pangenome lines.

The haplotypes observed in the wheat pangenome can act as a good baseline for interpreting other haplotypes in the Watkins collection. However, when the VCF file of SNPs in the Watkins collection is visualised in IGV, it is clear that some variation is not captured (**Figure 51**). There is a six bp insertion in Arina that is not called (due to the mapping of accessions to Chinese Spring, which does not have the insertion), and there are no SNPs called within the large intron insertion present in Chinese Spring despite the fact that there is presence/absence variation of this within the wheat pangenome lines. This is likely because the inserted region is transposon-rich, therefore difficult to assemble with lower-depth sequencing. Even in the case of Cadenza, sequenced to high quality, only Ns were recorded in this region. When blasted against *trep* (<http://botserv2.uzh.ch/kelldata/trep-db/blast/>), a hand-curated database of transposons, the top hits for this insertion were *Hordeum vulgare* retrotransposons RSX\_Hvul\_Xanti\_Gb3-2 and RSX\_Hvul\_Xanti\_Gb3-1. The length of this insertion is the only genotypic difference within the gene between CS and Paragon, which

have disparate phenotypes. It could be due to the insertion or to something else, like quantitative resistance.

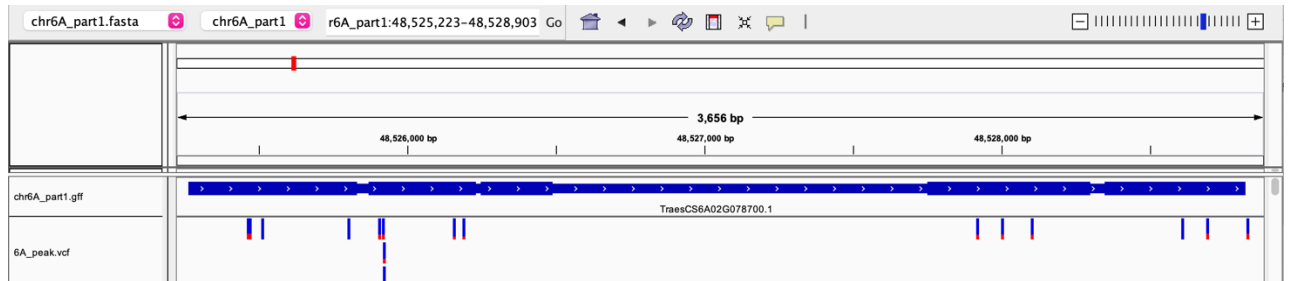


**Figure 51:** SNP calls within the *Stb15* locus, visualised in IGV.

A heatmap of the distance matrix generated for the SNPs in the TraesCS6A02G078700 locus in Watkins and wheat lines revealed four key haplotype groups (**Figure 52**). It is clear from the panel to the left of the heatmap that the Arina-Robigus group was exclusively associated with very low pycnidia scores.

An initial conservative estimate of  $k=10$  hierarchical clusters was made and these extracted from the pheatmap output, resulting in four haplotypes containing wheat lines and six unique to the Watkins collection (**Table 25**). However, upon closer inspection, these differences could be explained by missing data in several cases; it is not possible to tell from the VCF whether missing SNP calls (denoted by '.') are due to the absence of the SNP in the accession (eg due to a deletion) or to non-biological reasons (e.g. read mapping or filtering). From the wheat pangenome alignment of the gene above, it is clear that ArinaLrFor, Robigus and Claire have the same genotype. Therefore, the differences in genotype in the VCF seem to be due to data quality or processing. Similarly, it was not possible to discern whether the groups Watkins 1, 3 and 4 were the same as Chinese Spring or not, and, since these groups comprised only one accession each, it seemed reasonable to reallocate Watkins 1 and 4 to the Chinese Spring group and to exclude Watkins 3 (for which SNP data was available for only two datapoints). Upon closer inspection, Watkins 5 could be assorted into Watkins 5 and the Arina/Robigus group. Watkins 2 and 6 did appear to be unique, resulting in a total of four high-confidence haplotypes from the initial pool of ten (**Table 26**).

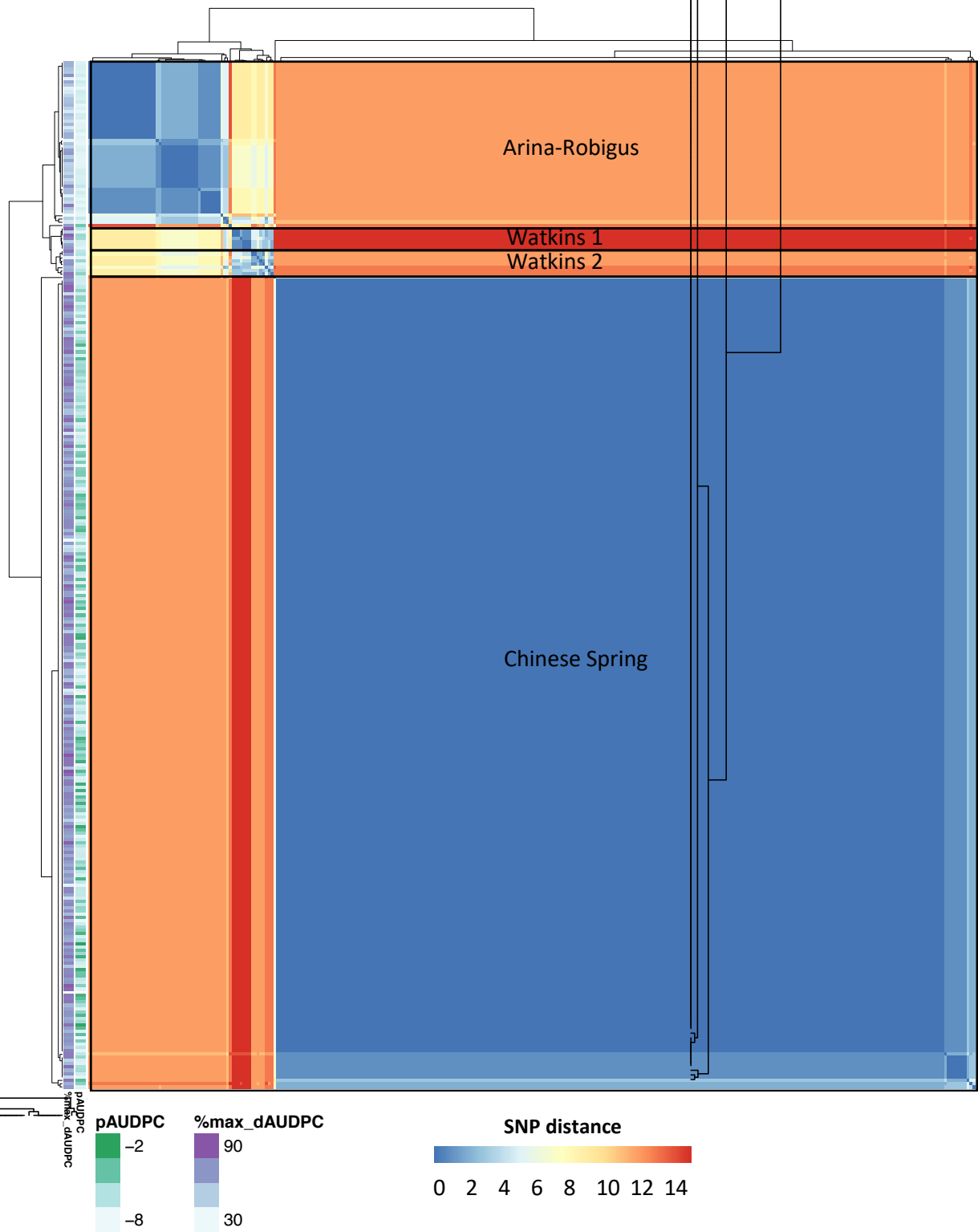


**Figure 52:** Heatmap of distance in SNPs within the TraesCS6A02G078700 locus between Watkins accessions. Panel on left shows phenotype scores. Major haplotype groups are outlined in black and labelled with the names of key lines.

**Table 25:** Haplotypes identified by pheatmap  $k=10$  and their SNP complement. Cells with the reference (Chinese Spring) genotype are in white. Cells with the ArinaLrFor genotype are in pink; other alternative alleles are in yellow cells.

Haplotype	No.	Distance from		SNP position chr6A_part1:4852...														
		Chinese Spring	ArinaLrFor	1	2	3	4	5	6	7	8	9	10	11	12	13	14	15
				5467	5473	5514	5805	5907	5922	5923	5925	6158	6193	7920	8004	8102	8609	8693
Chinese Spring	248	0	11-12	C	C	C	A	C	C	T	A	C	A	G	G	C	C	T
ArinaLrFor	1	12	0	.	.	C	A	A	A	C	G	.	.	.	T	.	C	C
Claire	2	11-12	7	A	G	C	A	A	A	C	G	.	.	A	T	A	C	C
Robigus	47	11-12	3-7	A	G	C	A	A	A	C	G	T	C	A	T	A	C	C
Watkins 1	1	6	9	.	.	.	A	C	C	T	A	C	A	G	G	C	C	T
Watkins 2	7	15	11	A	G	C	.	.	.	.	.	.	.	A	T	A	T	C
Watkins 3	1	13	8	.	.	.	.	.	.	.	.	.	.	.	.	.	C	T
Watkins 4	1	2	13	C	C	C	A	C	C	T	A	C	A	G	G	C	.	.
Watkins 5	3	13	9-11	A	G	C,T	.	.	.	.	.	.	.	A	T	A	C,T	C
Watkins 6	5	12	10-11	A	G	T	G	C	C	T	G	.	.	A	T	A	T	C
				EXON 1				EXON 2						EXON 4			EXON 5	

**Table 26:** Haplotypes identified by pheatmap  $k=10$  and their SNP complement, manually curated to remove haplotypes of low confidence. Cells with the reference (Chinese Spring) genotype are in white. Cells with the ArinaLrFor genotype are in pink; other alternative alleles are in yellow cells.

				SNP position chr6A_part1:4852...														
Distance from																		
Haplotype	No.	Distance from		1	2	3	4	5	6	7	8	9	10	11	12	13	14	15
		CS	ArinaLrFor	5467	5473	5514	5805	5907	5922	5923	5925	6158	6193	7920	8004	8102	8609	8693
CS	250	0-6	11-12	C	C	C	A	C	C	T	A	C	A	G	G	C	C	T
Robigus	51	11-12	0-7	A	G	C	A	A	A	C	G	T	C	A	T	A	C	C
Watkins 1	7	15	11	A	G	C	.	.	.	.	.	.	.	A	T	A	T	C
Watkins 2	7	12	10-11	A	G	T	G	C	C	T	G	.	.	A	T	A	T	C
				EXON 1				EXON 2						EXON 4			EXON 5	

The two unique Watkins haplotypes were rare in the panel (containing seven accessions each) and more similar to the Arina than the Chinese Spring haplotype. They contained three unique alleles: a C to T substitution at SNP position three, A to G at position four and C to T at position 14. Around half of the accessions in the Watkins groups fell within the phenotypic range of the Arina-Robigus group (Figure 53). There was a huge amount of phenotypic variation within the Chinese Spring haplotype group, from resistance on par with ArinaLrFor to susceptibility beyond that of Chinese Spring. Chinese Spring, Paragon, Norin 61 and Cadenza all carry the large intron insertion, and also all scored very highly for damage (>80% of max dAUDPC) in response to IPO88004, although pycnidia levels were variable.

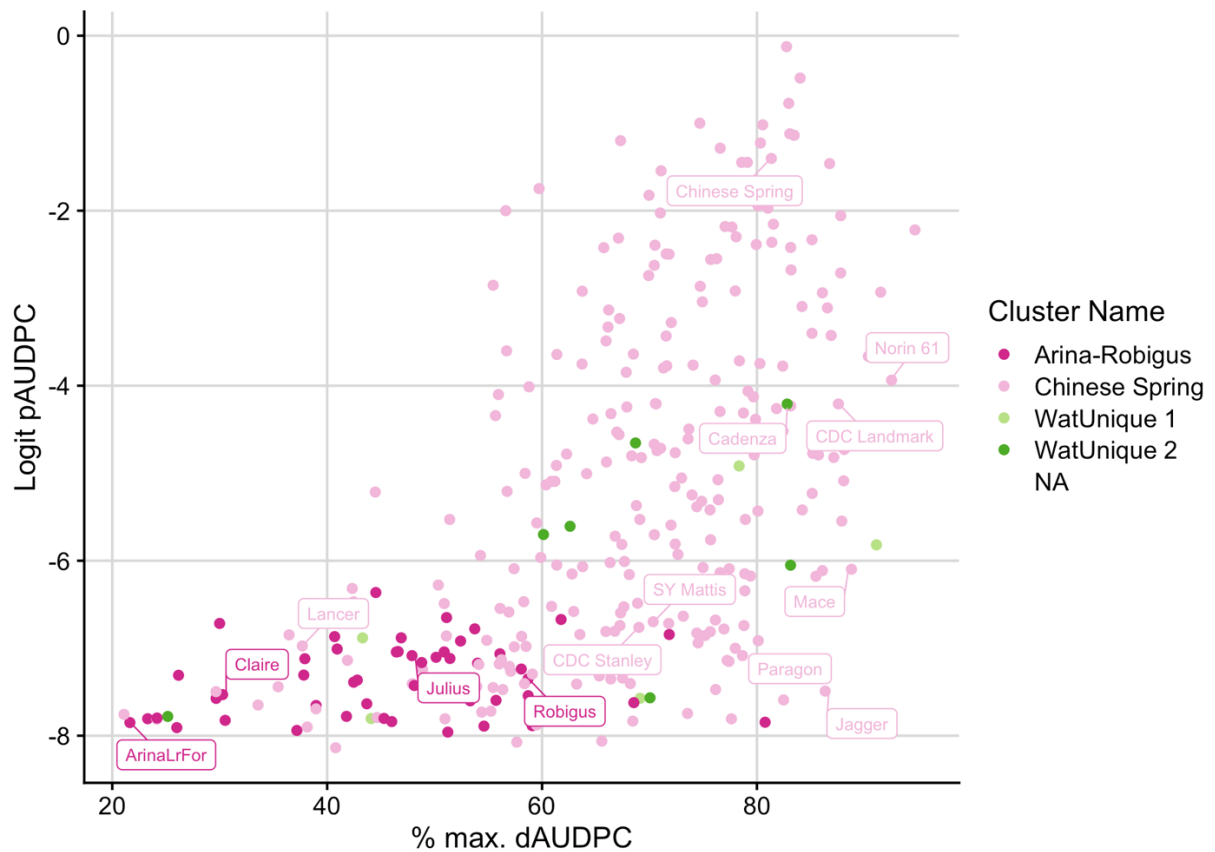


**Figure 53:** Pycnidia (logit pAUDPC) scores plotted against damage (% max. dAUDPC) scores in response to IPO88004, with colour coding to indicate haplotype clusters designated for *Stb15*.

#### 4.3.2.3. Stb15 in the Watkins 800 set

Seven major haplotype groups were estimated in the wider dataset of 800 Watkins and additional wheat lines (**Table 27**). Most lines had the Chinese Spring haplotype, and the Arina-Robigus genotype was also widespread. Group 7 included wheat cultivars such as Thatcher which were heterozygous at several loci.

**Table 27:** Haplotype groups in 800 Watkins lines and 250 additional wheat lines. ‘Distance from’ indicates the number of SNPs that are different in comparison to the named cultivar.

Haplotype	Example Cultivar	No.	Distance from		
			Chinese Spring	ArinaLrFor	Robigus
1	Chinese Spring	754	0-2	8-13	8-13
2	Robigus	229	11-12	4-6	0-3
3	Almus	8	5-7	4-8	4-8
4	ArinaLrFor	29	11-13	0-11	5-9
5	Druid	6	7-9	6	0-2
6	Spelt	20	13-15	7-12	9-14
7	Thatcher	4	1-2	6-7	6-8

#### 4.3.2.4. Using haplotype data for unmasking experiments

Lines that had functional (Arina) alleles of the *Stb15* candidate were removed from the dataset to test whether other effects could be unmasked as well as the importance of these lines for the association on 6A. This resulted in the association of the locus on 6A with IPO88004 response disappearing from the Manhattan plot, whilst the peak on 2B became more significant and refined (Figure 54). This gave us more confidence that the correct candidate gene had been selected.

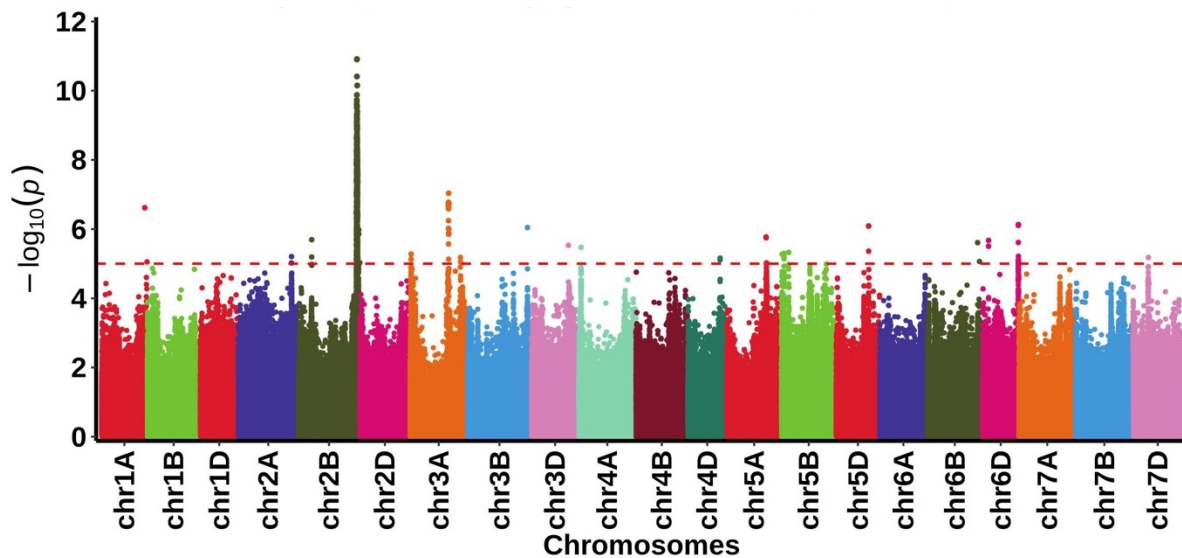
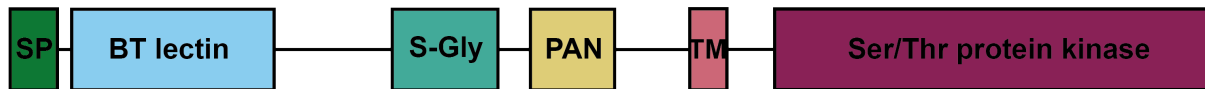


Figure 54: Manhattan plot of Watkins SNPs associated with IPO88004 pycnidia data, with lines carrying the functional haplotype of *Stb15* candidate TraesCS6A02G078700 removed.

#### 4.3.2.5. Predicted protein structure of the *Stb15* candidate

The *Stb15* candidate encodes a serine/threonine receptor-like kinase (S/TPK) with three extracellular domains: a bulb-type mannose-specific lectin, an S-locus glycoprotein, and a PAN/apple domain. The protein is therefore a G-type LecRK (lectin receptor kinase).



**Figure 55:** Protein domains of the *Stb15* candidate TraesCS6A02G078700 predicted from the amino acid sequence in the Uniprot online database (uniprot.org). Length in pixels of each domain corresponds to the number of amino acids. SP = signal peptide, BT = bulb-type, S-Gly = S-locus glycoprotein, PAN = PAN/apple, TM = transmembrane.

#### 4.3.3. Dissecting the response of Watkins landraces to IPO90012 by GWAS

Pycnidia data for IPO90012 did not appear to be associated with any loci in the Watkins collection (**Figure 56**). There was an association of both damage and super necrosis with a locus at 4DL; the *p*-value was much higher for the association with super necrosis, suggesting that the locus is more responsible for high/rapid necrosis responses. The peak for super necrosis ranged from 4D 462,738,168 to 484,035,393. The most highly associated SNPs were located between ~475,019,265 and 476,886,476 – the latter position being the most highly-associated SNP

<i>P</i> -value	Annotation	Gene function	Variant type
<b>4.63</b> <b>x10-20</b>	TraesCS4D02G308800- TraesCS4D02G308900		Intergenic region
<b>1.12</b> <b>x10-19</b>	TraesCS4D02G308600- TraesCS4D02G308700		Intergenic region

<b>5.66 x10-19</b>	TraesCS4D02G307100- TraesCS4D02G307300		Intergenic region
<b>3.76 x10-18</b>	TraesCS4D02G308700	Ras family protein	Upstream gene variant
<b>1.60 x10-17</b>	TraesCS4D02G307600- TraesCS4D02G307700		Intergenic region
<b>1.60 x10-17</b>	TraesCS4D02G307600- TraesCS4D02G307700		Intergenic region
<b>1.60 x10-17</b>	TraesCS4D02G307600- TraesCS4D02G307700		Intergenic region
<b>1.60 x10-17</b>	TraesCS4D02G307800	ARM repeat superfamily protein	Upstream gene variant
<b>1.60 x10-17</b>	TraesCS4D02G307800- TraesCS4D02G307900		Intergenic region
<b>1.60 x10-17</b>	TraesCS4D02G307800- TraesCS4D02G307900		Intergenic region
<b>1.60 x10-17</b>	TraesCS4D02G307800- TraesCS4D02G307900		Intergenic region
<b>2.88 x10-17</b>	TraesCS4D02G307500	Receptor-like protein kinase	Downstream gene variant
<b>3.21 x10-14</b>	TraesCS4D02G306300	Basic helix-loop- helix transcription factor	Upstream gene variant
<b>3.21 x10-14</b>	TraesCS4D02G306500	At1g04650-like protein	Upstream gene variant
<b>6.38 x10-14</b>	TraesCS4D02G305100	Ras-related protein	Downstream gene variant

(Table 28). With such a large region of interest, it is difficult to select one or a few candidate genes with confidence.

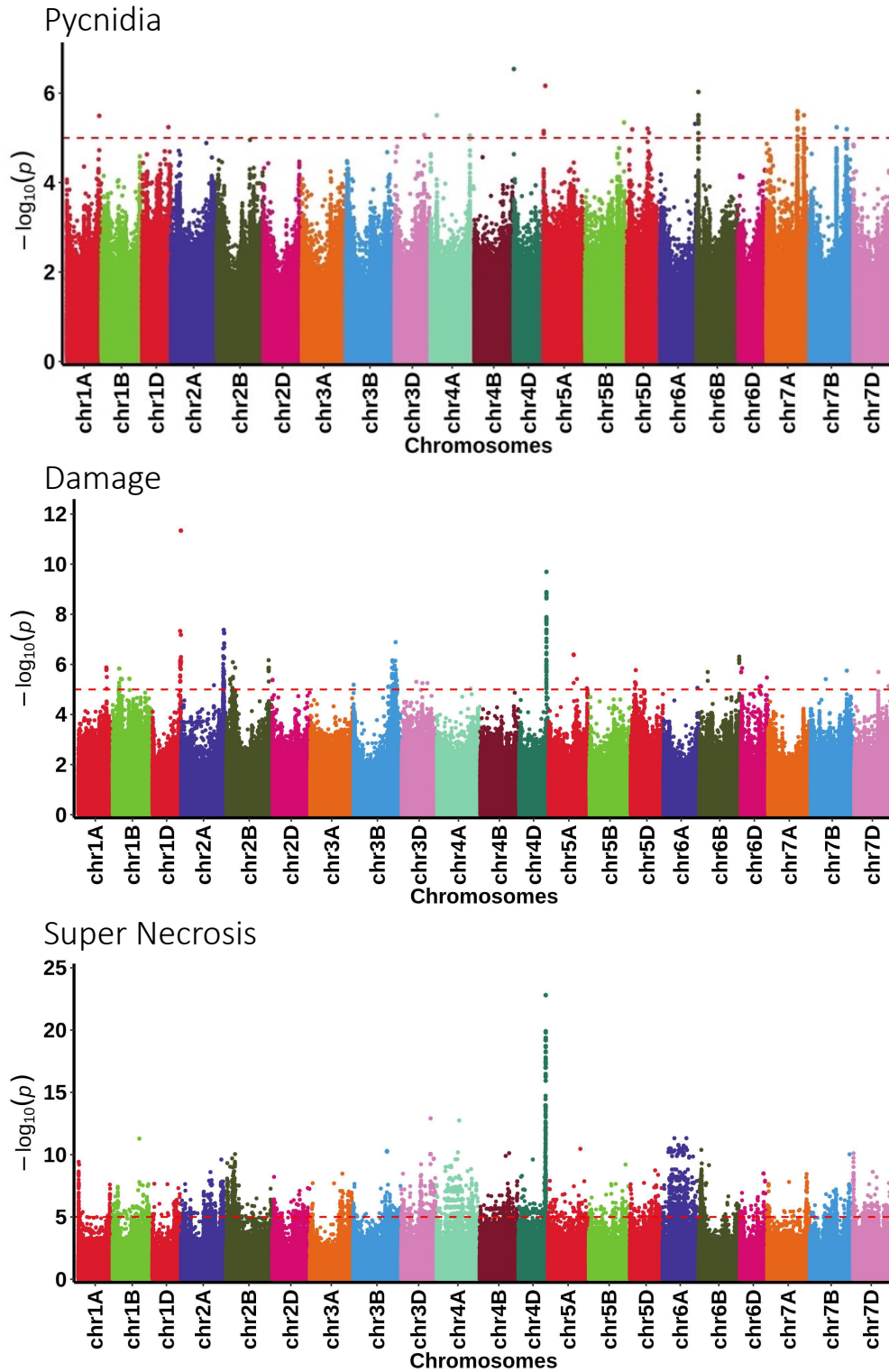


**Figure 56:** Manhattan plot showing associations between SNPs in the Watkins landrace collection and pycnidia, damage and super-necrosis responses to *Z. tritici* isolate IPO90012. Figures produced by Feng Cong.

**Table 28:** SNPs highly associated with super necrosis in response to IPO90012. Table provided by Shifeng Cheng and Feng Cong.

SNP position	P-value	Annotation	Gene function	Variant type
chr4D_476886476	4.63 $\times 10^{-20}$	TraesCS4D02G308800- TraesCS4D02G308900		Intergenic region
chr4D_476435335	1.12 $\times 10^{-19}$	TraesCS4D02G308600- TraesCS4D02G308700		Intergenic region
chr4D_475019265	5.66 $\times 10^{-19}$	TraesCS4D02G307100- TraesCS4D02G307300		Intergenic region
chr4D_476863477	3.76 $\times 10^{-18}$	TraesCS4D02G308700	Ras family protein	Upstream gene variant
chr4D_475289845	1.60 $\times 10^{-17}$	TraesCS4D02G307600- TraesCS4D02G307700		Intergenic region
chr4D_475310599	1.60 $\times 10^{-17}$	TraesCS4D02G307600- TraesCS4D02G307700		Intergenic region
chr4D_475680864	1.60 $\times 10^{-17}$	TraesCS4D02G307600- TraesCS4D02G307700		Intergenic region
chr4D_475957646	1.60 $\times 10^{-17}$	TraesCS4D02G307800	ARM repeat superfamily protein	Upstream gene variant
chr4D_475969312	1.60 $\times 10^{-17}$	TraesCS4D02G307800- TraesCS4D02G307900		Intergenic region
chr4D_475973262	1.60 $\times 10^{-17}$	TraesCS4D02G307800- TraesCS4D02G307900		Intergenic region
chr4D_476026671	1.60 $\times 10^{-17}$	TraesCS4D02G307800- TraesCS4D02G307900		Intergenic region
chr4D_475173303	2.88 $\times 10^{-17}$	TraesCS4D02G307500	Receptor-like protein kinase	Downstream gene variant
chr4D_474604773	3.21 $\times 10^{-14}$	TraesCS4D02G306300	Basic helix-loop- helix transcription factor	Upstream gene variant
chr4D_474861519	3.21 $\times 10^{-14}$	TraesCS4D02G306500	At1g04650-like protein	Upstream gene variant
chr4D_473812133	6.38 $\times 10^{-14}$	TraesCS4D02G305100	Ras-related protein	Downstream gene variant

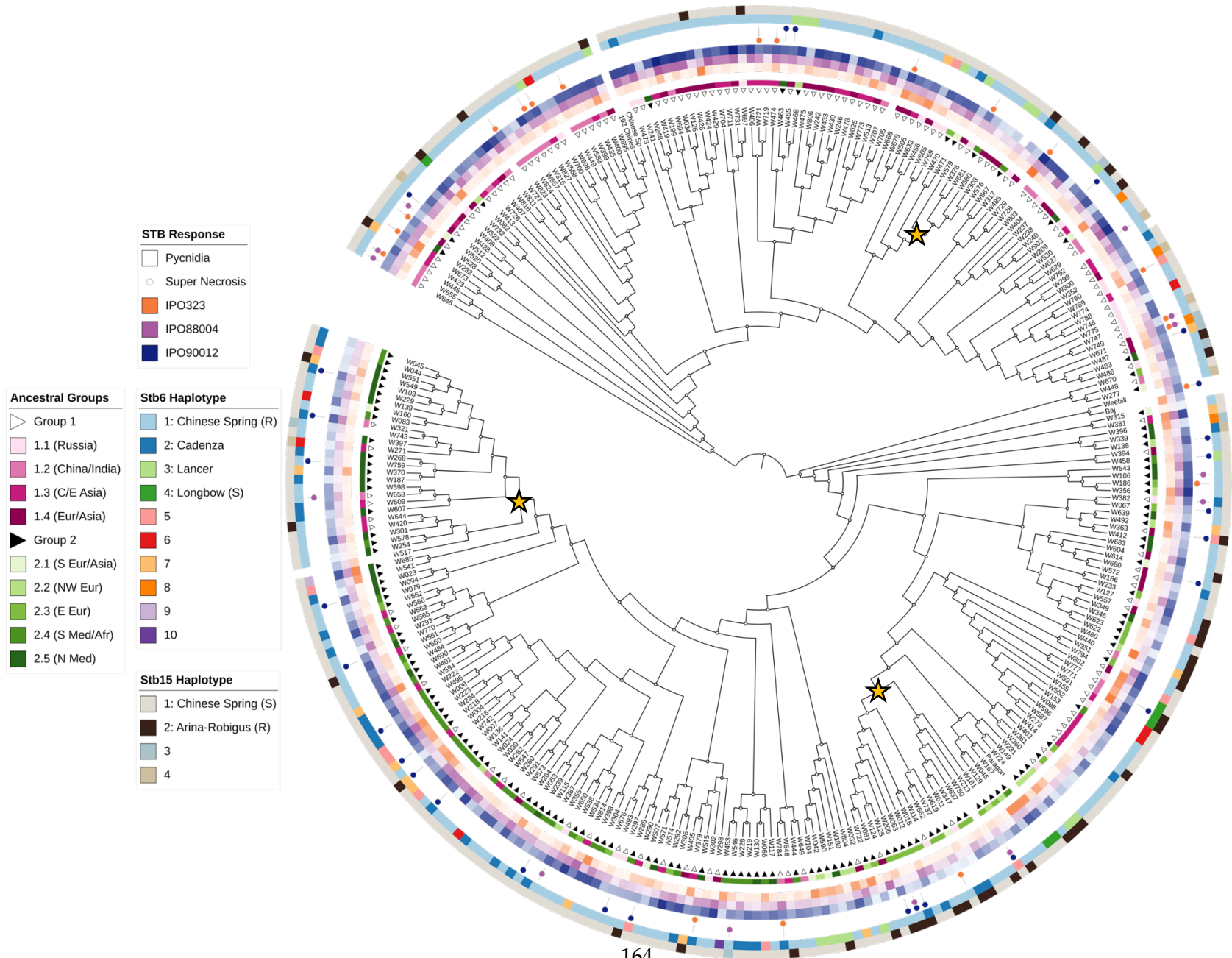
#### 4.3.4. Responses to *Z. tritici* in the Watkins collection in the context of its phylogeny

The phylogenetic tree of Watkins core 300 converged after 76 bootstrap calculations. The two main branches of the tree roughly corresponded to the two key ancestral groups previously designated in the Watkins collection (

Figure 57; Wingen et al., 2014). There appeared to be clades that had low pycnidia scores for all three isolates (marked with yellow stars). Only one of these was associated with the presence of functional *Stb15* alleles, so the locus on 2BL may play a role in resistance in some clades. These clades do not seem more or less likely to contain lines which exhibit super necrosis to one or more isolates.

**Figure 57 (overleaf):** Phylogenetic tree of the core 300 Watkins collection generated from Axiom breeder's array SNPs. Outer panels give additional information corresponding to each line. From the innermost panel: Ancestral group is indicated by colour (pink/green) and subgroups by colour intensity; STB response is indicated by lighter (more resistant) to darker (more susceptible) shades of

orange (IPO323), purple (IPO88004) or blue (IPO90012); super necrosis presence (filled circle) or absence (blank) is indicated for each isolate; *Stb6* haplotype is colour-coded (Chinese Spring in pale blue); and, finally, *Stb15* haplotype is represented with functional *Stb15* alleles in black. For gene haplotypes, example wheat cultivars are given and labelled with R (resistant allele) or S (susceptible allele) where known. Yellow stars mark out clades which appear to contain highly Septoria-resistant lines.



#### 4.4. DISCUSSION

The phenotyping and GWAS methods described in Chapters 3 and 4 proved sufficient to re-clone the resistance gene *Stb6*; this proof-of-concept provided us with the confidence needed to pursue the mapping of other *Stb* genes in the same way. This led to the identification of a high-confidence candidate for the previously-mapped gene *Stb15* to a region on 6AS, using the isolate IPO88004. An additional source of resistance to IPO88004 was mapped to chromosome 2B. We then attempted to use responses to the isolate IPO90012 to map a candidate for *Stb11*. No significant associations were detected when employing pycnidia data. This could be due to *Stb11* being rare in the Watkins collection; there was little resistance to IPO90012 compared to IPO323 and IPO88004. There appeared to be only one line, W453, which was specifically resistant to IPO90012; other sources of resistance to IPO90012 appeared to be broad-spectrum, especially in the case of the three clades marked with a star in **Figure 58**. If *Stb11* is rare in the panel, rather than absent, lines from the larger Watkins collection of 800 that are related to lines known to be resistant to IPO90012 could be selected and screened to enrich the panel for *Stb11*. Interestingly, an interval on 4D was associated with damage and super necrosis responses. This association was far more significant when mapped with SN, so it is likely that the interval is specific to this trait.

Haplotypes of *Stb6* and the *Stb15* candidate were explored in the Watkins collection. There appeared to be ten groups for *Stb6* and four key groups for *Stb15*. When haplotypes associated with resistance to IPO323 were removed from the analysis, the dataset appeared to be insufficient to map any additional intervals. However, the same analysis for IPO88004/*Stb15* resulted in the peak associated with resistance on 2B to become more refined and significant, facilitating future gene cloning efforts at this locus. Similarly, when the GWAS analyses on the IPO90012 damage and SN datasets are compared, the interval associated with these traits was more defined when mapping with SN data. These experiments demonstrate the utility of multiple, refined phenotype datasets for running different permutations of GWAS analyses.

With respect to the two *Stb* genes discussed in this chapter, haplotypes generally correlated well with phenotypes. In the case of *Stb15*, the presence of the Arina-Robigus version of the gene was a strong predictor of resistance to IPO88004, so much so that no lines which had this haplotype were scored as susceptible to IPO88004. This is a particularly clear-cut situation; markers could be developed to distinguish the Chinese Spring and Arina-Robigus haplotypes so that functional versions of *Stb15* could be

tracked in wheat germplasm. A good target for this would be the 6 bp insertion present in the first exon of the Arina. Although *Stb15* is no longer associated with field resistance, monitoring the *Stb* genes present in cultivars could aid in tracking the virulence profiles present in *Z. tritici* populations.

In the case of *Stb6*, the dominant resistant haplotype, that of Chinese Spring, was found to contain 13 exceptions where Watkins lines were susceptible to IPO323. It is possible that the gene is present but not expressed in these susceptible lines. This could be investigated by performing qRT-PCR on RNA samples from these plants when infected with IPO323. Another approach would be to generate a biparental mapping population with a resistant Watkins line carrying the same haplotype, to see how the resistance segregates. It is also possible that these lines do have a SNP relative to Chinese Spring, but that it was perhaps filtered out of the dataset that was used in this study. Ultimately, the Chinese Spring haplotype is incredibly widespread in bread wheat, as was found by Saintenac et al. (2018), and is a very good predictor of resistance to IPO323. It would be useful to develop markers distinguishing the resistant and susceptible haplotypes for stewardship of *Stb6*.

The methods used to investigate haplotypes in this chapter were relatively simple, and employed VCF files from our collaborators at AGIS, which had been filtered and appeared to have some missing data (particularly within the *Stb15* locus). Resequencing of the whole gene in the Watkins collection would be required in order to draw strong conclusions about the effect of particular variants on disease response. This may also shed light on the presence/absence of the large repetitive insertion present in Chinese Spring and its association with response to IPO88004. It would be interesting to discover whether whole exons or domains have indeed been deleted in some lines, as the SNP profiles in **Table 25** and **Table 26** might suggest, or whether this was due to limitations during mapping in the data we had at hand. Furthermore, homologues of *Stb15* could be studied in relatives of wheat to infer the age of the gene and when it may have been introduced into bread wheat.

Responses to IPO88004 varied within the Watkins-exclusive haplotype groups of *Stb15* – it is not possible to tell from the data at hand whether this is due to variations in background resistance or because the SNPs present in these groups hinder the function of *Stb15*. Arina is known to have very good background resistance and this may be true of many of the resistant Watkins lines, too.

In this study, there appeared to be more haplotypes of *Stb6* than *Stb15* in the Watkins core 300 collection. *Stb6* was likely introduced into wheat many times (Chartrain et al., 2005c);

since the gene is widespread in *Triticum dicoccum*, it is likely that it was first introduced very early during domestication (Saintenac et al., 2018). *Stb15* was detected in 60% of UK and European wheat varieties tested by Arraiano and Brown (2006) (Arraiano and Brown, 2006), but response to *Z. tritici* was not associated to the presence of *Stb15* in the field (Arraiano et al., 2009). Tests of Iranian isolates suggested that *Stb15* may provide resistance useful for wheat breeding in Iran (Makhdoomi et al., 2015). The gene may therefore be a useful source of resistance, in combination with quantitative genes, in regions outside of Europe where it may be less prevalent. The presence of the Arina haplotype of *Stb15* is often associated with broad-spectrum resistance (Figure x). Resequencing of the gene in a worldwide panel of wheat cultivars could allow inferences to be made of the association of *Stb15* with field resistance. Phenotypes of *Z. tritici* infection of the Watkins collection in the field could also be used to examine the current efficacy of *Stb15*.

The *Stb15* candidate encodes a serine/threonine receptor-like kinase (S/TPK) with three extracellular domains: a bulb-type mannose-specific lectin, an S-locus glycoprotein and a PAN/apple domain. If functional testing confirms the candidate, it would be the third in the series of *Stb* genes encoding RLKs from different subfamilies. *Stb16q* contains two DUF26 domains, which are similar to other proteins that bind mannose, whilst *Stb6* contains a galacturonan-binding (GUK-WAK) domain (Saintenac et al., 2018; Saintenac et al., 2021). Comparing a growing number of *Stb* genes would allow researchers to gain insight into how *Stb* genes have evolved and diversified, as well as the role of the polysaccharide composition of the apoplast during *Septoria* infection. No other membrane-bound lectin-type pathogen recognition receptors have been cloned in wheat (Gaurav et al. 2021, Table S16), so the molecular cloning of *Stb15* would be a substantial contribution.

#### 4.5. CONCLUSION

The association mapping experiments described in this chapter have led to the identification of a candidate for a well-known *Stb* gene, *Stb15*, as well as two novel loci associated with resistance to IPO88004 and high damage phenotypes. This work therefore provides new avenues for understanding wheat-*Septoria* interactions.

## 5. GENERAL DISCUSSION

**Z***ymoseptoria tritici* is the third most important pathogen of wheat in terms of yield losses and is the principle target of cereal fungicide in Europe (O'Driscoll et al., 2014; Savary et al., 2019). Sources of genetic resistance to this disease are therefore of high priority to breeders; in fact, STB resistance is the only disease-related trait listed as a minimum requirement for wheat cultivars in the UK Recommended List. Despite this, resistance continues to decline in the UK, especially in Cougar-derived varieties (<https://ahdb.org.uk/news/septoria-disease-rating-dip-revealed-by-early-rl-dataset-release>). New and durable sources of resistance are needed. To this end, in Chapters 2 and 3 Septoria responses in *Ae. tauschii* and wheat landrace diversity panels are investigated to identify lines exhibiting broad-spectrum resistance and investigated damage-associated resistance-related traits: SN and damage stability. Further testing of these traits, such as through microscopy, could reveal aspects of damage manifestation during *Z. tritici* infection that may be important for resistance.

A second problem in STB research is the lack of cloned *Stb* genes, which limits our understanding of how this interaction operates at the molecular level. We tested the applications of association genetics for gene cloning in this system, using both the *Ae. tauschii* and wheat landrace diversity panels. In Chapter 4, we rediscovered *Stb6* as a proof of concept for this method and went on to map a region highly associated with resistance to IPO88004. From here, we were able to identify a candidate for *Stb15*. The *Ae. tauschii* system proved less amenable to GWAS due to limited pathogen proliferation within this host. However, necrosis data in response to two isolates was used to map several associated regions, including one on 4DL which was also associated with SN responses to IPO90012 in the Watkins landrace collection.

There are many factors that may limit the success of GWAS approaches (Bartoli and Roux, 2017). A key one which became apparent in this study was the importance of having the

right distribution of, in particular, pycnidia cover phenotypes. In the *Ae. tauschii* system, there was too little pycnidia production. Even in the assay of cfz008, an isolate virulent on the *Ae. tauschii*-derived resistance gene *Stb16q*, no association with pycnidia data could be found using the WGS GWAS pipeline we employed (Gaurav et al., 2022). This led to the suggestion that *Ae. tauschii* may be a marginal host for wheat-adapted *Z. tritici*. The opposite appeared to be true in our assay of IPO90012 on wheat landraces – there was more pycnidia and susceptibility compared to the other two isolates we tested, and no association was found with pycnidia data. In both cases, resistance in the population was not suited to the isolates we tested; there was too much genetic resistance in *Ae. tauschii*, and too little resistance (notably, an apparent lack of *Stb11*) to IPO90012 in the Watkins collection. This highlights the fact that testing a diversity of host panel and pathogen isolate combinations is important for cloning genes *en masse*. Of course, the labour necessary to achieve this is considerable.

Another factor may be the distribution of genes within panels. Although there appears to be a concentration of functional *Stb15* resistance in one Watkins landrace clade, this allele is also fairly well distributed across the phylogenetic tree (

Figure 57). Similarly, functional *Stb6* resistance is widespread in the panel. If there were a major gene for resistance to IPO90012 in the landrace panel but it was located within a single clade, there would not be sufficient power to map it. It would not be possible to separate the effect of the gene from the effect of the population structure. So, genes that were introduced into wheat very early, like *Stb6* (Chartrain et al., 2005c), will be easier to map using worldwide diversity panels.

There are Watkins clades which exhibit strong resistance to all three of the *Z. tritici* isolates tested on the Watkins 300 panel (

Figure 57). Additionally, there are single lines within susceptible clades that exhibit strong non-race-specific resistance – which suggests that this could be the work of a major gene rather than quantitative resistance, which is more likely to be similar within clades due to its polygenic nature. It could be worth attempting to map traits associated with the line means across all of these isolates, and most ideally across a greater number of isolates. This may reveal traits for broad-spectrum resistance. This is an example of a key benefit of association genetics: continued rounds of phenotyping and genotyping have a combined value as well as the more immediate value of mapping traits associated with responses to specific isolates.

With continued exploration of diversity panels for *Stb* gene candidates, it is likely that a limit will quickly be reached when genes conferring clear, gene-for-gene resistance are exhausted. *Stb6*, *Stb15* and *Stb9* are likely the genes that can most easily be cloned with such an approach due to their strong effects (Brown et al., 2015b). Innovations in GWAS methods that increase their power will be essential for narrowing the mapping intervals of the huge number of QTLs associated with *Z. tritici* resistance. Hand-in-hand with this is the need for precise and consistent phenotypes, which is challenging when scores are confounded by strong genotype-by-environment interactions (Brown and Rant, 2013). If we can clone a greater number of *Stb* genes and generate more refined markers for QTLs, genetic resources for STB resistance could be better managed. Improved stewardship and deployment strategies could prolong the efficacy of *Stb* genes (Section 1.13), which have proven not to be durable in the field (Section 1.10).

There is no evidence that *Stb6* and *AvrStb6* directly interact (Saintenac et al., 2018), and there is no known effector that has a gene-for-gene relationship with *Stb16q*. We therefore have much to understand about how these molecular components interact during infection by *Z. tritici*, namely: the identity of the guardee of *Stb6*, the agents that interact with *Stb15* and whether there are *Avrs* that interact with *Stb16q*. *Stb16q* confers broad spectrum resistance (Ghaffary et al., 2012), so it may bind products that are conserved widely in *Z. tritici* and work at the basal level of plant immunity (Brown et al., 2015b). This would support the idea that *Stb16q* is a frontline component in *Ae. tauschii* resistance to *Z. tritici* (Section 2.4); similarly, LecRKs confer non-host or marginal host resistance to leaf rust in barley (Wang et al., 2019). The fact that the pathogen could quickly overcome *Stb16q* is therefore very concerning. Most likely, the DUF26 domains bind mannose, a building block of mannan in fungal cell walls (Miyakawa et al., 2014). Mannans are also a minor component of cell walls in wheat (Burton and Fincher, 2014). The G-type lectin domain of the *Stb15* candidate is also likely to bind mannose. *Z. tritici* does not appear to secrete cell wall degrading enzymes in the early stages of infection (Yang et al., 2013),

during which time it appears imperative for the host to initiate immune responses in resistant lines (Kema et al., 1996a). Lectins are known to form part of basal plant immunity and are involved in stomatal innate immunity responses in *A. thaliana* (Singh and Zimmerli, 2013). Therefore, it seems likely that *Stb16q* and *Stb15* detect a conserved PAMP such as mannose within or from fungal cell walls to initiate defence responses. Alternatively, an *Avr* could be involved; LecRKs have been found to bind to secreted proteins such as a *Phytophthora* spp. effector (Bouwmeester et al., 2011).

There are also questions that arise from the other domains present in the *Stb15* candidate. It has a PAN domain which is a superfamily of modules that appears in proteins of different families from different species (Tordai et al., 1999). PAN modules mediate a range of protein-protein and protein-carbohydrate interactions. S-locus glycoproteins are typically involved in the control of self-incompatibility in *Brassica* spp.; the similarity between these genes and domains found in monocot S/TPKs suggests that they have been conserved since at least the Cretaceous period when monocots and dicots diverged (Walker and Zhang, 1990).

Necrosis responses in both *Ae. tauschii* and Watkins wheat landraces were associated with a region on 4D. For Watkins data, the peak ranged from 462.7 Mb to 484.0 Mb whilst the peak ran between 468.4 Mb and 468.9 Mb with the *Ae. tauschii* dataset (mapped to Chinese Spring). Since the traits used to map these regions were very similar, it seems likely that the gene or genes underlying these two peaks are the same. The most highly associated SNPs found with the analysis of Watkins data were between 475.0 Mb and 476.9 Mb, but the difference to the *Ae. tauschii* peak could be due to linkage disequilibrium and differences in how this is dealt with between the two association genetics pipelines used or discrepancies in mapping reads from either of these two highly genetically diverse datasets to Chinese Spring. If the gene underlying these peaks could be identified, it could add much to our understanding of necrosis manifestation during *Z. tritici* infection. Haplotype diversity in the region could be studied in both *T. aestivum* and *Ae. tauschii* and compared with phenotypes to attempt to narrow down the candidate genes, similarly to analyses conducted in Chapter 4. Crosses between SN and green resistant lines as well as susceptible lines that exhibit high pycnidia cover could be carried out to see how the trait segregates with these two phenotypes. If a small number of candidates can be identified, they could be functionally tested in susceptible lines to test whether an SN-conferring gene is sufficient to induce a reduced pycnidia formation phenotype.

In this thesis, I have discussed dAUDPC or nAUDPC scores as well as the SN and damage stability phenotypes, but there could be further damage-related traits to unpick

in the wheat-*Z. tritici* pathosystem. The tan spot pathogen *Pyrenophora tritici-repentis* varies in its ability to induce tan necrosis and extensive chlorosis, which are under separate genetic control (Lamari and Bernier, 1991). Both phenotypes appear to be induced by an IGFG relationship with pathogen strains. A better understanding of damage-related traits could reveal more about the push-and-pull relationship between host defence responses that may elicit HR (to the benefit of *Z. tritici*) and those that do not. Genes underlying damage-related traits could also be host targets of *Z. tritici*, perhaps even guardees of genes like *Stb6*. In the same vein, increased precision in phenotyping pycnidia and lesions has resulted in the discovery of new QTLs involved in interactions with *Z. tritici* (Yates et al., 2019). Overall, an increased diversity of phenotyping methods seems to be beneficial to enhancing our understanding of this pathosystem.

Research efforts focus primarily on major-effect resistance, which provides only short-term 'froth' on top of the more vital 'coffee' of quantitative resistance genes that are less easily overcome and provide more reliable outcomes for growers (Brown, 2021; **Figure 6**). The study of resistance in diverse germplasm could lead to the discovery of that rare and elusive thing - major-gene resistance that is both highly effective and durable. In this project, we identified a candidate for a major *Stb* gene, *Stb15*, a yet-unexplored region associated with resistance on 2B, a region linked to necrosis-associated resistance in both wheat and *Ae. tauschii* and also explored broad-spectrum resistance in the Watkins collection that may contribute to wheat pre-breeding. We therefore hope to have bolstered both the froth and coffee of the wheat STB-resistance cappuccino.

## 6. REFERENCES

- Ajaz, S., Benbow, H. R., Christodoulou, T., Uauy, C., and Doohan, F. M.** (2021). Evaluation of the susceptibility of modern, wild, ancestral, and mutational wheat lines to *Septoria tritici* blotch disease. *Plant Pathol.* **70**:1123–1137.
- Altschul, S. F., Madden, T. L., Schäffer, A. A., Zhang, J., Zhang, Z., Miller, W., and Lipman, D. J.** (1997). Gapped BLAST and PSI-BLAST: a new generation of protein database search programs. *Nucleic Acids Res.* **25**:3389–3402.
- Arora, S., Singh, N., Kaur, S., Bains, N. S., Uauy, C., Poland, J., and Chhuneja, P.** (2017). Genome-Wide Association Study of Grain Architecture in Wild Wheat *Aegilops tauschii*. *Front. Plant Sci.* **8**:1–13.
- Arora, S., Steuernagel, B., Gaurav, K., Chandramohan, S., Long, Y., Matny, O., Johnson, R., Enk, J., Periyannan, S., Singh, N., et al.** (2019). Resistance gene cloning from a wild crop relative by sequence capture and association genetics. *Nat. Biotechnol.* **37**:139–143.
- Arora, S., Steed, A., Goddard, R., Gaurav, K., O'Hara, T., Schoen, A., Rawat, N., Elkot, A. F., Chinoy, C., Nicholson, M. H., et al.** (2022). A wheat kinase and immune receptor form the host-specificity barrier against the blast fungus. *bioRxiv* Advance Access published January 28, 2022, doi:10.1101/2022.01.27.477927.
- Arraiano, L. S., and Brown, J. K. M.** (2006). Identification of isolate-specific and partial resistance to *septoria tritici* blotch in 238 European wheat cultivars and breeding lines. *Plant Pathol.* **55**:726–738.
- Arraiano, L. S., Brading, P. A., and Brown, J. K. M.** (2001a). A detached seedling leaf technique to study resistance to *Mycosphaerella graminicola* (anamorph *Septoria tritici*) in wheat. *Plant Pathol.* **50**:339–346.
- Arraiano, L. S., Worland, A. J., Ellerbrook, C., and Brown, J. K. M.** (2001b). Chromosomal location of a gene for resistance to *septoria tritici* blotch (*Mycosphaerella graminicola*) in the hexaploid wheat “Synthetic 6x.” *Theor. Appl. Genet.* **103**:758–764.
- Arraiano, L. S., Chartrain, L., Bossolini, E., Slatter, H. N., Keller, B., and Brown, J. K. M.** (2007). A gene in European wheat cultivars for resistance to an African isolate of *Mycosphaerella graminicola*. *Plant Pathol.* **56**:73–78.
- Arraiano, L. S., Balaam, N., Fenwick, P. M., Chapman, C., Feuerhelm, D., Howell, P., Smith, S. J., Widdowson, J. P., and Brown, J. K. M.** (2009). Contributions of disease resistance and escape to the control of *septoria tritici* blotch of wheat. *Plant Pathol.* **58**:910–922.

- Assefa, S., and Fehrman, H.** (1998). Resistance in *Aegilops* species against leaf rust, stem rust, *Septoria tritici* blotch, eyespot and powdery mildew of wheat. *Zeitschrift Fur Pflanzenkrankheiten Und Pflanzenschutz-Journal Plant Dis. Prot.* **105**:624–631.
- Audano, P. A., Ravishankar, S., and Vannberg, F. O.** (2018). Mapping-free variant calling using haplotype reconstruction from k-mer frequencies. *Bioinformatics* **34**:1659–1665.
- Avni, R., Nave, M., Barad, O., Baruch, K., Twardziok, S. O., Gundlach, H., Hale, I., Mascher, M., Spannagl, M., Wiebe, K., et al.** (2017). Wild emmer genome architecture and diversity elucidate wheat evolution and domestication. *Science* **357**:93–97.
- Badet, T., Oggenfuss, U., Abraham, L., McDonald, B. A., and Croll, D.** (2020). A 19-isolate reference-quality global pangenome for the fungal wheat pathogen *Zymoseptoria tritici*. *BMC Biol.* **18**.
- Banke, S., and Mcdonald, B. A.** (2005). Migration patterns among global populations of the pathogenic fungus *Mycosphaerella graminicola*. *Mol. Ecol.* **14**:1881–1896.
- Bansal, U. K., Forrest, K. L., Hayden, M. J., Miah, H., Singh, D., and Bariana, H. S.** (2011). Characterisation of a new stripe rust resistance gene Yr47 and its genetic association with the leaf rust resistance gene Lr52. *Theor. Appl. Genet.* **122**:1461–1466.
- Bansal, U. K., Arief, V. N., DeLacy, I. H., and Bariana, H. S.** (2013). Exploring wheat landraces for rust resistance using a single marker scan. *Euphytica* **194**:219–233.
- Bartoli, C., and Roux, F.** (2017). Genome-Wide Association Studies In Plant Pathosystems: Toward an Ecological Genomics Approach. *Front. Plant Sci.* **8**:763.
- Bhatta, M., Morgounov, A., Belamkar, V., Poland, J., and Baenziger, P. S.** (2018). Unlocking the novel genetic diversity and population structure of synthetic Hexaploid wheat. *BMC Genomics* **19**:591.
- Borlaug, N.** (1968). Wheat breeding and its impact on world food supply. *Proc. 3rd Int. Wheat Genet. Symp. Canberra.*:1–36.
- Borlaug, N.** (2007). Feeding a Hungry world. *Science (80-. ).* **318**:359.
- Bouwmeester, K., de Sain, M., Weide, R., Gouget, A., Klamer, S., Canut, H., and Govers, F.** (2011). The Lectin Receptor Kinase LecRK-I.9 Is a Novel Phytophthora Resistance Component and a Potential Host Target for a RXLR Effector. *PLOS Pathog.* **7**:e1001327.
- Brading, P. A., Verstappen, E. C. P., Kema, G. H. J., and Brown, J. K. M.** (2002). A Gene-for-Gene Relationship Between Wheat and *Mycosphaerella graminicola*, the *Septoria Tritici* Blotch Pathogen. *Phytopathology* **92**:439–445.
- Brennan, C. J., Benbow, H. R., Mullins, E., and Doohan, F. M.** (2019). A review of the known unknowns in the early stages of *septoria tritici* blotch disease of wheat. *Plant Pathol.* **68**:1427–1438.

- Brown, J. K. M.** (2015). Durable Resistance of Crops to Disease: A Darwinian Perspective. <https://doi.org/10.1146/annurev-phyto-102313-045914> **53**:513–539.
- Brown, J. K. M.** (2021). Achievements in breeding cereals with durable disease resistance in Northwest Europe Northwest Europe. In *Burleigh Dodds Series In Agricultural Science*, p. Burleigh Dodds.
- Brown, J. K. M., and Rant, J. C.** (2013). Fitness costs and trade-offs of disease resistance and their consequences for breeding arable crops. *Plant Pathol.* **62**:83–95.
- Brown, J. K. M., Kema, G. H. J., Forrer, H.-R., Verstappen, E. C. P., Arraiano, L. S., Brading, P. A., Foster, E. M., Fried, P. M., and Jenny, E.** (2001). Resistance of wheat cultivars and breeding lines to septoria tritici blotch caused by isolates of *Mycosphaerella graminicola* in field trials. *Plant Pathol.* **50**:325–338.
- Brown, J. K. M., Chartrain, L., Lasserre-Zuber, P., and Saintenac, C.** (2015a). Genetics of resistance to *Zymoseptoria tritici* and applications to wheat breeding. *Fungal Genet. Biol.* **79**:33–41.
- Brown, J. K. M., Chartrain, L., Lasserre-Zuber, P., and Saintenac, C.** (2015b). Genetics of resistance to *Zymoseptoria tritici* and applications to wheat breeding. *Fungal Genet. Biol.* **79**:33–41.
- Brunner, P. C., and McDonald, B. A.** (2018). Evolutionary analyses of the avirulence effector AvrStb6 in global populations of *Zymoseptoria tritici* identify candidate amino acids involved in recognition. *Mol. Plant Pathol.* Advance Access published January 24, 2018, doi:10.1111/mpp.12217.
- Brunner, P. C., Torriani, S. F. F., Croll, D., Stukenbrock, E. H., and McDonald, B. A.** (2014). Hitchhiking Selection Is Driving Intron Gain in a Pathogenic Fungus. *Mol. Biol. Evol.* **31**:1741–1749.
- Brutus, A., Sicilia, F., Macone, A., Cervone, F., and De Lorenzo, G.** (2010). A domain swap approach reveals a role of the plant wall-associated kinase 1 (WAK1) as a receptor of oligogalacturonides. *Proc. Natl. Acad. Sci. U. S. A.* **107**:9452–9457.
- Buist, G., Steen, A., Kok, J., and Kuipers, O. P.** (2008). LysM, a widely distributed protein motif for binding to (peptido)glycans. *Mol. Microbiol.* **68**:838–847.
- Bunting, A. H.** (2001). John Percival - the man: his life and times. *Linn.* Advance Access published 2001.
- Burt, C., Griffe, L. L., Ridolfini, A. P., Orford, S., Griffiths, S., and Nicholson, P.** (2014). Mining the watkins collection of wheat landraces for novel sources of eyespot resistance. *Plant Pathol.* **63**:1241–1250.
- Burton, R. A., and Fincher, G. B.** (2014). Evolution and development of cell walls in cereal grains. *Front. Plant Sci.* **5**:456.
- Calvet-Mir, L., Calvet-Mir, M., Vaqué-Nuñez, L., and Reyes-García, V.** (2011). Landraces

- in situ Conservation: A Case Study in High-Mountain Home Gardens in Vall Fosca, Catalan Pyrenees, Iberian Peninsula. *Econ. Bot.* **65**:146–157.
- Camacho, C., Coulouris, G., Avagyan, V., Ma, N., Papadopoulos, J., Bealer, K., and Madden, T. L.** (2009). BLAST+: Architecture and applications. *BMC Bioinformatics* **10**:1–9.
- Chartrain, L., Brading, P. A., Makepeace, J. C., and Brown, J. K. M.** (2004). Sources of resistance to septoria tritici blotch and implications for wheat breeding. *Plant Pathol.* **53**:454–460.
- Chartrain, L., Berry, S. T., and Brown, J. K. M.** (2005a). Genetics and Resistance Resistance of Wheat Line Kavkaz-K4500 L.6.A.4 to Septoria Tritici Blotch Controlled by Isolate-Specific Resistance Genes Advance Access published 2005, doi:10.1094/PHYTO-95-0664.
- Chartrain, L., Joaquim, P., Berry, S. T., Arraiano, L. S., Azanza, F., and Brown, J. K. M.** (2005b). Genetics of resistance to septoria tritici blotch in the Portuguese wheat breeding line TE 9111. *Theor. Appl. Genet.* **110**:1138–1144.
- Chartrain, L., Brading, P. A., and Brown, J. K. M.** (2005c). Presence of the *Stb6* gene for resistance to septoria tritici blotch (*Mycosphaerella graminicola*) in cultivars used in wheat-breeding programmes worldwide. *Plant Pathol.* **54**:134–143.
- Chartrain, L., Sourdille, P., Bernard, M., and Brown, J. K. M.** (2009). Identification and location of *Stb9*, a gene for resistance to septoria tritici blotch in wheat cultivars Courtot and Tonic. *Plant Pathol.* **58**:547–555.
- Cock, P. J. A., Chilton, J. M., Grüning, B., Johnson, J. E., and Soranzo, N.** (2015). NCBI BLAST+ integrated into Galaxy. *Gigascience* **4**.
- Collett, D.** (2003). *Modelling binary data BT - Texts in statistical science*. Chapman & Hall/CRC.
- Cowger, C., and Brown, J. K. M.** (2019). Durability of Quantitative Resistance in Crops: Greater Than We Know? *Annu. Rev. Phytopathol.* **57**:253–277.
- Cowger, C., Hoffer, M. E., and Mundt, C. C.** (2000). Specific adaptation by *Mycosphaerella graminicola* to a resistant wheat cultivar. *Plant Pathol.* **49**:445–451.
- Cox, T. S., Raupp, W. J., Wilson, D. L., Gill, B. S., Leath, S., Bockus, W. W., and Browder, L. E.** (1992). Resistance to Foliar Diseases in a Collection of *Triticum tauschii* Germ Plasm. *Plant Dis.* **76**:1061–1064.
- Crookes, W., and Rew, R. H.** (1917). *The Wheat Problem*. Third Edit. London: Longmans, Green And Co.
- Daetwyler, H. D., Bansal, U. K., Bariana, H. S., Hayden, M. J., and Hayes, B. J.** (2014). Genomic prediction for rust resistance in diverse wheat landraces. *Theor. Appl. Genet.* **127**:1795–1803.

- Dangl, J. L., and Jones, J. D.** (2001). Plant pathogens and integrated defence responses to infection. *Nature* **411**:826–833.
- De La Concepcion, J. C., Franceschetti, M., Maclean, D., Terauchi, R., Kamoun, S., and Banfield, M. J.** (2019). Protein engineering expands the effector recognition profile of a rice NLR immune receptor. *Elife* **8**.
- De Wit, P. J. G. M.** (2016). *Cladosporium fulvum* Effectors: Weapons in the Arms Race with Tomato. *Annu. Rev. Phytopathol.* **54**:1–23.
- Delorean, E., Gao, L., Lopez, J. F. C., Mehrabi, A., Bentley, A., Sharon, A., Keller, B., Wulff, B., Steffenson, B., Steuernagel, B., et al.** (2021). High molecular weight glutenin gene diversity in *Aegilops tauschii* demonstrates unique origin of superior wheat quality. *Commun. Biol.* **2021** *41* **4**:1–9.
- Djidjou-Demasse, R., Moury, B., and Fabre, F.** (2017). Mosaics often outperform pyramids: Insights from a model comparing strategies for the deployment of plant resistance genes against viruses in agricultural landscapes. *New Phytol.* **216**:239–253.
- Dodds, P. N., and Rathjen, J. P.** (2010). Plant immunity: Towards an integrated view of plant-pathogen interactions. *Nat. Rev. Genet.* **11**:539–548.
- Dzyubenko, N.** (2018). Vavilov’s Collection of Worldwide Crop Genetic Resources in the 21st Century **16**.
- Ellis, J. G., Lagudah, E. S., Spielmeier, W., and Dodds, P. N.** (2014). The past, present and future of breeding rust resistant wheat. *Front. Plant Sci.* **5**:641.
- Estep, L. K., Torriani, S. F. F., Zala, M., Anderson, N. P., Flowers, M. D., McDonald, B. A., Mundt, C. C., and Brunner, P. C.** (2015). Emergence and early evolution of fungicide resistance in North American populations of *Zymoseptoria tritici*. *Plant Pathol.* **64**:961–971.
- Eyal, Z., L. S. A., M., P. J., and Ginkel, M. van** (1997). *The Septoria Diseases of Wheat: Concepts and Methods of Disease Management*. Mexico: CIMMYT.
- Faris, J. D., and Friesen, T. L.** (2020). Plant genes hijacked by necrotrophic fungal pathogens. *Curr. Opin. Plant Biol.* **56**:74–80.
- Feechan, A., Benbow, H., Tiley, A. M. M., Gibriel, H., Casey, E., and Doohan, F. M.** (2019). International Symposium on Cereal Leaf Blights (ISCLB) 2019: Book of Abstracts. In *International Symposium on Cereal Leaf Blights (ISCLB) 2019: Book of Abstracts*, .
- Fenton, A., Antonovics, J., and Brockhurst, M. A.** (2009). Inverse-gene-for-gene infection genetics and coevolutionary dynamics. *Am. Nat.* **174**.
- Ficiciyan, A., Loos, J., Sievers-Glotzbach, S., and Tschardtke, T.** (2018). More than Yield: Ecosystem Services of Traditional versus Modern Crop Varieties Revisited. *Sustain.* **2018**, *Vol. 10*, *Page 2834* **10**:2834.

- Flor, H. H.** (1971). Current Status of the Gene-For-Gene Concept. *Annu. Rev. Phytopathol.* **9**:275–296.
- Fones, H. N., Steinberg, G., and Gurr, S. J.** (2015). Measurement of virulence in *Zymoseptoria tritici* through low inoculum-density assays. *Fungal Genet. Biol.* **79**:89–93.
- FRAC** (2017). *Succinate Dehydrogenase Inhibitor (SDHI) Working Group Protocol of the discussions and use recommendations of the SDHI Working Group of the Fungicide Resistance Action Committee (FRAC)*.
- Frankin, S., Roychowdhury, R., Nashef, K., Abbo, S., Bonfil, D. J., and Ben-David, R.** (2021). In-Field Comparative Study of Landraces vs. Modern Wheat Genotypes under a Mediterranean Climate. *Plants 2021, Vol. 10, Page 2612* **10**:2612.
- French, E., Kim, B. S., and Iyer-Pascuzzi, A. S.** (2016). Mechanisms of quantitative disease resistance in plants. *Semin. Cell Dev. Biol.* **56**:201–208.
- Gaurav, K., Arora, S., Silva, P., Sánchez-Martín, J., Horsnell, R., Gao, L., Brar, G. S., Widrig, V., John Raupp, W., Singh, N., et al.** (2022). Population genomic analysis of *Aegilops tauschii* identifies targets for bread wheat improvement. *Nat. Biotechnol.* **40**:422–431.
- Gaut, B. S.** (2002). Evolutionary dynamics of grass genomes. *New Phytol.* **154**:15–28.
- Ghaffary, S. M. T., Faris, J. D., Friesen, T. L., Visser, R. G. F., van der Lee, T. A. J., Robert, O., and Kema, G. H. J.** (2012). New broad-spectrum resistance to septoria tritici blotch derived from synthetic hexaploid wheat. *Theor. Appl. Genet.* **124**:125–142.
- Gigot, C., Saint-Jean, S., Huber, L., Maumené, C., Leconte, M., Kerhornou, B., and de Vallavieille-Pope, C.** (2013). Protective effects of a wheat cultivar mixture against splash-dispersed septoria tritici blotch epidemics. *Plant Pathol.* **62**:1011–1019.
- Hafeez, A. N., Arora, S., Ghosh, S., Gilbert, D., Bowden, R. L., and Wulff, B. B. H.** (2021). Creation and judicious application of a wheat resistance gene atlas. *Mol. Plant* **14**:1053–1070.
- Harlan, J. R.** (1975). Our Vanishing Genetic Resources. *Science (80-. )*. **188**:618–621.
- Harlan, H. V., and Martini, M. L.** (1936). Problems and Results in Barley Breeding. *Yearb. Agric. Advance Access published 1936*.
- Hassani-Pak, K., Singh, A., Brandizi, M., Hearnshaw, J., Parsons, J. D., Amberkar, S., Phillips, A. L., Doonan, J. H., and Rawlings, C.** (2021). KnetMiner: a comprehensive approach for supporting evidence-based gene discovery and complex trait analysis across species. *Plant Biotechnol. J.* **19**:1670–1678.
- Hawkes, J. G.** (1999). The evidence for the extent of N.I. Vavilov’s new world Andean centres of cultivated plant origins. *Genet. Resour. Crop Evol.* **46**:163–168.
- Hillocks, R. J.** (2012). Farming with fewer pesticides: EU pesticide review and resulting

- challenges for UK agriculture. *Crop Prot.* **31**:85–93.
- Hovmøller, M. S., Walter, S., and Justesen, A. F.** (2010). Escalating threat of wheat rusts. *Science* **329**:369.
- Husenov, B., Muminjanov, H., Dreisigacker, S., Otambekova, M., Akin, B., Subasi, K., Rasheed, A., Shepelev, S., and Morgounov, A.** (2021). Crop Science Genetic diversity and agronomic performance of wheat landraces currently grown in Tajikistan Advance Access published 2021, doi:10.1002/csc2.20463.
- International Wheat Genome Sequencing Consortium (IWGSC), T. I. W. G. S. C., IWGSC RefSeq principal investigators, I. R. principal, Appels, R., Eversole, K., Feuillet, C., Keller, B., Rogers, J., Stein, N., IWGSC whole-genome assembly principal investigators, I. whole-genome assembly principal, Pozniak, C. J., et al.** (2018). Shifting the limits in wheat research and breeding using a fully annotated reference genome. *Science* **361**:eaar7191.
- Islam, M. T., Croll, D., Gladieux, P., Soanes, D. M., Persoons, A., Bhattacharjee, P., Hossain, M. S., Gupta, D. R., Rahman, M. M., Mahboob, M. G., et al.** (2016). Emergence of wheat blast in Bangladesh was caused by a South American lineage of *Magnaporthe oryzae*. *BMC Biol.* **14**:84.
- Jamieson, P. A., Libo, S., and He, P.** Plant Cell Surface Molecular Cypher: Receptor-Like Proteins and Their Roles in Immunity and Development Advance Access published doi:10.1016/j.plantsci.2018.05.030.
- Jing, H. C., Lovell, D., Gutteridge, R., Jenk, D., Korniyukhin, D., Mitrofanova, O. P., Kema, G. H. J., and Hammond-Kosack, K. E.** (2008). Phenotypic and genetic analysis of the *Triticum monococcum*-*Mycosphaerella graminicola* interaction. *New Phytol.* **179**:1121–1132.
- Johnson, R.** (1984). A Critical Analysis of Durable Resistance. *Annu. Rev. Phytopathol.* **22**:309–330.
- Jones, J. D. G., and Dangl, J. L.** (2006). The plant immune system. *Nature* **444**:323–329.
- Jørgensen, L. N., van den Bosch, F., Oliver, R. P., Heick, T. M., and Paveley, N. D.** (2017). Targeting Fungicide Inputs According to Need. *Annu. Rev. Phytopathol.* **55**:181–203.
- Jupe, F., Witek, K., Verweij, W., Sliwka, J., Pritchard, L., Etherington, G. J., Maclean, D., Cock, P. J., Leggett, R. M., Bryan, G. J., et al.** (2013). Resistance gene enrichment sequencing (RenSeq) enables reannotation of the NB-LRR gene family from sequenced plant genomes and rapid mapping of resistance loci in segregating populations. *Plant J.* **76**:530–544.
- Keen, N. T.** (1990). Gene-for-gene complementarity in plant-pathogen interactions. *Annu. Rev. Genet.* Advance Access published 1990,

doi:10.1146/annurev.ge.24.120190.002311.

- Keller, B., Wicker, T., and Krattinger, S. G.** (2018). Annual Review of Phytopathology Advances in Wheat and Pathogen Genomics: Implications for Disease Control Advance Access published 2018, doi:10.1146/annurev-phyto-080516.
- Kema, G. H. J., Yu, D., Rijkenberg, F. H. J., Shaw, M. W., and Baayen, R. P.** (1996a). Histology of pathogenesis of *Mycosphaerella graminicola* in wheat. *Phytopathology* 7:777-786.
- Kema, G. H. J., Annone, J. G., Sayoud, R., Van Silfhout, C. H., Van Ginkel, M., and de Bree, J.** (1996b). Genetic variation for virulence and resistance in the wheat-*Mycosphaerella graminicola* pathosystem I. Interactions Between Pathogen Isolates and Host Cultivars. *Phytopathology* 86:200-212.
- Kema, G. H. J., Mirzadi Gohari, A., Aouini, L., Gibriel, H. A. Y., Ware, S. B., van den Bosch, F., Manning-Smith, R., Alonso-Chavez, V., Helps, J., Ben M'Barek, S., et al.** (2018). Stress and sexual reproduction affect the dynamics of the wheat pathogen effector AvrStb6 and strobilurin resistance. *Nat. Genet.* Advance Access published February 12, 2018, doi:10.1038/s41588-018-0052-9.
- Keon, J., Antoniw, J., Carzaniga, R., Deller, S., Ward, J. L., Baker, J. M., Beale, M. H., Hammond-Kosack, K., and Rudd, J. J.** (2007). Transcriptional adaptation of *Mycosphaerella graminicola* to programmed cell death (PCD) of its susceptible wheat host. *Mol. Plant. Microbe. Interact.* 20:178-193.
- Kettles, G. J., Bayon, C., Sparks, C. A., Canning, G., Kanyuka, K., and Rudd, J. J.** (2018). Characterization of an antimicrobial and phytotoxic ribonuclease secreted by the fungal wheat pathogen *Zymoseptoria tritici*. *New Phytol.* 217:320-331.
- Kidane, Y. G., Hailemariam, B. N., Mengistu, D. K., Fadda, C., Pè, M. E., and Dell'Acqua, M.** (2017). Genome-Wide Association Study of Septoria tritici Blotch Resistance in Ethiopian Durum Wheat Landraces. *Front. Plant Sci.* 8.
- Kildea, S., Ransbotyn, V., Khan, M. R., Fagan, B., Leonard, G., Mullins, E., and Doohan, F. M.** (2008). *Bacillus megaterium* shows potential for the biocontrol of septoria tritici blotch of wheat. *Biol. Control* 47:37-45.
- Kildea, S., Byrne, J. ., Cucak, M., and Hutton, F.** (2020). First report of virulence to the septoria tritici blotch resistance gene *Stb16q* in the Irish *Zymoseptoria tritici* population. <http://ndrs.org.uk/article.php?id=041013> 41:13-13.
- Kildea, S., Sheppard, L., Cucak, M., and Hutton, F.** (2021). Detection of virulence to septoria tritici blotch (STB) resistance conferred by the winter wheat cultivar Cougar in the Irish *Zymoseptoria tritici* population and potential implications for STB control. *Plant Pathol.* Advance Access published 2021, doi:10.1111/PPA.13432.
- Kinene, T., Wainaina, J., Maina, S., and Boykin, L. M.** (2016). Rooting Trees, Methods

for. *Encycl. Evol. Biol.* Advance Access published April 14, 2016, doi:10.1016/B978-0-12-800049-6.00215-8.

- Lamari, L., and Bernier, C. C.** (1991). Genetics of Tan Necrosis and Extensive Chlorosis in Tan Spot of Wheat Caused by *Pyrenophora tritici-repentis*. *Phytopathology* **81**:1092.
- Lannoo, N., and Van Damme, E. J. M.** (2014). Lectin domains at the frontiers of plant defense. *Front. Plant Sci.* **5**:397.
- Larkan, N. J., Ma, L., Haddadi, P., Buchwaldt, M., Parkin, I. A. P., Djavaheri, M., and Borhan, M. H.** (2020). The Brassica napus wall-associated kinase-like (WAKL) gene Rlm9 provides race-specific blackleg resistance. *Plant J.* **104**:892–900.
- Letunic, I., and Bork, P.** (2021). Interactive Tree Of Life (iTOL) v5: an online tool for phylogenetic tree display and annotation. *Nucleic Acids Res.* **49**:W293–W296.
- Lewis, P. O.** (2001). A likelihood approach to estimating phylogeny from discrete morphological character data. *Syst. Biol.* **50**:913–925.
- Lin, X., Armstrong, M., Baker, K., Wouters, D., Visser, R. G. F., Wolters, P. J., Hein, I., and Vleeshouwers, V. G. A. A.** (2020). RLP/K enrichment sequencing; a novel method to identify receptor-like protein (RLP) and receptor-like kinase (RLK) genes. *New Phytol.* **227**:1264–1276.
- Linde, C. C., Zhan, J., and McDonald, B. A.** (2002). Population Structure of *Mycosphaerella graminicola*: From Lesions to Continents. *Phytopathology* **92**:946–955.
- Ling, H.-Q., Ma, B., Shi, X., Liu, H., Dong, L., Sun, H., Cao, Y., Gao, Q., Zheng, S., Li, Y., et al.** (2018). Genome sequence of the progenitor of wheat A subgenome *Triticum urartu*. *Nature* **557**:424–428.
- Liu, Z., Zhang, Z., Faris, J. D., Oliver, R. P., Syme, R., McDonald, M. C., McDonald, B. A., Solomon, P. S., Lu, S., Shelver, W. L., et al.** (2012). The cysteine rich necrotrophic effector SnTox1 produced by *Stagonospora nodorum* triggers susceptibility of wheat lines harboring *Snn1*. *PLoS Pathog.* **8**:e1002467.
- Loskutov, I. G.** (1999). *Vavilov and his institute: A history of the world collection of plant genetic resources in Russia*. IPGRI.
- Louriki, S., Rehman, S., El Hanafi, S., Bouhouch, Y., Al-Jaboobi, M., Amri, A., Douira, A., and Tadesse, W.** (2021). Identification of Resistance Sources and Genome-Wide Association Mapping of Septoria Tritici Blotch Resistance in Spring Bread Wheat Germplasm of ICARDA. *Front. Plant Sci.* **12**:600176.
- Luo, M. C., Gu, Y. Q., Puiu, D., Wang, H., Twardziok, S. O., Deal, K. R., Huo, N., Zhu, T., Wang, L., Wang, Y., et al.** (2017). Genome sequence of the progenitor of the wheat D genome *Aegilops tauschii*. *Nature* **551**:498–502.
- Luo, M., Xie, L., Chakraborty, S., Wang, A., Matny, O., Jugovich, M., Kolmer, J. A., Richardson, T., Bhatt, D., Hoque, M., et al.** (2021). A five-transgene cassette confers

- broad-spectrum resistance to a fungal rust pathogen in wheat. *Nat. Biotechnol.*  
Advance Access published 2021, doi:10.1038/s41587-020-00770-x.
- Makhdoomi, A., Mehrabi, R., Khodarahmi, M., and Abrinbana, M.** (2015). Efficacy of wheat genotypes and Stb resistance genes against Iranian isolates of *Zymoseptoria tritici*. *J. Gen. Plant Pathol.* **81**:5–14.
- Manser, B., Koller, T., Praz, C. R., Roulin, A., Zbinden, H., Arora, S., Steuernagel, B., Wulff, B. B. H., Keller, B., and Sánchez-Martín, J.** (2021). Identification of specificity-defining amino acids of the wheat immune receptor Pm2 and powdery mildew effector AvrPm2. *Plant J.* Advance Access published February 24, 2021, doi:10.1111/tbj.15214.
- Marcussen, T., Sandve, S. R., Heier, L., Spannagl, M., Pfeifer, M., Jakobsen, K. S., Wulff, B. B. H., Steuernagel, B., Mayer, K. F. X., Olsen, O. A., et al.** (2014). Ancient hybridizations among the ancestral genomes of bread wheat. *Science (80-. )*. **345**:1250092.
- Marshall, R., Kombrink, A., Motteram, J., Loza-Reyes, E., Lucas, J., Hammond-Kosack, K. E., Thomma, B. P. H. J., and Rudd, J. J.** (2011). Analysis of Two in Planta Expressed LysM Effector Homologs from the Fungus *Mycosphaerella graminicola* Reveals Novel Functional Properties and Varying Contributions to Virulence on Wheat. *PLANT Physiol.* **156**:756–769.
- McDonald, B. A.** (2014). Using dynamic diversity to achieve durable disease resistance in agricultural ecosystems. *Trop. Plant Pathol.* **39**:191–196.
- McDonald, B. A., and Mundt, C. C.** (2016). How Knowledge of Pathogen Population Biology Informs Management of Septoria Tritici Blotch. *Phytopathology* **106**:948–955.
- McFadden, E. S., and Sears, E. R.** (1947). The Genome Approach in Radical Wheat Breeding 1. *Agron. J.* **39**:1011–1025.
- McGrann, G. R. D., Stavrinides, A., Russell, J., Corbitt, M. M., Booth, A., Chartrain, L., Thomas, W. T. B., and Brown, J. K. M.** (2014). A trade off between mlo resistance to powdery mildew and increased susceptibility of barley to a newly important disease, *Ramularia* leaf spot. *J. Exp. Bot.* **65**:1025–1037.
- McKendry, A. L., and Henke, G. E.** (1994). Evaluation of Wheat Wild Relatives for Resistance to Septoria Tritici Blotch. *Crop Sci.* **34**:1080.
- Meile, L., Croll, D., Brunner, P. C., Plissonneau, C., Hartmann, F. E., McDonald, B. A., and Sánchez-Vallet, A.** (2018a). A fungal avirulence factor encoded in a highly plastic genomic region triggers partial resistance to septoria tritici blotch. *New Phytol.* **219**:1048–1061.
- Meile, L., Croll, D., Brunner, P. C., Plissonneau, C., Hartmann, F. E., McDonald, B. A., and Sanchez-Vallet, A.** (2018b). A fungal avirulence factor encoded in a highly

- plastic genomic region triggers partial resistance to septoria tritici blotch. *bioRxiv* Advance Access published February 23, 2018, doi:10.1101/264226.
- Miyakawa, T., Hatano, K. I., Miyauchi, Y., Suwa, Y. I., Sawano, Y., and Tanokura, M.** (2014). A secreted protein with plant-specific cysteine-rich motif functions as a mannose-binding lectin that exhibits antifungal activity. *Plant Physiol.* **166**:766–778.
- Morgounov, A., Özdemir, F., Keser, M., Akin, B., Dababat, A. A., Dreisigacker, S., Golkari, S., Koc, E., Küçükçongar, M., Muminjanov, H., et al.** (2021). Diversity and Adaptation of Currently Grown Wheat Landraces and Modern Germplasm in Afghanistan, Iran, and Turkey. *Crops* **1**:54–67.
- Mujeeb-Kazi, A., Rosas, V., and Roldan, S.** (1996). Conservation of the genetic variation of *Triticum tauschii* (Coss.) Schmalh. (*Aegilops squarrosa* auct. non L.) in synthetic hexaploid wheats (*T. turgidum* L. s.lat. x *T. tauschii*; 2n=6x=42, AABBDD) and its potential utilization for wheat improvement. *Genet. Resour. Crop Evol.* **1996** 432 **43**:129–134.
- Mundt, C.** (2018). Pyramiding for Resistance Durability: Theory and Practice. *Phytopathology* Advance Access published April 12, 2018, doi:10.1094/PHYTO-12-17-0426-RVW.
- Mundt, C. C., Brophy, L. S., and Schmitt, M. S.** (1995). Choosing crop cultivars and cultivar mixtures under low versus high disease pressure: A case study with wheat. *Crop Prot.* **14**:509–515.
- Nelson, R. R.** (1978). Genetics of horizontal resistance to plant diseases. *Ann. Rev. Phytopathol.* **16**:359–78.
- O’Driscoll, A., Kildea, S., Doohan, F., Spink, J., and Mullins, E.** (2014). The wheat–Septoria conflict: a new front opening up? *Trends Plant Sci.* **19**:602–610.
- O’Driscoll, A., Doohan, F., and Mullins, E.** (2015). Exploring the utility of *Brachypodium distachyon* as a model pathosystem for the wheat pathogen *Zymoseptoria tritici*. *BMC Res. Notes* **2015** 81 **8**:1–10.
- Ogbonnaya, F. C., Abdalla, O., Mujeeb-Kazi, A., Kazi, A. G., Xu, S. S., Gosman, N., Lagudah, E. S., Bonnett, D., Sorrells, M. E., and Tsujimoto, H.** (2013). Synthetic hexaploids: Harnessing species of the primary gene pool for wheat improvement. *Plant Breed. Rev.* **37**:35–122.
- Oggenfuss, U., Badet, T., Wicker, T., Hartmann, F. E., Singh, N. K., Abraham, L. N., Karisto, P., Vonlanthen, T., Mundt, C. C., McDonald, B. A., et al.** (2020). A population-level invasion by transposable elements in a fungal pathogen. *bioRxiv* Advance Access published February 12, 2020, doi:10.1101/2020.02.11.944652.
- Omrane, S., Audéon, C., Ignace, A., Duplaix, C., Aouini, L., Kema, G., Walker, A.-S., and Fillinger, S.** (2017). Plasticity of the MFS1 Promoter Leads to Multidrug

- Resistance in the Wheat Pathogen *Zymoseptoria tritici*. *mSphere* **2**:e00393-17.
- Orellana-Torrejon, C., Vidal, T., Boixel, A. L., Gélisse, S., Saint-Jean, S., and Suffert, F.** (2022). Annual dynamics of *Zymoseptoria tritici* populations in wheat cultivar mixtures: A compromise between the efficacy and durability of a recently broken-down resistance gene? *Plant Pathol.* **71**:289–303.
- Patterson, H. D., and Williams, E. R.** (1976). A new class of resolvable incomplete block designs. *Biometrika* **63**:83–92.
- Ponomarenko, A., Goodwin, S. B., and Kema, G. H. J.** (2011). Septoria tritici blotch (STB) of wheat Septoria tritici blotch (STB) of wheat. *Plant Heal. Instr.* Advance Access published 2011, doi:10.1094/PHI-I-2011-0407-01.
- Pont, C., Leroy, T., Seidel, M., Tondelli, A., Duchemin, W., Armisen, D., Lang, D., Bustos-Korts, D., Goué, N., Balfourier, F., et al.** (2019). Tracing the ancestry of modern bread wheats. *Nat. Genet.* **51**:905–911.
- Rahman, A., Hallgrímsdóttir, I., Eisen, M., and Pachter, L.** (2018). Association mapping from sequencing reads using k-mers. *Elife* **7**.
- Randhawa, M. S., Bariana, H. S., Mago, R., and Bansal, U. K.** (2015). Mapping of a new stripe rust resistance locus Yr57 on chromosome 3BS of wheat. *Mol. Breed.* **35**:65.
- Rehfus, A., Strobel, D., Bryson, R., and Stammler, G.** (2018). Mutations in *sdh* genes in field isolates of *Zymoseptoria tritici* and impact on the sensitivity to various succinate dehydrogenase inhibitors. *Plant Pathol.* **67**:175–180.
- Reynolds, M., Dreccer, F., and Trethowan, R.** (2007). Drought-adaptive traits derived from wheat wild relatives and landraces. *J. Exp. Bot.* **58**:177–186.
- Rimbaud, L., Papaïx, J., Barrett, L. G., Burdon, J. J., and Thrall, P. H.** (2018). Mosaics, mixtures, rotations or pyramiding: What is the optimal strategy to deploy major gene resistance? *Evol. Appl.* **11**:1791–1810.
- Robinson, J. T., Thorvaldsdóttir, H., Winckler, W., Guttman, M., Lander, E. S., Getz, G., and Mesirov, J. P.** (2011). Integrative genomics viewer. *Nat. Biotechnol.* **29**:24–26.
- Rudd, J. J., Kanyuka, K., Hassani-Pak, K., Derbyshire, M., Andongabo, A., Devonshire, J., Lysenko, A., Saqi, M., Desai, N. M., Powers, S. J., et al.** (2015). Transcriptome and metabolite profiling of the infection cycle of *Zymoseptoria tritici* on wheat reveals a biphasic interaction with plant immunity involving differential pathogen chromosomal contributions and a variation on the hemibiotrophic lifestyle definition. *Plant Physiol.* **167**:1158–1185.
- Saari, E. E., and Wilcoxson, R. D.** (1974). Plant Disease Situation of High-Yielding Dwarf Wheats in Asia and Africa. *Annu. Rev. Phytopathol.* **12**:49–68.
- Saintenac, C., Lee, W. S., Cambon, F., Rudd, J. J., King, R. C., Marande, W., Powers, S. J.,**

- Bergès, H., Phillips, A. L., Uauy, C., et al.** (2018). Wheat receptor-kinase-like protein Stb6 controls gene-for-gene resistance to fungal pathogen *Zymoseptoria tritici*. *Nat. Genet.* **50**:368–374.
- Saintenac, C., Cambon, F., Aouini, L., Verstappen, E., Ghaffary, S. M. T., Poucet, T., Marande, W., Berges, H., Xu, S., Jaouannet, M., et al.** (2021). A wheat cysteine-rich receptor-like kinase confers broad-spectrum resistance against *Septoria tritici* blotch. Advance Access published 2021.
- Salamini, F., Özkan, H., Brandolini, A., Schäfer-Pregl, R., and Martin, W.** (2002). Genetics and geography of wild cereal domestication in the near east. *Nat. Rev. Genet.* **3**:429–441.
- Sánchez-Martín, J., Steuernagel, B., Ghosh, S., Herren, G., Hurni, S., Adamski, N., Vrána, J., Kubaláková, M., Krattinger, S. G., Wicker, T., et al.** (2016). Rapid gene isolation in barley and wheat by mutant chromosome sequencing. *Genome Biol.* **17**:1–7.
- Sánchez-Vallet, A., McDonald, M. C., Solomon, P. S., and McDonald, B. A.** (2015). Is *Zymoseptoria tritici* a hemibiotroph? *Fungal Genet. Biol.* **79**:29–32.
- Savary, S., Willocquet, L., Pethybridge, S. J., Esker, P., McRoberts, N., and Nelson, A.** (2019). The global burden of pathogens and pests on major food crops. *Nat. Ecol. Evol.* **3**:430–439.
- Segretin, M. E., Pais, M., Franceschetti, M., Chaparro-Garcia, A., Bos, J. I. B., Banfield, M. J., and Kamoun, S.** (2014). Single amino acid mutations in the potato immune receptor R3a expand response to *Phytophthora* effectors. *Mol. Plant-Microbe Interact.* **27**:624–637.
- Seifbarghi, S., Razavi, M., Aminian, H., Zare, R., and Etebarian, H. R.** (2009). Studies on the host range of *Septoria* species on cereals and some wild grasses in Iran. *Phytopathol. Mediterr.* **48**:422–429.
- Shetty, N. P., Mehrabi, R., Lütken, H., Haldrup, A., Kema, G. H. J., Collinge, D. B., and Jørgensen, H. J. L.** (2007). Role of hydrogen peroxide during the interaction between the hemibiotrophic fungal pathogen *Septoria tritici* and wheat. *New Phytol.* **174**:637–647.
- Shi, G., Zhang, Z., Friesen, T. L., Raats, D., Fahima, T., Brueggeman, R. S., Lu, S., Trick, H. N., Liu, Z., Chao, W., et al.** (2016). The hijacking of a receptor kinase-driven pathway by a wheat fungal pathogen leads to disease. *Sci. Adv.* **2**:e1600822.
- Shipton, W. A., Boyd, W. R. J., Rosielle, A. A., and Shearer, B. I.** (1971). The common *Septoria* diseases of wheat. *Bot. Rev.* **37**:231–262.
- Shiu, S. H., and Bleecker, A. B.** (2003). Expansion of the receptor-like kinase/Pelle gene family and receptor-like proteins in *Arabidopsis*. *Plant Physiol.* **132**:530–543.

- Singh, P., and Zimmerli, L.** (2013). Lectin receptor kinases in plant innate immunity. *Front. Plant Sci.* **4**:124.
- Singh, B., Kaur, S., and Chhuneja, P.** (2018). Evaluation of plant resistance in progenitors of wheat against foliage feeding aphids. *Agric. Res. J.* **55**:117–121.
- Singh, N., Wu, S., Tiwari, V., Sehgal, S., Raupp, J., Wilson, D., Abbasov, M., Gill, B., and Poland, J.** (2019). Genomic analysis confirms population structure and identifies inter-lineage hybrids in *Aegilops tauschii*. *Front. Plant Sci.* **10**.
- Singh, S., Jighly, A., Sehgal, D., Burgueño, J., Joukhadar, R., Singh, S. K., Sharma, A., Vikram, P., Sansaloni, C. P., Govindan, V., et al.** (2021). Direct introgression of untapped diversity into elite wheat lines. *Nat. Food* **2**:819–827.
- Somasco, O. A., Qualset, C. O., and Gilchrist, D. G.** (1996). Single-gene resistance to *Septoria tritici* blotch in the spring wheat cultivar “Tadinia.” *Plant Breed.* **115**:261–267.
- Steinberg, G.** (2015). Cell biology of *Zymoseptoria tritici*: Pathogen cell organization and wheat infection. *Fungal Genet. Biol.* **79**:17–23.
- Stephens, C., Hammond-Kosack, K. E., and Kanyuka, K.** (2022). WAKsing plant immunity, waning diseases. *J. Exp. Bot.* **73**:22–37.
- Steuernagel, B., Periyannan, S. K., Hernández-Pinzón, I., Witek, K., Rouse, M. N., Yu, G., Hatta, A., Ayliffe, M., Bariana, H., Jones, J. D. G., et al.** (2016). Rapid cloning of disease-resistance genes in plants using mutagenesis and sequence capture. *Nat. Biotechnol.* **34**:652–655.
- Stotz, H. U., Mitrousia, G. K., de Wit, P. J. G. M., and Fitt, B. D. L.** (2014). Effector-triggered defence against apoplastic fungal pathogens. *Trends Plant Sci.* **19**:491–500.
- Stukenbrock, E. H., Banke, S., Javan-Nikkhah, M., and McDonald, B. A.** (2007). Origin and domestication of the fungal wheat pathogen *Mycosphaerella graminicola* via sympatric speciation. *Mol. Biol. Evol.* **24**:398–411.
- Suffert, F., Sache, I., and Lannou, C.** (2011). Early stages of *septoria tritici* blotch epidemics of winter wheat: Build-up, overseasoning, and release of primary inoculum. *Plant Pathol.* **60**:166–177.
- Tateda, C., Obara, K., Abe, Y., Sekine, R., Nekoduka, S., Hikage, T., Nishihara, M., Sekine, K. T., and Fujisaki, K.** (2019). The Host Stomatal Density Determines Resistance to *Septoria gentianae* in Japanese Gentian. *Mol. Plant-Microbe Interact.* **32**:428–436.
- Te Beest, D. E., Paveley, N. D., Shaw, M. W., and Van Den Bosch, F.** (2013). Accounting for the economic risk caused by variation in disease severity in fungicide dose decisions, exemplified for *Mycosphaerella graminicola* on winter wheat. *Phytopathology* **103**:666–672.
- Thind, A. K., Wicker, T., Šimková, H., Fossati, D., Moullet, O., Brabant, C., Vrána, J.,**

- Doležel, J., and Krattinger, S. G.** (2017). Rapid cloning of genes in hexaploid wheat using cultivar-specific long-range chromosome assembly. *Nat. Biotechnol.* **35**:793–796.
- Toda, Y., Tameshige, T., Tomiyama, M., Kinoshita, T., and Shimizu, K. K.** (2021). An Affordable Image-Analysis Platform to Accelerate Stomatal Phenotyping During Microscopic Observation. *Front. Plant Sci.* **12**:1–10.
- Toor, A. K., Bansal, U. K., Bhardwaj, S., Badebo, A., and Bariana, H. S.** (2013). Characterization of stem rust resistance in old tetraploid wheat landraces from the Watkins collection. *Genet. Resour. Crop Evol.* **60**:2081–2089.
- Tordai, H., Bányai, L., and Patthy, L.** (1999). The PAN module: The N-terminal domains of plasminogen and hepatocyte growth factor are homologous with the apple domains of the prekallikrein family and with a novel domain found in numerous nematode proteins. *FEBS Lett.* **461**:63–67.
- Torriani, S. F. F., Stukenbrock, E. H., Brunner, P. C., McDonald, B. A., and Croll, D.** (2011). Evidence for extensive recent intron transposition in closely related fungi. *Curr. Biol.* **21**:2017–22.
- Torriani, S. F. F., Melichar, J. P. E., Mills, C., Pain, N., Sierotzki, H., and Courbot, M.** (2015). Zymoseptoria tritici: A major threat to wheat production, integrated approaches to control. *Fungal Genet. Biol.* **79**:8–12.
- Vaattovaara, A., Brandt, B., Rajaraman, S., Safronov, O., Veidenberg, A., Luklová, M., Kangasjärvi, J., Löytynoja, A., Hothorn, M., Salojärvi, J., et al.** (2019). Mechanistic insights into the evolution of DUF26-containing proteins in land plants. *Commun. Biol.* **2**.
- Vagndorf, N., Nielsen, N. H., Edriss, V., Andersen, J. R., Orabi, J., Jørgensen, L. N., and Jahoor, A.** (2017). Genomewide association study reveals novel quantitative trait loci associated with resistance towards Septoria tritici blotch in North European winter wheat. *Plant Breed.* **136**:474–482.
- Van der Plank, J. E.** (1963). Plant diseases: epidemics and control. *Plant Dis. epidemics Control*. Advance Access published 1963.
- Vavilov, N. I.** (1922). The Law of Homologous Series in Variation. *J Genet* Advance Access published 1922.
- Vavilov, N. I.** (1931). The problem of the origin of the world's agriculture in the light of the latest investigations. In *Science at the Cross Roads (Routledge Revivals): Papers from The Second International Congress of the History of Science and Technology 1931*, pp. 97–106.
- Vidal, T., Boixel, A.-L., Durand, B., de Vallavieille-Pope, C., Huber, L., and Saint-Jean, S.** (2017). Reduction of fungal disease spread in cultivar mixtures: Impact of canopy architecture on rain-splash dispersal and on crop microclimate. *Agric. For. Meteorol.*

246:154–161.

- Villa, T. C. C., Maxted, N., Scholten, M., and Ford-Lloyd, B.** (2005). Defining and identifying crop landraces. *Plant Genet. Resour.* **3**:373–384.
- Voichek, Y., and Weigel, D.** (2020). Identifying genetic variants underlying phenotypic variation in plants without complete genomes. *Nat. Genet.* **52**:534–540.
- Voss-Fels, K. P., Stahl, A., Wittkop, B., Lichthardt, C., Nagler, S., Rose, T., Chen, T. W., Zetzsche, H., Seddig, S., Majid Baig, M., et al.** (2019). Breeding improves wheat productivity under contrasting agrochemical input levels. *Nat. Plants* **5**:706–714.
- Walker, J. C., and Zhang, R.** (1990). Relationship of a putative receptor protein kinase from maize to the S-locus glycoproteins of Brassica. *Nature* **345**:743–746.
- Walkowiak, S., Gao, L., Monat, C., Haberer, G., Kassa, M. T., Brinton, J., Ramirez-Gonzalez, R. H., Kolodziej, M. C., Delorean, E., Thambugala, D., et al.** (2020). Multiple wheat genomes reveal global variation in modern breeding. *Nature* **588**:277–283.
- Wang, J., Luo, M. C., Chen, Z., You, F. M., Wei, Y., Zheng, Y., and Dvorak, J.** (2013). *Aegilops tauschii* single nucleotide polymorphisms shed light on the origins of wheat D-genome genetic diversity and pinpoint the geographic origin of hexaploid wheat. *New Phytol.* **198**:925–937.
- Wang, Y., Subedi, S., de Vries, H., Doornenbal, P., Vels, A., Hensel, G., Kumlehn, J., Johnston, P. A., Qi, X., Blilou, I., et al.** (2019). Orthologous receptor kinases quantitatively affect the host status of barley to leaf rust fungi. *Nat. Plants* **5**:1129–1135.
- Watkins, A. E.** (1933). The Origin of Cultivated Plants. *Antiquity* **7**:73–80.
- Winfield, M. O., Allen, A. M., Wilkinson, P. A., BurrIDGE, A. J., Barker, G. L. A., Coghill, J., Waterfall, C., Wingen, L. U., Griffiths, S., and Edwards, K. J.** (2018). High-density genotyping of the A.E. Watkins Collection of hexaploid landraces identifies a large molecular diversity compared to elite bread wheat. *Plant Biotechnol. J.* **16**:165–175.
- Wingen, L. U., Orford, S., Goram, R., Leverington-Waite, M., Bilham, L., Patsiou, T. S., Ambrose, M., Dicks, J., and Griffiths, S.** (2014). Establishing the A. E. Watkins landrace cultivar collection as a resource for systematic gene discovery in bread wheat. *Theor Appl Genet* **127**:1831–1842.
- Wingen, L. U., West, C., Leverington-Waite, M., Collier, S., Orford, S., Goram, R., Yang, C.-Y., King, J., Allen, A. M., BurrIDGE, A., et al.** (2017). Wheat Landrace Genome Diversity Advance Access published 2017, doi:10.1534/genetics.116.194688.
- Wulff, B. B. H., and Moscou, M. J.** (2014). Strategies for transferring resistance into wheat: from wide crosses to GM cassettes. *Front. Plant Sci.* **5**:692.

- Yang, F., Li, W., and Jørgensen, H. J. L.** (2013). Transcriptional Reprogramming of Wheat and the Hemibiotrophic Pathogen *Septoria tritici* during Two Phases of the Compatible Interaction. *PLoS One* **8**:81606.
- Yang, N., Mcdonald, M. C., Peter, ; Solomon, S., and Milgate, A. W.** (2018). Genetic mapping of *Stb19*, a new resistance gene to *Zymoseptoria tritici* in wheat. *Theor. Appl. Genet.* **1**:3.
- Yates, S., Mikaberidze, A., Krattinger, S. G., Abrouk, M., Hund, A., Yu, K., Studer, B., Fouche, S., Meile, L., Pereira, D., et al.** (2019). Precision Phenotyping Reveals Novel Loci for Quantitative Resistance to *Septoria Tritici* Blotch. *Plant Phenomics* **2019**:1–11.
- Zhong, Z., Marcel, T. C., Hartmann, F. E., Ma, X., Plissonneau, C., Zala, M., Ducasse, A., Confais, J., Compain, J., Lapalu, N., et al.** (2017). A small secreted protein in *Zymoseptoria tritici* is responsible for avirulence on wheat cultivars carrying the *Stb6* resistance gene. *New Phytol.* **214**:619–631.
- Zhou, X., and Stephens, M.** (2012). Genome-wide efficient mixed-model analysis for association studies. *Nat. Genet.* **44**:821–824.
- Zhou, Y., Zhao, X., Li, Y., Xu, J., Bi, A., Kang, L., Xu, D., Chen, H., Wang, Y., Wang, Y. ge, et al.** (2020). Triticum population sequencing provides insights into wheat adaptation. *Nat. Genet.* **52**:1412–1422.
- Zhou, Y., Bai, S., Li, H., Sun, G., Zhang, D., Ma, F., Zhao, X., Nie, F., Li, J., Chen, L., et al.** (2021). Introgressing the *Aegilops tauschii* genome into wheat as a basis for cereal improvement. *Nat. Plants* **7**:774–786.
- Zurayk, R., and Khalidi, R.** (2011). *Food, farming, and freedom : sowing the Arab spring*. Just World Books.

## 7. APPENDIX

**Supplementary Table 1:** Mean responses of *Ae. tauschii* and wheat accessions to *Z. tritici* isolates cfz008 and IPO323. Means are estimated from a linear mixed model fitted to both datasets (Chapter 2).

Accession	cfz008		IPO323	
	Logit pAUDPC	% max dAUDPC	Logit pAUDPC	% max dAUDPC
Bastard II	-1.4	99.4	-	-
BW_01001	-7.1	28.9	-6.0	78.9
BW_01002	-6.0	61.0	-6.1	49.8
BW_01003	-5.2	79.9	-6.0	75.3
BW_01004	-6.3	15.5	-6.5	0.3
BW_01005	-6.9	35.3	-6.4	73.9
BW_01006	-3.9	15.9	-6.3	56.4
BW_01007	-5.6	72.3	-6.4	92.0
BW_01008	-5.4	56.6	-5.7	66.2
BW_01009	-3.9	58.6	-5.7	93.1
BW_01010	-6.1	14.8	-4.9	25.4
BW_01011	-3.9	29.9	-5.3	58.2
BW_01012	-5.3	12.7	-6.2	56.5
BW_01015	-4.1	91.8	-5.2	74.6
BW_01016	-3.7	50.3	-5.5	72.4
BW_01019	-5.6	25.7	-6.3	105.7
BW_01020	-5.2	23.3	-6.5	57.2
BW_01021	-3.5	96.0	-5.8	97.4
BW_01022	-5.1	44.5	-6.5	49.9
BW_01024	-5.8	65.6	-6.0	69.7
BW_01025	-4.9	25.3	-6.5	59.2
BW_01026	-5.6	62.2	-5.6	90.2
BW_01027	-5.4	17.0	-6.4	61.7
BW_01030	-4.5	47.3	-6.4	72.0
BW_01031	-3.5	85.2	-6.3	94.0
BW_01032	-2.5	38.2	-5.2	49.0
BW_01033	-2.7	50.7	-5.4	85.0
BW_01039	-3.6	38.8	-4.8	59.6
BW_01041	-5.6	30.3	-5.8	55.2
BW_01042	-3.7	86.0	-6.3	52.8
BW_01043	-5.8	65.1	-6.3	98.7
BW_01044	-6.2	66.6	-6.3	93.7
BW_01045	-2.5	94.5	-6.2	80.8
BW_01046	-3.4	47.3	-6.1	68.8
BW_01047	-5.6	37.4	-6.0	39.4
BW_01048	-5.4	25.3	-5.7	64.2
BW_01049	-4.6	101.6	-4.6	83.2

BW_01050	-6.1	46.5	-6.4	70.3
BW_01055	-5.8	92.3	-6.5	66.7
BW_01056	-5.1	41.1	-5.9	89.6
BW_01057	-2.4	43.1	-6.3	79.2
BW_01058	-3.4	65.2	-5.7	97.8
BW_01059	-3.6	78.6	-6.6	56.3
BW_01060	-4.1	67.0	-6.2	99.1
BW_01062	-4.6	84.2	-5.2	91.3
BW_01063	-5.1	58.1	-5.7	71.6
BW_01065	-3.2	56.1	-5.3	78.0
BW_01066	-6.4	6.1	-6.5	5.5
BW_01068	-6.2	6.5	-5.4	42.2
BW_01069	-6.0	18.0	-5.1	63.8
BW_01070	-5.6	16.5	-6.0	63.6
BW_01071	-7.1	49.7	-6.4	93.4
BW_01072	-6.0	37.3	-6.8	54.0
BW_01073	-7.1	16.5	-6.2	67.5
BW_01074	-5.3	30.1	-6.5	92.9
BW_01076	-4.4	19.3	-6.5	68.2
BW_01077	-5.6	37.0	-6.3	65.3
BW_01078	-2.5	51.6	-6.2	80.6
BW_01079	-4.5	63.0	-5.1	85.2
BW_01081	-3.0	63.0	-6.2	81.1
BW_01082	-4.3	65.2	-2.8	101.9
BW_01083	-7.1	43.3	-6.0	46.5
BW_01084	-4.9	16.0	-6.3	14.5
BW_01085	-6.1	7.5	-5.5	46.6
BW_01086	-3.2	73.0	-5.0	72.0
BW_01087	-2.5	99.9	-6.1	95.8
BW_01088	-6.7	6.0	-5.9	29.5
BW_01089	-5.5	88.9	-5.7	98.2
BW_01091	-5.6	14.6	-6.5	53.6
BW_01094	-3.0	42.9	-6.5	62.3
BW_01095	-2.5	96.8	-5.6	60.3
BW_01096	-5.0	94.6	-6.6	91.5
BW_01097	-5.8	71.1	-5.6	69.3
BW_01098	-7.1	23.7	-6.1	13.0
BW_01099	-2.5	92.2	-5.1	73.9
BW_01100	-4.8	49.5	-5.9	70.4
BW_01102	-3.4	68.0	-6.3	86.2
BW_01103	-1.6	83.6	-3.7	72.9
BW_01104	-3.4	88.1	-5.3	89.2
BW_01105	-4.3	32.4	-6.1	57.2
BW_01106	-2.5	94.7	-5.9	93.0
BW_01107	-5.3	56.2	-6.5	39.0
BW_01108	-5.1	59.9	-5.9	71.0

BW_01109	-5.7	12.9	-6.4	80.7
BW_01110	-5.0	68.1	-5.1	69.7
BW_01111	-5.3	32.0	-6.3	41.5
BW_01112	-4.0	53.5	-6.0	59.9
BW_01113	-3.1	66.7	-3.9	86.2
BW_01114	-6.1	30.8	-5.1	50.8
BW_01115	-3.0	52.3	-5.7	53.6
BW_01116	-2.8	88.3	-6.7	96.0
BW_01117	-5.4	59.9	-5.1	46.4
BW_01118	-3.5	49.5	-6.2	36.2
BW_01119	-7.1	74.6	-5.3	90.4
BW_01120	-4.2	73.6	-5.6	54.8
BW_01121	-5.2	54.7	-5.5	77.7
BW_01122	-4.4	32.2	-6.0	72.9
BW_01123	-4.9	25.4	-6.2	60.0
BW_01124	-4.6	46.2	-5.2	57.1
BW_01125	-2.5	100.4	-5.8	99.8
BW_01126	-6.3	25.8	-5.1	41.3
BW_01128	-3.1	76.6	-5.6	67.3
BW_01129	-5.1	49.5	-6.3	83.6
BW_01130	-4.1	47.6	-5.1	48.7
BW_01132	-6.4	32.5	-5.9	50.1
BW_01133	-3.5	44.0	-5.3	61.4
BW_01134	-4.4	23.5	-6.0	96.5
BW_01135	-1.8	99.4	-4.2	101.2
BW_01136	-4.8	98.2	-5.4	88.2
BW_01137	-6.9	2.0	-7.0	21.4
BW_01138	-5.8	25.4	-6.4	57.9
BW_01139	-5.2	92.9	-4.5	92.5
BW_01140	-6.0	37.4	-6.4	55.4
BW_01141	-6.9	41.6	-5.3	83.6
BW_01142	-5.5	12.8	-5.8	56.3
BW_01143	-6.1	78.2	-4.5	50.1
BW_01144	-5.7	67.1	-5.9	84.9
BW_01146	-2.3	67.5	-6.4	69.6
BW_01147	-4.6	88.2	-4.5	81.2
BW_01148	-3.4	56.1	-4.8	82.7
BW_01151	-6.8	11.3	-5.9	19.0
BW_01152	-3.5	49.6	-6.2	34.1
BW_01153	-5.2	15.7	-6.3	62.6
BW_01154	-5.1	37.5	-4.8	50.2
BW_01155	-4.6	10.1	-6.4	48.4
BW_01156	-3.1	49.7	-6.2	76.3
BW_01158	-3.7	75.7	-4.8	57.5
BW_01159	-4.8	33.8	-6.2	48.6
BW_01161	-5.8	32.6	-5.8	77.1

BW_01162	-4.2	27.3	-6.2	38.8
BW_01163	-6.9	5.2	-6.4	41.6
BW_01164	-7.5	54.1	-5.5	94.8
BW_01165	-4.5	28.9	-4.4	63.2
BW_01166	-5.2	39.8	-5.3	79.0
BW_01167	-4.7	77.7	-6.3	68.2
BW_01168	-4.2	66.1	-5.7	89.5
BW_01170	-3.4	92.4	-6.2	81.8
BW_01171	-2.8	91.2	-6.5	101.6
BW_01172	-3.6	60.2	-5.7	81.4
BW_01175	-0.8	48.1	-4.8	101.6
BW_01176	-3.1	48.3	-5.2	62.7
BW_01177	-6.1	23.9	-5.4	42.0
BW_01178	-6.3	13.4	-6.5	67.8
BW_01179	-4.0	68.3	-5.8	96.9
BW_01181	-5.9	75.6	-6.2	64.6
BW_01182	-4.6	62.5	-5.8	97.1
BW_01184	-3.5	94.8	-6.8	80.7
BW_01185	-5.4	87.5	-6.2	98.0
BW_01186	-3.6	83.8	-4.5	74.3
BW_01189	-5.7	40.2	-6.7	72.0
BW_01190	-5.3	42.6	-6.4	31.1
BW_01192	-5.6	31.3	-6.2	64.8
BW_01193	-6.5	30.8	-6.4	55.2
Cellule	1.2	99.2	-	-
CS stb16q (-)	2.2	95.1	-	-
CS Stb16q (+)	1.7	102.7	-	-
CS-Synthetic	-1.6	70.2	-	-
Flame	-	-	-6.0	13.3
Hereward	-	-	-6.4	19.5
KK	-1.0	98.7	-	-
Longbow	0.1	106.4	-0.6	94.3
Riband	-	-	-1.4	76.3
Tadinia	-0.1	97.4	-	-

**Supplementary Table 2:** Genes present in regions associated with necrosis response to *Z. tritici* isolate cfz008. Knetminer output for associated traits and functions of these genes is provided. Definitions of gene name acronyms are from The Arabidopsis Information Resource (TAIR; <https://www.arabidopsis.org/index.jsp>).

Chrm	Peak Name	Region St.	Region End	Exon St.	Gene	Gene Name	Trait	Function
2D	Blue 1	15460000	15960000	15594940	TRAESCS2D01G043400	MRG1 (mortality factor-related gene)	Disease resistance	BioProc: Response To Far Red Light, Response To Light Stimulus, Far-red Light Signaling Pathway, Long-day Photoperiodism. Publications: PMID:18667727, PMID:18683907, PMID:23135282, PMID:12938171, PMID:17653269, PMID:17227549, PMID:23261264.
				15629538	TRAESCS2D01G043500	CYP93D1 (cytochrome family gene)		Defense Response, Response To Stress, Response To Endogenous Stimuli., Response To Abiotic Stimulus, Response To Biotic Stimulus
				15933685	TRAESCS2D01G044000	NPF2.11 (nitrate excretion transporter)	Disease resistance	MolFunc, SAP Kinase Activity: Cellular Response To Ethylene, Response To Auxin, Response To Freezing, Response To Cold, Response To Karrikin, Response To Hypoxia, Response To Salt Stress, Response To Absence Of Light, Regulation Of Response To Osmosis, Response To Sucrose, Response To Light Stimulus, Response To Hormone. Publications: PMID:23007554, PMID:15978049, PMID:23962165, PMID:18849477, PMID:17227549, PMID:15381001, PMID:22783269, PMID:15272873.
				15920661	TRAESCS2D01G043800	AT14A (protein with integrin-related transmembrane domain)		Response To Zinc Ion, Response To UV-B, Response To Salt Stress, Response To Cytokinin, Defense Response To Fungus, Response To Endoplasmic Retic...: Publication, PMID:17587374, PMID:15978049, PMID:17916636, PMID:19656045, PMID:12773641, PMID:17061125, PMID:15282545
				15731041	TRAESCS2D01G043700	TRAESCS2D01G043700	Disease resistance	Response To Karrikin, Far-red Light Signaling Pathway, Response To Osmotic Stress, Defense Response To Fungus, Response To Light Stimulus, Defense Response To Fungus, Response To Auxin, Response To Heat, Innate Immune Response, Response To Ethylene, Response To Salt Stress, Regulation Of Defense Response, Response To Jasmonic Acid, Response To Cytokinin, Defense Response, Regulation Of Response To Osm..., Response To Far Red Light, Defense Response To Bacterium, Defense Response To Oomycetes, Response To Cadmium Ion: CelComp, Microtubule. Publications: PMID:24664204, PMID:23135282, PMID:15720654, PMID:25747881, PMID:23261264, PMID:18667727, PMID:15494554, PMID:19286969, PMID:18250078, PMID:23531533, PMID:17653269, PMID:15047901, PMID:12938171,

								PMID:17059409, PMID:17061125, PMID:21830950, PMID:16829591. Protein: Q9LTA6
				15587135	TRAESCS2D01G043300	AFH3 (Arabidopsis formin3)	Disease resistance, salt sensitivity	Publication: PMID:16776300
<b>3D</b>	Blue 2	43715000	44215000	44195808	TRAESCS3D01G087600	RAP (Octotricopeptide Repeat Protein)		Defense Response. Publication: PMID:15318736
				43738718	TRAESCS3D01G086200	TRAESCS3D01G086200		Defense Response
				43779270	TRAESCS3D01G086300	TPS21 (terpene synthase 21)		Defense Response, Response To Stress, Response To Herbivore, Response To Endogenous Stimuli, Response To Biotic Stimulus, Response To External Stimulus, Response To Extracellular Stimuli
				44007853	TRAESCS3D01G087300	OASB (O-acetylserine lyase B)	Salt sensitivity	Response To Cytokinin, Response To UV-B, Response To Cadmium Ion: Publications: PMID:17587374, PMID:12773641.
				44063865	TRAESCS3D01G087400	TRAESCS3D01G087400	Disease resistance	Response To Stress, Response To Endogenous Stimuli, Response To Abiotic Stimulus, Response To Biotic Stimulus, Response To Oxidative Stress, Response To Cadmium Ion: Publications: PMID:18596930, PMID:14645734, PMID:14617066.
				43994870	TRAESCS3D01G087100	DRT111 (recombination and DNA-damage resistance protein)	Disease resistance	Cellular Response To Potassium, Response To Freezing, Response To Cold, Cold Acclimation. Publications: PMID:25267732, PMID:15272873.
				43972447	TRAESCS3D01G087000	TRAESCS3D01G087000		Publication, PMID:15310832, Transcriptome profiling of the response of Arabidopsis suspension culture cells to Suc starvation
				43949085	TRAESCS3D01G086900	MFP2 (multifunctional protein 2)		Microtubule
				43798962	TRAESCS3D01G086600	TRAESCS3D01G086600	Disease resistance	Response To Stress, Response To Endogenous Stimuli, Response To Biotic Stimulus, Response To External Stimulus, Response To Abscisic Acid, Response To Extracellular Stimuli. Publications: PMID:16941220, PMID:17956627, PMID:15282545. Protein: Q8VZC7, POCB16
				44193535	TRAESCS3D01G087500	URH2 (uridine-ribohydrolase 2)		Cellular Response To DNA Damage, Response To Heat, Response To Stress, Response To Endogenous Stimuli, Response To Abiotic Stimulus, Response To Biotic Stimulus, Response To External Stimulus, Response To Extracellular Stimuli
<b>3D</b>	Red 1	594720000	595230000	594955199	TRAESCS3D01G509500	BOB2 (HSP20-like chaperones superfamily protein)		Phenotype, SHORTER HYPOCOTYLS IN THE DARK. Response To Cytokinin, Response To Auxin, Response To Heat, Heat Acclimation,

					Response To Abscisic Acid, Regulation Of Defense Response. Publications: PMID:15047901, PMID:15282545
594853731	TRAESCS3D01G509100	ndhO (NADH dehydrogenase-like complex)			Response To Glucose, Response To Water Deprivation, Response To Abscisic Acid
594807161	TRAESCS3D01G509000	PSD3 (phosphatidylserine decarboxylase 3)			Response To Stress, Response To Endogenous Stimuli, Response To Biotic Stimulus, Response To External Stimulus, Response To Extracellular Stimuli
595016277	TRAESCS3D01G509700	TRAESCS3D01G509700			Response To Stress, Response To Endogenous Stimuli, Response To Abiotic Stimulus, Response To Biotic Stimulus, Response To External Stimulus, Response To Extracellular Stimuli
594772175	TRAESCS3D01G508800	TRAESCS3D01G508800	Barley spot blotch resistance		Response To Stress, Response To Endogenous Stimuli, Response To Abiotic Stimulus, Response To Biotic Stimulus, Response To External Stimulus, Response To Extracellular Stimuli
594802584	TRAESCS3D01G508900	TRAESCS3D01G508900			Response To Stress, Response To Endogenous Stimuli, Response To Abiotic Stimulus, Response To Biotic Stimulus, Response To External Stimulus, Response To Extracellular Stimuli, Behavior
594748863	TRAESCS3D01G508600	TRAESCS3D01G508600			Response To Stress, Response To Endogenous Stimuli, Response To Abiotic Stimulus, Response To Biotic Stimulus, Response To External Stimulus, Response To Extracellular Stimuli, Behavior
594769919	TRAESCS3D01G508700	TRAESCS3D01G508700	Barley spot blotch resistance		Response To Stress, Response To Endogenous Stimuli, Response To Abiotic Stimulus, Response To Biotic Stimulus, Response To External Stimulus, Response To Extracellular Stimuli
595020229	TRAESCS3D01G509800	TRAESCS3D01G509800			Response To Heat, Heat Acclimation
595109906	TRAESCS3D01G510100	TRAESCS3D01G510100			Response To Freezing, Response To Cold: Publication, PMID:14617066
595062489	TRAESCS3D01G509900	RGLG3 (ring domain ligase 3)			Cellular Response To DNA Dama..., Response To Auxin, Defense Response To Bacterium, Response To Heat, Response To Gibberellin, Response To Wounding, Response To Hypoxia: Publication, PMID:15681342
594893048	TRAESCS3D01G509300	BOB2 (HSP20-like chaperones superfamily protein)			Phenotype, SHORTER HYPOCOTYLS IN THE DAR...: Response To Cytokinin, Response To Auxin, Response To Heat, Heat Acclimation, Response To Abscisic Acid, Regulation Of Defense Response: Publication, PMID:15047901, PMID:15282545
595070325	TRAESCS3D01G510000	RGLG3 (ring domain ligase 3)			Cellular Response To DNA Dama..., Response To Auxin, Defense Response To Bacterium, Response To Heat, Response To Gibberellin, Response To Wounding, Response To Hypoxia: Publication, PMID:15681342

4D	Blue 3	468400000	468900000	468601187	TRAESCS4D01G299800	FLDH (farnesol dehydrogenase)		Response To Stress, Response To Endogenous Stimuli, Plant-type Hypersensitive Res..., Response To Endoplasmic Retic..., Response To Biotic Stimulus, Response To External Stimulus, Response To Extracellular Stimuli: Publication, PMID:15047901
				468418135	TRAESCS4D01G299400	TRAESCS4D01G299400		Response To Stress, Response To Endogenous Stimuli, Response To Aluminum Ion, Response To Abiotic Stimulus, Response To Biotic Stimulus: Publication, PMID:23718947: Protein, Q0D8I9
				468603956	TRAESCS4D01G299900	ORC2 (origin recognition complex subunit 2)		Regulation Of Response To Osm..., Defense Response To Bacterium, Defense Response To Oomycetes, Response To Salt Stress, Regulation Of Defense Response
				468598548	TRAESCS4D01G299700	TRAESCS4D01G299700	Stem and stripe rust seedling and plant response	
				468588065	TRAESCS4D01G299500	PGSIP3 (plant glycogenin-like starch initiation protein 3)		Response To Stress, Response To Endogenous Stimuli, Response To Biotic Stimulus, Response To External Stimulus, Response To Extracellular Stimuli
6D	Red 3	430975000	431475000	431267503	TRAESCS6D01G324900	PME16 (pectin metylesterase 16)		Defense Response To Gram-negative bacteria, degradation pathway of pectin
				431469420	TRAESCS6D01G326600	EIL4 (ethylene insensitive 3 family protein)		Response To Karrikin, Cellular Response To Iron Ion
				431452669	TRAESCS6D01G326300	AVPL2 (pyrophosphate-energized membrane proton pump 2)	Stem and stripe rust seedling and plant response	Response To Freezing, Response To Water Deprivation, Response To Salt, Response To Osmotic Stress, Response To Salicylic Acid, Tropism, Defense Response To Bacterium..., Response To Abscisic Acid, Response To Cold, Response To Wounding, Defense Response, Response To Sucrose, Defense Response To Bacterium, Defense Response To Virus, Response To Endoplasmic Retic..., Response To Oxidative Stress, Response To Bacterium, Response To Hormone: Publication, PMID:17704230, PMID:12920300, PMID:16123132, PMID:16776300, PMID:14535883, PMID:14666423, PMID:15047901, PMID:12913158, PMID:14617066, PMID:18849477
				431252274	TRAESCS6D01G324700	TRAESCS6D01G324700		Response To Stress, Response To Endogenous Stimuli, Response To Biotic Stimulus, Response To External Stimulus, Response To Extracellular Stimuli

**Supplementary Table 3:** Mean logit pAUDPC and % maximum dAUDPC values estimated from linear mixed models for the interactions between the Watkins core 300 and wheat controls and 7 *Z. tritici* isolates.

Line	Isolate															
	CA30		IPO323		IPO88004		IPO89011		IPO90012		IPO92006		IPO94269		JIC040	
	Logit pAUDPC	% max. dAUDPC														
Baldus	-2.5	49.9	-1.5	56.8	-	-	-3.5	49.0	-	-	1.0	83.1	-	-	-	-
Bastard II	-	-	-	-	-	-	-	-	-	-	-3.3	67.1	-	-	-	-
Cellule	-	-	-	-	0.2	64.0	-	-	-	-	-5.4	44.3	-	-	-6.1	43.7
Chinese Spring	-	-	-5.6	47.2	-	-	-	-	-	-	-	-	-	-	-	-
Courtout	-	-	-	-	-	-	-0.7	68.2	-2.6	54.0	-	-	-	-	-	-
Flame	-	-	-6.0	46.2	-	-	-	-	-	-	-	-	-	-	-	-
Gene	-2.5	47.1	-	-	-	-	-	-	-	-	-	-	-9.6	8.1	-	-
KK	-	-	-	-	-1.9	52.2	-	-	-	-	-	-	-3.4	38.8	-0.5	51.0
Longbow	-	-	-3.1	28.9	-6.4	57.3	-	-	-	-	0.0	59.1	-	-	2.5	65.8
Olaf	-	-	-	-	-	-	-	-	-8.8	30.8	-	-	-	-	-	-
Paragon	-	-	-	-	-1.9	85.3	-	-	-	-	-	-	-	-	-1.0	75.7
W209	-2.3	52.4	-4.3	35.3	-5.6	39.5	-2.9	48.0	-6.2	25.4	-0.5	53.5	-3.5	39.0	-1.5	56.3
W219	-2.7	52.4	-6.7	20.3	-4.7	41.6	-3.8	49.0	-2.9	36.3	-0.2	60.9	-6.2	18.7	-1.5	48.6
W232	-2.2	57.0	-5.1	27.8	-3.3	48.3	-0.7	45.7	-5.1	36.3	-2.1	59.2	-3.4	46.7	-2.6	56.2
W240	-2.2	52.8	-3.8	47.6	-3.2	55.6	-0.8	52.6	-1.8	60.4	2.6	81.0	-1.1	61.7	-0.3	66.4
W242	-4.0	55.6	-3.8	26.1	-0.2	29.8	-0.5	67.3	-3.6	26.8	0.1	67.7	-4.0	14.0	-0.6	46.5
W268	-3.8	51.5	-7.3	27.2	-0.4	86.2	-2.3	61.2	-4.8	38.1	-2.5	38.0	-8.9	12.7	-4.8	56.3
W271	-3.6	49.4	-2.7	44.2	-0.4	81.3	-0.9	67.9	-9.0	34.8	1.3	84.0	-5.7	21.6	-3.8	54.8
W273	-2.2	51.9	-5.3	37.9	-2.4	64.4	-4.4	39.4	-4.2	51.5	0.5	82.0	-3.8	31.8	-0.9	66.0
W277	-2.7	50.8	-4.3	37.6	-1.4	52.0	-1.2	57.3	-7.3	18.9	-3.3	32.6	-2.7	45.3	-1.6	60.4

W292	-2.6	49.5	-3.8	32.7	-0.7	59.7	-2.1	52.9	-1.4	61.9	0.2	75.4	-2.7	42.5	-0.5	57.1
W297	-3.9	23.1	-7.2	43.3	-3.3	56.6	-0.8	60.7	-3.8	49.8	-1.6	76.2	-5.2	38.6	-2.2	57.4
W301	-2.7	45.4	-4.6	39.3	-1.2	69.4	-3.4	46.8	-5.2	32.1	0.8	85.7	-2.4	42.7	-1.4	57.1
W317	-3.6	37.3	-6.6	80.6	-6.7	54.3	-0.3	76.5	-6.0	27.5	-1.2	73.2	-7.0	25.5	-2.3	50.8
W381	-3.2	52.0	-2.4	24.5	1.4	45.8	-1.6	49.9	-1.9	46.1	0.1	62.0	-2.1	28.1	-0.6	37.1
W399	-2.1	73.4	-3.3	52.2	1.4	48.5	-2.4	43.3	-4.1	41.7	0.6	76.5	-4.1	34.4	-2.9	45.9
W404	-1.9	59.9	-6.1	71.9	0.8	58.3	-3.5	50.5	-2.9	55.0	0.9	80.4	-2.7	44.4	-0.2	72.4
W407	-4.7	40.9	-5.5	50.8	-2.6	63.5	-1.9	59.5	-4.0	43.2	-2.0	65.9	-2.8	47.3	-0.6	53.2
W423	-2.5	47.7	-3.0	30.2	-6.2	27.7	-3.5	48.3	-3.8	34.2	2.0	78.4	-2.4	45.9	-1.4	47.9
W426	-4.3	44.1	-6.6	40.4	-3.9	61.4	-2.9	57.6	-1.9	62.9	-1.3	83.6	-1.7	65.5	0.3	65.4
W449	-5.1	23.6	-2.8	78.9	-0.4	94.3	-2.2	45.4	-1.4	57.3	0.8	92.0	-2.4	60.6	-1.3	62.9
W580	-2.1	49.4	-6.8	21.3	-5.3	41.2	-4.7	40.8	-3.2	40.5	-2.9	46.4	-6.5	36.0	-3.8	48.8
W598	-1.7	58.1	-5.7	47.6	-2.6	63.5	-2.8	47.9	-4.5	62.3	-0.3	83.6	-5.8	38.0	-1.2	77.6
W650	-2.9	47.6	-6.1	50.3	1.5	73.5	-3.1	61.6	-3.8	42.5	1.1	73.3	-2.6	44.6	-1.0	70.6
W671	-4.2	50.2	-3.0	79.9	1.3	84.0	-1.6	69.3	-2.7	67.2	0.6	84.2	-1.2	75.5	-0.9	80.4
W680	-2.6	51.2	-3.7	73.9	-2.4	40.0	-2.3	61.1	-4.6	33.5	-0.6	66.0	-3.8	23.4	-2.6	48.9
W681	-2.3	51.7	-5.5	35.6	-2.8	33.9	-4.5	35.0	-6.1	10.8	0.1	78.8	-3.3	29.3	-3.0	35.9
W729	-2.9	51.6	-0.6	60.8	1.6	83.5	-2.4	77.6	-1.5	47.3	2.6	80.1	-3.1	37.0	1.5	71.1
W731	-1.5	58.8	-4.7	52.2	0.5	71.0	0.8	69.9	-1.4	59.7	1.3	90.2	-1.1	58.4	0.7	71.0
W747	-2.8	50.6	-5.0	57.4	-1.1	66.4	-1.2	60.9	-4.2	53.1	-0.3	83.2	-3.6	49.2	-2.7	80.7
W760	-1.5	60.6	-3.3	34.2	-4.3	36.3	-0.6	63.5	-9.6	4.2	-0.8	64.5	-3.2	31.6	-2.0	48.0
W769	-4.6	37.8	-4.4	35.3	-0.9	58.9	-3.1	44.1	-2.9	45.7	-0.4	66.7	-3.0	51.5	0.1	66.1
W771	-2.8	48.2	-1.8	56.6	-4.8	52.6	-1.1	56.4	-1.1	57.4	3.1	84.1	0.0	66.2	0.8	69.2
W773	-1.9	62.9	-2.7	59.8	-0.2	76.0	-5.4	49.5	-0.8	63.9	2.6	81.3	-1.7	58.7	0.3	65.2
W788	-2.8	54.1	-4.0	73.3	1.5	78.3	-0.2	68.6	-2.2	66.0	1.7	80.0	-1.9	66.4	1.5	73.6
W806	-2.0	55.8	-6.1	9.7	2.0	61.9	-1.9	57.0	-1.7	53.2	1.1	76.7	-1.0	62.7	1.2	68.1
W827	-4.0	61.2	-2.9	56.5	1.5	82.5	-3.1	60.4	-1.1	60.3	2.0	86.8	-3.4	46.5	-2.5	51.0

**Supplementary Table 4:** Mean logit pAUDPC and % maximum dAUDPC values estimated from linear mixed models for the interactions between the Watkins core 300 and wheat controls and *Z. tritici* isolates IPO323, IPO88004 and IPO90012. Super necrosis presence/absence is also given.

Line	IPO323			IPO88004				IPO90012		
	Logit pAUDPC	% max. dAUDPC	SN	Logit pAUDPC	% max. dAUDPC	SN	SN (R only)	Logit pAUDPC	% max. dAUDPC	SN
ArinalrFor	-8.29	49.11	0	-7.85	21.64	0	0	-8.43	29.90	0
Baj	-3.82	64.67	0	-7.30	36.89	0	0	-5.89	88.26	0
Cadenza	-8.05	46.23	0	-4.23	83.14	0	0	-3.38	88.56	0
CDC Landmark	-8.16	62.54	0	-4.21	87.58	1	1	-7.78	58.40	0
CDC Stanley	-	-	-	-6.76	69.02	0	0	-7.30	68.54	0
Chinese Spring	-7.56	33.44	0	-1.40	81.34	0	0	-1.09	58.06	0
Claire	-	-	-	-7.53	30.27	0	0	-2.78	62.55	0
Courtout	-	-	-	-	-	-	-	-2.74	87.62	1
Felder	-	-	-	-4.58	78.89	1	1	-	-	-
Flame	-8.15	30.99	0	-	-	-	-	-	-	-
Jagger	-	-	-	-7.49	86.35	1	1	-7.28	92.69	1
Julius	-	-	-	-7.08	47.90	0	0	-7.71	69.77	0
Kronos	-	-	-	-5.79	81.96	0	0	-5.78	78.82	0
Lancer	-8.07	55.30	0	-6.97	37.69	0	0	-4.30	85.96	0
Longbow	-2.15	60.34	0	-6.26	73.83	0	0	-3.15	82.02	0
Mace	-	-	-	-6.10	88.80	1	1	-0.18	84.93	0
Norin 61	-	-	-	-3.94	92.53	1	1	-3.29	89.58	0
Olaf	-	-	-	-	-	-	-	-8.63	62.35	0
Paragon	-2.40	73.46	0	-6.91	80.12	0	0	-2.76	91.33	0
Robigus	-8.30	41.34	-	-7.35	58.70	0	0	-8.13	64.96	0
SY Mattis	-	-	-	-6.70	70.34	0	0	-8.18	70.97	0
W004	-6.88	44.38	0	-6.16	68.12	0	0	-7.65	39.46	0
W007	-4.14	63.01	0	-2.92	77.99	0	0	-3.01	76.05	0
W008	-5.26	46.83	0	-5.07	76.37	0	0	-2.99	83.17	0
W012	-6.73	56.22	0	-2.62	70.44	0	0	-4.42	63.81	0
W015	-8.10	37.14	0	-4.13	79.67	0	0	-7.73	32.29	0
W023	-8.17	20.70	0	-5.96	59.88	0	0	-7.93	51.79	0
W024	-8.38	27.77	0	-2.92	63.74	0	0	-7.93	42.59	0
W030	-8.30	59.47	0	-1.45	78.58	0	0	-1.04	78.78	0
W032	-6.33	54.61	0	-3.04	74.92	0	0	-5.12	71.31	0
W034	-6.65	34.47	0	-1.00	74.68	0	0	-0.30	83.35	0
W042	-4.64	47.29	0	-7.24	48.88	0	0	-3.51	78.51	0
W044	-8.10	45.88	0	-6.81	75.65	0	0	-7.75	65.57	0

W045	-7.97	41.96	0	-6.74	78.79	0	0	-7.02	61.03	0
W046	-1.99	53.57	0	-5.70	70.45	0	0	-6.49	66.31	0
W053	-3.63	52.40	0	-5.05	72.98	0	0	-4.85	63.54	0
W063	-8.28	47.85	0	-7.82	30.51	0	0	-6.95	90.28	1
W066	-4.63	77.28	0	-6.17	79.40	0	0	-3.81	84.17	0
W067	-7.23	43.42	0	-7.30	59.09	0	0	-5.31	91.17	1
W079	-7.61	22.29	0	-7.81	77.62	0	0	-6.78	55.06	0
W081	-8.10	47.93	0	-7.60	53.31	0	0	-5.59	89.95	0
W082	-7.95	36.81	0	-2.06	87.80	0	0	-5.51	51.77	0
W083	-7.98	48.48	0	-7.02	67.88	0	0	-7.78	42.63	0
W088	-7.90	60.45	0	-7.19	54.12	0	0	-5.11	54.13	0
W094	-8.11	54.61	0	-5.32	74.85	0	0	-2.75	93.18	1
W103	-7.40	29.62	0	-5.72	66.80	0	0	-3.60	93.48	1
W104	-2.41	53.51	0	-6.49	68.89	0	0	-4.81	79.11	0
W106	-7.54	80.74	1	-6.86	51.10	0	0	-2.24	91.33	0
W114	-8.18	19.14	0	-7.01	40.93	0	0	-6.65	30.26	0
W115	-7.27	52.24	0	-4.67	70.44	0	0	-6.03	50.97	0
W117	-7.56	63.99	0	-5.93	72.64	0	0	-2.93	85.83	0
W124	-7.14	49.04	0	-1.46	86.76	0	0	-8.24	14.60	0
W125	-6.06	51.48	0	-7.39	42.47	0	0	-3.68	96.01	1
W126	-8.18	21.72	0	-1.14	83.47	0	0	-0.46	71.21	0
W127	-6.37	38.02	0	-7.04	50.89	0	0	-1.86	66.47	0
W129	-8.35	45.46	0	-8.14	40.79	0	0	-4.10	84.14	0
W130	-7.83	38.11	0	-7.50	29.66	0	0	-3.41	82.01	0
W136	-7.49	65.94	0	-2.18	77.04	0	0	-1.92	71.23	0
W138	-7.00	54.66	0	-6.18	85.49	0	0	-2.31	91.13	1
W139	-5.93	15.59	0	-4.74	70.69	0	0	-5.94	48.48	0
W141	-8.42	21.58	0	-2.56	75.70	0	0	-2.94	90.80	1
W145	-5.17	53.81	0	-7.81	23.29	0	0	-2.92	81.61	0
W149	-3.58	66.71	0	-7.65	38.97	0	0	-3.68	74.28	0
W151	-5.23	50.53	0	-7.04	46.61	0	0	-7.32	44.14	0
W153	-6.33	59.59	0	-7.41	47.91	0	0	-5.86	64.88	0
W155	-6.11	84.05	0	-5.59	72.00	0	0	-2.15	80.66	0
W160	-8.48	28.99	0	-6.58	62.94	0	0	-3.68	45.44	0
W164	-8.13	46.37	0	-7.40	58.37	0	0	-5.28	67.56	0
W166	-8.07	53.46	0	-7.88	59.48	0	0	-5.51	80.98	0
W167	-2.10	45.45	0	-5.53	78.92	0	0	-1.89	86.61	0
W181	-7.78	49.97	0	-7.85	80.76	0	0	-6.30	87.57	0
W186	-7.60	63.60	0	-4.52	82.43	1	0	-1.87	87.95	0
W187	-8.07	36.95	0	-7.90	38.14	0	0	-7.71	44.46	0

W189	-8.11	43.65	0	-7.34	67.49	0	0	-4.87	73.56	0
W199	-4.98	30.27	0	-0.13	82.75	0	0	0.39	81.17	0
W206	-8.25	91.87	1	-7.89	54.59	0	0	-7.43	97.59	1
W209	-8.14	43.44	0	-7.31	37.82	0	0	-6.67	64.37	0
W213	-7.21	83.98	1	-6.15	78.87	0	0	-6.84	98.84	1
W216	-3.96	71.31	0	-7.12	37.92	0	0	-4.59	95.07	1
W218	-3.83	52.57	0	-5.57	59.50	0	0	-4.05	95.53	1
W219	-7.61	41.91	0	-7.15	62.73	0	0	-2.73	78.88	0
W222	-6.26	43.96	0	-5.01	64.15	0	0	-2.52	79.15	0
W223	-2.61	59.67	0	-1.54	71.08	0	0	-1.57	61.94	0
W224	-4.05	52.98	0	-3.85	67.83	0	0	-2.98	80.46	0
W228	-8.01	39.60	0	-4.10	55.94	0	0	-4.58	61.52	0
W229	-8.24	26.88	0	-6.63	73.14	0	0	-5.69	80.67	0
W231	-5.45	89.27	0	-7.89	59.08	0	0	-7.48	69.62	0
W232	-8.26	46.63	0	-3.80	71.30	0	0	-5.33	56.26	0
W233	-7.72	38.89	0	-3.75	80.28	0	0	-2.96	79.32	0
W237	-8.18	68.41	0	-7.19	79.91	0	0	-7.77	84.23	0
W238	-7.04	40.77	0	-7.80	44.09	0	0	-3.70	56.40	0
W239	-8.13	53.51	0	-4.77	72.39	0	0	-3.84	88.32	0
W240	-6.81	59.97	0	-6.65	51.11	0	0	-3.04	89.94	1
W241	-7.39	36.32	0	-1.02	80.54	0	0	-1.41	79.87	0
W242	-7.14	47.44	0	-1.45	79.11	0	0	-1.37	64.62	0
W246	-7.39	35.24	0	-6.78	76.93	0	0	-6.37	60.24	0
W248	-8.32	30.36	0	-5.22	44.48	0	0	-6.60	36.92	0
W254	-8.14	37.37	0	-8.07	57.65	0	0	-7.85	71.28	0
W260	-7.12	13.89	0	-5.53	69.10	0	0	-2.08	76.46	0
W262	-7.58	40.76	0	-3.10	84.19	0	0	-6.56	54.28	0
W264	-7.38	22.83	0	-2.33	85.12	0	0	-1.93	72.65	0
W268	-8.23	29.35	0	-6.98	57.42	0	0	-6.52	48.73	0
W271	-7.41	39.97	0	-5.70	60.13	0	0	-7.86	61.30	0
W273	-8.32	69.14	0	-7.73	54.39	0	0	-3.20	80.91	0
W277	-7.21	40.04	0	-4.65	68.70	0	0	-5.20	70.31	0
W286	-8.35	48.21	0	-6.02	66.33	0	0	-5.52	90.59	0
W290	-6.32	43.34	0	-6.36	44.53	0	0	-5.30	64.56	0
W291	-7.89	42.48	0	-4.61	73.59	0	0	-2.06	85.06	0
W292	-8.11	78.86	0	-4.34	55.67	0	0	-0.30	75.81	0
W293	-7.67	30.29	0	-2.42	83.14	0	0	-7.88	55.37	0
W297	-8.25	45.17	0	-7.47	76.15	0	0	-5.67	97.65	1
W298	-8.23	21.43	0	-1.97	81.03	0	0	-0.74	80.17	0
W299	-7.61	59.94	0	-3.18	67.86	0	0	-3.55	73.74	0

W300	-7.90	51.92	0	-6.21	76.54	0	0	-4.68	54.23	0
W301	-7.15	61.22	0	-4.31	78.74	0	0	-2.58	82.55	0
W302	-7.48	31.97	0	-3.77	71.61	0	0	-2.64	64.01	0
W304	-7.00	60.92	0	-2.93	91.52	0	0	-1.43	85.86	0
W305	-8.03	52.71	0	-3.43	71.54	0	0	-2.22	67.37	0
W308	-8.40	36.06	0	-6.72	71.79	0	0	-7.44	73.42	0
W315	-8.09	21.47	0	-7.83	68.45	0	0	-7.94	41.09	0
W316	-7.15	29.20	0	-6.36	84.17	0	0	-0.97	59.24	0
W317	-7.83	45.27	0	-7.64	43.69	0	0	-5.60	70.35	0
W321	-7.49	54.81	0	-3.13	66.20	0	0	-2.53	92.57	1
W339	-6.69	68.57	0	-7.57	70.05	0	0	-3.95	65.88	0
W346	-7.41	42.35	0	-8.06	65.56	0	0	-7.13	66.22	0
W347	-8.05	71.57	0	-4.79	79.75	0	0	-4.18	68.92	0
W349	-4.33	71.97	0	-7.54	58.71	0	0	-6.67	71.43	0
W351	-7.28	55.72	0	-2.71	87.79	0	0	-1.56	82.13	0
W352	-8.19	75.59	0	-6.85	36.46	0	0	-4.30	64.79	0
W355	-8.11	36.78	0	-6.15	62.79	0	0	-4.52	85.62	0
W356	-3.78	40.84	0	-2.49	71.56	0	0	-0.52	73.99	0
W360	-8.42	45.00	0	-6.14	76.57	0	0	-6.35	55.58	0
W361	-8.41	49.49	0	-7.21	56.96	0	0	-7.28	26.82	0
W363	-4.50	48.05	0	-7.10	50.14	0	0	-6.46	93.83	1
W370	-4.04	55.35	0	-7.45	55.44	0	0	-4.08	78.13	0
W376	-7.94	44.18	0	-5.23	85.14	1	1	-3.10	86.43	0
W379	-3.57	40.77	0	-7.31	26.17	0	0	-4.20	57.99	0
W381	-2.69	44.15	0	-2.50	71.82	0	0	-1.25	55.27	0
W382	-5.07	78.44	1	-6.86	75.16	0	0	-3.13	65.32	0
W387	-8.31	40.11	0	-6.08	74.98	0	0	-5.13	96.40	1
W394	-7.62	26.53	0	-6.47	58.30	0	0	-4.99	76.79	0
W396	-3.71	49.19	0	-7.08	64.43	0	0	-7.33	56.92	0
W397	-8.24	40.55	0	-7.81	24.14	0	0	-6.28	33.91	0
W398	-2.09	54.61	0	-6.01	67.67	0	0	-1.50	77.25	0
W399	-7.43	29.00	0	-2.85	55.45	0	0	-1.83	61.35	0
W400	-2.99	56.99	0	-2.42	65.74	0	0	-1.47	76.99	0
W401	-2.42	52.28	0	-2.55	76.25	0	0	-1.80	82.87	0
W403	-6.69	37.82	0	-6.55	56.09	0	0	-7.48	38.34	0
W404	-8.14	44.62	0	-2.15	81.53	0	0	-1.58	78.97	0
W405	-8.38	24.77	0	-5.55	87.90	0	0	-1.49	64.18	0
W406	-8.41	31.00	0	-1.75	59.72	0	0	-0.65	68.76	0
W407	-7.54	55.98	0	-3.49	65.95	0	0	-4.64	65.70	0
W409	-8.23	38.04	0	-6.32	42.33	0	0	-4.93	50.94	0

W412	-8.14	49.54	0	-7.44	35.44	0	0	-5.80	64.08	0
W413	-8.09	23.41	0	-4.56	67.17	0	0	-3.65	56.03	0
W414	-7.15	40.12	0	-7.76	21.09	0	0	-4.71	29.36	0
W419	-7.60	24.46	0	-5.94	54.27	0	0	-1.93	59.32	0
W420	-8.29	26.08	0	-7.09	68.76	0	0	-5.67	86.72	0
W423	-3.74	52.03	0	-6.87	40.69	0	0	-5.29	59.64	0
W424	-1.33	52.00	0	-5.25	73.96	0	0	-5.44	64.79	0
W426	-7.90	30.17	0	-6.72	29.99	0	0	-1.41	81.90	0
W428	-8.14	55.64	0	-4.21	82.81	0	0	-2.61	79.74	0
W429	-7.27	64.05	0	-0.48	84.02	0	0	-1.68	82.95	0
W430	-8.06	53.20	0	-2.00	56.62	0	0	-0.54	54.97	0
W433	-6.73	34.94	0	-4.01	58.79	0	0	-1.68	65.90	0
W435	-6.95	50.02	0	-2.86	74.72	0	0	-1.76	74.33	0
W440	-8.14	18.53	0	-7.96	51.23	0	0	-5.54	51.38	0
W444	-7.17	42.31	0	-6.09	57.39	0	0	-3.60	75.36	0
W446	-8.17	31.60	0	-5.76	75.69	0	0	-2.38	75.27	0
W448	-8.31	50.35	0	-6.83	74.40	0	0	-5.87	55.24	0
W449	-6.81	25.13	0	-2.03	71.01	0	0	-2.08	68.21	0
W453	-3.41	71.19	0	-4.82	69.24	0	0	-7.13	70.84	0
W456	-6.60	80.49	0	-7.40	68.21	0	0	-5.82	47.77	0
W458	-6.68	20.80	0	-4.80	68.35	0	0	-4.74	92.60	1
W460	-0.98	69.94	0	-7.06	56.08	0	0	-4.86	52.17	0
W463	-8.30	69.72	0	-3.28	72.02	1	0	-2.33	93.25	1
W465	-7.56	45.07	0	-2.68	83.18	0	0	-2.72	95.11	1
W468	-8.09	40.39	0	-4.87	65.99	0	0	-1.10	86.43	0
W470	-8.18	47.35	0	-4.29	76.56	0	0	-2.09	88.43	0
W471	-7.67	44.67	0	-2.39	70.51	0	0	-2.32	65.06	0
W473	-6.95	45.51	0	-3.33	66.13	0	0	-1.06	76.94	0
W474	-5.47	29.60	0	-2.36	81.38	1	0	-1.87	71.01	0
W475	-5.62	33.37	0	-5.09	60.86	0	0	-6.43	47.34	0
W478	-5.73	21.65	0	-2.19	77.67	0	0	-1.26	72.49	0
W483	-7.78	47.11	0	-7.04	46.44	0	0	-4.06	82.55	0
W484	-8.19	34.09	0	-6.05	61.37	0	0	-2.98	74.68	0
W485	-7.88	19.58	0	-6.37	74.16	0	0	-6.59	67.91	0
W486	-8.13	56.08	0	-4.92	78.34	0	0	-3.58	66.44	0
W487	-5.28	86.08	0	-5.82	91.12	0	0	-4.67	91.81	1
W492	-3.07	52.46	0	-7.72	55.23	0	0	-2.84	69.52	0
W493	-7.29	38.30	0	-5.38	74.40	0	0	-6.00	54.19	0
W496	-6.95	49.04	0	-4.32	66.41	0	0	-4.61	93.82	1
W505	-3.68	56.62	0	-4.21	70.62	0	0	-3.53	94.81	0

W507	-6.22	70.85	0	-6.94	74.52	0	0	-5.08	100.27	1
W509	-8.09	28.76	0	-6.81	66.77	0	0	-4.53	59.90	0
W512	-7.92	35.91	0	-3.60	56.70	0	0	-4.48	88.26	1
W513	-6.09	52.02	0	-3.64	61.38	0	0	-4.85	52.31	0
W515	-8.15	38.85	0	-3.93	76.11	1	0	-3.90	75.85	0
W517	-6.03	28.21	0	-6.88	47.60	0	0	-6.18	51.76	0
W520	-8.24	70.98	1	-7.81	50.97	0	0	-6.23	88.09	0
W522	-6.68	29.81	0	-1.82	69.95	0	0	-1.61	63.37	0
W528	-6.64	47.60	0	-3.72	78.37	1	0	-3.71	79.18	0
W530	-2.44	50.64	0	-6.98	58.51	0	0	-3.50	52.60	0
W534	-8.16	33.74	0	-3.23	67.22	0	0	-0.76	76.56	0
W538	-5.34	31.00	0	-3.76	74.06	0	0	-3.35	69.31	0
W541	-3.14	54.32	0	-7.13	56.22	0	0	-6.51	59.47	0
W543	-7.49	68.02	0	-3.11	86.56	0	0	-2.23	83.81	0
W546	-6.42	64.16	1	-7.57	69.13	0	0	-3.96	74.79	0
W547	-7.50	50.32	0	-6.44	72.81	0	0	-5.48	83.47	0
W549	-4.83	43.60	0	-7.91	26.01	0	0	-7.59	47.48	0
W551	-7.15	66.70	0	-6.52	60.88	0	0	-7.43	55.36	0
W552	-7.13	53.14	0	-6.86	58.10	0	0	-1.55	79.65	0
W557	-8.07	43.91	0	-7.16	48.80	0	0	-3.52	63.74	0
W560	-6.90	42.52	0	-6.68	76.14	0	0	-3.64	79.66	0
W561	-6.65	35.38	0	-6.67	61.77	0	0	-2.12	87.10	0
W562	-8.23	23.89	0	-6.84	63.52	0	0	-5.72	46.29	0
W563	-7.22	47.81	0	-4.20	70.55	0	0	-1.59	82.98	0
W565	-7.26	69.10	0	-6.34	78.87	0	0	-6.26	75.10	0
W566	-6.61	36.06	0	-5.81	72.39	0	0	-4.03	62.67	0
W568	-6.31	40.02	0	-3.66	90.37	1	1	-1.69	75.03	0
W571	-5.48	39.80	0	-7.44	53.92	0	0	-6.33	86.93	0
W572	-7.49	49.60	0	-7.65	33.57	0	0	-7.02	38.64	0
W573	-8.24	51.89	0	-4.79	85.73	0	0	-5.64	83.27	0
W574	-6.90	55.45	0	-6.74	67.25	0	0	-3.19	88.37	0
W576	-8.08	39.91	0	-7.14	41.89	0	0	-6.71	88.26	0
W578	-8.16	60.51	0	-7.47	56.35	0	0	-6.83	72.99	0
W579	-8.32	29.80	0	-6.60	67.31	0	0	-6.20	53.33	0
W580	-8.19	60.89	0	-7.79	61.90	0	0	-7.25	82.51	0
W583	-7.30	37.37	0	-2.94	86.09	1	0	-2.13	76.47	0
W587	-7.83	43.58	0	-5.30	76.41	0	0	-7.60	67.82	0
W590	-4.07	57.13	0	-6.49	50.90	0	0	-6.18	82.59	0
W591	-7.90	43.76	0	-4.53	66.95	0	0	-3.69	92.06	0
W594	-8.28	52.42	0	-5.53	51.40	0	0	-4.18	66.15	0

W596	-7.52	38.36	0	-7.78	41.80	0	0	-5.64	47.26	0
W598	-8.26	61.17	0	-7.32	65.32	0	0	-4.92	81.08	0
W604	-8.34	63.52	0	-4.38	64.72	0	0	-2.56	71.34	0
W605	-5.87	64.60	0	-7.69	38.96	0	0	-1.90	71.72	0
W607	-7.85	27.08	0	-6.59	56.92	0	0	-6.99	39.50	0
W611	-8.39	46.09	0	-7.81	62.67	0	0	-8.25	44.35	0
W614	-7.36	57.70	0	-7.80	24.17	0	0	-4.86	37.11	0
W619	-7.28	33.08	0	-7.80	45.29	0	0	-7.79	58.19	0
W622	-8.09	57.84	0	-6.84	71.84	0	0	-7.82	67.29	0
W623	-7.60	27.81	0	-7.43	48.11	0	0	-4.24	49.14	0
W625	-6.87	41.76	0	-4.77	85.19	0	0	-1.70	92.85	0
W627	-8.24	56.81	0	-2.74	69.92	0	0	-1.31	73.87	0
W629	-8.14	48.71	0	-0.77	82.95	0	0	-0.25	79.37	0
W633	-2.26	69.64	0	-5.15	72.35	0	0	-2.93	88.48	0
W637	-7.48	54.57	0	-6.53	67.61	0	0	-5.05	71.65	0
W639	-8.15	28.79	0	-7.79	44.65	0	0	-6.19	55.39	0
W644	-7.67	30.77	0	-7.62	68.54	0	0	-5.97	71.21	0
W646	-8.07	71.40	1	-5.42	75.63	0	0	-4.63	84.12	0
W648	-8.19	31.72	0	-7.13	65.95	0	0	-5.01	82.03	0
W649	-7.74	54.16	0	-6.07	63.78	0	0	-3.88	92.37	0
W650	-7.31	74.91	1	-5.37	68.78	0	0	-2.25	86.13	0
W653	-8.14	100.70	1	-5.21	56.75	0	0	-5.01	83.50	0
W655	-6.78	64.27	1	-6.11	86.09	1	1	-4.55	93.82	0
W657	-6.85	36.65	0	-4.55	80.69	0	0	-6.95	73.18	0
W662	-8.15	37.12	0	-7.17	54.00	0	0	-7.72	57.78	0
W667	-7.04	69.87	0	-6.09	77.42	0	0	-	-	-
W668	-2.29	59.94	0	-4.71	71.03	1	1	-1.16	67.77	0
W670	-7.20	34.89	0	-7.57	29.66	0	0	-5.22	75.66	0
W671	-6.26	90.70	1	-4.65	88.91	1	1	-3.68	87.37	0
W673	-1.78	50.01	0	-4.06	79.16	1	1	-3.65	79.21	0
W676	-8.06	70.14	0	-4.91	61.34	0	0	-2.27	69.17	0
W678	-4.07	49.09	0	-4.73	88.13	0	0	-2.77	87.27	0
W680	-6.97	46.29	0	-5.81	67.42	0	0	-4.38	92.47	1
W681	-8.18	47.96	0	-5.09	61.19	0	0	-5.97	53.70	0
W683	-7.90	44.39	0	-7.20	62.63	0	0	-4.98	69.73	0
W685	-1.54	60.21	0	-3.64	68.50	0	0	-1.78	68.59	0
W690	-7.48	45.88	0	-5.13	60.38	0	0	-2.88	57.80	0
W694	-8.30	16.29	0	-1.29	76.58	0	0	-0.80	80.64	0
W695	-6.95	14.47	0	-7.36	42.80	0	0	-2.22	50.15	0
W697	-8.47	40.07	0	-7.12	51.43	0	0	-2.53	69.02	0

W698	-8.40	24.84	0	-4.50	73.66	0	0	-5.03	52.06	0
W700	-7.34	18.78	0	-5.00	58.42	0	0	-5.43	33.49	0
W704	-8.04	33.85	0	-2.30	78.06	0	0	-2.51	64.96	0
W705	-8.03	46.51	0	-7.00	77.98	0	0	-5.77	79.96	0
W707	-8.40	47.02	0	-1.20	67.31	0	0	-1.25	92.27	0
W711	-7.50	30.36	0	-2.31	67.11	0	0	-1.50	45.51	0
W719	-7.46	21.60	0	-7.26	57.08	0	0	-2.62	65.96	0
W721	-7.78	53.77	0	-3.43	86.91	1	1	-3.29	56.40	0
W722	-2.38	69.11	0	-6.81	65.94	0	0	-7.96	76.32	0
W724	-7.10	45.62	0	-6.78	53.73	0	0	-6.57	45.33	0
W726	-7.98	31.37	0	-7.14	77.22	0	0	-4.14	59.52	0
W727	-8.14	55.57	0	-1.94	80.10	0	0	-1.30	74.13	0
W728	-7.29	65.63	0	-4.38	79.87	0	0	-1.58	74.27	0
W729	-0.52	61.14	0	-3.78	82.40	1	0	-0.11	80.39	0
W731	-7.96	40.86	0	-1.23	80.33	0	0	0.52	66.44	0
W732	-2.29	57.11	0	-7.60	55.71	0	0	-2.46	69.21	0
W737	-8.17	61.23	0	-5.42	84.22	1	1	-7.96	25.13	0
W742	-2.99	55.05	0	-7.08	78.65	0	0	-5.11	87.73	0
W743	-8.28	27.61	0	-6.88	43.29	0	0	-7.13	53.25	0
W746	-8.33	58.36	0	-7.41	63.22	0	0	-7.87	69.74	0
W747	-8.17	75.32	0	-6.05	83.13	0	0	-2.70	73.63	0
W749	-7.51	96.98	1	-4.82	87.15	1	1	-7.07	76.72	0
W750	-8.12	50.57	0	-7.94	37.18	0	0	-5.89	73.52	0
W752	-7.70	87.64	1	-5.61	62.60	0	0	-3.38	69.86	0
W759	-8.16	65.78	0	-6.91	54.85	0	0	-7.19	95.44	1
W760	-5.62	56.27	0	-7.78	25.16	0	0	-6.99	44.67	0
W769	-8.08	34.08	0	-3.75	63.72	0	0	-2.43	73.98	0
W770	-8.40	35.67	0	-6.47	42.47	0	0	-4.24	95.95	1
W771	-0.99	83.09	0	-6.88	46.89	0	0	-2.09	92.97	0
W773	-3.42	50.00	0	-7.35	66.39	0	0	-3.13	60.09	0
W774	-8.33	54.87	0	-3.40	85.12	0	0	-2.95	96.32	0
W775	-8.01	57.40	0	-7.75	73.54	0	0	-3.05	76.74	0
W777	-3.80	83.80	0	-7.84	46.01	0	0	-4.85	92.26	1
W784	-7.71	38.17	0	-2.22	94.71	1	0	-3.68	67.39	0
W788	-7.43	37.70	0	-6.28	50.35	0	0	-4.54	78.04	0
W789	-4.27	61.33	0	-7.59	82.48	1	1	-3.67	75.43	0
W794	-1.91	68.30	0	-4.78	62.28	0	0	-1.69	67.56	0
W802	-2.71	54.55	0	-7.18	56.02	0	0	-3.02	72.00	0
W803	-7.99	36.94	0	-7.24	58.07	0	0	-1.43	72.80	0
W804	-3.35	80.20	0	-5.43	80.09	0	0	-2.16	90.62	0

<b>W806</b>	-6.77	46.46	0	-2.39	79.94	0	0	-0.79	81.91	0
<b>W811</b>	-7.32	39.88	0	-6.92	52.41	0	0	-0.51	84.80	0
<b>W814</b>	-6.07	38.60	0	-1.12	83.06	0	0	-3.49	65.06	0
<b>W816</b>	-8.24	66.50	0	-4.26	81.82	0	0	-2.69	79.53	0
<b>W823</b>	-7.60	46.55	0	-5.09	88.07	1	1	-3.32	78.85	0
<b>W824</b>	-8.09	30.08	0	-7.15	77.39	0	0	-6.15	79.46	0
<b>W827</b>	-8.13	62.12	0	-3.52	95.12	1	1	-2.52	85.10	0
<b>W903</b>	-7.81	36.34	0	-4.24	67.89	0	0	-1.65	83.99	0
<b>Weebill</b>	-	-	-	-5.52	90.62	0	0	-3.76	88.46	1

**Supplementary Table 5:** Haplotype groups assigned to each line in the Watkins core 300 based on SNPs within the *Stb6* and *Stb15* loci.

Line	WATDE	Stb6 Cluster	Stb15 Cluster	Stb15 Refined Cluster
ArinaLrFor	ArinaLrFor	1	1	Arina-Robigus
Cadenza	cadenza	2	2	Chinese Spring
CDC Landmark	landmark	1	2	Chinese Spring
CDC Stanley	stanley	1	2	Chinese Spring
Chinese Spring	Chinese_Spring	1	2	Chinese Spring
Claire	claire	2	10	Arina-Robigus
Fielder	fielder	1	2	Chinese Spring
Flame	Flame	1	2	Chinese Spring
Jagger	Jagger	1	2	Chinese Spring
Julius	Julius	1	3	Arina-Robigus
Lancer	lancer	3	2	Chinese Spring
Longbow	Longbow	4	3	Arina-Robigus
Mace	mace	1	2	Chinese Spring
Norin 61	Norin	1	2	Chinese Spring
Paragon	paragon	4	2	Chinese Spring
Robigus	robigus	1	3	Arina-Robigus
SY Mattis	SYMattis	1	2	Chinese Spring
W004	WATDE0001	1	2	Chinese Spring
W007	WATDE0002	5	2	Chinese Spring
W008	WATDE0126	2	2	Chinese Spring
W012	WATDE0133	1	2	Chinese Spring
W015	WATDE0138	2	2	Chinese Spring
W023	WATDE0003	2	2	Chinese Spring
W024	WATDE0149	1	2	Chinese Spring
W030	WATDE0156	1	2	Chinese Spring
W032	WATDE0004	1	2	Chinese Spring
W034	WATDE0005	1	2	Chinese Spring
W042	WATDE0007	3	2	Chinese Spring
W044	WATDE0008	2	2	Chinese Spring
W045	WATDE0009	2	4	Chinese Spring
W046	WATDE0171	1	2	Chinese Spring
W053	WATDE0180	2	2	Chinese Spring

W063	WATDE0192	2	3	Arina-Robigus
W066	WATDE0196	5	2	Chinese Spring
W067	WATDE0198	1	2	Chinese Spring
W079	WATDE0010	1	2	Chinese Spring
W081	WATDE0011	1	3	Arina-Robigus
W082	WATDE0215	1	2	Chinese Spring
W083	WATDE0216	1	2	Chinese Spring
W088	WATDE0222	1	2	Chinese Spring
W094	WATDE0228	1	2	Chinese Spring
W103	WATDE0013	2	2	Chinese Spring
W104	WATDE0238	3	2	Chinese Spring
W106	WATDE0241	1	2	Chinese Spring
W114	WATDE0249	1	3	Arina-Robigus
W115	WATDE0250	2	2	Chinese Spring
W117	WATDE0253	1	2	Chinese Spring
W124	WATDE0262	1	2	Chinese Spring
W125	WATDE0263	1	3	Arina-Robigus
W126	WATDE0015	1	2	Chinese Spring
W127	WATDE0016	1	3	Arina-Robigus
W129	WATDE0266	1	2	Chinese Spring
W130	WATDE0268	2	2	Chinese Spring
W136	WATDE0276	1	2	Chinese Spring
W138	WATDE0278	1	2	Chinese Spring
W139	WATDE0017	1	2	Chinese Spring
W141	WATDE0018	2	2	Chinese Spring
W145	WATDE0019	5	3	Arina-Robigus
W149	WATDE0020	3	3	Arina-Robigus
W151	WATDE0290	3	3	Arina-Robigus
W153	WATDE0292	1	2	Chinese Spring
W155	WATDE0294	6	2	Chinese Spring
W160	WATDE0021	6	2	Chinese Spring
W164	WATDE0305	2	2	Chinese Spring
W166	WATDE0308	1	2	Chinese Spring
W167	WATDE0310	4	2	Chinese Spring
W181	WATDE0022	1	3	Arina-Robigus
W186	WATDE0335	1	2	Chinese Spring

W187	WATDE0336	2	2	Chinese Spring
W189	WATDE0339	1	2	Chinese Spring
W199	WATDE0023	1	2	Chinese Spring
W206	WATDE0359	1	3	Arina-Robigus
W209	WATDE0024	1	3	Arina-Robigus
W213	WATDE0369	5	2	Chinese Spring
W216	WATDE0025	7	3	Arina-Robigus
W218	WATDE0026	7	2	Chinese Spring
W219	WATDE0027	2	2	Chinese Spring
W222	WATDE0375	2	2	Chinese Spring
W223	WATDE0028	5	2	Chinese Spring
W224	WATDE0029	5	2	Chinese Spring
W228	WATDE0381	2	2	Chinese Spring
W229	WATDE0382	1	2	Chinese Spring
W231	WATDE0030	3	3	Arina-Robigus
W232	WATDE0385	1	2	Chinese Spring
W233	WATDE0386	1	2	Chinese Spring
W237	WATDE0392	1	2	Chinese Spring
W238	WATDE0031	3	5	Watkins 1
W239	WATDE0032	1	2	Chinese Spring
W240	WATDE0394	1	3	Arina-Robigus
W241	WATDE0396	1	2	Chinese Spring
W242	WATDE0397	1	2	Chinese Spring
W246	WATDE0033	1	2	Chinese Spring
W248	WATDE0405	1	2	Chinese Spring
W254	WATDE0034	1	2	Chinese Spring
W260	WATDE0420	2	2	Chinese Spring
W262	WATDE0422	1	2	Chinese Spring
W264	WATDE0035	1	2	Chinese Spring
W268	WATDE0427	2	2	Chinese Spring
W271	WATDE0430	6	8	Watkins 2
W273	WATDE0036	1	2	Chinese Spring
W277	WATDE0435	1	9	Watkins 2
W286	WATDE0445	1	2	Chinese Spring
W290	WATDE0450	1	10	Arina-Robigus
W291	WATDE0037	1	2	Chinese Spring

W292	WATDE0038	1	2	Chinese Spring
W293	WATDE0451	1	2	Chinese Spring
W297	WATDE0455	1	2	Chinese Spring
W298	WATDE0456	1	2	Chinese Spring
W299	WATDE0039	1	6	NA
W300	WATDE0040	2	2	Chinese Spring
W301	WATDE0457	1	2	Chinese Spring
W302	WATDE0459	1	2	Chinese Spring
W304	WATDE0461	1	2	Chinese Spring
W305	WATDE0041	1	2	Chinese Spring
W308	WATDE0042	3	2	Chinese Spring
W315	WATDE0476	1	2	Chinese Spring
W316	WATDE0477	1	2	Chinese Spring
W317	WATDE0479	2	3	Arina-Robigus
W321	WATDE0486	2	2	Chinese Spring
W339	WATDE0509	2	9	Watkins 2
W346	WATDE0518	1	2	Chinese Spring
W347	WATDE0519	1	2	Chinese Spring
W349	WATDE0046	5	3	Arina-Robigus
W351	WATDE0521	1	2	Chinese Spring
W352	WATDE0047	1	2	Chinese Spring
W355	WATDE0048	2	2	Chinese Spring
W356	WATDE0526	1	2	Chinese Spring
W360	WATDE0049	1	2	Chinese Spring
W361	WATDE0532	1	2	Chinese Spring
W363	WATDE0534	5	3	Arina-Robigus
W370	WATDE0542	7	2	Chinese Spring
W376	WATDE0550	1	2	Chinese Spring
W379	WATDE0555	7	3	Arina-Robigus
W381	WATDE0557	7	2	Chinese Spring
W382	WATDE0558	2	2	Chinese Spring
W387	WATDE0050	1	2	Chinese Spring
W394	WATDE0571	1	2	Chinese Spring
W396	WATDE0051	8	5	Watkins 1
W397	WATDE0052	1	2	Chinese Spring
W398	WATDE0053	7	2	Chinese Spring

W399	WATDE0574	1	2	Chinese Spring
W400	WATDE0576	1	2	Chinese Spring
W401	WATDE0577	7	2	Chinese Spring
W403	WATDE0579	1	2	Chinese Spring
W404	WATDE0581	1	2	Chinese Spring
W405	WATDE0582	2	2	Chinese Spring
W406	WATDE0054	1	2	Chinese Spring
W407	WATDE0585	1	2	Chinese Spring
W409	WATDE0588	1	2	Chinese Spring
W412	WATDE0592	1	2	Chinese Spring
W413	WATDE0594	1	2	Chinese Spring
W414	WATDE0596	1	2	Chinese Spring
W419	WATDE0601	1	2	Chinese Spring
W420	WATDE0055	1	2	Chinese Spring
W423	WATDE0604	7	3	Arina-Robigus
W424	WATDE0606	1	2	Chinese Spring
W426	WATDE0609	1	3	Arina-Robigus
W428	WATDE0611	1	8	Watkins 2
W429	WATDE0612	1	2	Chinese Spring
W430	WATDE0613	1	2	Chinese Spring
W433	WATDE0056	1	7	Chinese Spring
W435	WATDE0617	1	2	Chinese Spring
W440	WATDE0057	1	3	Arina-Robigus
W444	WATDE0058	1	2	Chinese Spring
W446	WATDE0631	1	2	Chinese Spring
W448	WATDE0634	1	2	Chinese Spring
W449	WATDE0635	1	2	Chinese Spring
W453	WATDE0639	10	2	Chinese Spring
W456	WATDE0643	5	2	Chinese Spring
W458	WATDE0646	3	2	Chinese Spring
W460	WATDE0060	7	8	Arina-Robigus
W463	WATDE0651	1	2	Chinese Spring
W465	WATDE0653	3	2	Chinese Spring
W468	WATDE0061	3	2	Chinese Spring
W470	WATDE0659	2	2	Chinese Spring
W471	WATDE0062	3	2	Chinese Spring

W473	WATDE0661	2	2	Chinese Spring
W474	WATDE0063	1	2	Chinese Spring
W475	WATDE0064	3	2	Chinese Spring
W478	WATDE0664	1	2	Chinese Spring
W483	WATDE0066	1	3	Arina-Robigus
W484	WATDE0668	1	2	Chinese Spring
W485	WATDE0669	1	2	Chinese Spring
W486	WATDE0670	1	5	Watkins 1
W487	WATDE0671	7	5	Watkins 1
W492	WATDE0678	7	2	Chinese Spring
W493	WATDE0679	1	2	Chinese Spring
W496	WATDE0067	2	2	Chinese Spring
W505	WATDE0694	1	2	Chinese Spring
W507	WATDE0068	5	2	Chinese Spring
W509	WATDE0699	2	2	Chinese Spring
W512	WATDE0702	1	2	Chinese Spring
W513	WATDE0703	1	2	Chinese Spring
W515	WATDE0705	2	2	Chinese Spring
W520	WATDE0712	1	2	Chinese Spring
W522	WATDE0714	1	2	Chinese Spring
W528	WATDE0725	1	2	Chinese Spring
W530	WATDE0727	8	2	Chinese Spring
W534	WATDE0732	1	2	Chinese Spring
W538	WATDE0737	1	2	Chinese Spring
W541	WATDE0740	5	2	Chinese Spring
W543	WATDE0743	1	2	Chinese Spring
W546	WATDE0069	1	5	Watkins 1
W547	WATDE0747	6	2	Chinese Spring
W549	WATDE0749	7	3	Arina-Robigus
W551	WATDE0070	5	2	Chinese Spring
W552	WATDE0751	1	2	Chinese Spring
W557	WATDE0758	1	3	Arina-Robigus
W560	WATDE0071	1	2	Chinese Spring
W561	WATDE0761	1	3	Arina-Robigus
W562	WATDE0072	1	2	Chinese Spring
W563	WATDE0762	1	2	Chinese Spring

W565	WATDE0765	2	2	Chinese Spring
W566	WATDE0073	2	2	Chinese Spring
W568	WATDE0074	3	2	Chinese Spring
W571	WATDE0770	1	2	Chinese Spring
W572	WATDE0771	2	2	Chinese Spring
W573	WATDE0773	1	2	Chinese Spring
W574	WATDE0774	1	2	Chinese Spring
W576	WATDE0776	3	2	Chinese Spring
W578	WATDE0779	1	2	Chinese Spring
W579	WATDE0075	1	2	Chinese Spring
W580	WATDE0076	1	2	Chinese Spring
W583	WATDE0782	1	2	Chinese Spring
W587	WATDE0788	2	2	Chinese Spring
W590	WATDE0791	3	2	Chinese Spring
W591	WATDE0077	6	2	Chinese Spring
W594	WATDE0795	2	2	Chinese Spring
W596	WATDE0798	1	3	Arina-Robigus
W598	WATDE0801	1	2	Chinese Spring
W604	WATDE0808	1	2	Chinese Spring
W605	WATDE0078	3	2	Chinese Spring
W607	WATDE0811	2	2	Chinese Spring
W611	WATDE0816	2	3	Arina-Robigus
W614	WATDE0819	1	3	Arina-Robigus
W619	WATDE0827	2	3	Arina-Robigus
W622	WATDE0831	1	3	Arina-Robigus
W623	WATDE0833	1	3	Arina-Robigus
W625	WATDE0835	2	2	Chinese Spring
W627	WATDE0080	1	2	Chinese Spring
W629	WATDE0081	1	2	Chinese Spring
W633	WATDE0843	7	2	Chinese Spring
W637	WATDE0082	1	2	Chinese Spring
W639	WATDE0083	1	2	Chinese Spring
W644	WATDE0857	1	3	Arina-Robigus
W646	WATDE0861	1	2	Chinese Spring
W648	WATDE0863	1	3	Arina-Robigus
W649	WATDE0864	1	2	Chinese Spring

W650	WATDE0865	1	2	Chinese Spring
W653	WATDE0868	1	2	Chinese Spring
W655	WATDE0871	1	2	Chinese Spring
W657	WATDE0873	1	2	Chinese Spring
W662	WATDE0086	1	3	Arina-Robigus
W667	WATDE0882	1	2	Chinese Spring
W668	WATDE0883	1	2	Chinese Spring
W670	WATDE0087	1	3	Arina-Robigus
W671	WATDE0088	8	5	Watkins 1
W673	WATDE0888	1	2	Chinese Spring
W676	WATDE0892	1	2	Chinese Spring
W678	WATDE0895	1	2	Chinese Spring
W680	WATDE0089	1	2	Chinese Spring
W681	WATDE0898	1	2	Chinese Spring
W683	WATDE0090	1	2	Chinese Spring
W685	WATDE0091	9	2	Chinese Spring
W690	WATDE0092	1	2	Chinese Spring
W694	WATDE0093	1	2	Chinese Spring
W695	WATDE0909	3	3	Arina-Robigus
W697	WATDE0911	1	3	Arina-Robigus
W698	WATDE0094	1	2	Chinese Spring
W700	WATDE0095	6	2	Chinese Spring
W704	WATDE0096	1	2	Chinese Spring
W705	WATDE0097	1	2	Chinese Spring
W707	WATDE0098	1	2	Chinese Spring
W711	WATDE0919	1	2	Chinese Spring
W719	WATDE0929	1	2	Chinese Spring
W721	WATDE0932	1	2	Chinese Spring
W722	WATDE0099	3	2	Chinese Spring
W724	WATDE0934	1	3	Arina-Robigus
W726	WATDE0937	1	2	Chinese Spring
W727	WATDE0938	1	2	Chinese Spring
W728	WATDE0939	1	2	Chinese Spring
W729	WATDE0100	1	2	Chinese Spring
W731	WATDE0101	1	2	Chinese Spring
W732	WATDE0102	4	3	Arina-Robigus

W737	WATDE0950	1	2	Chinese Spring
W742	WATDE0104	7	2	Chinese Spring
W743	WATDE0954	1	5	Watkins 1
W746	WATDE0105	6	2	Chinese Spring
W747	WATDE0106	1	9	Watkins 2
W749	WATDE0107	1	2	Chinese Spring
W750	WATDE0108	1	3	Arina-Robigus
W752	WATDE0963	1	9	Watkins 2
W759	WATDE0971	1	2	Chinese Spring
W760	WATDE0973	8	9	Watkins 2
W769	WATDE0984	1	2	Chinese Spring
W770	WATDE0986	1	2	Chinese Spring
W771	WATDE0110	4	3	Arina-Robigus
W773	WATDE0989	1	2	Chinese Spring
W774	WATDE0991	1	2	Chinese Spring
W775	WATDE0993	1	2	Chinese Spring
W777	WATDE0111	4	3	Arina-Robigus
W784	WATDE0112	2	2	Chinese Spring
W788	WATDE0113	1	2	Chinese Spring
W789	WATDE0114	5	2	Chinese Spring
W794	WATDE1012	5	2	Chinese Spring
W802	WATDE1025	4	2	Chinese Spring
W803	WATDE1026	1	3	Arina-Robigus
W804	WATDE1027	7	2	Chinese Spring
W806	WATDE1030	1	2	Chinese Spring
W811	WATDE0115	1	3	Arina-Robigus
W814	WATDE0116	1	2	Chinese Spring
W816	WATDE0117	1	2	Chinese Spring
W823	WATDE1051	1	2	Chinese Spring
W824	WATDE1052	1	2	Chinese Spring
W827	WATDE0118	1	2	Chinese Spring
W903	WATDE1060	1	2	Chinese Spring

**Supplementary Script 1:** R code for transforming and fitting linear mixed models to STB phenotype data. Exported with *knitr*.

```
### Set up
# generate log file for checking output
logfile <- file("/path/STB_stats.log")
sink(logfile, append=TRUE)
sink(logfile, append=TRUE, type="message")

# read in file with raw phenotype data (scores on 0-100% cover scale over
several scoring days)
# column names for each scoring date eg 17 dpi must be 'p17, d17'.
dat <- read.csv("/path/STBdata.csv", head=T, na.strings = c("", "-"), str
ingsAsFactors = F);

### Function to calculate AUDPC
# 'insubset' gives the option to calculate the AUDPC differently for e.g.
different isolates
audpc <- function(df, day1, day2, day3, day4, day5,
insubset, ptype="p") {
  (day2-day1)*(df[df$Isolate %in% insubset, paste0(ptype,day1)] +
df[df$Isolate %in% insubset, paste0(ptype,day2)])/2 +
  (day3-day2)*(df[df$Isolate %in% insubset, paste0(ptype,day2)] +
df[df$Isolate %in% insubset, paste0(ptype,day3)])/2 +
  (day4-day3)*(df[df$Isolate %in% insubset, paste0(ptype,day3)] +
df[df$Isolate %in% insubset, paste0(ptype,day4)])/2 +
  (day5-day4)*(df[df$Isolate %in% insubset, paste0(ptype,day4)] +
df[df$Isolate %in% insubset, paste0(ptype,day5)])/2
}

# AUDPC for damage
dat[dat$Isolate %in% c("IPO323", "IPO88004", "IPO90012"), "dAUDPC"] <-
audpc(df=dat, 17,21,24,28,31, insubset = c("IPO323", "IPO88004", "IPO90
012"), ptype="d")
# AUDPC for pycnidia
dat[dat$Isolate %in% c("IPO323", "IPO88004", "IPO90012"), "dAUDPC"] <-
audpc(df=dat, 17,21,24,28,31, insubset = c("IPO323", "IPO88004", "IPO90
012"), ptype="p")

### Data transformation (depends on data distributions and model fits in
preliminary analyses)
# calculate minimum and maximum scores for the experiment
min_score = (4*(0+1)/2)/4
max_score = 100*(31-17)

# adjusted logit transformation for pycnidia
dat$lgt_pAUDPC <- log((dat$pAUDPC + min_score) /
((max_score + min_score) - dat$pAUDPC))

# percentage of the maximum possible dAUDPC for damage
dat$pmax_dAUDPC <- (dat$dAUDPC/max_score)*100

### Formatting
# format the data classes (factor or numeric)
dat[,1:8]<-lapply(dat[,1:8], factor);
dat[,9:ncol(dat)] <- sapply((sapply(dat[,9:ncol(dat)], as.character)), as
.numeric);

# filter out missing values
dat <- dat[!(is.na(dat$dAUDPC) & is.na(dat$pAUDPC)), ];

### Running linear mixed models with lmer
# if lmerTest is not already installed, install it and load the library
if(!require(lmerTest)){install.packages(lmerTest)}; library(lmerTest);
```

```

# generate the linear mixed model for pAUDPC
modp <- lmer(lgt_pAUDPC ~ Isolate*Line + Scorer + (1| Isolate:Batch) + (1
|Isolate:Batch:Rep) +
          (1|Isolate:Batch:Rep:Box), data=dat);
anova(modp);
summary(modp);

# generate the linear mixed model for dAUDPC
modd <- lmer(dAUDPC ~ Isolate*Line + Scorer + (1| Isolate:Batch) + (1|Iso
late:Batch:Rep) +
          (1|Isolate:Batch:Rep:Box) + (1|Isolate:Batch:Rep:Box:Tray)
, data=dat);
anova(modd);
summary(modd);

### Generate QQ-plots and histograms of residuals to check model fit
res.level <- resid(modp,scaled=T)
fit.fix <- predict(modp, re.form=~0)

jpeg("/path/pycnidia_residuals.jpg")
par(mfrow=c(2,2))
qqnorm(res.level)
plot(res.level~fit.fix, main="Fitted-Value Plot")
hist(res.level, main = "Histogram of Residuals")
mtext("lgt_pAUDPC", side = 3, line = -1, outer = TRUE)
dev.off()

res.level <- resid(modd,scaled=T)
fit.fix <- predict(modd, re.form=~0)

jpeg("/path/damage_residuals.jpg")
par(mfrow=c(2,2))
qqnorm(res.level)
plot(res.level~fit.fix, main="Fitted-Value Plot")
hist(res.level, main = "Histogram of Residuals")
mtext("lgt_dAUDPC", side = 3, line = -1, outer = TRUE)
dev.off()

### Calculate estimated means
# if emmeans is not already installed, install it and load the library
if(!require(emmeans)){install.packages(emmeans)}; library(emmeans);
# calculate estimated means for each combination of line and isolate for
both damage and pycnidia
emm.modp <- emmeans::emmeans(modp, specs="Isolate", by="Line");
est.modp <- as.data.frame(emm.modp);
emm.modd <- emmeans::emmeans(modd, specs="Isolate", by="Line");
ests.modd <- as.data.frame(emm.modd)

# format the dataframes and combine them to produce one .csv file with al
l estimated means
trimp <- est.modp[,1:3]
colnames(trimp)[3] <- "emmean_lgt_pAUDPC"
trimd <- ests.modd[,1:3]
colnames(trimd)[3] <- "emmean_dAUDPC"
means <- merge(trimp, trimd)
write.csv(means, "/path/estimated_means.csv")

### Finish writing to log file
sink()
sink(type="message")

```

**Supplementary Script 2:** Python programme for generating SNP distance matrices from regions extracted from VCF files.

```
1. import re
2.
3. gff_file = "chr6A_part1.gff"
4. vcf= "6A_peak.vcf"
5. outfile= open("TraesCS6A02G078700_distmatrix.tsv", "w")
6.
7. def getDistMatrix(acclist):
8.     """Generates distance matrix of appropriate size (based on
9.     no. samples in VCF)
10.     need as many lists in distmatrix as there are accessions and
11.     as many zeros in each list as there are accessions"""
12.
13.     noAccs = len(acclist)
14.
15.     distmatrix = [['NA' for x in range(noAccs)] for y in
16.                   range(noAccs)]
17.
18.     return distmatrix
19.
20. def addToDistMatrix(accl1, acc2, distance, acclist,
21.                    distmatrix):
22.     """Enters distance into correct position of distance
23.     matrix
24.     based on position of accs in acclist"""
25.
26.     # get indices of accl1 and acc2
27.     accl1 = acclist.index(accl1)
28.     acc2i = acclist.index(acc2)
29.     distmatrix[acc2i][accl1] = distance
30.
31.     return distmatrix
32.
33. def getAcc2(accl1, acclist):
34.     for acc in acclist:
35.         if acc != accl1:
36.             acc2index = acclist.index(acc)
37.
38.     done
39.
40.     acc2 = acc
41.
42.     return acc2
43.
44. def getAccList(accdict):
45.     for item in accdict.items():
46.         acclist.append(item[0])
```

```

37.
38.         return acclist
39.
40.     def calculateDistance(acc1, acc2, acclist, accdict):
41.         """Matches keys of vardict then does a string
comparison
42.         to assess distance between accessions"""
43.
44.         subdict1 = accdict.get(acc1)
45.         subdict2 = accdict.get(acc2)
46.
47.         distance = 0
48.
49.         for key in subdict1.keys():
50.             allele1 = subdict1.get(key)
51.             allele2 = subdict2.get(key)
52.
53.             split1=re.split('[/|]', allele1)
54.             split2=re.split('[/|]', allele2)
55.
56.             foundEqual=False
57.             for s1 in split1:
58.                 for s2 in split2:
59.                     if s1 == s2 or s1 in ['.', ','] or s2
in ['.', ',']:
60.                         foundEqual=True
61.                 if not foundEqual:
62.                     distance += 1
63.         return distance
64.
65.     def getAccDict(variation, accdict):
66.
67.         """Creates a dictionary with accession as they key,
68.         values are a dictionary with chrm, position tuple as
key
69.         and the variant as the value."""
70.         for acc in list(variation[4].keys()):
71.             vardict = {}
72.             if acc in accdict:
73.                 vardict= accdict[acc]
74.
75.             vardict[(variation[0], variation[1])] =
variation[4][acc]
76.             accdict[acc]= vardict

```

```

77.
78.         return accdict
79.
80.     def isexon(genedict, position):
81.         isinexon = False
82.         for gene in genedict:
83.             exonset = genedict[gene]
84.             for interval in exonset:
85.                 if position >= interval[0] and position <=
interval[1]:
86.                     isinexon = True
87.                     break
88.             if isinexon:
89.                 break
90.
91.         return isinexon
92.
93.     def getGenedict(gff_file, seqname):
94.         """Create dictionary of gene intervals"""
95.         genedict = {}
96.
97.         with open(gff_file) as gff:
98.             for line in gff:
99.                 if not(line.startswith("#") ): #make sure
this is not a comment line
100.                    splitLine = line.split("\t", -1) #
split line and store columns as list
101.                    start = int(splitLine[3]) # take the
fourth column and convert to a number
102.                    end = int(splitLine[4])      # take the
fifth column and convert to a number
103.                    # now, check if the chromosome is
correct and that the exon is within our interval. Also check that
this is an exon
104.                    if splitLine[0] == seqname and
splitLine[2]=="exon" and start >= 48563464 and end <= 48567367:
105.                        #print(splitLine)
106.                        gene =
splitLine[8].split("Parent=") [1].split(";") [0]
107.                        gene = gene.rstrip() # rstrip
removes potential newline characters.
108.                        interval = (start, end)
109.
110.                    if not gene in genedict:

```

```

111.             exonset = {interval}
112.             genedict[gene] = exonset
113.         else:
114.
115.             genedict[gene].add(interval)
116.
117.     return genedict
118.
119. def convertAlleleToBase(genotypes, refAllele, altAllele):
120.     """Convert X/X code for ref/alt allele to the base.
121.     Code = index of altAllele +1 (0 = refAllele)
122.     Alleles in altAllele comma separated eg GGTC A,GGTCG"""
123.     splitAlt = altAllele.split(",")
124.     for gt_key in genotypes.keys():
125.         gt = genotypes[gt_key]
126.         for i in re.split("[/|]", gt):
127.             if i == '0':
128.                 gt = gt.replace(i, refAllele)
129.             elif i not in ['1', '2', '3', '4']:
130.                 # account for weird gt values?
131.                 pass
132.             else:
133.                 gt = gt.replace(i, altAllele[int(i)-
134.                                     1])
135.         genotypes[gt_key] = gt
136.
137.     return genotypes
138.
139. def recordSampleNames(line):
140.     splitLine = line.split("\t")
141.     samples = []
142.     for i in range(9, len(splitLine)):
143.         samples.append(splitLine[i].strip())
144.     return samples
145.
146. def getGT_index(format_column):
147.     """check the format colum, at which position the GT
148.     field is. Return the index"""
149.     splitLine = format_column.split(":")
150.     for i in range(0, len(splitLine)):
151.         if splitLine[i] == "GT":
152.             return i
153.
154. def getGenotypes(splitLine, gt_index, sampleNames):

```

```

152.         genotypes = []
153.         for i in range(9, len(splitLine)):
154.             sample_field = splitLine[i]
155.             split_col = sample_field.split(":")
156.             genotypes.append(split_col[gt_index])
157.
158.         genotype_dict = {}
159.         for i in range(0, len(sampleNames)):
160.             genotype_dict[sampleNames[i]] = genotypes[i]
161.         return genotype_dict
162.
163.     def getvars(line, sampleNames, genedict):
164.         """Extract required information from each position
165.         (line)"""
166.         splitLine = line.split("\t", -1)
167.         chromosome = splitLine[0]
168.         position = int(splitLine[1])
169.         refAllele = splitLine[3]
170.         altAllele = splitLine[4]
171.         gt_index = getGT_index(splitLine[8])
172.
173.         if isexon(genedict, position):
174.             genotypes = getGenotypes(splitLine, gt_index,
175.             sampleNames)
176.             convertAlleleToBase(genotypes, refAllele,
177.             altAllele)
178.
179.             return(chromosome, position, refAllele,
180.             altAllele, genotypes)
181.
182.     with open(vcf) as infile:
183.         sampleNames = []
184.         accdict = {}
185.         acclist = []
186.         seqname = "chr6A_part1"
187.         genedict = getGenedict(gff_file, seqname)
188.         for line in infile:
189.             if line.startswith('#CHROM'):
190.                 sampleNames = recordSampleNames(line)
191.             elif not line.startswith('#'):
192.                 variation = getvars(line, sampleNames,
193.                 genedict)
194.                 if variation:

```

```

190.                                     accdict = getAccDict(variation,
      accdict)
191.
192.         acclist = getAccList(accdict)
193.         distmatrix = getDistMatrix(acclist)
194.         with outfile as record:
195.             record.write("Accessions" + "\t" +
      '\t'.join([str(x) for x in acclist]) + "\n")
196.             for acc1 in acclist:
197.                 print("Acc1 " + acc1)
198.                 acc1i = acclist.index(acc1)
199.                 record.write(acc1)
200.                 for acc2 in acclist:
201.                     distance = calculateDistance(acc1,
      acc2, acclist, accdict)
202.                     record.write("\t" + str(distance))
203.                     addToDistMatrix(acc1, acc2, distance,
      acclist, distmatrix)
204.
205.
206.             record.write("\n")

```

**Supplementary Script 3:** R code for generating heatmaps of haplotypes and defining clusters/haplotype groups.

```
1. isolate <- 'IP0323'
2. outfile <- "haplo_heatmap_C300_Stb6"
3. matrix <- read.csv("W300_Stb6_distmatrix_wholegene.tsv", sep="\t")
4. row.names(hm) <- matrix$Accessions
5. hm <- matrix[,-1]
6.
7. pt<-read.csv('estimated_means.csv',head=T)#phenotypes
8. wnames <- read.csv("Watcodes.csv", strip.white = T) #reference file
   for comparing different accession codes and filtering for lines in
   the Watkins core 300 set
9. pt<-pt[,-1]
10.   colnames(wnames)[1] <- 'Line'
11.   pt<-merge(pt,wnames,all.x=T)
12.
13.   pt <- pt[pt$Isolate==isolate,] #get scores for relevant isolate
14.   pto <- pt[match(colnames(hm),pt$WATDE),]
15.   row.names(pto) <- pto$WATDE #make rownames = accession names
16.   pto2 <- pto[,3:4] <- #remove excess columns
17.   colnames(pto2) <- c('pAUDPC','%max_dAUDPC')
18.
19.   fhm <- hm[row.names(hm) %in% wnames$WATDE, colnames(hm) %in%
   wnames$WATDE] #filter matrix for lines in Watkins core 300
20.
21.   pdf(file = outfile,
22.       width = 16, #The width of the plot in inches
23.       height = 16) #The height of the plot in inches
24.
25.   library(pheatmap)
26.   pheatmap(fhm,
27.           annotation_row = pto2,
28.           fontsize_row=3.5, fontsize_col=3.5)
29.   dev.off()
30.
31.   hmp <- pheatmap(fhm,
32.                 annotation_row = pto2,
33.                 fontsize_row=3.5, fontsize_col=3.5)
34.
35.   #Analyse plot and estimate number of clusters (k) needed
36.   #Add columns for distance from controls to aid analysis
37.   groups <-
   cbind(cbind(row.names(hmp),hmp$Chinese_Spring,hmp$Longbow),
38.       cluster = cutree(hmp$tree_row, k=10))
```

**Supplementary Script 4:** Python script employed to convert from hapmap to fasta format, written with Oliver Powell.

```
1. import pandas as pd
2.
3. hmp = pd.read_csv("Watkins_STB_panel_co_dominant_hmp2.txt",
    sep="\t")
4.
5. lineNames = hmp.columns.tolist()
6. lineNames = lineNames[11:]
7.
8. with open("Watkins_STB_panel_axiom_codominant_SNPs.fasta", "w+") as
    record:
9.     for line in lineNames:
10.         preseq = hmp[line].tolist()
11.         seq = "".join(preseq)
12.
13.         record.write(f">{line}\n")
14.         record.write(seq + "\n")
15.
```

**Supplementary Script 5:** Batch file used to run RaxML on the JIC high performance computing cluster, with arguments for tree generation specified.

```
1. #!/bin/bash
2. #SBATCH -J best_tree_Wat
3. #SBATCH --mem 125G
4. #SBATCH -n 10
5. #SBATCH -N 1
6. #SBATCH -p jic-long,nbi-long
7. #SBATCH -o best_tree.%j.out
8. #SBATCH -e best_tree.%j.err
9.
10.      source raxml-8.2.10
11.      raxmlHPC -s
      Watkins_STB_panel_axiom_codominant_SNPs_variable.phy -m ASC_GTRGAMMA
      --asc-corr=lewis -p 12345 -x 12345 -# autoMRE -n Wat_axiom_tree
12.
13.      #-s is sequence file name
14.      #-m is substitution model (ASC_GTRGAMMA - General Time
      Reversible model of nucleotide substitution under the Gamma model of
      rate heterogeneity with an ascertainment bias correction)
15.      ##-n output file name
16.      #-p parsimony random seed
17.      #-# number of bootstrap replicates. autoMRE will execute a
      maximum of 1000 BS replicate searches, but it may, of course converge
      earlier.
```

## THE VISITOR

I fall upon your flag leaf,  
germ tubes latching, latticing,  
slithering past your guard cells,  
creeping along corridors, around corners,  
masked amid the apoplast,  
my mycelia multiplying, matting,  
marauding through your mesophyll,  
cramming between cracks in the walls,  
deploying proteins to distract and disarm.

I am espoused to shadows, recesses;  
you scry for my old guise,  
that eternal nemesis needling you  
since civilisation began;  
your limbs were longer, your ears lighter,  
but I've evolved with you,  
gaining ground with each generation,  
shuffling chromosomes with my kin.

My hyphae cobweb your walls  
because we are talking in different tongues -  
I am too strange to conjugate,  
you have allowed me to settle in.

Your cells shrink as I indulge in the finale;  
walls crack and crash around you,  
blight unravelling in blanched lesions  
as I ravage the scraps to birth spores  
that swell through your sacked stomata.  
My children will corrupt your countless siblings,  
crowded around you, choking on air  
dead with stringencies -  
a mass rigor mortis of monoculture.  
If only you had recognised me.